
Doctoral

Science

2011-3

Eco and In Vitro Mammalian Toxicological Assessment of Polymeric Nanomaterials

Pratap Naha

Technological University Dublin

Follow this and additional works at: <https://arrow.tudublin.ie/sciendoc>

Recommended Citation

Naha, P. (2011). *Eco and In Vitro Mammalian Toxicological Assessment of Polymeric Nanomaterials*. Doctoral Thesis. Technological University Dublin. doi:10.21427/D7VS31

This Theses, Ph.D is brought to you for free and open access by the Science at ARROW@TU Dublin. It has been accepted for inclusion in Doctoral by an authorized administrator of ARROW@TU Dublin. For more information, please contact arrow.admin@tudublin.ie, aisling.coyne@tudublin.ie, vera.kilshaw@tudublin.ie.

Eco and *In Vitro* Mammalian Toxicological Assessment of Polymeric nanomaterials

By

Pratap C. Naha
(M. Pharm; Pharmacology)

**A thesis submitted to the Dublin Institute of Technology
for the degree of Doctor of Philosophy (Ph.D)**



**RESC & NanoLab; FOCAS research Institute
School of Physics
Dublin Institute of Technology
Kevin Street, Dublin 8**

Supervisor

Prof. Hugh J. Byrne

March 2011

Abstract

Eco and *in vitro* mammalian toxicological assessment of *N*-isopropylacrylamide (NIPAM) / *N*-tert-butylacrylamide (BAM) copolymer nanoparticles and Poly-amidoamine (PAMAM) dendrimers were performed in a range of test models. The particle sizes of the copolymer nanoparticles and PAMAM dendrimers (G4, G5 and G6) were measured in Milli-Q water, Algae Media, Daphnia Media, Microtox Diluent and cell culture media. The zeta potential of PNIPAM (Poly- *N*-isopropylacrylamide) and NIPAM/BAM copolymer nanoparticles measured in the different media was seen to correlate well with the ratio of BAM monomer and therefore the hydrophobicity of the particles. Ecotoxicological studies of the NIPAM/BAM copolymer nanoparticles and PAMAM dendrimers was performed using four test species; *Vibrio fischeri*, *Pseudokirchneriella subcapitata*, *Daphnia magna*, *Thamnocephalus platyurus*. The cytotoxicity of PNIPAM, NIPAM/BAM 85:15 copolymer nanoparticles and PAMAM dendrimers (G4, G5 and G6) was evaluated in RTG-2 (rainbow trout gonadal cells) and PLHC-1 (hepatocellular carcinoma in an adult female topminnow (*Poeciliopsis lucida*) cells. The generation of intracellular reactive oxygen species, genotoxicity and apoptosis was evaluated upon the exposure of PLHC-1 cells to PAMAM dendrimers. The mammalian cyto- and geno- toxicity of PNIPAM nanoparticles were analysed in HaCaT (an immortal non-cancerous human keratinocyte cell line) and SW 480 (a primary adenocarcinoma cell line of the colon) cells. The immunotoxicity of PAMAM dendrimers was evaluated in mouse macrophages (J774A.1 cells). Inflammatory markers like IL-6 (Interleukin-6), TNF- α (Tumour necrosis factor- α) and MIP-2 (Macrophage inflammatory protein-2) expression were measured by ELISA (Enzyme linked immuno sorbent assay). In the case of the NIPAM/BAM series of nanoparticles,

the ecotoxicological response was seen to vary systematically with the ratio of BAM monomer and therefore with the zeta potential of the nanoparticles. The toxic response in *Daphnia magna* was seen to also vary systematically with the reduction in zeta potential pointing towards a contribution of secondary effects due to modification of the medium. PNIPAM nanoparticles show excellent biocompatibility in HaCaT (immortalised non-cancerous human keratinocyte) and SW480 (primary adenocarcinoma of colon) cells, as no significant cyto or genotoxicity response has been observed even at high dose, although the particles were internalised by the cells within 24h.

In the case of PAMAM dendrimers, a significant eco and cytotoxicological response was recorded at particle concentrations from 0.129 μM (7.4 mg l^{-1}) to 16.55 μM (235.1 mg l^{-1}) and *Daphnia magna* was found to be the most sensitive test species, the RTG-2 fish cell line the least sensitive. Consistent with the results of the cytotoxicity assays, a generation dependent intracellular ROS, DNA damage and apoptosis was observed in PLHC-1 cells upon exposure to PAMAM dendrimers. The immunotoxicity of PAMAM dendrimers was investigated in mouse macrophage cells (J774A.1) *in vitro* within a concentration range of 0.013 to 6 μM . A generation dependent immunotoxicological response of PAMAM dendrimer was observed ($G6 > G5 > G4$). A similar generation dependence of the increased production of intracellular ROS and inflammatory mediators was observed. The toxicological response of PAMAM dendrimers varied systematically with the dendrimer generation and therefore with the number of surface amino groups per particle. The mechanism of the toxic response is proposed to be one of localisation of the cationic particles in the mitochondria, leading to significant increase in ROS generation, induction of cytokines production, DNA damage, apoptosis and ultimately cell death. For the cell lines, although spectroscopic studies indicated an

interaction with the serum supplement, trends for this interaction do not correlate to those observed for the toxic response. The clear and systematic variations of the observed toxic response with the measured physico-chemical properties point towards underlying structure activity relationships.

Declaration

I certify that this thesis which I now submit for examination for the award Doctor of Philosophy (Ph.D), is entirely my own work and has not been taken from the work of others, and to the extent that such work has been cited and acknowledged within the text of my work.

This thesis was prepared according to the regulations for postgraduate study by research of the Dublin Institute of Technology and has not been submitted in whole or in part for an award in any other Institute or University.

The work reported in this thesis conforms to the principles and requirements of the Institute's guidelines for ethics in research.

The Institute has permission to keep, or lend or to copy this thesis in whole or in part, on condition that any such use of the material or the thesis be duly acknowledged.

Signature _____ Date ____/____/____
Candidate

Acknowledgements

I would like to sincerely thank the following people without whom the completion of this thesis would not have been possible. First of all, I would like to thank my supervisor Prof. Hugh. J. Byrne. It wouldn't have been possible to do this work without all his supervision and constructive ideas. His compassionate nature and great knowledge in every aspect of life are the qualities to be emulated. I would also like to present my gratitude to Dr. Maria Davoren who guided and encouraged me at the initial stage of my Ph.D. I would like to specially thank them both for letting me develop my skill in taking initiative of difficult endeavour and see through its end.

Special thanks to Prof. Kenneth A. Dawson and Dr. Iseult Lynch from the Centre for BioNano Interactions (CBNI) University College Dublin, Belfield, Dublin 4, Ireland for provide us NIPAM/BAM series of nanoparticles for my toxicological study under the INSPIRE collaboration.

I would like to present my gratitude to Dr. Fiona Lyng, manager RESC for providing me with the lab space and helping me with experiments. I also thank to Dr. Kunal Bhattacharya and Dr. Alan Casey for their help in performing nanoparticles genotoxicity and metrology studies. I would present my thanks to the technical staff of RESC Mrs. Amaya Gracia and Karina Carey for their help with experiments. Finally, a huge thanks to all the postdoctoral and postgraduate fellows in RESC and NanoLab research centre, Focas Institute for making my time fruitful and enjoyable here.

At every step of my venture my beloved Mother, Father and Brother shared with me all the moments of different colours with immense of love and ever available patience. My respect and profound affection for them is beyond the range of inscription of words. They are really emblems of love and care.

Abbreviations

AB	Alamar Blue™
ABTS	2,2'-Azino-Bis(3-Ethylbenzthiazolin-6-Sulfonic acid)
AFM	Atomic force microscopy
AK	Adenylate kinase
AM	Algae media
ANOVA	Analysis of variances
AP-1	Activator protein 1
ApoE	Apolipoprotein E
Apop	Apoptotic cells
ATCC	American type culture collection
BAM	N-tert-butylacrylamide
BEAS-2B	Normal human bronchial epithelial cell line
BSA	Bovine serum albumin
Ca	Calcium
Carboxy-H ₂ DCFDA	6-carboxy-2',7'-dichlorodihydrofluorescein diacetate
CLSM	Confocal laser scanning microscope
CO ₂	Carbon dioxide
CI	Confidence interval
COX-2	Cyclooxygenase-2
DLS	Dynamic light scattering
DM	<i>Daphnia</i> media
DMEM-F12	Dubecco's modified essential medium-F12 nutrient mix
DMSO	Dimethylsulfoxide

DNA	Deoxyribonucleic acid
EC	European Commission
EC ₅₀	Effective concentration leading to a 50% response
ECACC	European collection of cell cultures
EDTA	Ethylenediaminetetraacetic acid
ELISA	Enzyme linked immunosorbant assay
ENU	Ethyl Nitrosourea
EPA	Environmental Protection Agency
EtOH	Ethanol
FACS	Fluorescence associated cell sorter
FBS	Foetal bovine serum
Fe	Iron
FITC	Fluorescein isothiocyanate
FP7	7th Research Framework Programme
FU	Fluorescent units
GSH	glutathione
h	Hours
H ₂ O ₂	Hydrogen peroxide
HaCaT	Normal human keratinocyte cell line
HRP	Horseradish peroxidase
IgG	Immunoglobulin G
IL	Interleukin
iNOS	Inducible nitric oxide synthase
J774A.1	Mouse macrophage cells
LPS	Lipopolysaccharide

mA	milliampere
MCP-1	Macrophage-chemoattractant protein-1
MD	Microtox diluents
Mg	Magnesium
MIP	Macrophage inflammatory protein
mM	millimolar
ml	millilitre
μ M	Micromolar
μ l	microliter
mRNA	Messenger RNA
Mt	Mitochondria
MTT	3-(4,5-Dimethylthiazol-2-yl)-2,5diphenyltetrazoliumbromid
mV	millivolt
NADPH	reduced nicotinamide adenine dinucleotide phosphate
Nec	Necrotic cell
NIPAM	N-isopropylacrylamide
NF- κ B	Nuclear factor- κ -B
nm	Nanometer
NPs	Nanoparticles
NR	Neutral Red
Nuc	Nucleus
OECD	Organisation for Economic Development
8-OHdG	8-hydroxy-2'-deoxyguanosine
OTM	Olive Tail Moment
PAMAM	Poly (amido)amine

PBS	Phosphate buffered saline
PBS-T	Phosphate buffer saline with 0.05% of Tween 20
PCR	Polymerase chain reaction
PGE ₂	Prostaglandin E2
PI	Propidium iodide
PLHC-1	Hepatocellular carcinoma cells (<i>Poeciliopsis lucida</i>)
PNIPAM	Poly-N-isopropylacrylamide
ppm	Parts per million
RNA	Ribonucleic acid
ROS	Reactive oxygen species
RT	Room temperature
RTG-2	Rainbow trout gonadal cells
RT-PCR	Reverse transcriptase PCR
RRR	Reduction, Replacement and Refinement
SD	Standard deviation
SDS	Sodium dodecylsulphate
SW 480	Primary adenocarcinoma cell line of colon
TEM	Transmission electron microscopy
TiO ₂	Titanium dioxide
TNF- α	Tumour-necrosis-factor- α
TM	<i>Thamnocephalus media</i>
Tween	Polysorbate
UV	ultraviolet

Table of Contents

Abstract	i
Declaration	iv
Acknowledgements	v
Abbreviations	vi
Table of Contents	x
List of Tables.....	xiii
List of Figures	xv
Chapter 1	1
1. Introduction	2
1.1 Introduction to Nanotechnology	2
1.2 Polymeric nanoparticles	3
1.2.1 PNIPAM and NIPAM/BAM nanoparticles	5
1.2.2 PAMAM dendrimers.....	7
1.3 Nanotoxicology	9
1.4 Eco (Nano) Toxicology.....	11
1.5 Aims, Objectives and Methodology.....	12
References	21
Chapter 2	32
2. Materials and Experimental protocols	33
2.1 Materials.....	33
2.1.1 PNIPAM and NIPAM/BAM co-polymer nanoparticles	33
2.1.2 PAMAM (Poly amidoamine) dendrimers.....	33
2.2 Experimental protocol.....	34
2.2.1 Particle Characterisation	34
2.2.1.1 Particle size measurement	34
2.2.1.2 Zeta potential measurement	36
2.2.1.3 Spectroscopic analysis	36
2.2.1.4 Surface Area measurement	37
2.2.1.5 Transmission electron microscopy (TEM) study.....	38
2.2.2 Ecotoxicity tests	38
2.2.2.1 Microtox [®] test	38
2.2.2.2 Microalgae growth inhibition assay.....	40
2.2.2.3 Thamnotoxkit F TM	43
2.2.2.4 Daphnia magna acute immobilisation assay	45
2.2.2.5 Cell culture	47
2.2.2.6 Cytotoxicity assays.	49
2.2.2.7 Internalisation study of fluorescently labelled PNIPAM nanoparticles	52
2.2.2.8 Study of Co-localisation of the fluorescently labelled PNIPAM nanoparticles with lysosomes.....	53
2.2.2.9 Intracellular Reactive Oxygen Species (ROS).....	54
2.2.2.10 Cytokines assay.....	57
2.2.2.11 Oxidative DNA damage.....	59
2.2.2.12 Alkaline Comet assay.....	63
2.2.2.13 Apoptosis assay.....	64
2.2.2.14 Statistics	65

References	67
Chapter 3	70
3.1. Introduction	71
3.2 Experimental methods.....	72
3.3 Results	72
3.3.1 Nanoparticles characterisation	72
3.3.1.1 Particle size measurement	72
3.3.1.2 Zeta potential measurement	75
3.3.1.3 Surface Area measurement	76
3.3.2 Ecotoxicity	77
3.3.2.1 Ecotoxicity test results with PNIPAM	83
3.3.2.2 Ecotoxicity test results with NIPAM/BAM 85:15.....	84
3.3.2.3 Ecotoxicity tests with NIPAM/BAM 65:35.....	85
3.3.2.4 Ecotoxicity tests with NIPAM/BAM 50:50.....	86
3.4 Discussion	87
3.5 Conclusions	94
References	96
Chapter 4	101
4.1 Introduction	102
4.2 Experimental methods.....	103
4.3 Results	103
4.3.1 Characterisation of PNIPAM nanoparticles.....	103
4.3.2 Intracellular uptake study.....	106
4.3.3 Cytotoxicity assessment of PNIPAM nanoparticles	112
4.3.4 Genotoxicity assessment of PNIPAM nanoparticles	114
4.4 Discussion	117
4.4.1 Characterisation of PNIPAM nanoparticles.....	117
4.4.2 Intracellular uptake study.....	118
4.4.3 Cytotoxicity.....	118
4.4.4 Genotoxicity.....	119
4.5 Conclusion	121
References	122
Chapter 5	129
5.1 Introduction	130
5.2 Experimental methods.....	131
5.3 Results	132
5.3.1 Characterisation of particles.....	132
5.3.1.1 Particle size	132
5.3.1.2 Zeta potential.....	133
5.3.1.3 Spectroscopic analysis	134
5.3.2 Ecotoxicity	136
5.3.2.1 Ecotoxicity tests with PAMAM Dendrimer G4, G5 and G6	137
5.4 Discussion	144
5.5 Conclusion	149
References	150
Chapter 6	156
6.1 Introduction	157
6.2 Experimental methods.....	159
6.3 Results	159
6.3.1 Particle characterization and Cytotoxicity	159

6.3.2 Intracellular reactive oxygen species (ROS).....	159
6.3.3 Genotoxicity response of PAMAM dendrimers	165
6.3.4 8-OHdG assay	170
6.3.5 Apoptosis Assay.....	171
6.4 Discussion	176
6.5 Conclusion	180
References	181
Chapter 7	184
7.1 Introduction	185
7.2 Experimental methods.....	187
7.3 Results	187
7.3.1 Characterisation of PAMAM dendrimers	187
7.3.2 Cytotoxicity assay	188
7.3.3 Intracellular Reactive oxygen species (ROS)	191
7.3.4 Cytokines production	196
7.3.4.1 Macrophage inflammatory protein-2 (MIP-2)	196
7.3.4.2 Interleukin-6 (IL-6)	198
7.3.4.3 Tumour necrosis factor- α (TNF- α)	199
7.4 Discussion	202
7.5 Conclusions	209
Reference.....	210
Chapter 8	217
References	224
Appendices	225
Appendix I: Supporting Information.....	226
1.1 PNIPAM and NIPAM/BAM co-polymer nanoparticles	226
1.2 Transmission electron microscopy (TEM) study.....	227
Appendix II: Publications	229
Appendix III: Presentations.....	231
Appendix IVI: Conference and Workshop Attendance	232
Curriculum Vitae.....	233

List of Tables

Table 2.1. Composition of stock solutions for Jaworskis algal media.

Table 3.1. Hydrodynamic diameter of PNIPAM and NIPAM/BAM copolymer nanoparticles in different test media and temperature.

Table 3.2. Ecotoxicity data for poly-*N*-isopropylacrylamide P(NIPAM) nanoparticles on selected test species and endpoints.

Table 3.3. Ecotoxicity data for *N*-isopropylacrylamide-co-*N*-*tert*-butylacrylamide (NIPAM/BAM 85:15) copolymer nanoparticles on selected test species and endpoints.

Table 3.4. Ecotoxicity data for *N*-isopropylacrylamide-co-*N*-*tert*-butylacrylamide (NIPAM/BAM 65:35) copolymer nanoparticles on selected test species and endpoints.

Table 3.5. Ecotoxicity data for *N*-isopropylacrylamide-co-*N*-*tert*-butylacrylamide (NIPAM/BAM 50:50) copolymer nanoparticles on selected test species and endpoints

Table 4.2. Zeta potential of NIPAM nanoparticles in different media

Table 5.1. Hydrodynamic diameter of PAMAM dendrimers in different test media.

Table 5.2: Ecotoxicity of PAMAM dendrimer G4.

Table 5.3 :Ecotoxicity of PAMAM dendrimer G5.

Table 5.4: Ecotoxicity of PAMAM dendrimer G6.

Table 6.1. Level of 8-OHdG formation upon the exposure of PAMAM dendrimers to PLHC-1 cells.

Table 6.2. Percentage of cell population in different stages of apoptosis upon the exposure of PAMAM dendrimers in PLHC-1 cells at 6h exposure.

Table 6.3. Percentage of cell population in different stages of apoptosis upon the exposure of PAMAM dendrimers in PLHC-1 cells at 12h exposure.

Table 6.4. Percentage of cell population in different stages of apoptosis upon the exposure of PAMAM dendrimers in PLHC-1 cells at 24h exposure

Table 7.1. Zeta potential of PAMAM dendrimers in different media

Table 7.2. EC₅₀ data of PAMAM dendrimer G4, G5 and G6 in Alamar blue (AB) and MTT assay for 24 hour exposure in J774A.1 cells.

List of Figures

Figure 1.1. Increase in hydrophobicity of the NIPAM/BAM copolymer nanoparticles as a function of BAM ratio.

Figure 1.2. PAMAM dendrimer G4

Figure 1.3. Fresh water ecosystem representing different trophic levels.

Figure 2.1. PAMAM dendrimer G4 , G5 and G6

Figure 2. 2. Schematic diagram of a conventional dynamic light scattering instrument.

Figure 2.3. Microtox[®] Model 500 analyser and the Morphology of *Vibrio fischeri*.

Figure 2.4. Morphology of *Pseudokirchneriella subcapitata*.

Figure 2.5. Morphology of *Thamnocephalus platyurus*

Figure 2.6. Morphology of *Daphnia magna*

Figure 2.7. Morphology of, A. RTG-2 cells, B. PLHC-1 cells, C. HaCaT cells. D. SW 480 cells, E. J774A.1 cells.

Figure 2.8. Conversion of Caroxy H₂DCFDA to DCF

Figure 2.9. Time kinetic study of ROS production with 200 μ M of H₂O₂ exposure to PLHC-1 cells. The concentration of Carboxyl H₂DCFDA used 10 μ M.

Figure 2.10. Principle of ELISA (Sandwich technique)

Figure 2.11. Schematic diagram of the conversion of Deoxyguanosine to 8-hydroxyguanosine.

Figure 3.1. Hydrodynamic diameter of PNIPAM and NIPAM/BAM copolymer nanoparticles. Figure a, represents for MQ water and figure b, represents for in Microtox diluent (MD) as a function of increasing temperature.

- Figure 3.2. Zeta potential of PNIPAM and NIPAM/BAM copolymer particles in different media.
- Figure 3.3. Effect of NIPAM and NIPAM/BAM nanoparticles on algal growth inhibition.
- Figure 3.4. Effect of PNIPAM (A); NIPAM/BAM 85:15 (B); NIPAM/BAM 65:35 (C) and NIPAM/BAM 50:50 (D) particles on immobilisation of *Daphnia magna*.
- Figure 3.5. Effect of PNIPAM (□) and NIPAM/BAM 85:15 (■) (A); NIPAM/BAM 65:35 (B); and NIPAM/BAM 50:50 (C) particles on lethality of *Thamnocephalus platyurus*.
- Figure 3.6. Cytotoxicity of PNIPAM and NIPAM/BAM nanoparticles in RTG-2 cells. Figure A. represents for PNIPAM and figure B represents for the NIPAM/BAM 85:15 nanoparticles.
- Figure 3.7. Relationship between 24 hour (□) and 48 hour (■) EC₅₀ for immobilisation of *Daphnia magna* following exposure to PNIPAM and different NIPAM/BAM copolymer particles.
- Figure 3.8. Effect of PNIPAM and different NIPAM/BAM copolymer nanoparticles on 24 h LC₅₀ in *Thamnocephalus platyurus*.
- Figure 3.9. Effect of zeta potential of different copolymer nanoparticles on immobilisation of *Daphnia magna* based on the (□) 24 hour; (■) and 48 hour EC₅₀ results.
- Figure 3.10. Correlation between change in zeta potential and EC₅₀ in immobilisation of *Daphnia magna* with different NIPAM and NIPAM/BAM copolymer.
- Figure 4.1. Representative TEM image of the labelled PNIPAM nanoparticles.

- Figure 4.2. Confocal laser scanning micrograph (CLSM) of internalisation of fluorescent labelled PNIPAM nanoparticles in HaCaT and SW 480 cells after 24h of exposure. Panel 1 represents the uptake study in the HaCaT cells and panel 2 represents the uptake study in SW 480 cells.
- Figure 4.3. CLSM optical sections (z-sections) of the HaCaT and SW 480 cells showing the localisation of the nanoparticles at different sections. Each optical section represents a particular plane of focus and nanoparticles have a different plane of focus indicating that they are internalised completely. Panel 1 represents the HaCaT cells (optical section thickness is 0.41 μm), panel.2 represents the SW 480 cells (optical section thickness is 1.0 μm) with exposure concentration 50mg/l.
- Figure 4.4. CLSM images of co-localisation of NIPAM nanoparticles with lysosomes, by co-staining the HaCaT cells with lysotracker (green). (1) and (2) are the 24 hour exposure to labelled PNIPAM nanoparticles at concentrations of 30 and 50 mg/l respectively.
- Figure 4.5. Cytotoxicological response of HaCaT cells after 24, 48, 72 and 96 h of exposure to increasing concentrations of PNIPAM nanoparticles.
- Figure 4.6. Cytotoxicological response of SW 480 cells after 24, 48, 72 and 96 h of exposure to increasing concentrations of PNIPAM nanoparticles.
- Figure 4.7. Genotoxicity response of PNIPAM nanoparticles to HaCaT cells. Panel A represents the % tail DNA and Panel B represents the olive tail moment after exposure of the particles at three different time points.
- Figure 4.8. Genotoxicity response of PNIPAM nanoparticles to SW 480 cells. Panel A represents the % tail DNA and Panel B represents the olive tail moment after exposure of the particles at three different time points.

- Figure 5.1. Zeta potential of PAMAM dendrimer in different test media.
- Figure 5.2. Medium interaction study of PAMAM (G4, G5 and G6) dendrimers in PLHC-1 media by UV-Visible absorption spectroscopy. Figure a. represents UV-Visible absorption spectra of DMEM F-12 HAM, PLHC-1 and RTG-2 media; Figure b. represents. UV-Visible absorption spectra of RTG-2 media with PAMAM (G4, G5 and G6) dendrimers. Figure c. represents. UV-Visible absorption spectra of PLHC-1 media with PAMAM (G4, G5 and G6) dendrimers.
- Figure 5.3. Dose dependent response of PAMAM dendrimers in *T. platyurus* , Figure A, B and C represents for the PAMAM dendrimer G4, G5 and G6 respectively.
- Figure 5.4. Dose dependent response of PAMAM dendrimers in *D.magna* , Figure A, B and C represents for the PAMAM dendrimer G4, G5 and G6 respectively.
- Figure 5.5. Cytotoxicity of PAMAM dendrimer in PLHC-1 cells as quantified using the AB Assay. a, b and c represent G4, G5 and G6 respectively.
- Figure 5.6. Cytotoxicity of PAMAM dendrimer in RTG-2 cells as quantified using the AB Assay. a, b and c represent G4, G5 and G6 respectively.
- Figure 5.7. Toxicity profile of PAMAM dendrimers based on EC_{50}/LC_{50} values in different test models.
- Figure 5.8. Correlation between measured surface areas of PAMAM dendrimers with EC_{50}/LC_{50} in different test models
- Figure 5.9. Correlation between change of zeta potential and EC_{50} of PAMAM dendrimer (G4, G5 and G6) in immobilisation of *Daphnia magna*.
- Figure 6.1 Confocal laser scanning micrograph (CLSM) of PLHC-1 cells showing intracellular ROS production upon exposure of PAMAM dendrimers to the PLHC-1 cells.

Figure 6.2 Concentration and time dependent intracellular ROS generation, upon the exposure of PAMAM dendrimers (A) G4 (B) G5 and (C) G6.

Figure 6.3: Plot showing the generation dependent intracellular ROS production at a concentration of 0.6 μ M for G6.

Figure 6.4 (A) Plot showing the relationship between the intracellular ROS production and the number of surface primary amino group of the PAMAM dendrimers at 2 hour exposure time period of 0.6 μ M concentration; (B) relationship between maximum surface amino group and the intracellular ROS production in PLHC-1 cells.

Figure 6.5. Representative micrograph showing comets of PLHC-1 cells after 24 hour exposure of PAMAM dendrimers.

Figure 6.6. Genotoxicity response of PAMAM dendrimers at 6h, 12h and 24h exposure, Panel A, B and C represents for PAMAM G4, G5 and G6.

Figure 6.7. Generation dependent genotoxicity response of PAMAM dendrimers at 6h, 12h and 24h exposure.

Figure 6.8. Correlation between the % Tail DNA and number of primary surface amino groups of the PAMAM dendrimers.

Figure 6.9. Correlation between maximum DNA damage and maximum intracellular ROS production upon the exposure of PAMAM dendrimer G4, G5 and G6.

Figure 6.10. Generation dependent different stages of apoptosis upon the exposure of PAMAM dendrimers for G4, G5 and G6 at concentration of 5.2, 2 and 1.2 μ M respectively in PLHC-1 cells.

Figure 7.1. Comparison of cytotoxicity assay between AB and MTT of (a) G4, (b) G5 and (c) G6 PAMAM dendrimers in J774A.1 cells after 24h exposure. The data shown in mean \pm SD (n=3).

- Figure 7.2. (a) Time and generation dependence of toxic response of PAMAM dendrimers (G4, G5, G6). (b) Correlation between number of surface amino group and the toxic response of PAMAM dendrimers at 24h exposure (AB assay).
- Figure 7.3. Confocal fluorescence and phase contrast micrographs of intracellular ROS generation following exposure to (a) negative control, (b) positive control (H_2O_2), (c) PAMAM G4, (d) PAMAM G5 and (e) PAMAM G6. The data are shown after 2h exposure of PAMAM dendrimers.
- Figure 7.4. Concentration and time dependent intracellular ROS generation by G4, G5 and G6 at (a) 1, (b) 2, (c) 4 and (d) 6 h exposure time points.
- Figure 7.5. (a) generation dependent intracellular reactive oxygen species (ROS) production following exposure to PAMAM dendrimers (G4, G5 and G6) in J774A.1 cells at an exposure concentration of $1\mu M$. (b) correlation between the production of intracellular ROS and number of surface primary amino groups.
- Figure 7.6. The level of MIP-2 secreted after exposure of J774A.1 cells to (a)G4, (b) G5 and (c) G6 PAMAM dendrimers for 6h, 12h, 24h, 48h and 72h.
- Figure 7.7. Secretion of IL-6 following exposure of (a) G4, (b) G5 and (c) G6 in J774A.1 cells at 6, 12, 24and 48 h time points.
- Figure 7.8. Secretion of TNF- α upon the exposure of (a) G4, (b) G5 and (c) G6 in J774A.1 cells at 6, 12, 24 and 48 h time points.
- Figure 7.9. Generation dependent MIP-2, IL-6 and TNF- α secretion after 24h exposure of PAMAM dendrimers (G4, G5 and G6) in J774A.1 cells.
- Figure 7.10. Correlation between inflammatory mediator (a) MIP-2, (b) IL-6 and (c) TNF- α response and the surface area of PAMAM dendrimers (G4, G5 and

G6). Figure 7.11. Schematic of the systematic sequence of events in J774A.1 cells following exposure to PAMAM dendrimers.

Figure 7.12. Graphical representation of the of different responses as a function of time upon the exposure of PAMAM dendrimers(for the case of G4) in J774A.1 cells.

Chapter 1

Introduction, Aims and Objective

1. Introduction

1.1 Introduction to Nanotechnology

Nanotechnology is a new and fast emerging field that involves the design, production, and exploitation of structures at the nanoscale. A nanomaterial is a material that has one or more external dimensions in the nanoscale or which is nanostructured. A nano-object with all three external dimensions in the nanoscale is defined as a nanoparticle (<http://www.nanoimpactnet.eu/index.php?page=nomenclature>, accessed on 16th June 2011). Nanotechnology can also be defined as the design, synthesis and application of materials and devices whose size and shape have been engineered at the nanoscale. It exploits unique chemical, physical, electrical and mechanical properties that emerge when materials are structured at the nanoscale. Nanotechnology is a highly promising and exciting technology that spans many areas of science and technological applications and is one of the hitherto unexplored frontiers of science. It offers a broad range of exciting prospects for technological innovation. Nanoscience has exploded in the last decade, primarily as the result of the development of new tools that have made the characterization and manipulation of nanostructures practical, and also as a result of new methods for preparation of these physical and chemical structures. Nanotechnology is a sector of the materials manufacturing industry that has already created a multibillion market which is widely expected to grow to 1 trillion \$US by 2015 (Lux Research).

Numerous applications of nanoparticles are already on the market, in products such as paints, sunscreens, cosmetics, self-cleaning glass, industrial lubricants, advance tyres, semiconductor devices and food (Garland 2009, Mueller and Nowack 2008, Jaroenworuluck, 2006). In the biomedical field, nanotechnology is also projected to have a significant impact. For example, polymeric nanomaterials such as poly

aminoamide (PAMAM) dendrimers have already been explored for applications such as targeted drug delivery in cancer therapy, gene delivery and also the mannosylated form of PAMAM dendrimers are already used in vaccine delivery systems (Sheng et al., 2008).

Optimisation of nanoparticle design and delivery strategies for such biomedical applications requires however a detailed understanding of how such nanoparticles interact with biological fluids, tissues and cells. Cellular uptake mechanisms, intracellular trafficking, oxidative stress and inflammatory responses have already been widely explored (see for example the review by Nel et al., 2009), but there is much to be learned about the dependences on the physico-chemical properties of the particles. Furthermore, the proliferation of nanotechnology in general has prompted concerns over the safety of engineered nanoparticles, as exposure to humans and/or the environment may occur intentionally or accidentally. Therefore it is important to understand the interaction of nanomaterials with living organisms in terms of potential toxicological impacts on both the environment and human health. Well characterised, chemically and physically well defined materials are critical in this respect and, ultimately, quantitative structure activity relationships (QSARS) governing the interaction of engineered nanoparticles with organisms and the resultant biological responses are desirable.

The aim of this study was to explore structure activity relationships governing the toxicological responses model eco and mammalian cell culture systems to polymeric nanoparticles of systematically varied physico-chemical properties.

1.2 Polymeric nanoparticles

Polymeric nanoparticles have been proposed for a wide range of medical applications in terms of diagnosis, tissue engineering and as drug delivery devices (Storrie and Mooney, 2006). Several polymeric micro- and nanoparticles have been used for the

delivery of drugs and therapeutic proteins. In particular, polylactic-*co*-glycolic acid (PLGA) and poly-lactic acid (PLA) polymers, which are biodegradable in nature, show great potential and have been widely used in drug delivery systems (Ito et al., 2008; Naha et al., 2008 and 2009). Currently, four other nanoparticles, namely polymer coated iron oxide nanoparticles, PEGylated (process of covalent attachment of polyethylene glycol) liposomes, dendritic fullerenes, and fullerene derivative nanoparticles, are being investigated in clinical trials for their anticancer activity (Dobrovolskaia and McNeil, 2007).

Poly *N*-isopropylacrylamide (PNIPAM), *N*-isopropylacrylamide-*co*- *N*-tert-butylacrylamide (NIPAM/BAM) nanoparticles, and Poly (amido) amine (PAMAM) dendritic nanoparticles have been used in this study. These nanomaterials have systematically varied physico-chemical properties and were so chosen in an attempt to explore structure activity relationships governing the toxicological responses. PAMAM dendrimers also have potential applications as intracellular drug, protein and vaccine delivery systems.

Poly *N*-isopropylacrylamide (PNIPAM) nanoparticles have been developed and proposed for controlled release of ophthalmic drops for glaucoma therapy (Hsiue et al., 2003; Hsiue et al. 2002). Polyamidoamine (PAMAM) dendrimers are widely used in the field of biomedical applications, such as drug delivery, targeted drug delivery in cancer therapy, gene delivery, and also the mannosylated form of PAMAM dendrimers is used in vaccine delivery systems (Sheng et al., 2008). There was no complete report on ecotoxicity of PAMAM dendrimers, PNIPAM and NIPAM/BAM series of nanoparticles are available in the literature.

PAMAM dendrimers are molecularly defined, in that they have a precise molecular structure and molecular weight. NIPAM/BAM particles are less well defined and have

an average molecular weight, depending on particle size. Although PAMAM dendrimers may more accurately be defined as macromolecules, throughout this work they are considered polymeric nanoparticles, for simplicity.

1.2.1 PNIPAM and NIPAM/BAM nanoparticles

Poly *N*-isopropylacrylamide (PNIPAM) is a well known thermoresponsive polymer (Hsiue et al. 2002). Thermoresponsive is a general term which means a material changes its properties as a function of temperature, above or below its Lower Critical Solution Temperature (LCST), defined as the temperature below which the component of a mixture are miscible for all components. PNIPAM exhibits a LCST of ~ 32 °C in aqueous media (Xu et al., 2006). Copolymerisation of NIPAM with the more hydrophobic monomer *N*-tert-butylacrylamide (BAM) reduces the LCST of the resultant co-polymer compared to that of PNIPAM, increasingly so as the ratio of the BAM monomer in the co-polymer is increased. As the ratio of BAM increases, the amount of N-H groups exposed at the surface decreases, and the amount of -C-(CH₃)₃ groups increases, reducing the hydrophilicity of the resulting copolymer (Figure 1.1). For example, LCSTs for the polymers with monomer ratios NIPAM/BAM 85:15, NIPAM/BAM 65:35, NIPAM/BAM 50:50 are 25°C, 17°C and 12°C respectively (Lynch et al., 2005). Adjustment of the LCST to near body temperature (Zhang and Misra 2007) is essential, particularly for ‘smart’ drug delivery applications (Peppas et al. 2000; Lin and Metters 2006). Above its LCST, the polymer particles form large agglomerates and this could be affect to release of the drug from this composite polymer. As a result, the concentration of the released drug will not reach the minimum effective concentration (MEC) level in the blood. Thus, it is always necessary to maintain the LCST near to normal body temperature. Because of this reversible phase

transition, PNIPAM has been widely used in the preparation of stimuli responsive systems for biomedical applications, such as in the controlled release of drugs and in tissue engineering (Kavanagh et al. 2005; Xu et al., 2006; Xu et al. 2004; Zhang et al., 2005). NIPAM/BAM copolymer nanoparticles of varying size and copolymer ratios have been observed to adsorb plasma proteins on to their surface with potential implications for selective biological interactions (Cedervall et al. 2007). Recently, NIPAM/BAM copolymer particles have been shown to retard or even reverse the fibrillation of amyloid- β , the protein involved in Alzheimer's disease (Cabaleiro-Lago et al. 2008), also in solution experiments, indicating that such processes are complex and depend on the nature of both the particle and the protein.

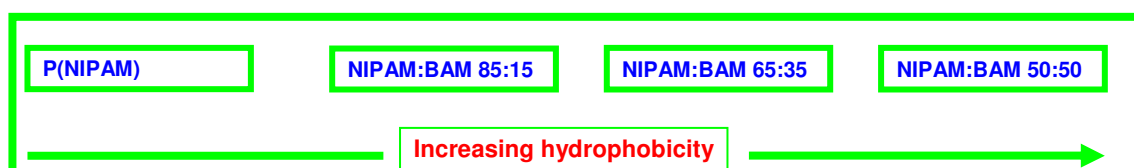
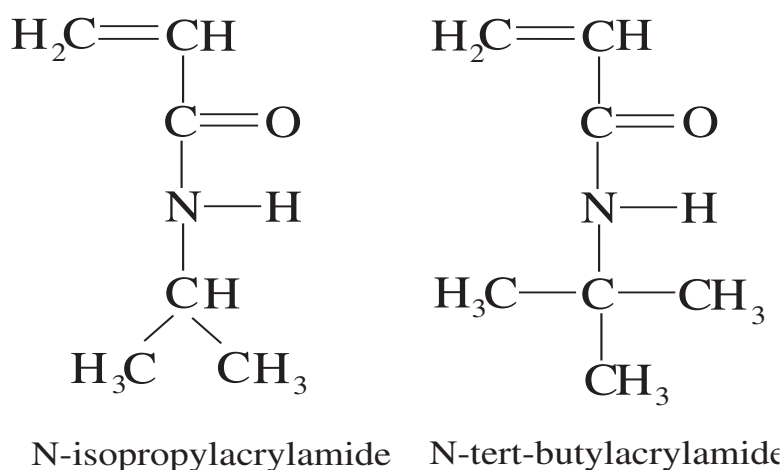


Figure 1.1. Increase in hydrophobicity of the NIPAM/BAM copolymer nanoparticles as a function of BAM ratio.

Notably, in addition to their potential biomedical applications, the variable size and surface chemistry of such polymeric particles renders them valuable probes of the underlying structure activity relationships determining biological responses.

1.2.2 PAMAM dendrimers

Dendrimers have well-defined nanoscale architecture and potential novel applications in the biomedical field (Lee et al., 2005). Polyamidoamine (PAMAM) dendrimers contain a 2-carbon ethylenediamine core and primary amino groups on the surface (<http://www.dendritech.com/pamam.html>, accessed on 16th June 2009). The systematically variable structural architecture and the large internal free volume make these dendrimers an attractive option for drug delivery and other biomedical applications (Venuganti and Perumal 2008; Svenson and Tamalia 2005; Emanuele and Attwood 2005; Ducan and Izoo 2005). It is possible to passively target PAMAM dendrimers to a tumour because of the increased permeability of tumour vasculature to macromolecules and also due to the limited lymphatic drainage (Maeda and Matsumura 1986). The unique properties of dendrimers, as compared to linear polymers, render them of interest for intracellular drug delivery system for cancer therapy (Gillis and Frechet 2005). Amino terminated PAMAM dendrimers result in enhanced anti-ovalbumin immunoglobulin-G and immunoglobulin-M levels and have also been used as adjuvants in vaccine delivery systems (Rajananthanan et al., 1999). In a recent study it has been shown that N-acetyl-D-glucosamine modified PAMAM dendrimers improve the immunogenicity by up-regulation of antibody formation via activation of natural killer cells (Hulikova et al., 2009) and the mannosylated form of PAMAM dendrimers potentiate the immunogenicity and have been proposed for vaccine delivery systems (Sheng et al., 2008). PAMAM dendrimers have also been proposed for intracellular

drug, protein and vaccine delivery systems. Because of the potential widespread use of these systems, a complete evaluation of their toxicology to humans is required.

Furthermore, although not yet in widespread use, future uses may result in significant environmental exposure, notably in fresh water via industrial effluent and domestic waste, warranting a comprehensive ecotoxicological study in a model freshwater ecosystem.

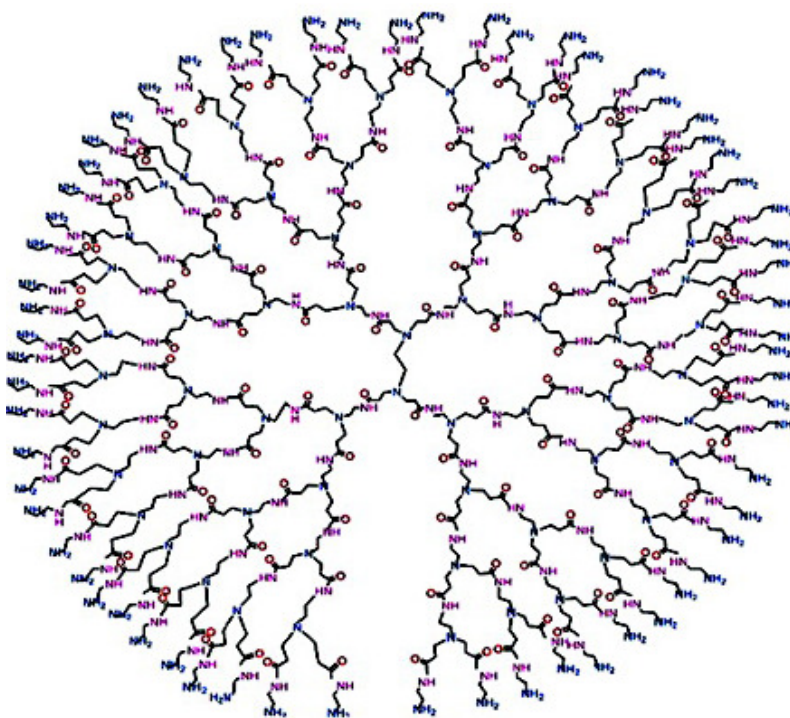


Figure 1.2. PAMAM dendrimer G4 (Lubic, 2009. *Environ. Sci. Technol.* 43, 1247–1249).

For the purpose of this work, similar to the NIPAM/BAM based structures, the structurally well defined and variable macromolecules can also provide a further basis upon which to establish structure activity relationships governing eco- and mammalian toxicological responses which may serve to develop a fundamental understanding of their interactions and as guidelines for the future prediction of responses.

1.3 Nanotoxicology

Nanotoxicology is an evolving sub-specialty of particle toxicology. It addresses the toxicology of nanoparticles, which in general appear to elicit toxic effects that are peculiar and not seen with larger particles. The important mechanistic toxicity pathways of different nanoparticles are intracellular reactive oxygen species (ROS) production, expression of inflammatory markers, DNA adduct formation, DNA damage, chromosomal aberration, mutation, apoptosis and finally cell death. To date, typical nanoparticles that have been studied are titanium dioxide, alumina, zinc oxide, carbon black, carbon nanotubes, and "nano-C₆₀" (Brown et al., 2001, 2004; Vevers et al., 2008; Jeng et al., 2006; Colvin et al., 2003; Herzog et al., 2007; Davoren et al., 2007). Surface area is also an important factor in the toxicity of a nanoparticle, as the greater the surface area, the more reactive centers are exposed to the cellular environment, and the more pro-inflammatory and toxic effects' (Brown et al., 2001; Stoeger et al., 2009). In addition, some nanoparticles seem to be able to translocate from their site of deposition to more remote sites such as the blood and the brain (Wang et al., 2008). This has resulted in a dramatic change in how particle toxicology is viewed. Instead of being confined to the lungs, nanoparticle toxicologists now study the brain, blood, liver, skin and gut. Nanotoxicology has therefore revolutionised and rejuvenated the field of particle toxicology. The smaller a particle is, the larger its surface area to volume ratio and thus the associated chemical and biological activity of the material is increased. The greater chemical reactivity of nanomaterials results, for example, in increased production of reactive oxygen species (ROS) (Nel et al., 2006; Stoeger et al., 2009), including free radicals.

Reactive Oxygen species in mammalian cells include Hydroxyl radicals ($\cdot\text{OH}$), Hydroxyl ion (OH^-), Superoxide anion (O_2^-), Singlet oxygen ($^1\text{O}_2$), Hydrogen peroxide

(H₂O₂) and Hypochlorite ion (OCl⁻) and increased production acts to suppress the antioxidant system and results in oxidative stress. Oxidative stress is an imbalance of the intracellular redox equilibrium and can cause localised degradation of organelles. Oxidative stress leads to inflammation, a biological response of tissues to harmful stimuli, such as pathogens, damaged cells, or irritants (pollutant, nanomaterials etc) and genotoxicity effects, in which the genetic material (DNA) is damaged. The effects are likely to be DNA damage, micronucleus formation, chromosomal aberrations or the formation of DNA adducts. An excess of ROS can cause oxidation of lipids, proteins, DNA etc and the adverse effects depend upon the different species of ROS. For example, hydroxyl radical can lead to adduct formation in the base pairs of DNA, such as 8-OHdG (8-hydroxy-2'-deoxyguanosine), which mediates the pathophysiology of a wide variety of diseases including cancer, atherosclerosis, neurodegenerative disorders and the aging process (Halliwell and Gutteridge, 1999). In the case of nanotoxicology, increased levels of intracellular ROS as a result of nanoparticle exposure has been identified as a fundamental precursor to inflammation, genotoxicity and apoptosis (Xia et al., 2006). Oxidative stress induces signaling pathways of MAPK and transcription factors such as NFκB, AP-1. These transcription factors induce mRNA expression of pro-inflammatory mediators, finally causing inflammation. Persistent inflammation can lead to cell damage, induced by chemical/physical injury, anoxia or nanoparticles. Cell damage means leakage of cell contents into the adjacent tissues, resulting in the capillary transmigration of granulocytes to the injured tissue. The accumulation of neutrophils and release of enzymes and oxygen radicals enhances the inflammatory reaction which will lead to apoptotic cell death.

Increased ROS production has been found for a diverse range of nanomaterials including fullerenes, carbon nanotubes and metal oxide nanoparticles. ROS and free

radical production is one of the primary mechanisms of nanoparticle toxicity, it may result in oxidative stress, inflammation and consequent damage to proteins, membranes and DNA (Risom et al., 2005).

Despite the increasing body of literature relating to the toxicity of nanoparticles, there remains a dearth of systematic studies in which the physic-chemical properties of the nanoparticles are systematically varied and the toxicological response and mechanism monitored and related to the particle variations. In this study, the toxicological response to systematically varied polymeric nanoparticle exposure is monitored in mammalian cell lines *in vitro*. Although *in vitro* cell lines are only an approximation of *in vivo* studies, it is anticipated that the systematic variation of the polymeric nanoparticle properties can point towards structure activity relationships governing the responses and help elucidate underlying mechanisms. Mouse macrophage, as well as human skin and intestinal models are used.

1.4 Eco (Nano) Toxicology

In addition to potential hazards to humans, those to the environment should also be considered. The assessment of environmental effects of nanoparticles requires an understanding, for example, of their mobility, reactivity, ecotoxicity and persistency (Nowack and Buchelli, 2007). Recently reports on the ecotoxicity of various nanomaterials have started to emerge in the literature. Of the studies conducted to date, the majority have focused on carbon based materials (Lovern and Klaper, 2006; Zhu et al., 2006; Cheng et al., 2007; Lin and Xing, 2007; Smith et al., 2007; Baun et al., 2008; Lovern et al., 2007) but there have also been reports of ecotoxicological studies of various metal based nanoparticulate materials (Lovern et al., 2007; Federici et al., 2007; Heinlaan et al., 2008; Gagné et al., 2008; Mortimer et al., 2008) as well as polymeric dendrimers (Mortimer et al., 2008). A recent study has explored the toxicity of

PAMAM dendrimers (G 3.5 and G4) in a zebra fish embryo model (Heiden et al., 2007).

1.5 Aims, Objectives and Methodology

Due to the potential widespread use of both series of polymeric nanomaterials (PAMAM dendrimers, PNIPAM and NIPAM/BAM copolymer nanoparticles), there is an increasing need for information regarding the human health and environmental implications of exposure to these polymeric nanomaterials. The structurally well defined and variable macromolecules can also provide a further basis upon which to establish structure activity relationships governing eco and mammalian-toxicological responses which may serve to develop a fundamental understanding of their interactions and as guidelines for the future prediction of responses. However, the field of eco-(nano) toxicology is still relatively new and there is a dearth of quantitative structure activity relationships established for nanomaterials.

To date, little is known about the metabolism and excretion, ecotoxicity and *in vitro* mammalian toxicity for the case of PNIPAM and the NIPAM/BAM series of NPs. These particles were chosen under the INSPIRE collaborative programme as model particles due to their variable physico-chemical properties. For the case of the PAMAM dendrimers, no complete ecotoxicity data set is available, although a recent study has explored the toxicity of PAMAM dendrimers (G 3.5 and G-4) in a zebra fish embryo model (Heiden, et al., 2007). In this study, ecotoxicological assessment is performed in a range of fresh water ecological organisms, constituting a multi-trophic model ecosystem. In comparison, there are several reports on the mammalian toxicity of PAMAM dendrimers. They have been shown to reduce the transmembrane potential and hinder the influx of Ca^{2+} ions to the mitochondria (Labieniec and Gabryelak 2008). Mitochondrial Ca^{2+} overload in combination with oxidative stress and ATP depletion

induces mitochondrial permeability which results in ischemia reperfusion, oxidative stress and apoptosis (Vergun and Reynolds, 2005). The toxicity of PAMAM dendrimers in mammalian cells has been demonstrated to depend upon the generation and surface functional groups (Roberts et al., 1996; Malik et al., 2000). They have been shown to induce membrane disruption, including the formation of holes and membrane erosion in supported lipid bilayers (Leroueil et al., 2007 and 2008; Hong et al., 2004). A recent study shows that the pathway of the toxic response induced by PAMAM dendrimers is by apoptosis mediated by mitochondrial dysfunction. (Lee et al., 2009). However, despite their proposed applications, the pharmacokinetics i.e ADME (Absorption, Distribution, Metabolism and Excretion) of PAMAM dendrimers is still unclear.

PAMAM dendrimers are chemically stable and soluble in water, and thus it can reasonably be expected that they will remain in an intact form in the environment, at least in the earlier stages. In order to assess the potential environmental and human impact of these materials, a systematic battery of bioassays representing multitrophic levels of a fresh water ecosystem was employed for the ecotoxicological study, while *in vitro* cell models were employed for the mammalian toxicological study.

In this study, ecotoxicological assessment of nanoparticles is probed using various aquatic species representing the different trophic levels (decomposer, primary producer, invertebrates and vertebrates), as shown in figure 1.3. Assessment of the toxicological response to nanoparticle exposure of all the fresh water ecological test models is carried out according to international guide lines, described in section 2.2.2, of chapter 2. In brief, *Vibrio fischeri* is a marine bacterium which acts as a decomposer; *Pseudokirchneriella subcapitata* acts as a primary producer; *Thamnocephalus platyurus*

and *Daphnia magna* act as primary consumers, and fish act as a secondary consumer. Together, they represent the different trophic levels of a fresh water ecosystem.

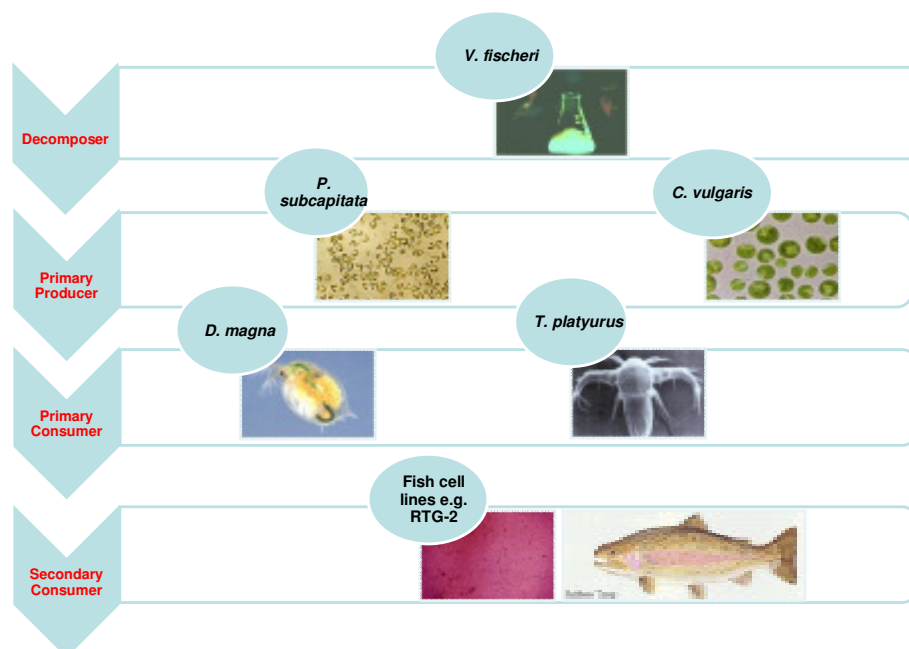


Figure 1.3. Fresh water ecosystem representing different trophic levels.

The test models employed in this study were selected for a number of reasons. As no individual test will have a universal sensitivity to all toxicants a ‘battery’ of tests was used to provide an accurate assessment of the potential ecotoxicity of the test compound. The test battery included bacteria, a protozoan, algae, an invertebrate and fish cell lines. The test models are routinely used in our laboratory and others (Zurita et al., 2007), and have well established standardised protocols. The tests are also low cost and require small volumes of sample in comparison to whole organism tests (e.g. *in vivo* acute lethality test with fish). Both of these factors are important to take into consideration when screening nanomaterials, as most nanomaterials are available in only small quantities (when compared to their bulk counterparts) and are normally significantly more expensive to obtain.

In accordance with the EU policy of Reduction, Replacement and Refinement (RRR), *in vitro* models rather than animal studies have been employed to explore the cytotoxicity of these materials. (Directive 86/609/EEC on the protection of animals used for experimental and scientific purposes). The fish cells lines were chosen to represent a vertebrate model and have the advantage of requiring the smallest volume of sample when compared to the other test models. Both cells lines have routinely been used for the assessment of toxic effects of chemicals and evaluation of environmental samples in our laboratory and it has been found that *in vitro* cytotoxicity is positively correlated with acute toxicity *in vivo*. (Fent, 2001; Davoren and Fogarty. 2006). The RTG-2 cell line, derived from the Rainbow trout, has direct environmental relevance to an Irish freshwater system. The PLHC-1 cell line was chosen to test alongside, as it has been shown to have increased sensitivity to toxicants compared to the RTG-2 cell line and while this particular species is not as environmentally relevant its inclusion does allow a comparison of different test species and different fish organs.

For the mammalian study, three different cell lines have been selected for the toxicological evaluation. In the case of PNIPAM nanoparticles, HaCaT (Skin model) and SW480 (intestinal model) cell lines were chosen, to compare the *in vitro* toxicity profile of the nanoparticles. These two cells are isolated from the different organs of the human, and also have different morphology, metabolism and also antioxidant defence mechanisms. The choice of skin and intestinal cell models is also influenced by proposed applications of polymeric nanoparticles for drug delivery, likely to be applied transdermally or by ingestion.

In the case of PAMAM dendrimers, the immunotoxicity was investigated in mouse macrophages, as several studies have shown that N-acetyl-D-glucosamine modified

PAMAM dendrimers improve the immunogenicity by up-regulation of antibody formation via activation of natural killer cells (Hulikova et al., 2009) and the mannosylated form of PAMAM dendrimers potentiate the immunogenicity and have been proposed for vaccine delivery systems (Sheng et al., 2008) and also employed for the intracellular drug and gene delivery system.

When nanoparticles enter into the bloodstream, they immediately encounter a complex environment of plasma proteins and immune cells. The interaction of nanoparticles with immune cells may occur both in the blood stream via monocytes, platelets, leukocytes, and dendritic cells (DC) and in tissues by resident phagocytes, e.g., Kupffer cells in liver, DC in lymph nodes, macrophages and B cells in the spleen (Dobrovolskaia et al., 2008). As PAMAM dendrimers are potentially proposed for vaccine and intracellular gene delivery applications, and macrophages are the main target cells to produce/improve the immunogenicity of the different antigens, this study explores the understanding of the interaction with and toxicity to macrophages cells of PAMAM (G-4, G-5 and G-6) dendrimers. J774A.1 cells, derived from the blood of female BALB/c mouse, are chosen for the *in vitro* model.

For each toxicological evaluation, a range finding study was performed to establish the dose range resulting in a mortality/toxicity between 10 % - 90 %, allowing the calculation of EC_{50}/LD_{50} . The calculated EC_{50} s indicate that the materials are at most mildly toxic.

In the cases of the PNIPAM and NIPAM/BAM series of nanoparticles, concentrations employed were based on extensive range finding tests which revealed the PNIPAM and NIPAM/BAM copolymers to have low acute toxicity to the chosen battery of test species. However, the results are of merit as there is currently no ecotoxicity data available for these nanoparticles and these results therefore address this lack of

environmental data by providing acute toxicity data (5 min – 72 h) for these nanoparticles to a range of test models.

In the case of PAMAM dendrimers, intracellular ROS generation, concentrations were kept constant (0.031 to 3 μ M of PAMAM dendrimers) for the three generations of PAMAM dendrimers to observe any generation dependent ROS production. In the case of cytokine production, concentrations were chosen (for G-4 - 0.08 to 6 μ M; for G-5 - 0.03 to 2 μ M; and for G-6 - 0.013 to 1 μ M) on the basis of the cytotoxicity assay, to establish the point of maximum production of TNF- α , MIP-2 and IL-6.

Furthermore, the concentration range selected for the dendrimers is of therapeutic relevance for their potential applications, according to the study of Kukowska-Latallo et al., 2005, which indicated that the therapeutically relevant concentrations are $\leq 3 \mu$ M.

Potentially the greatest value of the study, independent of relevance of dose, is the emphasis on relating the observed responses to the systematically varied physico-chemical properties of the two polymer nanoparticle series. In this field, establishing structure activity relationships upon which a greater understanding of relevant materials parameters is of critical importance.

For the ecotoxicity study, the endpoints are the inhibition of *Vibrio fischeri*, growth inhibition of *Pseudokirchneriella subcapitata*, immobilisation of *Daphnia magna*, mortality of *Thamnocephallus platyurus*, and cytotoxicity of RTG-2 and PLHC-1 cells. In the case of mammalian toxicity, *in vitro* cytotoxicity assessment was investigated in HaCaT, SW480 and J774A.1 cells.

The aim of the present investigation was thus the particle characterisation, and toxicological assessment (of both environmental and human effects) of these polymeric nanomaterials. PNIPAM and NIPAM/BAM (Poly N-isopropylacrylamide and N-isopropylacrylamide-co-N-tert-butylacrylamide) copolymer nanoparticles (provided by

University College Dublin under the Integrated NanoScience Platform for Ireland (<http://www.inspirenano.ie/>) and the commercially available PAMAM (Polyamidoamine) dendrimers (G4, G5 and G6) were chosen. Variation of the copolymerisation ratio from 100% PNIPAM through NIPAM/BAM 85:15, NIPAM/BAM 65:35 and NIPAM/BAM 50:50 allowed a systematic variation of the surface chemistry which manifested as changes in the zeta potential, facilitating the establishment of structure-activity relationships. In the case of the PAMAM dendrimers, the surface chemistry was kept constant, while the size, molecular weight and number of surface primary amino groups were systematically varied. Particle characterisation, in terms of hydrodynamic diameter, zeta potential and specific surface area (BET) measurement was performed. Since PNIPAM and NIPAM/BAM nanoparticles are thermosensitive, the particle size was measured as a function of temperature. The prime aim of the thesis was to elucidate and understand correlations between the physicochemical properties and the observed toxicological responses, followed by the underlying mechanism of the toxicity due to these nanomaterials.

Investigation of the acute ecotoxicological effects of PNIPAM and NIPAM/BAM copolymer particles and PAMAM dendrimers (G4, G5 and G6) was conducted using a battery of bioassays representing different trophic levels. The tests employed included a bacterial species, a unicellular algae species and two crustaceans. In addition, the cytotoxicity of PNIPAM, and NIPAM/BAM (85:15) copolymer particles and PAMAM dendrimers (G4, G5 and G6) was investigated in two fish cell lines. UV/visible spectroscopic analysis of PAMAM dendrimers (G4, G5 and G6) in two different cell culture media was performed to investigate any potential changes to the effective medium composition which could contribute to an indirect or secondary toxicity. The

intracellular reactive oxygen species (ROS), genotoxicity, DNA adduct (8-OHdG), apoptosis assay was performed to understand the underlying mechanism of toxicity upon the exposure of PAMAM dendrimers in PLHC-1 cells.

The mammalian toxicological assessment of PNIPAM nanoparticles was carried out in human skin and gastrointestinal cell lines. The uptake and co-localisation study was performed using fluorescently labelled nanoparticles. The geno-toxicological assessment was performed using the alkaline comet assay in both the cell lines, to understand the fate, biodistribution, biocompatibility/cytotoxicological response to the PNIPAM nanoparticles. Due to the lower LCST of the copolymer nanoparticles (NIPAM/BAM 85:15, NIPAM/BAM 65:35, NIPAM/BAM 50:50 are 25°C, 17°C and 12°C respectively) it was not possible to assess their toxicity in the mammalian cell culture systems (37°C).

Due to potential applications in intracellular drug, gene and also in vaccine delivery system, the immunotoxicity assessment of PAMAM dendrimers was performed in a mouse macrophage cell line (J774A.1 cells). This was followed by the cytotoxicological assessment, and the generation of intracellular reactive oxygen species (ROS), and the inflammatory markers IL-6 (Interleukin-6), TNF- α (Tumour necrosis factor alpha) and MIP-2 (Macrophage inflammatory protein-2) were monitored to understand the origin of the toxic response by the PAMAM dendrimer in these cells.

In the case of the PAMAM dendrimers, by keeping the surface chemistry (functional group) constant while increasing the molecular weight, and consequently the number of surface amino groups and the particle surface area, a systematic variation of toxic response was observed. As the generation increases the toxic responses increases. Also, in the case of PNIPAM and NIPAM/BAM copolymer nanoparticles, a clear structurally dependent toxic response has been observed. However the PNIPAM nanoparticles show

excellent biocompatibility to the mammalian cells. The systematic increase in the intracellular reactive oxygen species (ROS), inflammatory markers (IL-6, TNF- α , and MIP-2), genotoxicity and apoptosis was observed with the increase in generation of PAMAM dendrimers. By systemically changing the surface chemistry and particle size, the foundations of structure activity relationships determining the toxic response have been established.

The study aims to identify and elucidate the underlying mechanisms of biological responses which vary systematically as a function of the systematically varied physico-chemical properties of the polymeric nanoparticles. Such empirical or qualitative correlations may lay the foundation of quantitative structure-activity relationships. As such, although it can have specific quantitative meaning in a statistical context, the concept of correlation is evoked throughout this work in a purely qualitative context.

References

- Baun, A., Sorensen, S.N., Rasmussen, R.F., Hartmann, N.B., Koch, C.B., 2008. Toxicity and bioaccumulation of xenobiotic organic compounds in the presence of aqueous suspensions of aggregates of nano-C₆₀. *Aquat. Toxicol.* 86, 379-387.
- Brown, D. M., Donaldson, K., Borm, P. J., Schins, R. P., Dehnhardt, P., Gilmour, M., Jimenez, L. A., Stone, V. 2004. Calcium and ROS-mediated activation of transcription factors and TNF- α cytokine gene expression in macrophages exposed to ultrafine particles. *Am. J. Physiol. Lung Cell. Mol. Physiol.* 286, 344-353.
- Brown, D. M., Wilson, M. R., MacNee, W., Stone, V., Donaldson, K. 2001. Size-Dependent Proinflammatory Effects of Ultrafine Polystyrene Particles: A Role for Surface Area and Oxidative Stress in the Enhanced Activity of Ultrafines. *Toxicology and Applied Pharmacology*, 175, 191–199.
- Cabaleiro-Lago, C., Quinlan-Pluck, F., Lynch, I., Lindman, S., Minogue, A.M., Thulin, E., Walsh, D.M., Dawson, K.A., Linse, S. 2008. Inhibition of amyloid β protein fibrillation by polymeric nanoparticles. *JACS*, 19; 15437-43.
- Cedervall, T., Lynch, I., Foy, M., Berggård, T., Donnelly, S.C., Cagney, G., Linse, S., Dawson, K.A., 2007. Detailed identification of plasma proteins adsorbed on copolymer nanoparticles. *Angew. Chem. Int. Ed. Engl.* 46, 5754-5756.
- Cheng, J., Flahaut, E., Cheng, S.H., 2007. Effect of carbon nanotubes on developing zebrafish (*Danio rerio*) embryos. *Environmental Toxicology and Chemistry*. 26, 708-716.
- Cheng, Y., Xu, Z., Ma, M., Xu, T. 2008. Dendrimers as drug carrier: applications in different routes of drug administration. *J. Pharm. Sci.* 97, 123-143.

-
- Colvin, V. L. 2003. The potential environmental impact of engineered nanomaterials. *Nat. Biotechnol.* 21, 1166–70.
- Davoren, M., Herzog, E., Casey, A., Cottineau, B., Chambers, G., Byrne, H.J., Lyng, F.M. 2007. *In vitro* toxicity evaluation of single walled carbon nanotubes on human A549 lung cells. *Toxicol In vitro*, 21, 438-48.
- Davoren, M. and Fogarty, A.M. 2006. *In vitro* cytotoxicity assessment of the biocidal agents sodium o-phenylphenol, sodium o-benzyl-p-chlorophenol, and sodium p-tertiary amyphenol using established fish cell lines. *Toxicology in vitro*, 7, 1190-1201.
- Dendritech, Inc. <http://www.dendritech.com/pamam.html>, accessed on 16th June 2009.
- Dobrovolskaia, M.A., McNeil, S.C., 2007, Immunological properties of engineered nanomaterials. *Nat. Nanotechnol.* 2, 469-478.
- Duncan, R., Izzo, L. 2005. Dendrimer biocompatibility and toxicity. *Adv. Drug Delivery Rev.* 57, 2215–2237
- Emanuele, A. D., Attwood, D. 2005. Dendrimer-drug interactions. *Adv. Drug Delivery Rev.* 57, 2147–2162.
- Federici, G., Shaw, B.J., Handy, R.D., 2007. Toxicity of titanium dioxide nanoparticles to rainbow trout (*Oncorhynchus mykiss*): Gill injury, oxidative stress, and other physiological effects. *Aquat. Toxicol.* 84, 415-430.
- Fent, K. 2001. Fish cell lines as versatile tools in ecotoxicology: assessment of cytotoxicity, cytochrome P4501A induction potential and estrogenic activity of chemicals and environmental samples *Toxicology in vitro*, 15, 477-488.

- Gagné, F., Auclair, J., Turcotte, P., Fournier, M., Gagnon, C., Sauve, S., Blaise, C., 2008. Ecotoxicity of CdTe quantum dots to fresh water mussels: Impacts on immune system, oxidative stress and genotoxicity. *Aquat. Toxicol.* 86, 333-340.
- Gillies, E.R., Frechet, J.M.J. 2005. Dendrimers and dendritic polymers in drug delivery. *Drug Discovery Today* 10, 35-43.
- Garland, A. 2009. The Global market for carbon nanotubes to 2015: (<http://www.nanoposts.com/indx.php?mod=nanotube> accessed on 20th March 2011).
- Gillies, E.R., Frechet, J.M.J. 2005. Dendrimers and dendritic polymers in drug delivery. *Drug Discovery Today* 10, 35-43.
- Heiden, T. C., Dengler, E., Kao, W. J., Heideman, W., Peterson, R. E. 2007. Developmental toxicity of low generation PAMAM dendrimers in zebrafish. *Toxicol Appl Pharmacol.* 225, 70-79.
- Heinlaan, M., Ivask, A., Blinova, I., Dubourguier, H.C., Kahru, A., 2008. Toxicity of nanosized and bulk ZnO, CuO and TiO₂ to bacteria *Vibrio fischeri* and crustaceans *Daphnia magna* and *Thamnocephalus platyurus*. *Chemosphere.* 71, 1308-1316.
- Herzog, E., Casey, A., Lyng, F.M., Chambers, G., Byrne, H. J., Davoren, M. 2007. A new approach to the toxicity testing of carbon-based nanomaterials--the clonogenic assay. *Toxicol Lett.* 2007, 174, 49-60.
- Hong, S. P., Bielinska, A. U., Mecke, A., Keszler, B., Beals, J. L., Shi, X. Y., Balogh, L., Orr, B. G., Baker, J. R., Holl, M. M. B. 2004. Interaction of poly(amidoamine) dendrimers with supported lipid bilayers and cells: hole formation and the relation to transport. *Bioconjugate Chem.* 15, 774-782.

- Hsiue, G. H., Chang, R. W., Wang, C. H., Lee, S. H. 2003. Development of in situ thermosensitive drug vehicles for glaucoma therapy. *Biomaterials*, 24, 2423-30.
- Hsiue, G. H., Hsu, S. H., Yang, C. C., Lee, S. H., Yang, I. K. 2002. Preparation of controlled release ophthalmic drops, for glaucoma therapy using thermosensitive poly-N-isopropylacrylamide. *Biomaterials* 23, 457-62.
- Huang, R.Q., Qu, Y.H., Ke, W.L., Zhu, J.H., Pei, Y.Y., Jiang, C. 2007. Efficient gene delivery targeted to brain using a transferrin conjugated polyethylene glycol modified polyamidoamine dendrimer. *FASEB J.* 21, 1117-1125.
- Hulikova, K., Benson, V., Svoboda, J., Sima, P., Fiserova, A. 2009. N-Acetyl-D-glucosamine-coated polyamidoamine dendrimer modulates antibody formation via natural killer cell activation. *International Immunopharmacology* 9, 792–799.
- Ito, F., Fujimori, H., Honnami, H., Kawakami, H., Kanamura, K., Makino, K. 2008. Effect of polyethylene glycol on preparation of rifampicin-loaded PLGA microspheres with membrane emulsification technique. *Colloids Surf B Biointerfaces* 66, 65-70.
- Jaroenworarluck, A., Sunsaneeyametha, W., Kosachan, N., Stevens, R. 2006. Characteristics of silica coated TiO₂ and its UV absorption for sunscreen cosmetics applications. *Surface and Interface Analysis*, 38, 473-477.
- Jeng, H. A., Swanson, J. 2006. Toxicity of Metal Oxide Nanoparticles in Mammalian Cells. *J. Environ. Sci. Health A.* 41, 2699–2711
- Kang, H., De-Long, R., Fisher, MH., Juliano, R.L. 2005. Tat-conjugated PAMAM Dendrimers as delivery agents for antisense and siRNA oligonucleotides. *Pharmaceutical research* 22, 2099-2106.

- Kavanagh, C.A., Gorelova, T.A., Selezneva, I.I., Rochev, Y.A., Dawson, K.A., Gallagher, W.M., Gorelov, A.V., Keenan, A.K. 2005. Poly(N-isopropylacrylamide) copolymer films as vehicles for the sustained delivery of proteins to vascular endothelial cells. *J. Biomed. Mater. Res. A.* 72, 25-35.
- Kukowska-Latallo, J.F., Candido, K.A., Cao, Z., Nigavekar, S.S., Majoros, I.J., Thomas, T.P., Balogh, L.P., Khan, M.K., Baker, J.R. 2005. Nanoparticle targeting of anticancer drug improves therapeutic response in animal model of human epithelial cancer. *Cancer Res.* 65, 5317-24.
- Labieniec, M., Gabryelak, T. 2008. Preliminary biological evaluation of poli(amidoamine) (PAMAM) dendrimer G3.5 on selected parameters of rat liver mitochondria. *Mitochondrion*, 8, 305–312
- Lee, J.H., Cha, K.E., Kim, M.S., Hong, H.W., Chung, D.J., Ryu, G., Myung, H. 2009. Nanosized polyamidoamine (PAMAM) dendrimer-induced apoptosis mediated by mitochondrial dysfunction. *Toxicol Lett.* 190 , 202–207.
- Lee, C.C., MacKay, J.A., Frechet, J.M.J., Szoka, F.C., 2005. Designing dendrimers for biological applications. *Nat. Biotechnol.* 23, 1517–1526.
- Leroueil, P. R., Berry, S. A., Duthie, K., Han, G., Rotello, V. M., McNerny, D. Q., Baker, J. R., Orr, B. G., Holl, M. M. B. 2008. Wide varieties of cationic nanoparticles induce defects in supported lipid bilayers. *Nano Letters.* 8, 420-424.
- Leroueil, P. R., Hong, S. Y., Mecke, A., Baker, J. R., Orr, B. G., Holl, M. M. B. 2007. Nanoparticle interaction with biological membranes: Does nanotechnology present a janus face? *Acc. Chem. Res.* 40, 335-342.
- Lin, C. C., and Metters. A. T. 2006. Hydrogels in controlled release formulations: network design and mathematical modeling. *Adv Drug Deliv Rev* 58, 1379-408.

-
- Lin, D., Xing, B., 2007. Phytotoxicity of nanoparticles: Inhibition of seed germination and root growth. *Environ. Pollut.* 150, 243-50.
- Lovern, S.B., Klaper, R., 2006. *Daphnia magna* mortality when exposed to titanium dioxide and fullerene (C₆₀) nanoparticles. *Environmental Toxicology and Chemistry*. 25, 1132-1137.
- Lovern, S.B., Strickler J.R., Klaper, R., 2007. Behavioral and physiological changes in *Daphnia magna* when exposed to nanoparticle suspensions (titanium dioxide, nano-C60, and C60HxC70Hx). *Environ. Sci. Technol.* 41, 4465-7.
- Lubick, N. 2009. Promising Green Nanomaterials. *Environ. Sci. Technol.* 43, 1247–1249
- Lux Research 2008. Nanomaterial state of the market Q3 2008: Stealth success, Board Impact, LRNI-SMR-08-01, Lux Research, New York, US.
- Lynch, I., Blute, I.A., Zhmud, B., MacArtain, P., Tosetto, M., Allen, L.T., Byrne, H.J., Farrell, G.F., Keenan, A.K., Gallagher, W.M., Dawson, K.A. 2005. Correlation of the Adhesive Properties of Cells to *N*-Isopropylacrylamide/*N*-*tert*-Butylacrylamide Copolymer Surfaces with Changes in Surface Structure Using Contact Angle Measurements, Molecular Simulations, and Raman Spectroscopy. *Chem. Mater.* 17, 3889 - 3898.
- Maeda, H., Matsumura, Y. 1986. A new concept on macromolecular therapeutics in cancer chemotherapy: mechanism of tumouritropic accumulation of proteins and the antitumour agents SMANCS. *Cancer Res.* 46, 6387-6392.
- Malik, N., Wiwattanapatapee, R., Klopsch, R., Lorenz, K., Frey, H., Weener, J. W., Meijer, E. W., Paulus, W., Duncan, R. 2000. Dendrimers: relationship between structure and biocompatibility *in vitro*, and preliminary studies in the biodistribution

- of 125I-labelled polyamidoamine dendrimers *in vivo*. Journal of Controlled Release. 65, 133-148.
- Meng, H., Chen, Z., Xing, G., Yuan, H., Chen, C., Zhao, F., Zhang, C., Zhao, Y., 2007. Ultrahigh reactivity provokes nanotoxicity: Explanation of oral toxicity of nano-copper particles. Toxicology Letters, 175, 102-110
- Mortimer, M., Kasemets, K., Heinlaan, M., Kurvet, I., Kahru, A., 2008. High throughput kinetic *Vibrio fischeri* bioluminescence inhibition assay for study of toxic effects of nanoparticles. Toxicol. In Vitro, 22, 1412-1417.
- Muller, N. C and Nowack B. 2008. Exposure modelling of engineered nanoparticles to the environment. Environ. Sci Technol. 42, 4447-4453.
- Naha, P. C., Kanchan, V., Manna, P. K., and Panda. A. K. 2008. Improved bioavailability of orally delivered insulin using Eudragit-L30D coated PLGA microparticles. J Microencapsul. 25 , 248-56.
- Naha, P. C., Kanchan, V., and A. K. Panda. 2009a. Evaluation of parenteral depot insulin formulation using PLGA and PLA microparticles. J Biomater Appl. 24, 309-25.
- Nel, A.E., Mädler, L., Velegol, D., Xia, T., Hoek, E.M.V., Somasundaran, P., Klaessig, F., Castranova V., and Thompson, M. 2009. Understanding biophysicochemical interactions at the nano-bio interface. Nature materials, 8, 543-557.
- Nel, A., Xia, T., Madler, L., Li, N. 2006. Toxic potential of materials at the nanolevel. Science 311, 622-7.
- Nowack, B., Bucheli, T.D., 2007. Occurrence, behavior and effects of nanoparticles in the environment. Environmental Pollution. 150, 5-22.

- Peppas, N. A., Bures, P., Leobandung, W., Ichikawa, H., 2000. Hydrogels in pharmaceutical formulations. *Eur J Pharm Biopharm* 50, 27-46.
- Perinotto, A. C., Caseli, L., Hayasaka, C. O., Riul, A., Oliveira, O. N., Zucolotto, V. 2008. Dendrimer-assisted immobilization of alcohol dehydrogenase in nanostructured films for biosensing: Ethanol detection using electrical capacitance measurements, *Thin Solid Films*, 516, 9002–9005.
- Rajananthanan, P., Attard, G. S., Sheikh, N. A., Morrow, W. J. 1999. Evaluation of novel aggregate structures as adjuvants: composition, toxicity studies and humoral responses. *Vaccine* 17, 715–730.
- Risom, L., Moller, P., Loft, S. 2005. Oxidative stress-induced DNA damage by particulate air pollution. *Mutat Res.* 592, 119-137.
- Rothschild, A., Cohen, S.R., Tenne, R. 1999. WS2 nanotube as tips in scanning probe microscopy, *Applied Physics Letters*, 25, 4025-4027.
- Roberts, J. C., Bhalgat, M. K., Zera, R. T. 1996. Preliminary biological evaluation of polyamidoamine (PAMAM) Starburst™ dendrimers. *J. Biomed. Material Research*, 30, 53-65.
- Sheng, K. C., Kalkanidis, M., Pouniotis, D.S., Esparon, S., Tang, C.K., Apostolopoulos, V., Geoffrey, A., Pietersz, G.A. 2008. Delivery of antigen using a novel mannosylated dendrimer potentiates immunogenicity *in vitro* and *in vivo* *Eur. J. Immunol.* 38, 424–436.
- Smith, C.J., Shaw, B.J., Handy, R.D., 2007. Toxicity of single walled carbon nanotubes to rainbow trout, (*Oncorhynchus mykiss*): respiratory toxicity, organ pathologies, and other physiological effects. *Aquat. Toxicol.* 82, 94-109.
- Storrie, H., Mooney, D. J., 2006. Sustained delivery of plasmid DNA from polymeric scaffolds for tissue engineering. *Adv. Drug. Del. Rev.* 58, 500-514.

- Stoeger, T., Takenaka, S., Frankenberger, B., Ritter, B., Karg, E., Maier, K., Schulz, H., Schmid O. 2009. Deducing *in vivo* Toxicity of Combustion-Derived Nanoparticles from a Cell-Free Oxidative Potency Assay and Metabolic Activation of Organic Compounds. *Environmental Health Perspectives*, 117, 54-60.
- Svenson, S., Tomalia, D. A. 2005. Dendrimers in biomedical applications-reflections on the field. *Adv. Drug Delivery Rev.* 57, 2106–2129.
- Venuganti, V. V. K., Perumal, O. P. 2008. Effect of Poly(amidoamine) (PAMAM) dendrimer on skin permeation of 5-fluorouracil. *Int. J. Pharm.* 361, 230–238.
- Vergun, O., Reynolds, I. J. 2005. Distinct characteristics of Ca²⁺ induced depolarization of isolated brain and liver mitochondria. *Biochim. Biophys. Acta.* 1709, 127–137.
- Vevers, W.F., Jha, A.N. 2008. Genotoxic and cytotoxic potential of titanium dioxide nanoparticles on fish cell *in vitro*. *Ecotoxicology*, 17, 410-420.
- Wang, J., Liu, Y., Jiao, F., Lao, F., Li, W., Gu, Y., Li, Y., Ge, C., Zhou, G., Li, B., Zhao, Y., Chai, Z., Chen, C. 2008. Time-dependent translocation and potential impairment on central nervous system by intranasally instilled TiO₂ nanoparticles. *Toxicology*. 254, 82-90.
- Xia, T., Kovoichich, M., Brant, J., Hotze, M., Sempf, J., Oberley, T., Sioutas, C., Yeh, J. I., Wiesner, M. R., Nel, A. E. 2006. Comparison of the Abilities of Ambient and Manufactured Nanoparticles to Induce Cellular Toxicity According to an Oxidative Stress Paradigm. *Nano Lett.* 6, 1794–1807.
- Xu, F.J., Kang, E.T., Neoh, K.G., 2006. pH and temperature responsive hydrogel from crosslinked triblock copolymers prepared via consecutive atom transfer radical polymerization. *Biomaterials*. 27, 2787-2797.

- Xu, F.Z., Zhong, S.P., Yung, L.Y.L., Kang, E.T., Neoh, K.G., 2004. Surface-active and stimuli-response polymer-Si(100) hybrid from surface-initiated atom transfer radical polymerization for control of cell adhesion. *Biomacromolecules*. 5, 2392-2403.
- Xu, Y. H., Zhao, D.Y. 2005. Removal of copper from contaminated soil by use of poly(amidoamine) dendrimers. *Environ. Sci. Technol.* 39, 2369-2375
- Xu, Y. H., Zhao, D. Y. 2006. Removal of lead from contaminated soils using poly(amidoamine) dendrimers. *Ind. Eng. Chem. Res.* 45, 1758-1765
- Yoo, H., Juliano, R.L. 2000. Enhanced delivery of antisense oligonucleotides with fluorophore-conjugated PAMAM dendrimers. *Nucleic acid Research*. 28, 4225-4231.
- Yang, Y., Gupta, M.C., Dudley, K.L. 2007. Studies on electromagnetic interference shielding characteristics of metal nanoparticles and carbon nanostructure field polymer composites in the Ku-band frequency. *Micro and Nano Letters*, 2, 85-89.
- Yoo, H., Juliano, R.L. 2000. Enhanced delivery of antisense oligonucleotides with fluorophore-conjugated PAMAM dendrimers. *Nucleic acid Research*. 28, 4225-4231.
- Zhang, J., Misra, R.D.K. 2007. Magnetic drug-targeting carrier encapsulated with thermosensitive smart polymer: Core-shell nanoparticle carrier and drug release response. *Acta Biomaterialia* 3, 838-850
- Zhang, X.Z., Lewis, P.J., Chu, C.C., 2005. Fabrication and characterization of a smart drug delivery system: microsphere in hydrogel. *Biomaterials*. 26, 3299-3309.
- Zhu, Y., Zhao, Q., Li, Y., Cai, X., Li, W., 2006. The interaction and toxicity of multi-walled carbon nanotubes with *Stylonychia mytilus*. *J. Nanosci. Nanotechnol.* 6, 1357-1364.

Zurita, J. L., Repetto, G., Jos, A., Salguero, M., López-Artíguez, M., Cameán, A. M.
2007. Toxicological effects of the lipid regulator gemfibrozil in four aquatic
systems *Aquatic Toxicology*, 2007, 81, 106-115.

Chapter 2

Materials and Experimental protocols

2. Materials and Experimental protocols

2.1 Materials

2.1.1 PNIPAM and NIPAM/BAM co-polymer nanoparticles

Poly *N*-isopropylacrylamide (PNIPAM) and *N*-isopropylacrylamide-co-*N*-*tert*-butylacrylamide (NIPAM/BAM) copolymer particles with systematically varied ratios of the respective monomers (85:15, 65:35, and 50:50 NIPAM/BAM) were synthesised by the staff of University College Dublin through the “Integrated NanoScience Platform for Ireland” collaborative programme (www.inspirenano.ie). They were synthesised by free radical polymerisation (Cedervall, et al., 2007). The synthesis procedures for both labelled and unlabelled particles are given in Appendix-1.

2.1.2 PAMAM (Poly amidoamine) dendrimers

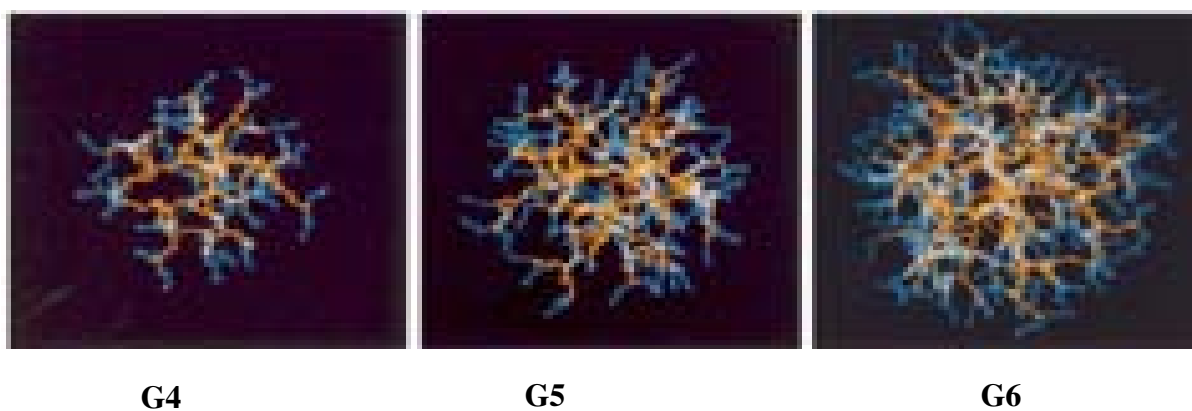


Figure 2.1 : PAMAM dendrimer G4 , G5 and G6 (Svenson and Tomalia. 2005, Advance Drug Delivery Review, 57, 2106-2129.)

Polyamidoamine (PAMAM) dendrimers G4, G5 and G6 (Figure 2.1) having an ethylenediamine core (StarburstTM, Dendritech Inc.) were purchased from Sigma-Aldrich (Ireland). The average molecular weight of G4, G5 and G6 is 14,215, 28,825

and 58,048 and they contain 64, 128 and 256 surface amino groups respectively (www.dendritech.com, accessed on 16th June 2009).

2.2 Experimental protocol

2.2.1 Particle Characterisation

2.2.1.1 Particle size measurement

Dynamic Light Scattering (DLS) is commonly employed for the measurement of the particle size and size distribution of particles and molecules dispersed or dissolved in a liquid. The scattered intensities undergo random fluctuations due to the Brownian motion of the particles in suspension and analysis of these fluctuation yields the particle size distribution. The relevant diameter that is measured in DLS is the hydrodynamic diameter and refers to how a particle diffuses within a fluid. The basic construction of the dynamic light scattering instrument is shown in figure 2.2.

The particle size distributions of PNIPAM and NIPAM/BAM copolymer nanoparticles in the appropriate assay media were analyzed using a Zeta sizer (Malvern Instruments, UK). For a typical experiment, approximately 1000 µg/ml suspensions of nanoparticles in MQ water and the respective assay media (*i.e.* algal medium [AM], *Daphnia* medium [DM] and Microtox[®] diluent [MD]) were analysed as a function of temperature from 0°C to 30°C with an interval of 5°C due to the thermoresponsive nature of these particles. The hydrodynamic diameter of PNIPAM nanoparticles was measured in the cell culture media as a function of temperature from 30 to 38 °C, as the mammalian cells are grown at 37 °C, to understand the behaviour of these particles in the appropriate experimental conditions. 1000 µg/ml is the highest concentration used for the ecotoxicity study, as identified by the initial range finding tests. Agglomeration is

generally known to be a concentration dependent phenomenon, and thus this concentration represents the extreme agglomeration behaviour. To confirm this, PNIPAM nanoparticles were measured at concentrations of 100 $\mu\text{g/ml}$ and 1000 $\mu\text{g/ml}$ in the cell culture media for the mammalian toxicity assessment.

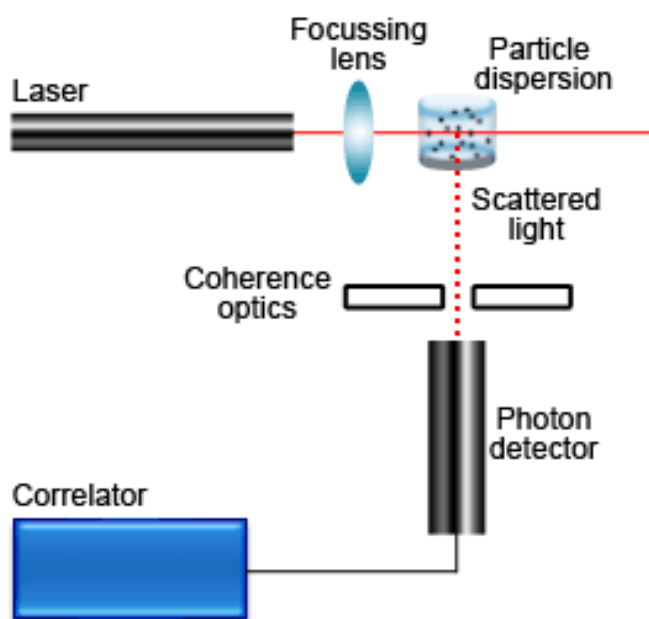


Figure 2.2. Schematic diagram of a conventional dynamic light scattering instrument. (http://www.malvern.com/LabEng/technology/dynamic_light_scattering/classical_90_degree_scattering.htm accessed on 16th June 2009).

In the case of PAMAM dendrimers, approximately 20 μM suspensions of dendrimer nanoparticles in the respective assay media DM, MD and *Thamnocephalus* medium (TM), and the cell culture medium, Dulbecco's Modified Medium Nutrient Mixture/F-12 Ham [DMEM], with 5% foetal calf serum (FCS) supplement (PLHC-1) and 10% serum supplement (RTG-2) were analysed at 20°C. The pH of the various test media, before and after exposure to G4, G5 and G6 dendrimers was measured using a HQ11d Single-Input pH meter (Hach Company, Colorado).

2.2.1.2 Zeta potential measurement

Zeta potential is used to determine the stability of a particle dispersion, as it is a measure of one of the main forces that governs inter-particle interactions. Zeta potential is measured by applying an electric field across the dispersion. Particles within the dispersion with a zeta potential will migrate toward the electrode of opposite charge with a velocity which depends on the interaction with the dispersion medium and is therefore proportional to the magnitude of the zeta potential (<http://www.malvern.jp> accessed on 16th June 2009). More precisely, it measures the potential across the electrical double layer which exists between the particle itself and the dispersion medium. It is commonly an indicator of hydrophilicity or surface charge.

The zeta potential of PNIPAM and NIPAM/BAM nanoparticles and PAMAM dendrimers was measured in the respective assay media using a Zeta sizer (Malvern Instruments, UK, Figure 2.3A). The zeta potential measurements of PNIPAM and NIPAM/BAM copolymer nanoparticles were conducted at 20 °C, using a concentration of 1000 µg/ml. In the case of PAMAM dendrimers, measurements were conducted at 20°C, using a 20 µM concentration.

2.2.1.3 Spectroscopic analysis

As it has previously been demonstrated that some nanoparticles can interact and bind with various molecular constituents of cell culture media (Casey et al., 2008), absorption spectroscopic analysis of each dendrimer in the different cell culture media (DMEM, RTG-2 and PLHC-1) was performed using a Perkin Elmer Lambda 900 UV/visible/NIR absorption spectrometer. Changes to the spectroscopic profile of the medium can result from changes to the effective composition of the medium due to

molecular adsorption to the particles. This may lead to secondary toxic effects due to medium depletion (Casey et al., 2008).

In the case of NIPAM/BAM 65:35 and NIPAM/BAM 50:50, large agglomerates are formed, and as a result, for both materials, large amounts of precipitated material is visually observed floating in the cell culture media. Thus, these two particles were deemed unsuitable for cytotoxicity assessment. PNIPAM and NIPAM/BAM 85:15 particles were well dispersed in the respective media, but were found to be nontoxic to the fish cells. Therefore the indirect toxicity by PNIPAM and NIPAM/BAM copolymer particles, due to medium depletion effect was not analysed.

2.2.1.4 Surface Area measurement

BET theory governs the physical adsorption of gas molecules on a solid surface and serves as the basis for an important analysis technique for the measurement of the specific surface area of a material. In 1938, Stephen Brunauer, Paul Hugh Emmett, and Edward Teller published an article about the BET theory (Brunauer et al., 1938) for the first time; “BET” consists of the first initials of their family names. The concept of the theory is an extension of the Langmuir theory, which is a theory for monolayer molecular adsorption, to multilayer adsorption with the following hypotheses: (a) gas molecules physically adsorb on a solid in layers infinitely; (b) there is no interaction between each adsorption layer; and (c) the Langmuir theory can be applied to each layer. BET surface area measurements of PNIPAM and NIPAM/BAM co-polymer nanoparticles were performed using a Gemini series surface area analyser (Micromeritics, USA) (Figure 2.4). For the experiment, approximately 0.5 g particles of each of the materials were degassed with helium gas at a constant temperature of 25 °C for two hours prior to surface area measurements being recorded. However, in the case of the PAMAM dendrimers it was not possible to measure BET surface area because

the dendrimers are supplied by the manufacturer in methanol (in suspension form) and for BET surface area measurement, powdered samples are required.

2.2.1.5 Transmission electron microscopy (TEM) study

In the case of PNIPAM particles, particle size was also determined by Electron Microscopy by the staff of UCD and the detailed procedure is described in Appendix-1.

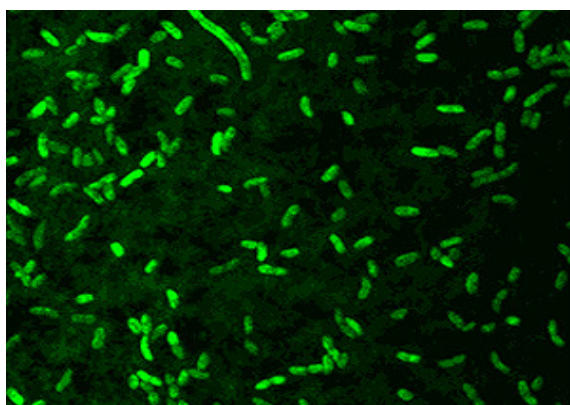
2.2.2 Ecotoxicity tests

Each ecotoxicity test was performed in two stages. A preliminary or range finding test was conducted which determined the range of concentrations of interest for the definitive test. The definitive test used a concentration range (at least five concentrations) in which effects were likely to occur, thereby permitting the calculation of the respective Effective Concentrations (EC_{50} is the concentration at which 50% effect was observed) or Lethal Concentrations (LC_{50} is the concentration at which 50% mortality was observed), No Observed Effect Concentration (NOEC), and Lowest Observed Effect Concentration (LOEC). The acute toxicity of each dendrimer was investigated in the four test systems representing different trophic levels. The cytotoxicity of the dendrimers was also evaluated in two fish cell lines, RTG-2 and PLHC-1, to represent vertebrate species. The details of each of the cell lines are given in sections 2.2.2.5.1 and 2.2.2.5.2, respectively.

2.2.2.1 Microtox[®] test

The acute toxicity of each dendrimer and NIPAM/BAM series of nanoparticles to the marine bacterium *Vibrio fischeri* was determined using the 90% basic test for aqueous extract protocol (Azur Environmental, 1998). Lyophilised *Vibrio fischeri* bacteria (NRRL B-11177) and all Microtox[®] reagents were obtained from SDI Europe,

Hampshire, UK. Phenol was used as a reference chemical and a basic test for phenol was run for every fresh vial of bacteria to ensure the validity of all tests. Readings of bioluminescent response were measured using a Microtox[®] Model 500 analyser (Figure 2.3) and the acute toxicity data was obtained and analysed using the Microtox Omni software (SDI Europe, Hampshire, UK). Five, fifteen and thirty minute EC₅₀ tests were performed.



Morphology of *Vibrio fischeri*

Figure 2.3. Morphology of *Vibrio fischeri* (<http://www.google.ie/images>, accessed on 16th June 2009).

In brief, phenol was used as positive control, in accordance with the manufacturer's instructions. Five concentrations of phenol (6.25, 12.5, 25 and 50 mg/l) were used. All concentrations of positive control and nanoparticles were dispersed in Microtox diluent (SDI, Europe). If the EC₅₀ (5 minutes exposure time) of the Phenol falls within the range 13 to 26 mg/l, then the bacteria are considered valid for performing the experiments (Azur Environmental, 1998). After the initial range finding study, (toxicity range from 10-90%) the concentration ranges for the nanoparticle exposures were chosen. In the case of the PNIPAM and NIPAM/BAM series of nanoparticles, the top concentration used was 1000 mg/l.

After the positive control experiments, the bacteria were exposed to nanoparticle suspensions of 9 different concentrations and the readings were taken at 5, 15 and 30 minutes after exposure. For PNIPAM and NIPAM/BAM nanoparticles, the top concentration of 1000 mg/l was serially diluted (1:2) with the Microtox diluents to produce the range of concentrations (900, 450, 225, 112.5, 56.25, 28.13, 14.06, 7.031 and 3.516 mg/l). For the case of PAMAM dendrimers, a maximum concentration of 50 μM for G4 was used to generate 1:2 serially diluted concentrations (50, 25, 12.5, 6.25, 3.125, 1.56, 0.78, 0.39, 0.19 μM). For G-5, the maximum concentration used was 25 μM , which was 1:2 serially diluted (25, 12.5, 6.25, 3.125, 1.56, 0.78, 0.39, 0.19, 0.097 μM). For G-6, the maximum concentration used was 12.5 μM , serially diluted to produce a similar range (12.5, 6.25, 3.125, 1.56, 0.78, 0.39, 0.19, 0.097, 0.048 μM). The end point is the determination of inhibition of luminescence of the bacteria after 5, 15 and 30 minutes exposure time.

2.2.2.2 Microalgae growth inhibition assay

Assessment of the acute toxicity of the materials to the freshwater algae *Pseudokirchneriella subcapitata* (Figure 2.6) was conducted in accordance with OECD Guideline 201 (2002). *Pseudokirchneriella subcapitata* CCAP 278/4 was obtained from the Culture Collection of Algae and Protozoa (CCAP) Argyll, Scotland. All microalgae growth inhibition tests were conducted at $20 \pm 1^\circ\text{C}$ with continuous shaking at 100 rpm and continuous illumination of 10,000 lx (OECD Guideline 201 (2002)). The initial algal density of all flasks was 1×10^4 cell ml^{-1} in a final volume of 20 ml. Negative controls were incorporated for each test containing only algal growth media and algal inoculum. The composition of the growth medium is described in table 2.1. The cell density of each replicate was measured after 72 h using a Neubauer Improved

(Bright-Line) chamber (Brand, Germany). The concentrations of PNIPAM and NIPAM/BAM nanoparticles studied were 10, 50, 100, 500 and 1000 mg/l. In brief, the experiments were carried out in 20 ml conical flasks. 10,000 algal cells were seed in each flask, whereupon they were exposed to the nanoparticles and the final volume was made up to 20 ml with Jaworskis Algal Media. The flask was incubated in an incubator shaker with continuous shaking at 100 rpm and continuous illumination of 10,000 lx at $20 \pm 1^\circ\text{C}$ according to the OECD Guideline 201 (2002). After a 72 hour exposure period, the algal cells were counted and the mean inhibition was calculated by using the formulae below. Each experiment was run with three duplicates and three individual experiments were performed for each nanoparticle concentration (n=3).

Average growth rate = $[\text{LN}(\text{Number of Algal cells after exposure to nanoparticles}) - \text{LN}(10000)]/72$.

Growth rate % of Control = $(\text{Average growth rate after nanoparticle exposure} / \text{Average growth rate of control}) * 100$.

Mean Inhibition = $100 - \text{Growth rate \% of Control}$.

Average specific growth rate (μ) and percentage inhibition of average specific growth rate (%Ir) relative to controls were calculated for each concentration. The reference chemical potassium dichromate was employed as a positive control to ensure validity of the test method and the 72 hour EC_{50} for algal growth inhibition was found to be 1.3 mg/l.



Figure 2.4. *Pseudokirchneriella subcapitata*. (<http://www.google.ie/images>, accessed on 16th June 2009)

Table 2.1 Stock Solutions for Jaworskis Algal Media.

Stocks	Concentrations (g / 200ml)
Calcium nitrate tetrahydrate	4.0
Potassium phosphate monobasic	2.48
Magnesium sulfate heptahydrate	10.0
Sodium Bicarbonate	3.18
Ethylenediaminetetraacetic acid	0.45
Ethylenediaminetetraacetic acid tetrasodium salt	0.45
Boric acid	0.496
Manganese chloride tetrahydrate	0.278
Ammonium molybdate tetra hydrate	0.2
Cyanocobalamine	0.008
Thiamin HCl	0.008
Biotin	0.008
Sodium Nitrate	16.0
Sodium phosphate dibasic dihydrate	7.2

- Prepare Stock solutions as per Table 1, store @ 4°C. Label stock bottles with preparation date, initials and give an expiry appropriate for the stock e.g. 6 months.

- When new Jaworskis media needs to be prepared, remove stock solutions from fridge.
- Pipette 10ml of each stock solution into 10L carboy.
- Fill carboy with deionised water up to 10L mark, mix.
- Using pump & filters, sterile filter media into 1L sterile, clean Duran bottles.
- Label; Jaworskis media, preparation date, initials, filtered, allocate expiry date e.g. 6 months.
- Store at RT in the dark.

2.2.2.3 *Thamnotoxkit FTM*

The acute toxicity of the materials was also evaluated using the freshwater shrimp *Thamnocephalus platyurus* (Figure 2.7.). This toxicity test was purchased in kit form from SDI Europe (Hampshire, UK) and the test was performed according to manufacturer's instructions (Thamnotoxkit, FTM. 1995). Briefly, the test is a 24 h LC₅₀ bioassay, which is performed in a 24-well test plate using instars II–III larvae of the shrimp, which are hatched from cysts. Hatching was initiated 24 h prior to the start of the test. The hatching medium was prepared by transferring 2.5 ml standard freshwater into a vial and 17.5 ml deionized water was added to it. (i.e. dilution 1:8). An opened tube with cysts was filled with hatching medium (approx. 1 ml), the tube was closed and was shaken at regular intervals for approximately 30 minutes. Then 10 ml hatching medium was taken into a small Petri dish and the contents of the vial with prehydrated cysts were transferred into this Petri dish, making sure most of the cysts are transferred by rinsing the tube with hatching medium. The Petri dish was swirled gently to distribute the cysts evenly. The hatching Petri dish was covered and incubated at 25°C for 20-22 hours, under continuous illumination (light source of 3000-4000 lux). Upon hatching, the shrimp were exposed to various concentrations of each nanoparticle and were incubated at 25°C for 24 h in the dark (Thamnotoxkit, FTM. 1995). The bioassay is

conducted in a disposable 24 well plate. 1 ml standard freshwater was added to the four wells of control group. This procedure (1ml) was repeated for the other wells with the respective nanoparticle concentrations. Using a dissection microscope, 10 larvae were transferred to each well. Care was taken, during this operation, to minimize the transfer of medium along with the larvae. The 24 well plate was covered with aluminum foil and incubated at 25°C in dark. After 24 hours, the dead larvae in each test well were counted under the microscope and the % mortality was calculated. Concentrations of PNIPAM and NIPAM/BAM 85/15 nanoparticles of 500, 800, 1000, 1250 and 1500 mg/l were studied. For NIPAM/BAM 65/35 nanoparticles, concentrations of 200, 400, 600, 800 and 1000 mg/l were used, and for NIPAM/BAM, 50/50 nanoparticles, concentrations of 200, 300, 400, 500, and 600 mg/l were used after range finding experiments. For the case of PAMAM dendrimers G-4 (1, 2, 3, 5 and 7 μ M), G-5 (0.5, 1, 2, 4 and 6 μ M) and G-6 (0.5, 1, 2, 3 and 4 μ M) were used after range finding experiments. The test endpoint was mortality. The number of dead shrimp for each concentration was recorded and the respective LC₅₀ was determined. The 24 hour EC₅₀ was determined to be 0.1 mg/l for potassium dichromate which was used as a positive control to validate the experimental protocol. Each experiment was run with three duplicates and three individual experiments were performed for each nanoparticle concentration (n=3).

Potassium dichromate was used as positive control in different assays as recommended by manufacture's guideline (Thamnotoxkit, FTM. 1995) and also reported in the literature (Minagh et al., 2009,).



Figure 2.5. *Thamnocephalus platyurus* . (<http://www.google.ie/images>, accessed on 16th June 2009)

2.2.2.4 *Daphnia magna* acute immobilisation assay

Acute toxicity immobilization tests were performed on each of the dendrimers according to the British standard (BS EN ISO 6341, 1996). *Daphnia magna* (Figure 2.8) were originally obtained from TNO laboratories (the Netherlands) and were cultured in static conditions at $20 \pm 1^\circ\text{C}$ over a 16 h/8 h light/dark photoperiod. The culture was maintained by using daphnia growth media, which is composed of Calcium chloride-11.76 g/l, sodium bicarbonate-2.59 g/l, potassium chloride-0.23 g/l and Magnesium sulphate-4.93 g/l. The media was changed twice in a week and algae were given to daphnia as food for their growth. Daphnia were separated according to those carrying eggs, which were placed in a separate vessel to collect the neonates of same age. Acute toxicity tests were performed on *Daphnia magna* neonates that were less than 24 h old. In brief, the Immobilisation (no independent movement after gentle agitation of the test liquid for 15 seconds) was carried out in 10 ml tubes. For each

independent experiment, five different concentrations of nanoparticles and one control group was run with four replicates and three independent experiments were performed. The control group contains only the daphnia medium whereas the other tubes contained different concentration of nanoparticles, and the nanoparticles were dispersed in the daphnia medium. Then five daphnia neonates were transferred to each control and tubes containing different concentrations of nanoparticles. After 24 and 48 hour, the immobilisation of daphnia neonates was observed visually and the percentage of immobilization was calculated. There was no feeding during the tests. Daphnid sensitivity was verified by determining the 24 h EC₅₀ using potassium dichromate. The 24 h EC₅₀ of potassium dichromate on immobilization of *Daphnia magna* was observed to be 0.1 mg/l. The concentrations of PNIPAM nanoparticles were 250, 500, 750, 1000, and 1250 mg/l, for NIPAM/BAM 85/15 nanoparticles 100, 250, 500, 750 and 1000 mg/l, for NIPAM/BAM 65/35 nanoparticles 100, 200, 300, 400 and 500 mg/l, for NIPAM/BAM 50/50 nanoparticles 50, 100, 150, 200 and 250 mg/l. The concentrations used in the case of PAMAM dendrimers were (0.25, 0.5, 1, 2 and 3 μ M) for G4, 0.1, 0.25, 0.75, 1 and 1.5 μ M for G-5 , and 0.05, 0.1, 0.25, 0.5 and 0.75 μ M for G-6, as established by respective range finding studies.



Figure 2.6 . *Daphnia magna*. (<http://www.google.ie/images>, accessed on 16th June 2009)

2.2.2.5 Cell culture

The rationale behind the choice of *in vitro* models (cell lines) employed in this study was described in Section 1.5 of Chapter-1.

2.2.2.5.1 RTG-2, rainbow trout gonadal cells

RTG-2, rainbow trout gonadal cells (Catalogue no. 90102529) (Figure 2.7a) were obtained from the European Collection of Cell Cultures (Salisbury, UK). Cells were maintained in Dulbecco's modified Eagle's medium (DMEM) supplemented with 10% fetal calf serum (FCS), 45 IU ml⁻¹ penicillin and 45 µg ml⁻¹ streptomycin. The RTG-2 medium was also supplemented with 25 mM 4-(2-hydroxyethyl)-1-piperazineethanesulfonic acid (HEPES) and 1% non-essential amino acids. Cultures were maintained in a refrigerated incubator (Leec, Nottingham, UK) at a temperature of 20°C. For subculture the cells were detached using Versene/trypsin solution (1 mM EDTA/0.25 % trypsin) in Ca²⁺ and Mg²⁺ free Hanks Balanced Salts Solution (HBSS).

2.2.2.5.2 PLHC-1 cells

PLHC-1 cells (CRL-2406) (Figure 2.7b) were derived from a hepatocellular carcinoma in an adult female topminnow (*Poeciliopsis lucida*) and were obtained from the American Type Culture Collection (ATCC). Cells were maintained in DMEM supplemented with 5 % FCS, 45 IU ml⁻¹ penicillin, and 45 µg ml⁻¹ streptomycin. Cultures were maintained in a refrigerated incubator (Leec, Nottingham, UK) at a temperature of 30°C under normoxic atmosphere. For subculture the cells were detached using Versine/trypsin solution (1 mM EDTA/0.25 % trypsin) in Ca²⁺ and Mg²⁺ free Hanks Balanced Salts Solution (HBSS).

2.2.2.5.3 SW4 80 cells

SW480 cells (ATCC, CCL-228) (Figure 2.7c) a primary adenocarcinoma cell line of the colon, were cultured in DMEM F-12 HAM with 2mM L-glutamine supplemented with 10% FCS, 45 IU ml⁻¹ penicillin and 45 IU ml⁻¹ streptomycin at 37°C in 5% CO₂. For subculture, the cells were detached using Versene/trypsin solution (1 mM EDTA/0.25 % trypsin) in Ca²⁺ and Mg²⁺ free Hanks Balanced Salts Solution (HBSS).

2.2.2.5.4 HaCaT cells

HaCaT cells, an immortal non-cancerous human keratinocyte cell line (Figure 2.7d) (Kindly provided by Prof. Dr. Boukamp, Heidelberg), were also cultured in DMEM F-12 HAM with the addition of 1µg/ml hydrocortisone (Smola et al., 1993). For subculture, the cells were detached using Versene/trypsin solution (1 mM EDTA/0.25 % trypsin) in Ca²⁺ and Mg²⁺ free Hanks Balanced Salts Solution (HBSS).

2.2.2.5.5 J774A.1 cells

J774A.1 is a mouse macrophage cell line, (ECACC, 91051511) (Figure 2.7e) derived from a tumour in a female BALB/c mouse. J774A.1 cells were cultured in DMEM with 2mM L-glutamine supplemented with 10% FCS, 45 IU ml⁻¹ penicillin and 45 IU ml⁻¹

streptomycin at 37°C in 5% CO₂. For subculture, the cells were detached using Versene/trypsin solution (1 mM EDTA/0.25 % trypsin) in Ca²⁺ and Mg²⁺ free HBSS.

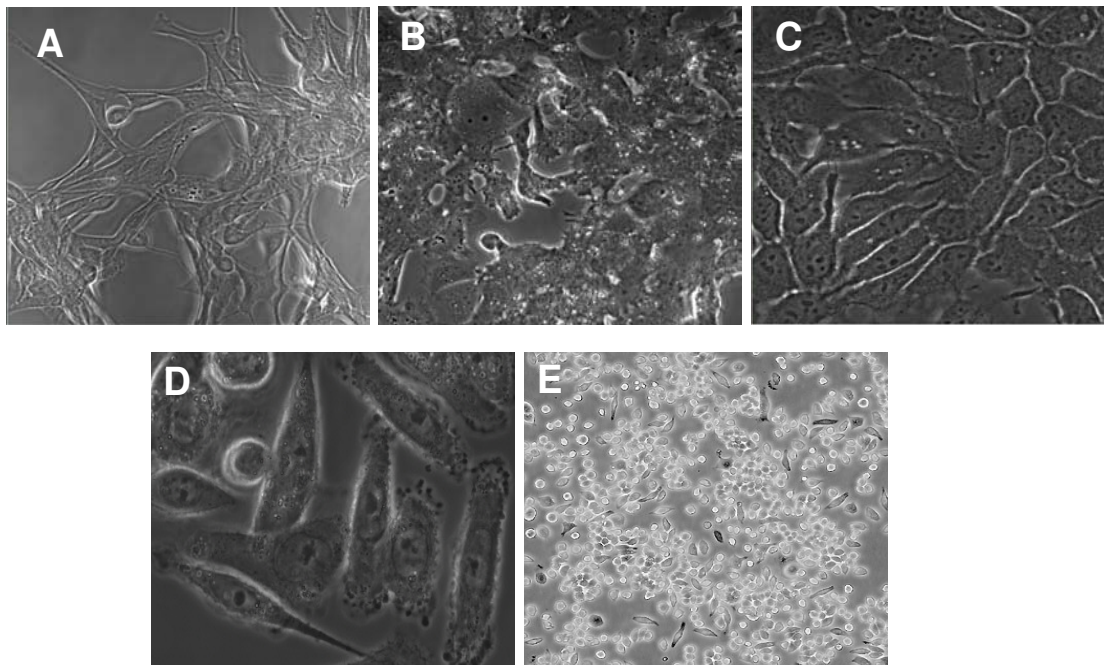


Figure 2.7. Morphology of, A. RTG-2 cells, B. PLHC-1 cells, C. HaCaT cells. D. SW 480 cells, E. J774A.1 cells. Magnification at 63x for panel A, B, C, and D, and 20x for panel E.

2.2.2.6 Cytotoxicity assays.

For cytotoxicity tests, with the RTG-2 cells, 96 well plates were seeded with 100 μ l of the following cell suspension concentrations: 2×10^5 cells per ml for 24 h exposure periods, 1.8×10^5 cells per ml for the 48 h exposures, and 1.6×10^5 cells per ml for the 72 and 96 h exposure periods (Davoren et al., 2005). For PLHC-1 cell exposures, 100 μ l of the following cell suspension concentrations: 8×10^5 cells per ml for 24 h, 6×10^5 cells per ml for 48 h, 4×10^5 cells per ml for 72 and 2×10^5 cells per ml for the 96 h exposure (Minagh et al., 2009). In the case of HaCaT and SW 480, cells are plated at a

seeding density of 1×10^5 cells/ml for the 24 hour test, 6×10^4 cells/ml for the 48 hour test, 4×10^4 cells/ml for the 72 hour and 2×10^4 cells/ml for the 96 hours in 96 well plates. Note that, due to the nature of the assay, and the need for lower cell numbers for the longer duration exposure experiments (to allow sufficient room for the cells to proliferate), for each exposure concentration the ratio of particles: cells (and hence the exposure dose) was different for each time-point, with the dose per cell being a factor of 2.5 different between the 24 and 96 hour exposures initially, and the dose being distributed among the daughter cells during proliferation. The cell numbers were determined according to previous literature, (Davoren et al., 2005, Casey et al., 2008, Minagh et al., 2009). An alternative protocol is the clonogenic assay (Herzog et al. 2007). For the J774A.1 tests, cells were plated at a seeding density of 1×10^5 cells/ml for 24 hour exposure experiments. The plates were kept in a CO₂ incubator for 24 hours for proper attachment of cells on the surface of the 96 well plates.

Particles were prepared in reduced serum medium (5%), following the protocol of Casey et al 2008. It should be noted, however, that at even at reduced serum levels, the nanoparticles are likely to bind to the proteins (Lynch et al., 2007). For the cytotoxicity of all test particles, a range of concentrations of nanoparticles was tested to establish a preliminary range (within 10 to 90 % cytotoxic response) with each cell line. Six replicate wells were used for each control and test concentration per microplate and three individual experiments were performed. After each incubation period (24, 48, 72, or 96 h), the test medium was removed, cell monolayers washed with phosphate buffered saline (PBS) and prepared for the cytotoxicity assays. In the case of NIPAM/BAM copolymer nanoparticles, the cytotoxicity of PNIPAM and NIPAM/BAM 85:15 was studied in RTG-2 cells. NIPAM/BAM 65:35 and NIPAM/BAM 50:50 were demonstrated to form large aggregates at this temperature,

due to the low LCST, which led to both materials floating in the cell culture media. For a cytotoxicity assessment the particles should be fully dispersed and capable of interaction with the cells so in this case it was not considered practical to test these particles with the cell line.

2.2.2.6.1 Alamar blue (AB) assay

Alamar blue (AB) is a water-soluble dye which is frequently employed for *in vitro* quantification of the viability of cells (Fields and Lancaster, 1993; Ahmed et al., 1994). When added to cell cultures, the dye diffuses into the cytosol and the oxidised form is reduced by the mitochondrial enzyme activity (Al-Nasiry et al., 2007). This conversion results in a change in colour of the dye from indigo blue to fluorescent pink, which can be easily measured by its absorption or fluorescence (Al-Nasiry et al., 2007). Reduced conversion compared to controls is a measure of reduced cellular viability. Alamar Blue (AB) uptake and conversion was therefore used throughout this work as a cytotoxicity assay. The assay was carried out according to the manufacturer's instructions. Briefly, control media or test exposures were removed, the cells were rinsed once with PBS and 100µl of AB medium (5% v/v solution of AB) prepared in fresh media (without FCS or supplements) were added to each well. After 3 h of incubation, AB fluorescence was measured at the excitation and emission wavelengths of 540 nm and 595 nm respectively, in a microplate reader (TECAN GENios, Grodig, Austria). The percentage of cell viability was determined by comparison with cells which were not exposed to nanoparticles i.e. the control group. Interference of nanoparticles with colorimetric assays has been documented for the case of carbon nanotubes (Casey et al., 2007). It should be noted, however, that this is the case for insoluble nanoparticles, which were seen to adhere strongly to the cell surfaces, even after repeated washing (Davoren et al., 2007). In the case of highly soluble polymeric nanoparticles, such effects are likely to

be much less dramatic. In order to confirm this, the fluorescence intensity of AB media in the absence and presence of PNIPAM particles was compared, and no difference was observed, which indicates that the PNIPAM nanoparticles do not interact or interfere with the AB assay.

2.2.2.6.2 MTT Assay

The MTT test is a colorimetric assay that measures the reduction of yellow 3-(4,5-dimethylthiazol-2-yl)-2,5-diphenyl tetrazolium bromide (MTT) by mitochondrial succinate dehydrogenase. A parallel set of plates was set up for the MTT assay and seeded and exposed in an identical manner to that described in the AB assay. After the desired exposure time the control medium or test exposures was removed, the cells were washed with PBS and 100 μ l of freshly prepared MTT in media (0.5 mg/ml of MTT in un-supplemented media) were added to each well. The MTT enters the cells and passes into the mitochondria where it is reduced to an insoluble dark purple formazan product. After 3 h incubation, the medium was discarded and the cells were rinsed with PBS and 100 μ l of DMSO were added to each well to extract the dye. The plates were shaken at 240 rpm for 10 min and the absorbance was measured at 595 nm in a microplate reader (TECAN GENios, Grodig, Austria). Since reduction of MTT can only occur in metabolically active cells the level of activity is a measure of the viability of the cells.

2.2.2.7 Internalisation study of fluorescently labelled PNIPAM nanoparticles

Fluorescently labelled particles were not evaluated for their toxicity but rather were employed to visualise the particle uptake and localisation. Methacryloxyethyl thiocarbamoyl rhodamine B labelled PNIPAM nanoparticles were used for the uptake study in the HaCaT and SW480 cells. HaCaT and SW480 cells were seeded at a density of 25,000 in glass-bottomed petri dishes. The Petri dishes were kept in a CO₂ incubator at 37 °C for 24 h. After attachment, the cells were exposed to different

concentrations of fluorescent nanoparticles and after a 24 hour exposure the monolayer of cells was washed with PBS to remove external particles. The particles in the cells were visualised by excitation at 543 nm and fluorescence emission was collected above 560 nm using a confocal laser scanning microscope (LSM 510 META, Zeiss, Germany). Fluorescence and phase contrast images were recorded from a minimum of 3 areas per sample. The internalisation of the PNIPAM nanoparticles was confirmed by taking optical sections (z-sections) of the HaCaT and SW 480 cells. Each optical section represents a particular plane of focus and it is clear that the nanoparticles have been internalised completely, rather than being accumulated in or at the cell membrane. For HaCaT cells 18 z section and for SW 480 cells 21 z sections were taken. Each section is separated by 0.41 and 1 μ m for HaCaT and SW 480 cell respectively.

2.2.2.8 Study of Co-localisation of the fluorescently labelled PNIPAM nanoparticles with lysosomes

Co-localisation studies of the labelled PNIPAM nanoparticles to lysosome were performed on the HaCaT cells using lysotracker green (<http://probes.invitrogen.com> accessed on 16th June 2009). LysoTracker® probes are fluorescent acidotropic probes for labelling and tracking acidic organelles in live cells. These probes have several important features, including high selectivity for acidic organelles and effective labelling of live cells at nanomolar concentrations (<http://products.invitrogen.com>). In this study, lysotracker green was used for staining lysosomes as the particles were labelled with the red rhodamine B dye.

Methacryloxyethyl thiocarbamoyl Rhodamine B is the fluorescent label used to track the particle within the cells and this fluorescent labels is stable in the pH conditions and

has previously been used for both *in vitro* and *in vivo* imaging of expansile nanoparticles in murine models (Colson et al., 2010).

HaCaT cells were seeded at a density of 25,000 in glass-bottomed petri dishes. The Petri dishes were kept in a CO₂ incubator at 37 °C for 24 h to attach the cells on the glass surface. After attachment, the cells were exposed to different concentrations (30 and 50 mg/l) of fluorescent nanoparticles and after 24 h exposure the monolayer of cells was washed with PBS. The cells were then incubated for 30 minutes with 75nM concentration of lysotracker in a CO₂ incubator at 37 °C. The particles in the cells were visualised using excitation at 543 nm and fluorescence emission was collected above 560 nm, whereas fluorescence from lysosomes was recorded using 488 nm excitation, emission being measured through a 505-530 nm bandpass filter in both cases using a confocal microscope (LSM 510 META, Zeiss, Germany). Fluorescence and phase contrast images were recorded from a minimum of 3 areas per sample.

2.2.2.9 Intracellular Reactive Oxygen Species (ROS)

Intracellular reactive oxygen species were measured by a fluorimetric assay using Carboxy H₂DCFDA [5 (and-6)-Carboxy-2', 7'-dichloro-dihydrofluorescein diacetate)] as the probe (<http://probes.invitrogen.com>) Carboxy H₂DCFDA was used because it carries an additional negative charge that improves its retention compared to non-carboxylated forms (<http://probes.invitrogen.com/media/pis/g002.pdf>, accessed on 16th June 2009). Intracellular oxidation of (6-carboxy-2',7'-dichlorodihydrofluorescein diacetate (Carboxy H₂DCFDA) to 2', 7'-di-chlorofluorescein (DCF) (Figure 2.11) was monitored according to the increase in fluorescence as measured by a plate reader and using confocal fluorescence microscopy.

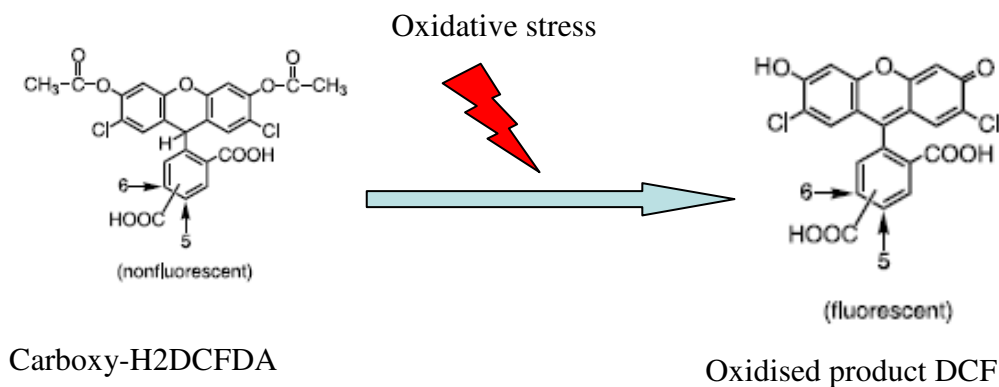


Figure 2.8. Conversion of Carboxy H₂DCFDA to DCF.

The optimal loading time for the Carboxyl H₂DCFDA was determined to be 40 minutes by a kinetic study of the response to H₂O₂ as a control (Figure 2.9). This time point was found to be substantially below the saturation point of the assay for exposure to 200 μM H₂O₂. Thus increase in ROS levels as a result of nanoparticle exposure to this level and beyond can be measured.

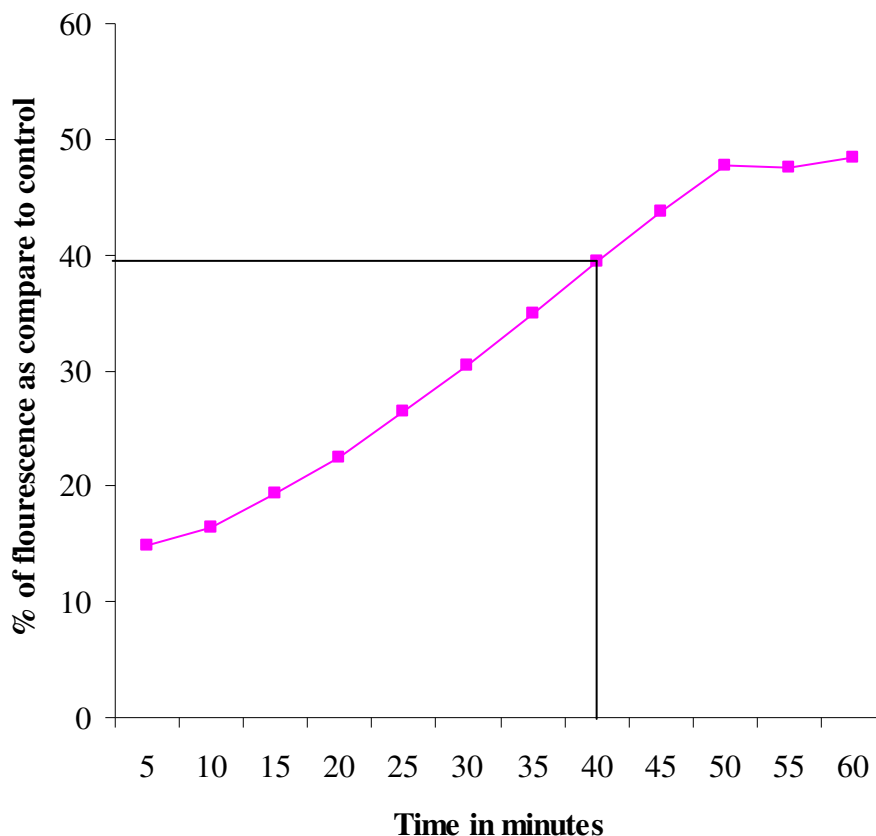


Figure 2.9. Time kinetic study of ROS production with 200 μM of H_2O_2 exposure to PLHC-1 cells. The concentration of Carboxyl H_2DCFDA used 10 μM .

In brief, the assay was performed in black 96 well microplates (Nunc, Denmark). The J774A.1 cells were seeded in 100 μl of cell suspension in each well at a density of 4×10^5 cells/ml and at 8×10^5 cells/ml for PLHC-1 cells. After 24 h of cell attachment, plates were washed with 100 μl /well PBS and the cells were treated with increasing concentrations of each generation of dendrimer prepared in 5% FCS containing media. Hydrogen peroxide (400 μM) was used as positive control to validate the protocol. All incubations were performed at 37°C in a 5% CO_2 humidified incubator. Six replicate wells were used for each control and test concentrations per 96 well microplates. After the specified incubation time period (1, 2, 4 and 6 h) the plates were washed with 100

$\mu\text{l/well}$ PBS and then 100 $\mu\text{l/well}$ of 10 μM Carboxy H_2DCFDA was added to each well. The plates were incubated at 37°C for a period of 40 minutes. The fluorescence was quantified using a plate reader, which provides an average of the statistically variable response of individual cells (Elbekai and El-Kadi, 2005). Fluorescence was measured using an excitation of 485nm and emission of 530nm, in a TECAN GENios (Grodig, Austria) microplate reader. For visualisation of the intracellular fluorescence, carboxy H_2DCFDA was excited at 488 nm and fluorescence emission at 520 nm (with a 505 nm long pass filter) was recorded using a confocal laser scanning microscope (LSM 510 META, Zeiss, Germany). Fluorescence and phase contrast images were recorded from a minimum of 3 areas per sample.

2.2.2.10 Cytokines assay

An enzyme linked immunosorbant assay (ELISA) was performed to quantify the proinflammatory mediators (IL-6, TNF- α and MIP-2) after the exposure of the J774A.1 cells to PAMAM dendrimers. The basic principle of ELISA is shown in figure 2.10. LPS (lipo-polysaccharide) was used as positive control to stimulate the TNF- α and MIP-2 and validate the ELISA protocol. After the exposure period, the supernatant was collected, and then centrifuged and stored at -80°C for ELISA. Although some loss of protein due to adsorption onto the nanoparticles may have occurred, the extent was not measured. The principle of the ELISA is based on the sandwich technique, in which the capture antibody (primary antibody) at concentrations of $1\mu\text{g/ml}$ (TNF- α), $2\mu\text{g/ml}$ (IL-6) and $0.5\mu\text{g/ml}$ (MIP-2) in PBS (pH -7.4), was coated in the 96 well plate (Nunc-immuno plate, Denmark).

The plates were incubated overnight at room temperature. The wells were aspirated to remove the liquid and the plates were washed four times with PBS-T (phosphate buffer

saline with 0.05% of Tween 20) and then blocked with 1% BSA solution at room temperature for 1 hour. The plates were again washed with PBS-T four times and 100 μ l of different dilutions of supernatant were added to the respective wells and standards of IL-6, TNF- α and MIP-2 at a concentration from 10 to 800 pg/ml in duplicate were added to the first two columns of the 96 well plates and incubated for 2h at room temperature. The plates were aspirated and washed four times, whereupon 100 μ l of the detection antibody against the respective marker (secondary antibody) were added to the 96 well ELISA plate at a concentration of 0.25 μ g/ml (for TNF- α and MIP-2), or 0.5 μ g/ml (IL-6) and the plates were incubated at room temperature for 2h. The plates were aspirated and washed four times, 100 μ l of avidine-HRP (1:2000 dilutions in blocking buffer) were added to each well and the plates were incubated for 30 minutes at room temperature. The plates were washed four times with washing buffer and 100 μ l of substrate solution (2,2'-Azino-Bis(3-Ethylbenzthiazolin-6-Sulfonic acid)) were added to each well and the plates were incubated at room temperature to develop the colour. The colour development time was optimised to be 15 minutes for each assay using the standards and the absorbance was measured at 405 nm in a VICTOR³VTM 1420 Multilabel Counter plate reader (Perkin Elmer, USA).

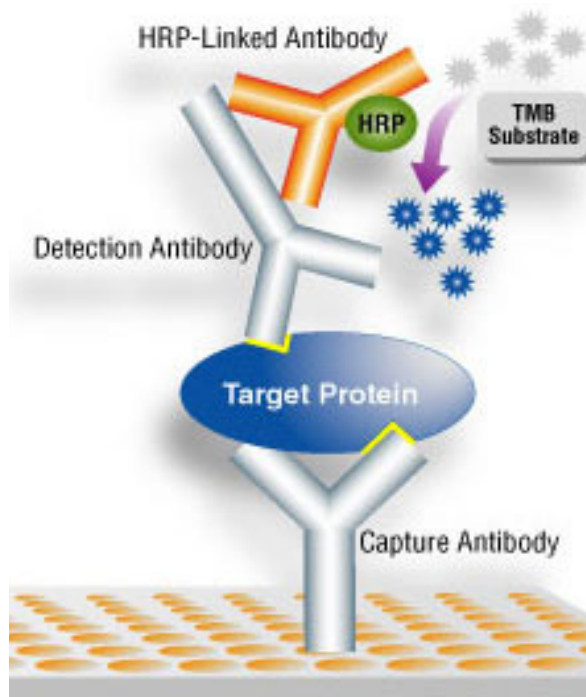


Figure 2.10. Principle of ELISA (Sandwich technique)

(http://www.synchronium.net/wpcontent/uploads/2009/09/sandwich_elisa.jpg&imgrefurl, accessed on 16th June 2009).

2.2.2.11 Oxidative DNA damage

8-hydroxy-2'-deoxyguanosine (8-OHdG) is formed when DNA is oxidatively modified by ROS, as shown schematically in Figure 2.11. Oxidative stress has been demonstrated to play a potential role in the initiation, promotion, and progression of malignancy. Lesions such as 8-OHdG are coupled with their potential mutagenicity in mammalian cells and this has led to their proposed potential as intermediate markers of a disease endpoint for example, cancer.

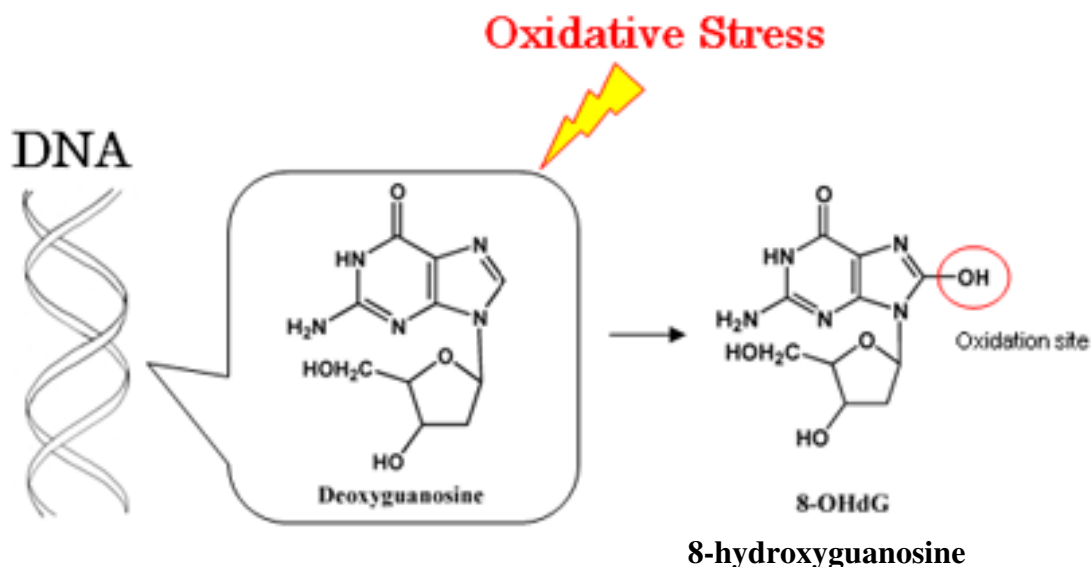


Figure 2.11. Schematic diagram of the conversion of Deoxyguanosine to 8-hydroxyguanosine.

2.2.2.11.1 DNA Extraction from PLHC-1 cells

DNA was extracted using the DNA extractor WB kit (Wako pure chemicals Industries, LTD, Osaka, Japan). In brief, the cells were plated in a T-25 culture flask (Nunc, Denmark), at a seeding density of 1×10^6 and kept for 24h to allow for attachment. They were then exposed to different concentrations of PAMAM dendrimer solutions for the different time points (6, 12, 24, 48 and 72h). The exposure was terminated after the appropriate exposure time by removing the medium and rinsing with PBS. The cells were then trypsinized and centrifuged to remove the supernatant, 0.5 ml of lysis solution was added to the pellet and the suspension was mixed gently by inversion of the microfuge tube. The cell suspension was then centrifuged at 10,000x g for 20 seconds at 4 °C. One millilitre of lysis solution was then added to the pellet and the suspension was again mixed gently by inversion of the microfuge tube, and subsequently centrifuged at 10,000x g for 30 second at 4 °C. The lysis step was repeated one more time.

The resultant pellet was suspended in 200 μ l of enzyme reaction solution and 10 μ l of protease solution was added and the suspension was mixed gently by inversion. The reaction mixture was incubated at 37 $^{\circ}$ C for 1 hour and the solution was mixed several times by inversion. After the incubation time, 0.3 ml of sodium iodide followed by 0.5 ml of isopropyl alcohol was added to the reaction mixture and the solution was mixed by inversion of the microfuge tube until a whitish material appears. It was then centrifuged at 10,000 g for 10 minutes at room temperature. The pellet was rinsed with washing solution A and then washing solution B. The pellet was reconstituted in MQ water and maintained at 4 $^{\circ}$ C. The purity of the extracted DNA was determined by UV-visible spectroscopy at 260 and 280 nm. The absorbance (the ratio of 260/280 nm) value was obtained \sim 1.8, which indicates that the extracted DNA is pure.

After DNA extraction, the DNA was digested for the determination of 8-OHdG by the ELISA method. The DNA was converted to single strand by incubating the sample at 95 $^{\circ}$ C for 5 minutes and then rapidly chilling on ice. The DNA sample was then digested to nucleotides by incubating the denatured DNA with 5 units of nuclease P1 for 2 hour at 37 $^{\circ}$ C in 20 mM Sodium Acetate, pH 5.2. Subsequently it was treated with 5 units of alkaline phosphatase for 1 hour at 37 $^{\circ}$ C in 100 mM Tris buffer, pH 7.5. The reaction mixture was centrifuged for 5 minutes at 6000 g and the supernatant was used for the 8-OHdG assay.

2.2.2.11.2 Measurement of 8-OHdG by ELISA

The 8-OHdG ELISA kit is a competitive *in vitro* enzyme linked immuno-sorbent assay for quantitative measurement of the oxidative DNA adduct 8-hydroxy, 2' deoxyguanosine (8-OHdG). All reagents and samples were equilibrated to room temperature before use (20-25 $^{\circ}$ C). The ELISA was carried out according to the

manufacturer's instructions. In brief, the primary antibody was reconstituted with the primary antibody solution and allowed to dissolve completely.

Fifty microlitres of sample (extracted DNA) or standard was added per well, and then 50µl of reconstituted primary antibody was added per well. The plate was shaken from side to side and the solution mixed fully. The container was covered with adhesive strip, making sure it was sealed tightly, and incubated at 4 °C overnight. The contents of the plate were removed. 250 µl of washing solution were pipetted into each well. After washing thoroughly by shaking the plate from side to side, the washing solution was removed. The plate was inverted and blotted using a clean paper towel to remove any remaining washing buffer. The washing process was repeated twice more.

The secondary antibody was reconstituted with the secondary antibody solution. 100 µl of constituted secondary antibody was added per well. The plate was shaken from side to side to mix fully. The plate was covered with an adhesive strip and incubated at room temperature for 1 hour. At the end of the incubation period, the plates were washed twice with washing buffer. The chromatic solution (enzyme substrate solution) was reconstituted with 100 times the volume of the diluting solution. 100 µl of the reconstituted enzyme substrate was added per well. The plate was shaken from side to side to mix fully and incubated at room temperature for 15 minutes in the dark.

100 µl of the reaction terminating solution was added per well. The plate was shaken from side to side to mix fully. After terminating the reaction, the absorbance at 450 nm was measured. A standard curve was used to determine the amount of 8-OHdG present in test samples.

2.2.2.12 Alkaline Comet assay

The alkaline comet assay, also known as single cell gel electrophoresis (SCGE), is a rapid and sensitive technique for analysis and quantification of DNA damage in individual living cells. It probes damage such as single and double strand breaks and alkali-labile sites (Collins et al., 2004). Individual cells are embedded in a thin agarose gel on a microscope slide. All cellular proteins are then removed from the cells by lysing and the sample is stained with a DNA specific fluorescent dye. The DNA is then allowed to denature under alkaline/neutral conditions. Under an applied voltage, damaged DNA or DNA fragments migrate and thus the process produces an image with a pronounced head and tail, resembling a comet. The head consists of remaining undamaged DNA, while the tail consists of damaged (single stranded or double stranded breaks) or fragments of DNA. The gel is analysed fluorescence in the head and tail and the length of tail. The extent of DNA liberated from the head of the comet is directly proportional to the amount of DNA damage.

The olive tail moment (OTM) is one of the most important parameters and is calculated as the product of two factors: the percentage of DNA in the tail (tail percentage DNA) and the distance between the intensity centroid of the head (head mean) and the tail (tail mean) along the x-axis of the comet. It is calculated by the formula-

$$\text{Olive Tail Moment (OTM)} = (\text{Tail.mean} - \text{Head.mean}) \times \% \text{Tail DNA} / 100.$$

The genotoxicity of NIPAM nanoparticles was assessed using the micro-comet assay technique in three cell lines (HaCaT, SW480 and PLHC-1 cells). For a typical experiment, 100 μl of 1×10^5 cells/ml for 24h; 8×10^4 cells/ml for 48h; 6×10^4 cells/ml for 72h exposure of nanoparticles were plated in 96 well microplate and incubated at 37°C in 5% CO_2 for 24 hours to ensure cell attachment. The PLHC-1 cells were incubated at

30 °C during the whole experimental time period. The cell monolayers were then washed with PBS and exposed to varying particle concentrations (12.5 mg/l, 25 mg/l, 100 mg/l, 200 mg/l, 400 mg/l, and 800 mg/l) for different time intervals (24, 48 and 72h). For PAMAM dendrimers, cells were exposed to different concentrations (0.125, 0.25, 0.5, 0.75 and 1 µM) of G4, G5 and G6 for 6, 12 and 24h. After the appropriate exposure time, cells were washed once with PBS, trypsinized and suspended in low melting point agarose and cast onto a gel bond film fixed with chamber slides. After the agarose solidified, it was suspended in freshly prepared and pre-cooled cell lysis buffer overnight. The following day, electrophoresis was conducted in alkaline electrophoresis buffer (pH 12.7) for 15 mins (conditions: 300 mA, 1.5 V/cm at 4°C). After completion of the electrophoresis run time, the Gelbond™ film was treated with neutralisation buffer (pH 7.5) for 30 minutes to neutralise the DNA embedded gels and then dehydrated in absolute ethanol for 2 h. Gels were stored in the dark overnight at 4°C, allowed to dry completely, and were then stained with SYBR-Green nucleic acid stain. Image analysis was performed using Komet 5.5 software (ANDOR™, UK) and a Nikon Eclipse E600 microscope attached to a CCD camera. 50 comets were imaged per slide and 4 slides per each concentration were prepared. Three independent experiments were performed. Values of OTM and percentage of tail DNA were automatically calculated by the software. Ethyl Nitrosourea (ENU) 100 µM was used as a positive control to validate the experimental protocol.

2.2.2.13 Apoptosis assay

Apoptosis is a programmed cell death process, and during apoptosis the cytoplasmic membrane increases slightly in permeability. The increase of apoptosis induced cell death as a result of exposure to nanoparticles was investigated by using a kit containing

both YO-PRO®-1 and PI dyes. YO-PRO®-1, is a green fluorescent dye which can enter apoptotic cells. Propidium iodide (PI), a red fluorescent dye, on the other hand cannot enter in to the cells. When employed in parallel, they provide a sensitive indicator for apoptosis (Idziorek et al., 1995; Estaquier et al., 1996). After incubation of a cell population with YOPRO®-1 and PI, apoptotic cells show green fluorescence, dead cells show red and green fluorescence, and no fluorescence is observed from live cells (<http://probes.invitrogen.com/media/pis/mp13243.pdf>). The relative populations can easily be distinguished by a flow cytometer that uses the 488 nm line of an argon-ion laser for excitation.

The PLHC-1 cells were plated in a 6 well plate at a seeding density of 1×10^6 cells/ml well. The plates were incubated at 30 °C for 24 hour to ensure proper attachment. The cell monolayer were washed with PBS and then exposed with a range of concentrations of PAMAM dendrimers (G4, G5 and G6) for different time points (6, 12, 24, 48 and 72h). After the appropriate exposure time, cells were washed once with PBS, trypsinized, centrifuged, the supernatant removed and then the cell pellets were suspended in 1 ml PBS. One microlitre of YO-PRO®-1 dye and 1µl PI were added to the cell suspension and it was incubated on ice for 30 minutes. After the incubation time, the fluorescence of the cell suspension was measured in flow cytometer (CyFlow® space). The experimental protocol was validated by using camptothecin as positive control.

2.2.2.14 Statistics

All experiments were conducted in at least triplicate (three independent experiments). Ecotoxicity was expressed as mean percentage inhibition for the case of Microtox® (inhibition of bioluminescence), *D. magna* (immobilisation) and percentage mortality was measured for the *T. platyurus* assay. Fluorescence (AB assay) as fluorescent units

(FUs) was quantified using a microplate reader (TECAN GENios, Grödig, Austria). Raw data from cell cytotoxicity assays were collated and analyzed using Microsoft Excel[®] (Microsoft Corporation, Redmond, WA). Cytotoxicity and the intracellular ROS (Reactive oxygen species) were expressed as mean percentage inhibition relative to the unexposed control \pm standard deviation (SD). MIP-2, IL-6 and TNF- α data were calculated from their respective standards and were expressed in mean (pg/ml) \pm standard deviation (SD). Three independent genotoxicity assay was performed, which was expressed in terms of percentage tail DNA and OTM, and the data shown as the mean percentage \pm standard deviation (SD). The distributions of the data were checked and found to be normal and thus the data is deemed to be suitable for analysis using one way ANOVA. Statistical analyses were carried out using one-way analyses of variance (ANOVA) followed by Dunnett's multiple comparison tests. Statistical significance was accepted at $P \leq 0.05$ for all tests. Toxicity data was fitted to a sigmoidal curve and a four parameter logistic model used to calculate EC/LC₅₀ values. This analysis was performed using Xlfit3[™] a curve fitting add-in for Microsoft[®] Excel (ID Business Solutions, UK).

References

- Azur Environmental (1998). Microtox[®] acute toxicity basic test procedures, Report, Carlsbad, CA. pp 1-13.
- Batista, M.L Jr., Santos, R.V., Cunha, L.M., Mattos, K., Oliveira, E.M., Seelaender, M.C., Costa Rosa, L.F. 2006. Changes in the pro-inflammatory cytokine production and peritoneal macrophage function in rats with chronic heart failure. *Cytokine*, 34, 284-290.
- Barnden, M. J., Allison, J., Heath, W. R., Carbone, F.R. 1998. Defective TCR expression in transgenic mice constructed using cDNA-based alpha- and beta-chain genes under the control of heterologous regulatory elements. *Immunol Cell Biol.* 76, 34-40.
- Brunauer, B., Emmett, P. H., Teller. E. 1938. Adsorption of gases in Multimolecular Layers. *J. Am. Chem. Soc.* 60, 309–319.
- BS EN ISO 6341 (1996). Water Quality Determination of the Inhibition of the Mobility of *Daphnia magna* Strauss (Cladocera, Crustacea) Acute Toxicity Test. British Standards Institution, London.
- Casey, A., Herzog, E., Lyng, F.M., Byrne, H.J., Chambers, G., Davoren, M., 2008. Single walled carbon nanotubes induce indirect cytotoxicity by medium depletion in A549 lung cells. *Toxicol. Lett.* 179, 78-84.
- Casey, A., Davoren, M., Herzog, E., Lyng, F. M., Byrne, H. J., Chambers, G. 2007. Probing the interaction of single walled carbon nanotubes within cell culture medium as a precursor to toxicity testing. *Carbon*, 45, 34–40.
- Colson, Y. L., Liu, R., Southard, E. B., Schulz, M. D., Wade, J. E., Griset, A. P., Zubris, K. A., Padera, R. F., Grinstaff M. W. 2010. The performance of expansile

- nanoparticles in a murine model of peritoneal carcinomatosis. *Biomaterials*, 32, 832-840.
- Davoren, M., Fogarty, M., 2006. *In vitro* cytotoxicity assessment of the biocidal agents sodium o-phenylphenol, sodium o-benzyl-p-chlorophenol, and sodium p-tertiary amylphenol using established fish cell lines. *Toxicol. In Vitro*, 20, 1190–1201.
- Davoren, M., Ní Shúilleabháin, S., Hartl, M. G, Sheehan, D., O'Brien, N. M., O'Halloran, J., Van Pelt FN, Mothersill C. 2005. Assessing the potential of fish cell lines as tools for the cytotoxicity testing of estuarine sediment aqueous elutriates. *Toxicology In vitro*, 19, 421-431.
- Darzynkiewicz, Z., Juan, G., Li, X., Gorczyca, W., Murakami, T., Traganos, F. 1997. Cytometry in cell neurobiology: analysis of apoptosis and accidental cell death (necrosis). *Cytometry*. 27, 1-20.
- Estaquier, J., Tanaka, M., Suda, T., Nagata, S., Golstein, P., Ameisen, J. C. 1996. Fas-mediated apoptosis of CD4+ and CD8+ T cells from human immunodeficiency virus-infected persons: differential *in vitro* preventive effect of cytokines and protease antagonists. *Blood*. 87, 4959-66.
- Elbekai, R.H and El-Kadi, A.O.S., 2005. The role of oxidative stress in the modulation of aryl hydrocarbon receptor-regulated genes by As³⁺, Cd²⁺, and Cr⁶⁺. *Free Radical Biol. Med.* 39, 1499–1511.
- Gorelov, A.V., DuChesne, A., Dawson, KA. 1997. Phase separation in dilute solutions of poly (N-isopropylacrylamide). *Physica A*. 240, 443-452.
- <http://probes.invitrogen.com/media/pis/g002.pdf>, accessed on 16th June 2009
- <http://www.inspirenano.com>, accessed on 16th June 2009
- <http://www.dendritech.com>, accessed on 16th June 2009

- Idziorek, T., Estaquier, J., De Bels, F., Ameisen, J. C. 1995. YOPRO-1 permits cytofluorometric analysis of programmed cell death (apoptosis) without interfering with cell viability. *J Immunol Methods*. 185, 249-58.
- Minagh, E., Hernan, R., O'Rourke, K., Lyng, F. M, Davoren, M. 2009. Aquatic ecotoxicity of the selective serotonin reuptake inhibitor sertraline hydrochloride in a battery of freshwater test species. *Ecotoxicology and Environmental Safety*, 72, 434-440.
- Nyholm, N. 1990. Expression of results from growth inhibition toxicity tests with algae. *Arch. Environ. Contam. Toxicol.* 19, 518-522.
- OECD, 2002. Guideline for testing of chemicals. In: *Freshwater Alga and Cyanobacteria, Growth Inhibition Test, Method 201*, OECD.
- Osuchowski, M.F., Siddiqui, J., Copeland, S., Remick D.G. 2005. Sequential ELISA to profile multiple cytokines from small volumes. *Journal of Immunological Methods*, 302, 172–181
- Osuchowski, M.F., Welch, K., Siddiqui, J., Remick, D.G. 2006. Circulating Cytokine/Inhibitor Profiles Reshape the Understanding of the SIRS/CARS Continuum in Sepsis and Predict Mortality. *Journal of Immunology*, 177, 1967-74.
- Smola, H., Thiekotter, G., Fusenig, N.E., 1993. Mutual Induction of Growth Factor Gene Expression by Epidermal-Dermal Cell Interaction. *J. Cell Biol.* 122, 417–429.
- Thamnotoxkit, FTM., 1995. Crustacean toxicity screening test for freshwater. Standard Operating Procedure, Creasal, Deinze, Belgium.

Chapter 3

Characterisation and Ecotoxicology of PNIPAM and NIPAM/BAM Copolymer Nanoparticles

Adapted from “Preparation, Characterization of *NIPAM* and *NIPAM/BAM* Copolymer Nanoparticles and their Acute Toxicity Testing using an Aquatic test battery”. *Aquatic Toxicology*, 2009. 92, 146-154.

Authors: Pratap C. Naha, Alan Casey, Tiziana Tenuta, Iseult Lynch, Kenneth A.

Dawson, Hugh J. Byrne, Maria Davoren

3.1. Introduction

As nanomaterials are currently being widely used in modern technology, there is an increasing need for information regarding the human health and environmental implications of these nanomaterials. To date, the human health impacts of nanomaterials have received the greatest attention and it has been demonstrated through both *in vivo* and *in vitro* studies with mammalian test systems that the properties that make nanomaterials so attractive from a commercial application viewpoint (*e.g.* nanoparticle size and increased surface area) can also potentially be responsible for undesirable health effects (Oberdörster et al., 2005, Meng et al., 2007; Papageorgiou et al., 2007; Singh et al., 2007; Poland et al., 2008).

The assessment of environmental effects requires an understanding of their mobility, reactivity, ecotoxicity and persistency (Nowack and Buchelli, 2007). Recently reports on the ecotoxicity of various nanomaterials have started to emerge in the literature. Of the studies conducted, the majority have focused on the carbon based materials (Lovern and Klaper, 2006; Zhu et al., 2006; Cheng et al., 2007; Lin and Xing, 2007; Smith et al., 2007; Baun et al., 2008; Lovern et al., 2007) but there have also been recent reports on the ecotoxicological evaluation of various metal based nanomaterials (Lovern et al., 2007; Federici et al., 2007; Heinlaan et al., 2008; Gagné et al., 2008; Mortimer et al., 2008) and dendrimers (Mortimer et al., 2008). These studies have looked at various aquatic species representing the different trophic levels (decomposer, primary producer, invertebrates and vertebrates).

The aim of the present investigation was therefore the preparation, characterisation and ecotoxicological assessment of PNIPAM and NIPAM/BAM copolymer nanoparticles. Variation of the co-polymerisation ratio from 100% NIPAM through NIPAM/BAM 85:15, NIPAM/BAM 65:35 and NIPAM/AM 50:50 allowed a systematic variation of

the surface chemistry which manifested as changes in the Zeta potential, facilitating the establishment of structure-activity relationships. Since these particles are thermosensitive, the particle size was measured as a function of temperature. The surface area of the particles was measured by BET. Investigation of the acute ecotoxicological effects of PNIPAM and NIPAM/BAM copolymer particles was conducted using a battery of bioassays representing different trophic levels. The tests employed included a bacterial species, a unicellular algae species and two crustaceans. In addition, the cytotoxicity of PNIPAM and NIPAM/BAM (85:15) copolymer particles was investigated in a salmonid fish cell line.

3.2 Experimental methods

All the experimental methods are described in chapter 2. Specifically, particle size measurement, zeta potential and BET surface area measurement are described in chapter 2, section 2.2.1.1 , 2.2.1.2 and 2.2.1.4 respectively. All the ecotoxicity protocols and cytotoxicity assays are described in section 2.2.2 and 2.2.2.6.

3.3 Results

3.3.1 Nanoparticles characterisation

3.3.1.1 Particle size measurement

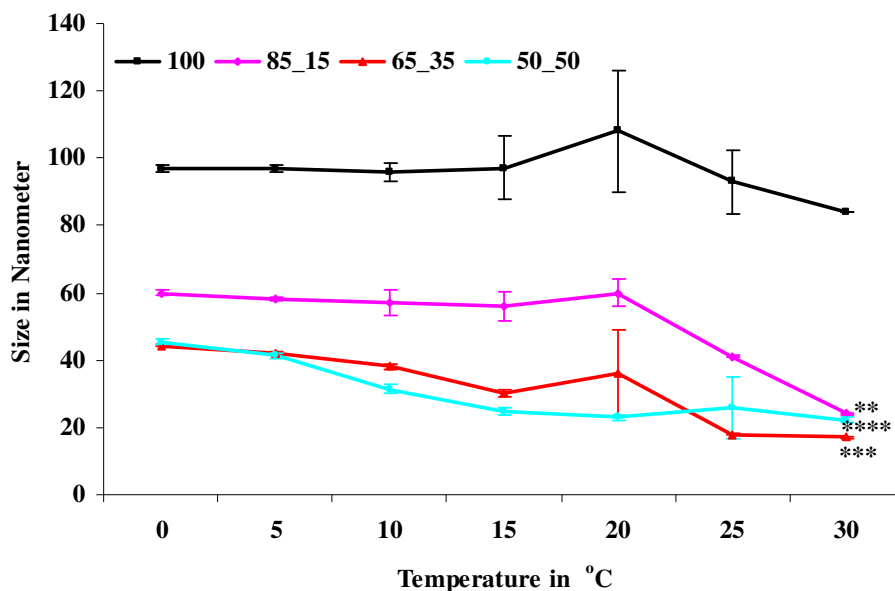
The average particle sizes of PNIPAM and the various NIPAM/BAM copolymer nanoparticles were measured as a function of increasing temperature. PNIPAM and NIPAM/BAM copolymers are thermoresponsive in nature. When the temperature is raised above the LCST the polymer undergoes a phase transition and the random coil structure (hydrophilic state) collapses to form a globular structure (hydrophobic state) (Xu et al., 2006).

This behaviour of decreasing particle size with increasing temperature is demonstrated well by the temperature dependence of the nanoparticles when prepared in MQ water (shown in figure 3.1A). The particle size of NIPAM and NIPAM/BAM copolymer nanoparticles was found to increase with increasing temperature when they were prepared in other media, however, as presented in Figure 3.1B for the example of the Microtox[®] diluent, MD. For the NIPAM/BAM 50:50 copolymer nanoparticles, the particle size is seen to begin to increase significantly at ~10°C, close to its LCST and the particle size becomes as high as microns. This dramatic increase of particle size is characteristic of agglomeration. The 63:35 and 85:15 copolymer particles remain unagglomerated until ~ 15°C and 20°C respectively and the 100% PNIPAM until 25°C. Table 3.1 lists the average particle size of the various co-polymer particles in the respective test media, at the temperatures at which the respective tests were conducted. With the exception of the 50:50 copolymer, all particles are unagglomerated at the concentrations and temperatures employed for the eco- toxicological studies. Whereas in algal media the particles are measured to be 61nm, in cell culture medium, both the 50:50 and 65:35 copolymer particles were highly agglomerated at 20°C, and so were not tested for the cytotoxicity assessment.

Table 3.1. Hydrodynamic diameter of PNIPAM and NIPAM/BAM copolymer nanoparticles in different test media and temperature.

Test Medium	Test Temperature °C	PNIPAM	NIPAM/BAM 85:15	NIPAM/BAM 65:35	NIPAM/BAM 50:50
Microtox Diluent	15	98 nm	69 nm	42 nm	2131 nm
Algal Medium	20	105 nm	60 nm	61 nm	5765 nm
<i>Daphnia</i> medium	20	102 nm	58 nm	200 nm	2789 nm

A



B

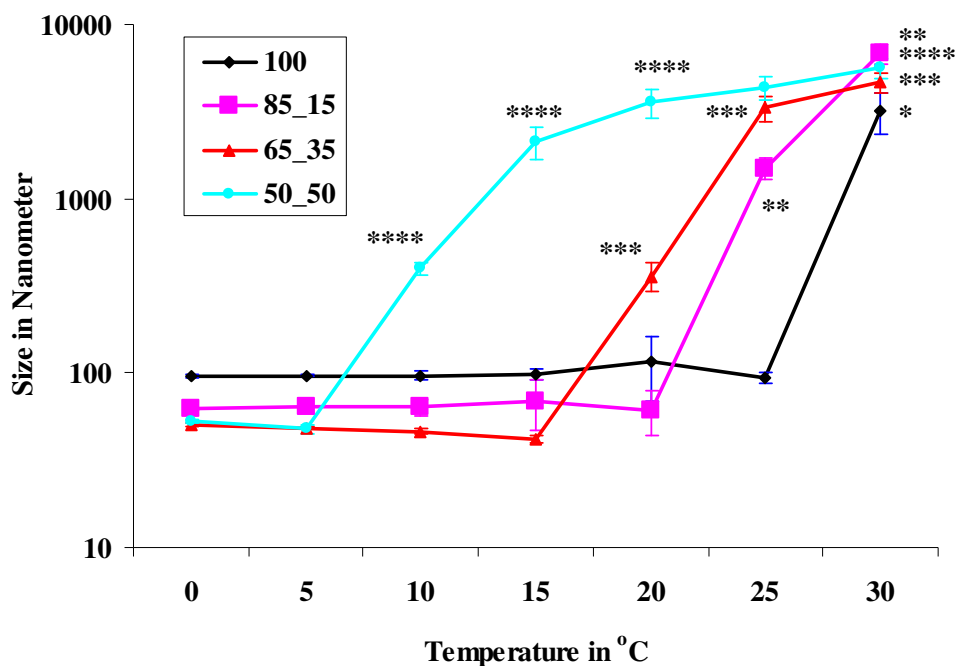


Figure 3.1. Hydrodynamic diameter of PNIPAM and NIPAM/BAM copolymer nanoparticles. (A) MQ water (There is a significant difference of decreasing of particle size of all the series of nanoparticles except PNIPAM nanoparticles between 0 °C and 30 °C); and figure (B) Microtox diluent (MD) as a function of increasing temperature. Data is presented as the mean \pm SD (N=6). * indicate a significant difference of particle size as compare to 0 °C ($p < 0.05$). *, **, *** and **** denotes for PNIPAM, NIPAM/BAM 85:15, NIPAM/BAM 65:35 and NIPAM/BAM 50:50 respectively.

3.3.1.2 Zeta potential measurement

The zeta potentials of PNIPAM and the different NIPAM/BAM copolymer particles was measured in the various test media; MQ water, MD, AM, and DM. The results are shown in Figure 3.2. Significant difference ($p < 0.05$) of zeta potential in each respective media as compared to milli-Q water with the PNIPAM and NIPAM/BAM

series of nanoparticles was observed. For all media types, increasing the ratio of BAM in the copolymer nanoparticles was shown to cause a decrease in their zeta potential. No correlation between zeta potential and particle size was observed.

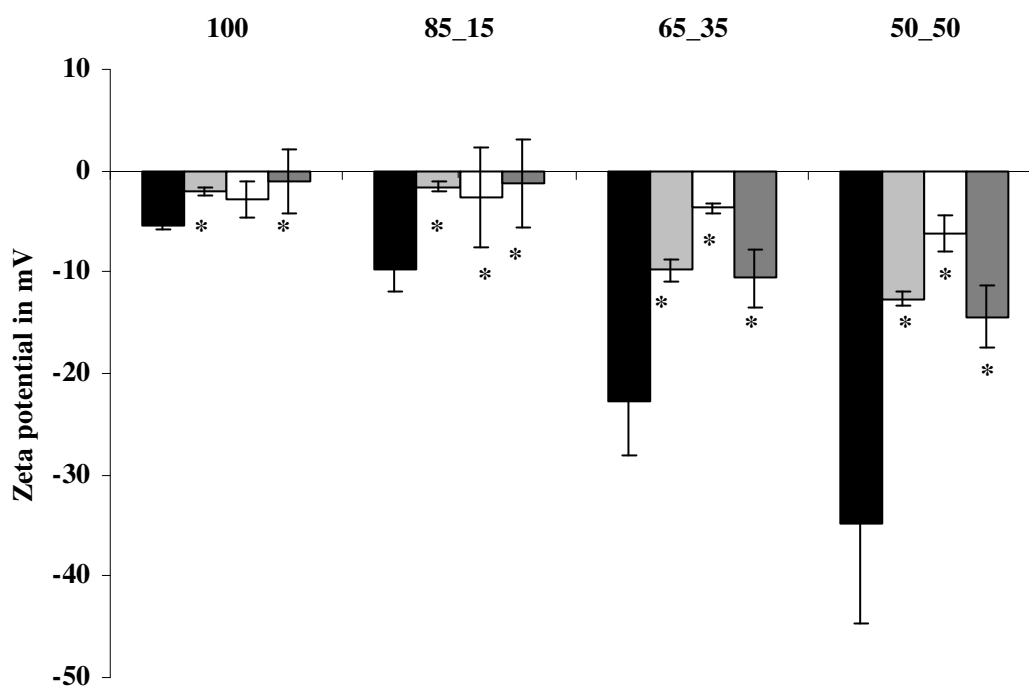


Figure 3.2. Zeta potential of PNIPAM and NIPAM/BAM copolymer particles in different media. (■) MQ; (◻) AM; (□) MD; (◼) DM. Data is presented as the mean \pm SD (N=6). * denotes significant difference ($p < 0.05$) of zeta potential in different media as compare to milli-Q water.

3.3.1.3 Surface Area measurement

The surface area of PNIPAM, NIPAM/BAM 85:15, NIPAM/BAM 65:35 and NIPAM/BAM 50:50 particles was found to be 5.77 ± 0.07 m²/g, 9.57 ± 0.06 m²/g, 14.1 ± 0.1 m²/g and 8.5 ± 0.1 m²/g respectively. With the exception of the 50:50 copolymers, the surface areas correlate reasonably with the particle size.

3.3.2 Ecotoxicity

Testing of reference chemicals in tandem with the polymer nanoparticles was carried out to ensure the validity of each test method. Phenol was used as the reference chemical to validate the Microtox[®] acute test and the 5 min EC₅₀ was determined as 16.5 mg/l. This was in accordance with the Microtox[®] acute toxicity basic test procedures (Azur Environmental, 1998) which stipulates values between 13 and 26 mg/l. In the algal growth inhibition test with *P. subcapitata* a 72 h EC₅₀ of 1.3 mg/l was determined for the reference toxicant potassium dichromate which showed good agreement with published results (Nyholm, 1990). The *T. platyurus* bioassay determined a 24h LC₅₀ value of 0.1 mg/l for the reference chemical potassium dichromate. This value was within the range reported in the test procedure Thamnotoxkit F (1995) protocol. In the *D. magna* test a 24h EC₅₀ value of 0.1 mg/l was determined with the reference chemical potassium dichromate which was consistent with that published in the standard test guideline (BS EN ISO 6341, 1996).

The dose dependent effects of the PNIPAM and NIPAM/BAM particles in the algal tests are shown in Figure 3.3. In the cases of PNIPAM and the NIPAM/BAM series of nanoparticles, concentrations employed were based on extensive range finding tests which revealed the PNIPAM and NIPAM/BAM copolymers to have low acute toxicity to the algal model. However, the results are of merit as there is currently no ecotoxicity data available for these nanoparticles and these results therefore address this lack of environmental data by providing acute toxicity data (72 h) for these nanoparticles.

The calculation of growth inhibition of algae was performed according to (Minagh et al., 2009), as described in chapter 2, section 2.2.2.2. No growth inhibition was observed in the control group (negative control). Statistically significant differences between the treatment and the control group were observed. An increase in algal growth inhibition

with increasing nanoparticles exposure concentration is observed. The growth inhibition was significant ($p < 0.05$) as compared to control group. Maximum algal growth inhibition was observed for NIPAM/BAM 50:50 particles, the least growth inhibition being observed for PNIPAM particles.

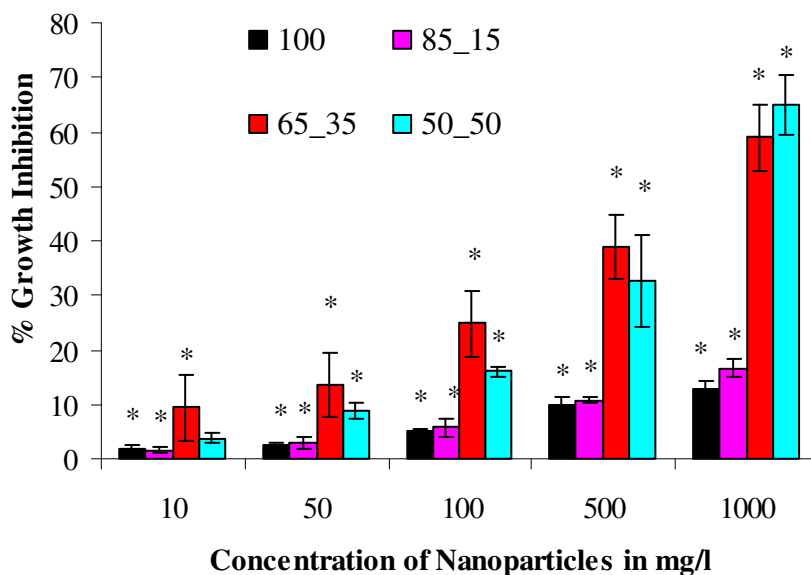


Figure 3.3. Effect of NIPAM and NIPAM/BAM nanoparticles on *P. subcapitata* growth inhibition. Data is presented as the mean \pm SD (N=3). *Denotes significant difference from control ($P \leq 0.05$).

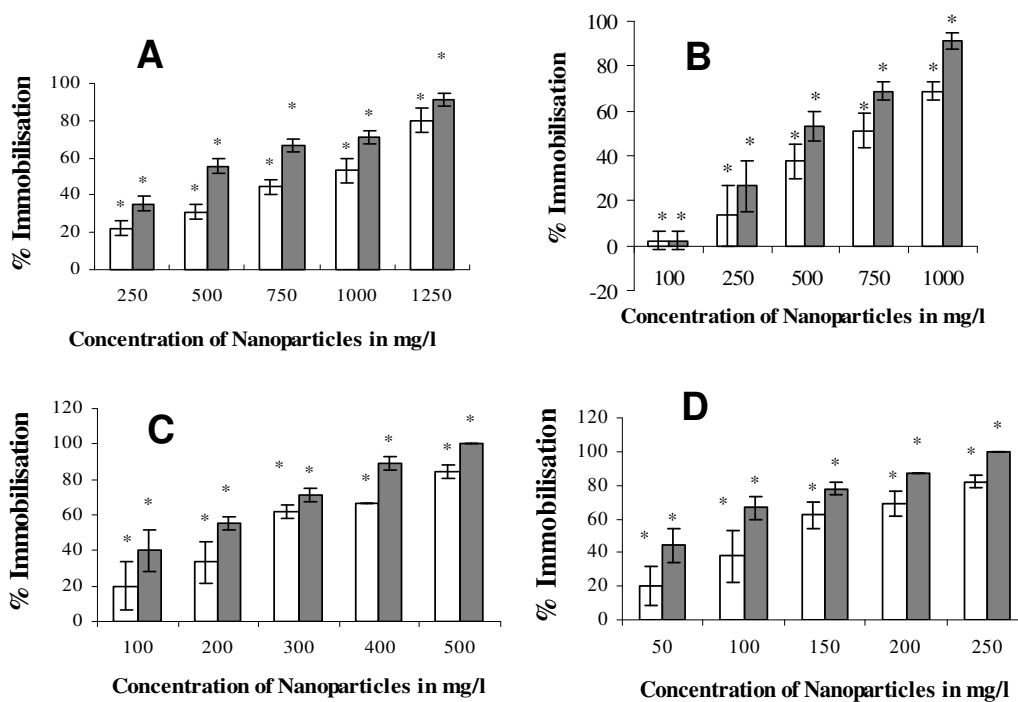


Figure 3.4. Effect of PNIPAM (A); NIPAM/BAM 85:15 (B); NIPAM/BAM 65:35 (C); and NIPAM/BAM 50:50 (D) particles on immobilisation of *Daphnia magna* after (□) 24 hour and (■) 48 hours. Data is presented as the mean \pm SD (N=3). *Denotes significant difference from control ($P \leq 0.05$).

The effects of each of the materials on the invertebrate *Daphnia magna* and *Thamnocephalus platyurus* are presented in Figures 3.4 and 3.5 respectively. Based on initial range finding studies, the exposure concentrations were chosen for the ecotoxicity study of the PNIPAM and NIPAM/BAM series of nanoparticles. Similar dose dependent responses were observed in the *Daphnia magna* after 24 h and 48 h exposures. For all of the NIPAM/BAM series of nanoparticles, with increasing dose, an increase in the immobilisation of *Daphnia magna* was observed for both 24h and 48 h exposures. A significant immobilisation of *Daphnia magna* after nanoparticles exposure was observed as compared to the untreated control group ($P \leq 0.05$) (figure 3.4). The

trend of toxicity of the PNIPAM and NIPAM/BAM series of nanoparticles is PNIPAM < NIPAM/BAM 85:15 < NIPAM/BAM 65:35 < NIPAM/BAM 50:50.

In the case of *Thamnocephalus platyurus*, a similar dose dependent response is observed (figure 3.5). A significant ($P \leq 0.05$) mortality of *Thamnocephalus platyurus* after nanoparticle exposure was observed as compared to the untreated group (figure 3.5). The mortality of *Thamnocephalus platyurus* increases with increased concentration of PNIPAM and NIPAM/BAM nanoparticles after 24 h exposure. The trend of mortality of *Thamnocephalus platyurus* due exposure to the PNIPAM and NIPAM/BAM series of nanoparticles is PNIPAM \leq NIPAM/BAM 85:15 < NIPAM/BAM 65:35 < NIPAM/BAM 50:50.

The cytotoxicity of PNIPAM and NIPAM/BAM 85:15 particles was tested in the concentration range 25-1000 mg l⁻¹ in the RTG-2 cell line at four time points i.e 24 h, 48 h, 72 h and 96 h. NIPAM/BAM 65:35 and NIPAM/BAM 50:50 nanoparticles are not stable in the cell culture media due to a high degree of agglomeration. No significant toxicity was found for PNIPAM and NIPAM/BAM 85:15 nanoparticles at any of the test concentrations with either of the endpoints studied at any of the time points (shown in figure 3.6).

XlfitTM software was employed to evaluate the the EC₅₀/LC₅₀ values for the respective assays and these are listed in Tables 3.2-3.5. In cases where the endpoint does not reach a value of 50%, the software cannot calculate a value for EC₅₀. For these cases, a return of “not calculated” has been recorded. In tables 3.2-3.5, the Lowest Observed Effective Concentration (LOEC) was calculated where a statistically significant ($P \leq 0.05$) effect was observed at the lowest concentration. However the No Observed Effective

Concentration (NOEC) is the concentration where no statistically significant ($P \leq 0.05$) effects were observed. As in some cases, significant effects have been observed at the lowest concentrations, the NOEC values are presented as less than (<) the LOEC value.

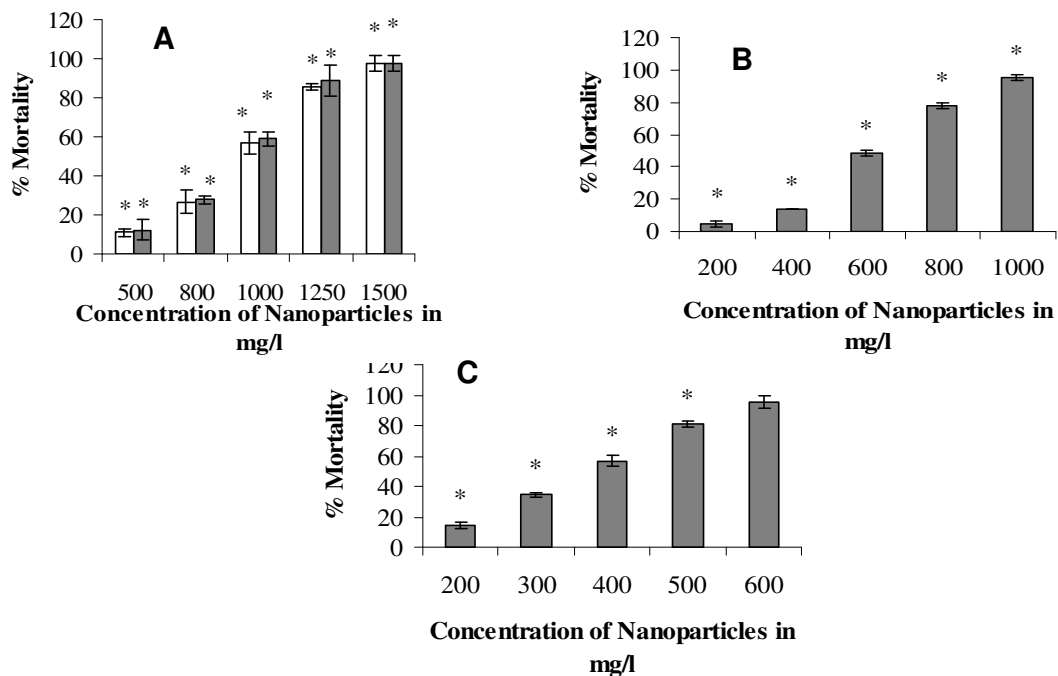
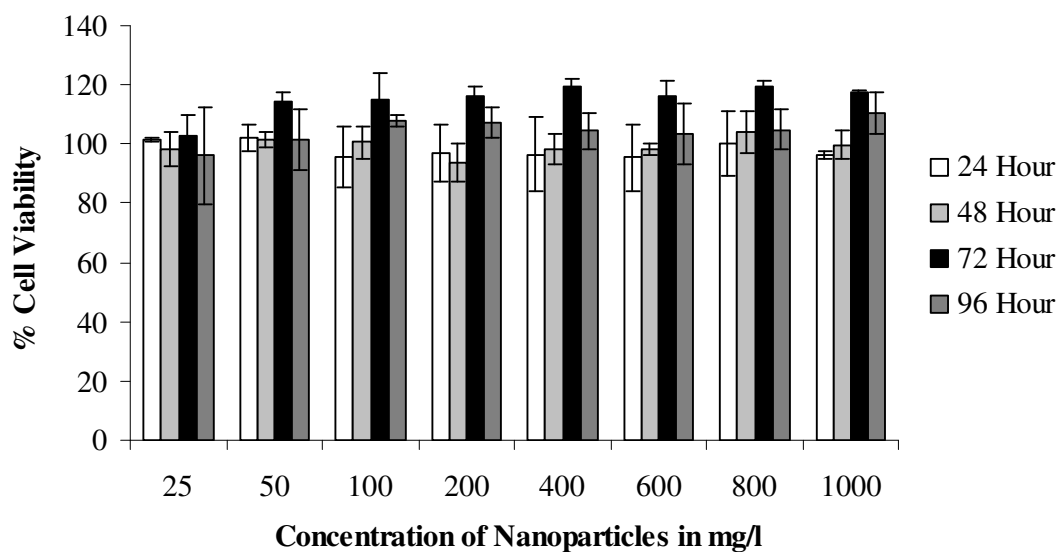


Figure 3.5 : Effect of PNIPAM (□) and NIPAM/BAM 85:15 (■) (A); NIPAM/BAM 65:35 (B); and NIPAM/BAM 50:50 (C) particles on lethality of *Thamnocephalus platyurus*. Data is presented as the mean \pm SD (N=3). *Denotes significant difference from control ($P \leq 0.05$).

A



B

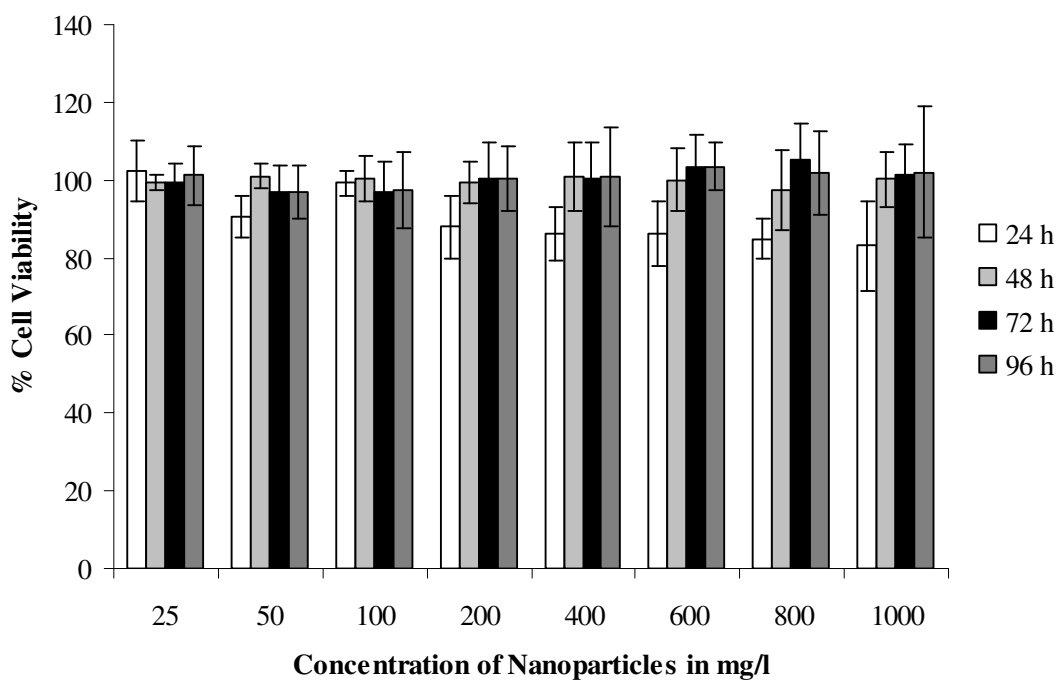


Figure 3.6. Cytotoxicity of (A) PNIPAM and (B) NIPAM/BAM 85/15 nanoparticles in RTG-2 cells. Data is presented as the mean \pm SD (N=3).

3.3.2.1 Ecotoxicity test results with PNIPAM

The results of the ecotoxicity assessment of PNIPAM particles with the four test systems are presented in Table 3.2. Employing the calculated ecotoxicity value (EC_{50}/LC_{50}), in terms of species sensitivity the ranking order for PNIPAM particles is as follows *Daphnia magna* > *Thamnocephalus platyurus*. The EC_{50} for *V. fischeri* and *P.subcapitata* was not calculated as the toxicity did not reach 50 % at the highest concentration. LOEC was calculated where a statistically significant ($P \leq 0.05$) effect was observed at the lowest concentration and the details are given in table 3.2. The LOEC of PNIPAM NPs is 10, 250 and 500 mg/l for *P.subcapitata*, *D. magna* and *T. Platyurus* respectively. The NOEC is the concentration at which no significant difference of toxicity was observed as compared to control. However, in some cases, significant toxicity was observed at the lowest concentration employed in this study and so the NOEC value is recorded as less than the lower concentration employed.

Table 3.2. Ecotoxicity data for poly-*N*-isopropylacrylamide PNIPAM nanoparticles on selected test species and endpoints.

Test Species	End Point and Concentration Range tested (mg l ⁻¹)	EC ₅₀ /LC ₅₀ (mg l ⁻¹) ± SD	Maximum Toxicity (%)	NOEC (mg l ⁻¹)	LOEC (mg l ⁻¹)
<i>V. fischeri</i>	5 min inhibition (3.5-900)	Not calculated	21.5	-	-
<i>P.subcapitata</i>	72 h inhibition (10-1000)	Not calculated	12.75	< 10	10
<i>D. magna</i>	24 h immobilisation (250-1250)	771 ± 103	80	< 250	250
<i>D. magna</i>	48 h immobilisation (250-1250)	413 ± 43	91	< 250	250
<i>T. platyurus</i>	24 h lethality (500-1500)	943 ± 38	97.7	< 500	500

3.3.2.2 Ecotoxicity test results with NIPAM/BAM 85:15

The results of the ecotoxicity evaluation of NIPAM/BAM 85:15 with the test systems are presented in Table 3.3. Based on the calculated ecotoxicity value (EC₅₀/LC₅₀), in terms of species sensitivity, the ranking order for NIPAM/BAM 85:15 nanoparticles is as follows *Daphnia magna* > *Thamnocephalus platyurus*, as was the case for the parent polymer PNIPAM. The EC₅₀ for *V. fischeri* and *P.subcapitata* was not calculated as the toxicity did not reach 50 % at the highest concentration. LOEC was calculated where a statistically significant ($P \leq 0.05$) effect was observed at the lowest concentration and the details were given in table 3.3. The LOEC of NIPAM/BAM 85:15 NPs is 10, 250,

500 and 900 mg/l for *P.subcapitata*, *D. Magna*, *T. Platyurus* and *V. Fischeri* respectively.

Table 3.3. Ecotoxicity data for *N-isopropylacrylamide-co-N-tert-butylacrylamide* (NIPAM/BAM 85:15) copolymer nanoparticles on selected test species and endpoints.

Test Species	End Point and Concentration Range tested (mg l ⁻¹)	EC ₅₀ /LC ₅₀ ± SD (mg l ⁻¹)	Maximum Toxicity (%)	NOEC (mg l ⁻¹)	LOEC (mg l ⁻¹)
<i>V. fischeri</i>	5 min inhibition (3.5-900)	Not calculated	44.3	14.0	900
<i>P. subcapitata</i>	72 h inhibition (10-1000)	Not calculated	16.6	< 10	10
<i>D. magna</i>	24 h immobilisation (100-1000)	675± 121	68.9	250	500
<i>D. magna</i>	48 h immobilisation (100-1000)	449± 80	91.1	100	250
<i>T. platyurus</i>	24 h lethality (500-1500)	931 ± 26	97.7	< 500	500

3.3.2.3 Ecotoxicity tests with NIPAM/BAM 65:35

The results of the ecotoxicity assessment of NIPAM/BAM 65:35 particles with the different test systems are presented in Table 3.4. Employing the calculated ecotoxicity value (EC₅₀/LC₅₀), in terms of species sensitivity the ranking order for NIPAM/BAM 65:35 particles is as follows *Vibrio fischeri* > *Daphnia magna* > *Pseudokirchneriella subcapitata* > *Thamnocephalus platyurus*. The maximum toxicity was observed 100 % with *D. magna*, while it was 58.9 % with *P.subcapitata*. The LOEC of NIPAM/BAM 65:35 NPs is 10, 14.6, 100 and 200 mg/l for *P.subcapitata*, *V. Fischeri*, *D. Magna* and *T. Platyurus* respectively.

Table 3.4. Ecotoxicity data for *N-isopropylacrylamide-co-N-tert-butylacrylamide* (NIPAM/BAM 65:35) copolymer nanoparticles on selected test species and endpoints.

Test Species	End Point and Concentration Range tested (mg l ⁻¹)	EC ₅₀ /LC ₅₀ ± SD (mg l ⁻¹)	Maximum Toxicity (%)	NOEC (mg l ⁻¹)	LOEC (mg l ⁻¹)
<i>V. fischeri</i>	5 min inhibition (3.5-900)	50± 25	62	7.0	14.06
<i>P. subcapitata</i>	72 h inhibition (10-1000)	562±209	58.9	<10	10
<i>D. magna</i>	24 h immobilisation (100-500)	245 ± 42	84	100	200
<i>D. magna</i>	48 h immobilisation (100-500)	114± 32	100	< 100	100
<i>T. platyurus</i>	24 h lethality (200-1000)	602 ± 8	95.5	< 200	200

3.3.2.4 Ecotoxicity tests with NIPAM/BAM 50:50

The results for NIPAM/BAM 50:50 particles from the different test systems are presented in Table 3.5. Employing the calculated ecotoxicity value (EC₅₀/LC₅₀) in terms of species sensitivity the ranking order for NIPAM/BAM 50:50 nanoparticles to the test species is as follows *Vibrio fischeri* > *Daphnia magna* > *Thamnocephalus platyurus* > *Pseudokirchneriella subcapitata*. The LOEC of NIPAM/BAM 50:50 NPs is 28.3, 50, 50 and 200 mg/l for *V. Fischeri*, *P.subcapitata*, *D. Magna* and *T. Platyurus* respectively.

Table 3.5. Ecotoxicity data for *N-isopropylacrylamide-co-N-tert-butylacrylamide* (NIPAM/BAM 50:50) copolymer nanoparticles on selected test species and endpoints

Test Species	End Point and Concentration Range tested (mg l ⁻¹)	EC ₅₀ /LC ₅₀ ± SD (mg l ⁻¹)	Maximum Toxicity (%)	NOEC (mg l ⁻¹)	LOEC (mg l ⁻¹)
<i>V. fischeri</i>	5 min inhibition (3.5-900)	24± 0.5	71.3	14.0	28.3
<i>P. subcapitata</i>	72 h inhibition (10-1000)	707 ±66	65	10	50
<i>D. magna</i>	24 h immobilisation (50-250)	119± 31	82.2	50	100
<i>D. magna</i>	48 h immobilisation (50-250)	60± 14	100	< 50	50
<i>T. platyurus</i>	24 h lethality (200-600)	353± 8	95.5	< 200	200

3.4 Discussion

The particle size of the different materials was measured in different media. The expected particle size decrease as a function of temperature expected for these thermoresponsive polymers is observed only in the MQ environment. The particle size of PNIPAM and NIPAM/BAM copolymer nanoparticles was found to increase with increase in temperature in AM, DM, and MD media, however, with the average particle size increasing to several microns as the materials undergo the phase transition. This behaviour is characteristic of agglomeration, as a consequence of the screening effect of the salts in the various test media. It is proposed therefore that the particles interact with different components of the media and agglomerates when the temperature is increased above the respective LCST.

The zeta potential of PNIPAM and the different NIPAM/BAM copolymer nanoparticles was shown to decrease (NIPAM < NIPAM/BAM 85:15 < NIPAM/BAM 65:35 < NIPAM/BAM 50:50) with increasing BAM ratio as presented in Figure 3.2. This increasingly negative value of the zeta potential of the co-polymer particle surface is consistent with the reduced hydrophilicity (as determined by contact angle measurements) as a result of the increased BAM content (Lynch et al., 2005; Allen et al., 2003). A similar trend was observed with all the media tested but was most significant when the nanoparticles were tested in MQ water. Such a decrease in the zeta potential of nanoparticles in growth media is commonly observed (Hang et al., 2007) and is attributable to shielding of the potential due to adsorption of and/or interaction with components of the medium by the nanoparticles, supporting the conclusions of the particle size measurements.

In terms of response, Poly *N*-isopropylacrylamide particles were found to be the least toxic among all the NIPAM/BAM copolymer particles tested in this study. The most sensitive test species to PNIPAM nanoparticles was the *Daphnia magna* (48 hour EC₅₀ 413.6 mg l⁻¹) and the least sensitive test species was the *Pseudokirchneriella subcapitata* (72 hour EC₅₀ > 1000 mg l⁻¹).

The NIPAM/BAM 85:15 nanoparticles demonstrated a very similar toxicity profile to PNIPAM with *Daphnia magna* being the most sensitive test species (48 hour EC₅₀ is 449.6 mg l⁻¹) and *Pseudokirchneriella subcapitata* the least sensitive (72 hour EC₅₀ is > 1000 mg l⁻¹). NIPAM/BAM 65:35 nanoparticles were shown to be more toxic than PNIPAM and this increase in toxicity was attributed to the increase in BAM ratio in the copolymer nanoparticles. There was a change in the test species sensitivity to this particle in comparison to PNIPAM and NIPAM/BAM 85:15 nanoparticles with the bacterium *Vibrio fischeri* (5 minutes EC₅₀ 40.5 mg l⁻¹) showing greater sensitivity than

the *Daphnia magna* bioassay in this case. The least sensitive test species are *Pseudokirchneriella subcapitata* (72 hour EC₅₀ 727.1 mg l⁻¹).

NIPAM/BAM 50:50 nanoparticles were found to be the most toxic to the test battery compared to the other three copolymer nanoparticles. The species sensitivity to these particles was found to be in the same order as that of the NIPAM/BAM 65:35 nanoparticles with *Vibrio fischeri* (5 minutes EC₅₀ 25.7 mg l⁻¹) as the most sensitive and *Pseudokirchneriella subcapitata* (72 hour EC₅₀ 706.7 mg l⁻¹) as the least sensitive test. The sensitivity of the test species varied as the physicochemical characteristics of the PNIPAM and NIPAM/BAM copolymer particles changed. The most sensitive bioassay for PNIPAM and NIPAM/BAM 85:15 particles were found to be the immobilisation of *Daphnia magna* (48 hour EC₅₀) followed by mortality of *Thamnocephalus platyurus* (24 hour LC₅₀). The most sensitive test for NIPAM/BAM 65:35 and NIPAM/BAM 50:50 particles was the Microtox[®] assay (*Vibrio fischeri*, 5 minutes EC₅₀) followed by the immobilisation of *Daphnia magna* (48 hour EC₅₀) and mortality of *Thamnocephalus platyurus* (24 hour LC₅₀). The least sensitive bioassay was the *Pseudokirchneriella subcapitata* (72 hour LC₅₀) for the four test particles. The cytotoxicity of PNIPAM and NIPAM/BAM 85:15 were studied in RTG-2 cells and from this study it was observed that there was no significant difference in terms of cell viability between control and cells exposed to the polymer particles. Neither the PNIPAM nor NIPAM/BAM 85:15 particles were found to be toxic to the fish cells at the concentrations and time points tested in this study (shown in figure 3.6). Cytotoxicity in RTG-2 was assessed at the recommended growth temperature of 20°C. NIPAM/BAM 65:35 and NIPAM/BAM 50:50 were demonstrated to form large aggregates at this temperature, due to the low LCST, which led to both materials floating in the cell culture media. For a cytotoxicity assessment the particles should be fully dispersed and capable of interaction with the

cells so in this case it was not considered practical to test these particles with the cell line.

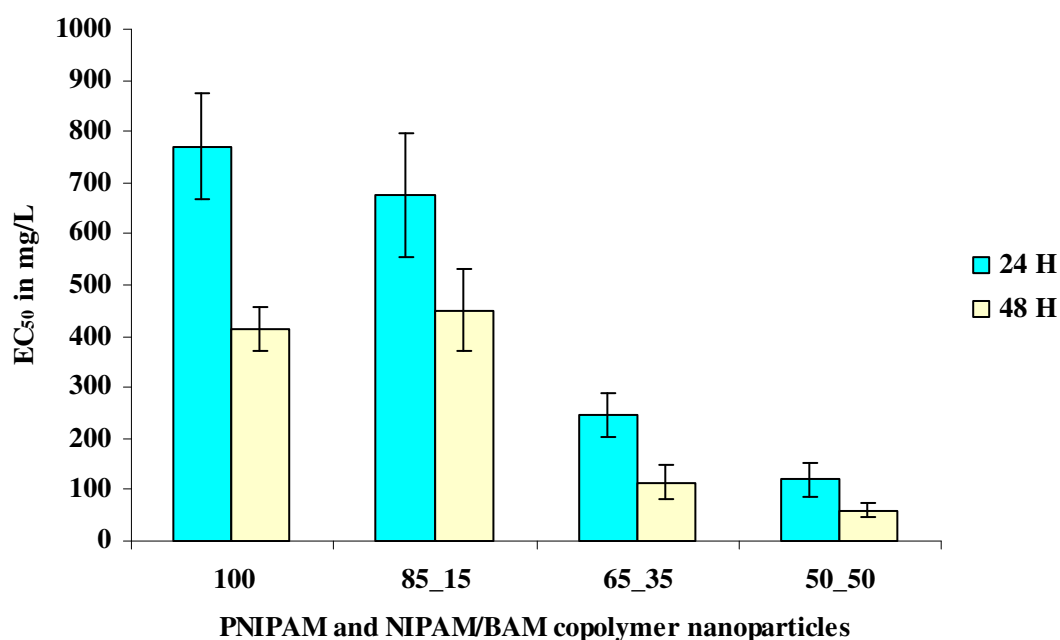


Figure 3.7. Relationship between EC_{50} for immobilisation of *Daphnia magna* following exposure to PNIPAM and different NIPAM/BAM copolymer particles.

The toxicity of the polymer nanoparticles gradually increased in the entire test species (except RTG-2 cells) as a function of increasing BAM ratio. This relationship with increasing ratio of BAM is shown for the EC_{50} of the 24 and 48 h acute immobilisation test with *Daphnia magna* in Figure 3.7. An increase in the ratio of the monomer BAM was also shown to cause a concomitant decrease in the LC_{50} value (i.e. more toxic) following 24 h exposure of the invertebrate *Thamnocephalus platyurus* (Figure 3.8). The monomer ratio has, however, also been shown to be related to the measured zeta potential and therefore the measured ecotoxicity response may be associated with the zeta potential as indicated in Figure 3.9.

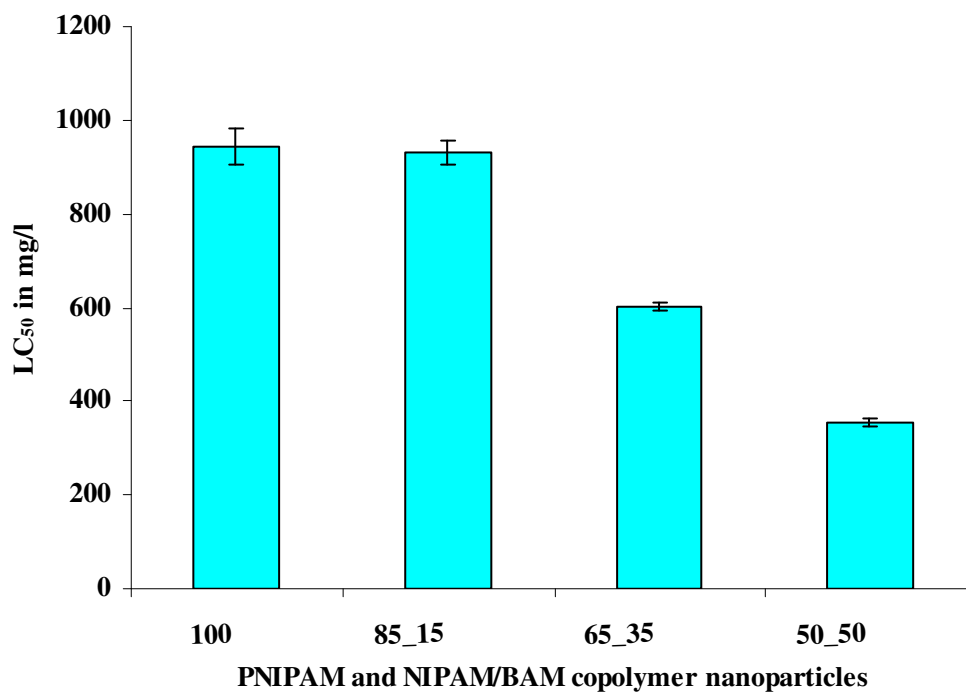


Figure 3.8. Effect of PNIPAM and different NIPAM/BAM copolymer nanoparticles on 24 h LC₅₀ in *Thamnocephalus platyurus*.

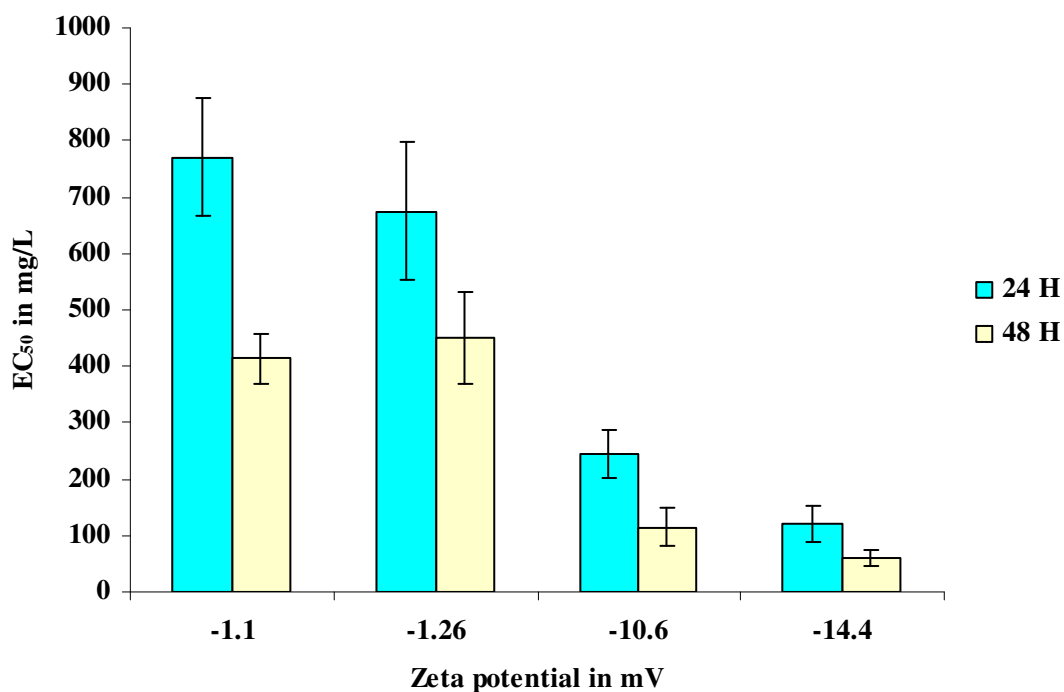


Figure 3.9. Association of zeta potential of different copolymer nanoparticles on immobilisation of *Daphnia magna* based on the EC₅₀ results.

No correlation with particle size was observed for the test results and thus the increased toxic response must be associated with the decreased hydrophilicity and therefore zeta potential of the copolymer particles with increasing BAM content. For a given particle composition, the zeta potentials are significantly reduced in all growth media, indicating a further decrease of hydrophilicity and higher agglomeration due to surface charge screening, as evidenced by the reduction of zeta potential, by the ionic salts of the media. It is worth noting that, for the 50:50 and 65:35 NIPAM/BAM copolymer nanoparticles, the degree of screening (i.e. reduction of zeta potential) is highest for the Microtox diluent (Figure 3.2), and that this assay shows the highest sensitivity for these particles. For the PNIPAM and 85:15 NIPAM/BAM particles, the largest reduction of zeta potential is in the *Daphnia* medium, and again the *Daphnia* assay was seen to be the most sensitive assay for these particles. This observation may point towards a better understanding of the mechanisms of the toxic response. In, for example, studies of the toxic response of mammalian cells to carbon nanotubes, it has been seen that medium depletion by interaction with the molecular components of the medium results in a significant indirect toxic response (Casey et al., 2008). The interaction with the medium components implied here could similarly contribute to the toxic response observed. Figure 3.10 indicates an association of the observed toxic response in the *Daphnia magna* system after 24 h with the change in the zeta potential of the polymer nanoparticles in the *Daphnia* medium.

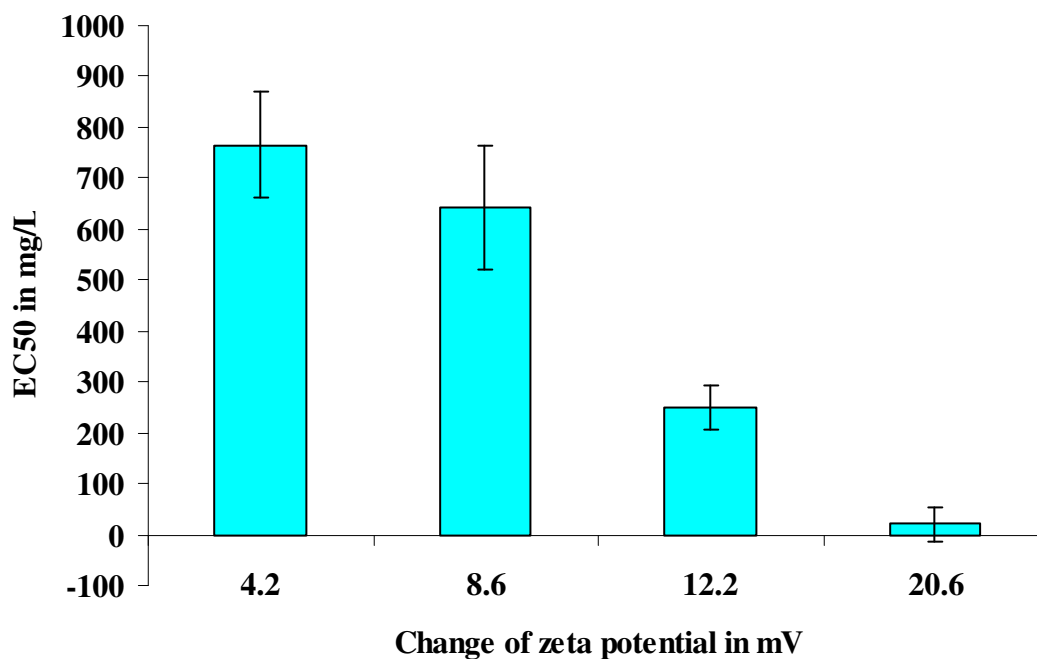


Figure 3.10. Relation between change in zeta potential and EC_{50} in immobilisation of *Daphnia magna* with different PNIPAM and NIPAM/BAM copolymer.

Thus the interaction of the particles with the medium may be associated with the toxic response suggesting a secondary toxic mechanism, similar to that observed in mammalian cells exposed to single walled carbon nanotube samples. Although the media for the test species employed here is very different in nature to that used for mammalian cytotoxicity, in that it is made up of salts to modify the aqueous environment rather than essential nutrients, the interaction with the medium components suggested here could result in changes in the ionic strength of the media and similarly contribute to the toxic response observed. This correlation of response to reduction of zeta potential does not simply correlate to all endpoints for a given particle composition however, and the association with the remnant particle zeta potential indicated in Figure 3.9 implies an intrinsic primary toxic response which is dependent on nanoparticle composition. Further studies of particle uptake by the different species are therefore merited to further understand the mechanisms underlying the toxic response. Additionally, parallel studies on the test species in media

systematically depleted of individual salt components may shed additional light on the toxicity mechanism.

3.5 Conclusions

PNIPAM and NIPAM/BAM nanoparticles are well known thermoresponsive particles and to the best of our knowledge there is no ecotoxicity data of NIPAM/BAM nanoparticles available to date. The most sensitive ecotoxicological assay for PNIPAM and NIPAM/BAM 85:15 nanoparticles was the immobilisation of *Daphnia magna* (48 hour EC₅₀) and for NIPAM/BAM 65:35 and NIPAM/BAM 50:50 nanoparticles was the Microtox[®] assay (*Vibrio fischeri*, 5 minutes EC₅₀). The least sensitive bioassay was *Pseudokirchneriella subcapitata* (72 h EC₅₀) except NIPAM/BAM 65:35 nanoparticles among the four nanomaterials tested. An important conclusion from the study therefore is that the sensitivity of each assay is dependent on the physico-chemical characteristics of the particle, emphasising the importance of a multi-trophic approach. As the ratio of BAM increases in the copolymer nanoparticle the toxicity was increased in all the test species, despite the fact that the particles with the highest ratio of BAM were highly agglomerated. The toxicity trend for different nanoparticles was NIPAM < NIPAM/BAM 85:15 < NIPAM/BAM 65:35 < NIPAM/BAM 50:50, which suggests that there is a significant effect due to particle hydrophobicity and the surface free energy (Lynch et al., 2005). This is supported by the association of the toxic response with the observed zeta potential of the particles in the medium. The correlation of the toxic response in *Daphnia magna* with the reduction in zeta potential points towards a contribution of secondary effects due to modification of the medium. No dependence of the toxic response on the particle size was observed however. Nevertheless the study indicates a clear dependence of the toxic response on the particle composition pointing

towards structure-activity relationships. The mammalian toxicity of PNIPAM nanoparticles is discussed in chapter 4. Due to the lower LCST of the NIPAM/BAM 85:15, 65:35 and 50:50 nanoparticles are unstable at 37 °C and thus their mammalian toxicity was not studied.

References

- Allen, L. T., Fox, E.J., Blute, I., Kelly, Z.D., Rochev, Y., Keenan, A.K., Dawson, K.A., Gallagher, W.M., 2003. Interactions of soft condensed materials with living cells: phenotype/transcriptome correlations for the hydrophobic effect. *Proc. Natl. Acad. Sci. USA.* 100, 6331-6336.
- Azur Environmental (1998). Microtox[®] acute toxicity basic test procedures, Report, Carlsbad, CA. pp 1-13.
- Baun, A., Sorensen, S.N., Rasmussen, R.F., Hartmann, N.B., Koch, C.B., 2008. Toxicity and bioaccumulation of xenobiotic organic compounds in the presence of aqueous suspensions of aggregates of nano-C₆₀. *Aquat. Toxicol.* 86, 379-387.
- BS EN ISO 6341 (1996). Water Quality Determination of the Inhibition of the Mobility of *Daphnia magna* Strauss (Cladocera, Crustacea) Acute Toxicity Test. British Standards Institution, London.
- Cabaleiro-Lago, C., Quinlan-Pluck, F., Lynch, I., Lindman, S., Minogue, A.M., Thulin, E., Walsh, D.M., Dawson, K.A., Linse, S. 2008. Inhibition of amyloid β protein fibrillation by polymeric nanoparticles. *JACS*, in press.
- Casey, A., Herzog, E., Lyng, F.M., Byrne, H.J., Chambers, G., Davoren, M., 2008. Single walled carbon nanotubes induce indirect cytotoxicity by medium depletion in A549 lung cells. *Toxicol. Lett.* 179, 78-84.
- Cedervall, T., Lynch, I., Foy, M., Berggård, T., Donnelly, S.C., Cagney, G., Linse, S., Dawson, K.A., 2007. Detailed identification of plasma proteins adsorbed on copolymer nanoparticles. *Angew. Chem. Int. Ed. Engl.* 46, 5754-5756.

- Cheng, J., Flahaut, E., Cheng, S.H., 2007. Effect of carbon nanotubes on developing zebrafish (*Danio rerio*) embryos. *Environmental Toxicology and Chemistry*. 26, 708-716.
- Federici, G., Shaw, B.J., Handy, R.D., 2007. Toxicity of titanium dioxide nanoparticles to rainbow trout (*Oncorhynchus mykiss*): Gill injury, oxidative stress, and other physiological effects. *Aquat. Toxicol.* 84, 415-430.
- Gagné, F., Auclair, J., Turcotte, P., Fournier, M., Gagnon, C., Sauve, S., Blaise, C., 2008. Ecotoxicity of CdTe quantum dots to fresh water mussels: Impacts on immune system, oxidative stress and genotoxicity. *Aquat. Toxicol.* 86, 333-340.
- Hang, J. Z., Zhang, Y. F., Shi, L. Y., Feng, X., 2007. Electrokinetic properties of barite nanoparticles suspensions in different electrolyte media. *Journal of Materials Science*. 42, 9611-9616.
- Heinlaan, M., Ivask, A., Blinova, I., Dubourguier, H.C., Kahru, A., 2008. Toxicity of nanosized and bulk ZnO, CuO and TiO₂ to bacteria *Vibrio fischeri* and crustaceans *Daphnia magna* and *Thamnocephalus platyurus*. *Chemosphere*. 71, 1308-1316.
- Hsiue, G.H., Chang, R.W., Wang, C.H., Lee, S.H., 2003. Development of in situ thermosensitive drug vehicles for glaucoma therapy. *Biomaterials*. 24, 2423-2430.
- Hsiue, G.H., Hsu, S.H., Yang, C.C., Lee, S.H., Yang, I.K., 2002. Preparation of control release ophthalmic drops, for glaucoma therapy using thermosensitive poly-*N*-isopropylacrylamide. *Biomaterials*. 23, 457-462.
- Kavanagh, C.A., Gorelova, T.A., Selezneva, I.I., Rochev, Y.A., Dawson, K.A., Gallagher, W.M., Gorelov, A.V., Keenan, A.K. 2005. Poly(*N*-isopropylacrylamide) copolymer films as vehicles for the sustained delivery of proteins to vascular endothelial cells. *J. Biomed. Mater. Res. A*. 72, 25-35.

- Lin, D., Xing, B., 2007. Phytotoxicity of nanoparticles: Inhibition of seed germination and root growth. *Environ. Pollut.* 150, 243-50.
- Linse, S., Lago, C.C., Xue, W.F., Lynch, I., Lindman, S., Thulin, E., Radford, S.E., Dawson, K.A., 2007. Nucleation of protein fibrillation by nanoparticles. *Proc. Natl. Acad. Sci. USA.* 104, 8691-8696.
- Lovern, S.B., Klaper, R., 2006. *Daphnia magna* mortality when exposed to titanium dioxide and fullerene (C₆₀) nanoparticles. *Environmental Toxicology and Chemistry.* 25, 1132-1137.
- Lovern, S.B., Strickler J.R., Klaper, R., 2007. Behavioral and physiological changes in *Daphnia magna* when exposed to nanoparticle suspensions (titanium dioxide, nano-C60, and C60HxC70Hx). *Environ. Sci. Technol.* 41, 4465-7.
- Lynch, I., Blute, I.A., Zhmud, B., MacArtain, P., Tosetto, M., Allen, L.T., Byrne, H.J., Farrell, G.F., Keenan, A.K., Gallagher, W.M., Dawson, K.A. 2005. Correlation of the Adhesive Properties of Cells to *N*-Isopropylacrylamide/*N*-*tert*-Butylacrylamide Copolymer Surfaces with Changes in Surface Structure Using Contact Angle Measurements, Molecular Simulations, and Raman Spectroscopy. *Chem. Mater.* 17, 3889 - 3898.
- Meng, H., Chen, Z., Xing, G., Yuan, H., Chen, C., Zhao, F., Zhang, C., Zhao, Y., 2007. Ultrahigh reactivity provokes nanotoxicity: Explanation of oral toxicity of nano-copper particles. *Toxicology Letters*, 175, 102-110
- Mortimer, M., Kasemets, K., Heinlaan, M., Kurvet, I., Kahru, A., 2008. High throughput kinetic *Vibrio fischeri* bioluminescence inhibition assay for study of toxic effects of nanoparticles. *Toxicol. In Vitro*, 22, 1412-1417.
- Nowack, B., Bucheli, T.D., 2007. Occurrence, behavior and effects of nanoparticles in the environment. *Environmental Pollution.* 150, 5-22.

- Nyholm, N. 1990. Expression of results from growth inhibition toxicity tests with algae. Arch. Environ. Contam. Toxicol. 19, 518-522.
- Oberdörster, G., Oberdörster, E., Oberdörster, J., 2005. Nanotoxicology: an emerging discipline evolving from studies of ultra fine particles. Environ. Health Perspect. 113, 823-839.
- OECD, 2002. Guideline for testing of chemicals. In: Freshwater Alga and Cyanobacteria, Growth Inhibition Test, Method 201, OECD.
- Papageorgiou, I., Brown, C., Schins, R., Singh, S., Newson, R., Davis, S., Fisher, J., Ingham E., Case C.P. 2007. The effect of nano- and micron-sized particles of cobalt–chromium alloy on human fibroblasts *in vitro*. Biomaterials 28, 2946-2958.
- Poland, C.A., Duffin, R., Kinloch, I., Maynard, A., Wallace, W.A.H., Seaton, A., Stone, V., Brown, S., MacNee, W., Donaldson, K., 2008. Carbon nanotubes introduced into the abdominal cavity of mice show asbestos like pathogenicity in a pilot study. Nat. Nanotechnol. 3, 423-428.
- Singh,S., Shi, T., Duffin, R Albrecht, C., van Berlo, D., Höhr, D., Fubini, B., Martra, G., Fenoglio, I., Borm, P.J.A., Schins, R.P.F. 2007. Endocytosis, oxidative stress and IL-8 expression in human lung epithelial cells upon treatment with fine and ultrafine TiO₂: Role of the specific surface area and of surface methylation of the particles. Toxicol Appl Pharmacol. 222, 141-151
- Smith, C.J., Shaw, B.J., Handy, R.D., 2007. Toxicity of single walled carbon nanotubes to rainbow trout, (*Oncorhynchus mykiss*): respiratory toxicity, organ pathologies, and other physiological effects. Aquat. Toxicol. 82, 94-109.
- Thamnotoxkit, FTM., 1995. Crustacean toxicity screening test for freshwater. Standard Operating Procedure, Creasal, Deinze, Belgium.

-
- Xu, F.J., Kang, E.T., Neoh, K.G., 2006. pH and temperature responsive hydrogel from crosslinked triblock copolymers prepared via consecutive atom transfer radical polymerization. *Biomaterials*. 27, 2787-2797.
- Xu, F.Z., Zhong, S.P., Yung, L.Y.L., Kang, E.T., Neoh, K.G., 2004. Surface-active and stimuli-response polymer-Si(100) hybrid from surface-initiated atom transfer radical polymerization for control of cell adhesion. *Biomacromolecules*. 5, 2392-2403.
- Zhang, X.Z., Yang, Y.Y., Chung, T.S., Ma, K.X., 2001. Preparation and Characterization of Fast Response Macroporous Poly(*N*-isopropylacrylamide) Hydrogels. *Langmuir*. 17, 6094-6099.
- Zhang, X.Z., Lewis, P.J., Chu, C.C., 2005. Fabrication and characterization of a smart drug delivery system: microsphere in hydrogel. *Biomaterials*. 26, 3299-3309.
- Zhu, Y., Zhao, Q., Li, Y., Cai, X., Li, W., 2006. The interaction and toxicity of multi-walled carbon nanotubes with *Stylonychia mytilus*. *J. Nanosci. Nanotechnol.* 6, 1357-1364.

Chapter 4

In vitro mammalian toxicology of PNIPAM nanoparticles

Adapted from “Intracellular localisation, Geno- and Cytotoxic response of Poly *N*-isopropylacrylamide (PNIPAM) nanoparticles to human keratinocyte (HaCaT) and colon cells (SW 480)” *Toxicology Letters*, 2010. 198, 134-143.

Authors: Pratap C. Naha, Kunal Bhattacharya, Tiziana Tenuta, Kenneth A.

Dawson, Iseult Lynch, Amaya Gracia, Fiona M. Lyng, Hugh J. Byrne

4.1 Introduction

Poly *N*-isopropylacrylamide (PNIPAM) is a well known thermoresponsive polymer (Hsiue et al. 2002) which exhibits a lower critical solution temperature (LCST) of about 32°C in aqueous media (Xu et al., 2006). Adjustment of the LCST to near body temperature (Zhang and Misra 2007) is essential, particularly for ‘smart’ drug delivery applications (Peppas et al. 2000; Lin and Metters 2006). Because of this reversible phase transition, PNIPAM has been widely used as stimuli responsive polymer for biomedical applications, such as in the controlled release of drugs and in tissue engineering (Kavanagh et al. 2005; Xu et al., 2006; Xu et al. 2004; Zhang et al., 2005). Given their potential widespread use, there is an increasing need for information regarding the human health and environmental implications of these polymeric nanomaterials. To date the human health impacts of nanomaterials have received the greatest attention, and it has been demonstrated through both *in vivo* and *in vitro* studies with mammalian test systems that the properties that make nanomaterials so attractive from a commercial application viewpoint (*e.g.* nanoparticle size and increased surface area) can also potentially be responsible for undesirable health effects (Meng et al. 2007; Oberdorster et al., 2005; Papageorgiou et al. 2007; Poland et al. 2008; Singh et al. 2007). However, to date, no conclusive links between engineered nanoparticles and a biological or health impact have been observed, and insufficient data exists to make generalisations about the biocompatibility or safety of nanomaterials in general, or even about a specific nanoparticle type.

The aim of the present investigation, therefore, is the measurement, characterisation and assessment of the mammalian cytotoxicity and genotoxicity of PNIPAM nanoparticles in immortalised non-cancerous human keratinocyte (HaCaT) and a primary adenocarcinoma of human colon (SW480) cell line, as dermal and intestinal models

respectively, these being considered two of the potential routes of exposure to nanomaterials. Physico-chemical characterisation of PNIPAM nanoparticles was performed in terms of measurement of hydrodynamic diameter and zeta potential in the appropriate cell culture media. As the particles are thermoresponsive in nature, the particle size was measured as a function of temperature, because all exposures were performed at 37 °C. Cellular uptake and co-localisation studies were carried out with fluorescently-labelled PNIPAM nanoparticles, synthesised in the presence of a fluorescent co-monomer, using Confocal Laser Scanning Microscopy (CLSM).

4.2 Experimental methods

All experimental methods and protocols are described in chapter 2. Specifically, particle size measurement, zeta potential and BET surface area measurement are described in chapter 2, section 2.2.1.1, 2.2.1.2 and 2.2.1.4 respectively. Intracellular uptake and co-localisation of PNIPAM nanoparticles protocols are described in section 2.2.2.7 and 2.2.2.8. Cytotoxicity assay and genotoxicity protocols are described in section 2.2.2 and 2.2.2.12.

4.3 Results

4.3.1 Characterisation of PNIPAM nanoparticles

The hydrodynamic diameter of PNIPAM nanoparticles was measured as a function of increasing temperature due to its thermoresponsive nature. When the temperature is raised above the LCST, the polymer undergoes a phase transition and the random coil structure (hydrophilic state) collapses to form a globular structure (hydrophobic state) (Xu et al., 2006). This behaviour of decreasing particle size with increasing temperature is demonstrated well by the temperature dependence of the nanoparticles when prepared

in MQ water (Table 4.1). In our experiments, the measured particle size of PNIPAM nanoparticles was found to increase with increasing temperature when they were prepared in cell culture media (Table 4.1), although in MQ water the particle size decreases with increasing temperature. Transmission Electron Microscopy confirmed the as produced particles to have a dry size of 40 ± 10 nm, as shown in the representative TEM image of Figure 4.1.

The BET surface area of the unlabelled PNIPAM nanoparticles was found previously to be 5.77 ± 0.07 m²/g (Section 3.2.1.3 of Chapter 3 and Naha et al., 2009b). Zeta potentials of the PNIPAM nanoparticles were measured in MQ water, DMEM and supplemented cell culture media (Table 4.2). Zeta potential is a measure of the electrophoretic mobility of the nanoparticles in the medium. In the absence of change of the agglomeration state of the nanoparticles, or the content of the medium, no change in mobility is expected as a function of concentration.

Table 4.1. Hydrodynamic diameter (nm) of NIPAM nanoparticles with increasing temperature in different media

Conc. of Nanoparticles	Type of Media	Size nm (30 °C)	Size (nm) (32 °C)	Size (nm) (34 °C)	Size (nm) (36 °C)	Size (nm) (38 °C)
1000 mg/l	Water	90.6 ± 4.5	84.3 ± 2.4	74.7 ± 3.1	57.36 ± 2.3	52.72 ± 1.1
100 mg/l	Water	88.9 ± 3.6	82.2 ± 1.9	75.3 ± 3.4	55.3 ± 2.5	49.2 ± 1.1
1000 mg/l	DMEM	90.9 ± 3.6	343 ± 32	1324 ± 179	1781 ± 86	2936 ± 150
100 mg/l	DMEM	85.7 ± .66	88.1 ± 4.9	708 ± 65	1424 ± 97	1497 ± 77
1000 mg/l	DMEM with 5% FBS	88.1 ± 2.9	422 ± 45	1129 ± 140	1266 ± 36	1259 ± 93
100 mg/l	DMEM with 5% FBS	83.4 ± 4.3	81.5 ± 6.5	407.8 ± 16.1	563.2 ± 11.9	641.5 ± 82.9
1000 mg/l	DMEM with 10 % FBS	89.9 ± 7.9	368.9 ± 31.1	879.4 ± 34.6	950.6 ± 55.7	853.1 ± 11.5
100 mg/l	DMEM with 10 % FBS	86.8 ± 6.5	71.3 ± 17.4	285.8 ± 77.6	461.8 ± 34.43	473.3 ± 51.4

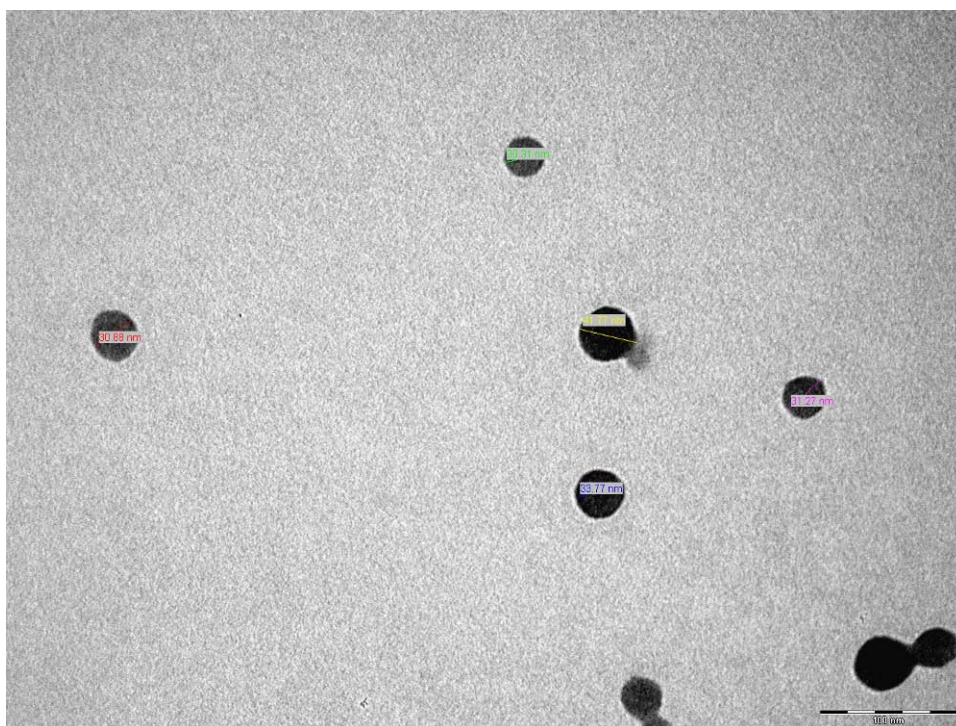


Figure 4.1: Representative TEM image of the labelled PNIPAM nanoparticles. Scale bar is 100 nm.

Table 4.2. Zeta potential of NIPAM nanoparticles in different media

Type of media	Zeta potential in mV
Milli-Q Water	-5.38 ± 0.52
DMEM	-1.33 ± 0.66
DMEM with 5% FBS	-7.09 ± 0.34
DMEM with 10% FBS	-7.93 ± 0.63

4.3.2 Intracellular uptake study

An intracellular uptake study was performed with the fluorescently labelled PNIPAM nanoparticles, the uptake and localisation of the particles in HaCaT and SW480 cells being visualised by CLSM after 24 hours of exposure. As the cytotoxicity and genotoxicity of PNIPAM nanoparticles were investigated in these two cell lines, the uptake study was performed with the same cell lines. The internalisation of the particles

is illustrated in Figure 4.2 and optical sections (z-sections) of the HaCaT and SW 480 cells are shown in Figure 4.3. Each optical section represents a particular plane of focus and it is clear that the nanoparticles have been internalised completely, rather than being accumulated in or at the cell membrane. Washing of the cells prior to observation in the confocal microscope also ensured that non-internalised particles were removed. Each optical section represents a particular plane of focus and it is clear that the nanoparticles have been internalised completely, rather than being accumulated in or at the cell membrane. For HaCaT cells 18 z section and for SW 480 cells 21 z sections were taken. Each section is separated by 0.41 and 1 μ m for HaCaT and SW 480 cell respectively. The results demonstrate that the PNIPAM nanoparticles were taken up and distributed throughout the cell within 24 hrs of exposure.

A common mechanism which has been identified for the cellular uptake of nanoparticles is by endocytosis, after which the particles are trafficked through endosomes and later lysosomes (Nel et al., 2009; Salvati, et al., 2011; Shapero et al., 2011). In order to confirm that the PNIPAM nanoparticles are indeed taken up by the cells, and to explore their intracellular localisation, LysoTracker was used. LysoTracker has previously been used for tracking of the nanoparticles in the lysosomes in confocal microscopy (Contreras et al., 2010; Shi et al., 2010; Neun and Stern, 2011).

Figure 4.4 (1D and 2D) shows an overlay of the LysoTracker and PNIPAM nanoparticle fluorescence in HaCaT cells for exposure doses of 30 and 50 mg/l respectively, after 24hrs. Although the lateral resolution does not allow a precise visualization, the observations are consistent with a localization of the nanoparticles predominantly in lysosomal compartments, although some nanoparticle fluorescence is distributed elsewhere in the cytoplasm. Unfortunately a quantitative assessment of the degree of colocalisation was not possible, as the protocol and data sheet of LysoTracker dye

(invitrogen), lysotracker dye only stains a fraction of the cells (Lysotracker Data Sheet, Invitrogen) .

The results of the co-localisation study, in which lysosomes were co-stained using lysotracker green, are consistent with localisation of the PNIPAM nanoparticles in lysosomes (Figure 4.4). No evidence of localisation within the cell nuclei was observed. This is not unexpected, given the large size of the agglomerates in the cell culture medium. From the images of Figures 4.2 and 4.4, it appears that further particle agglomeration may be occurring intracellularly, or that particles are being accumulated into the lysosomes. Lysosomes have also been shown to be the final destination for polystyrene and silica nanoparticles following uptake by a range of cell types (Shapero et al., 2011, Salvati et al. 2011). Additionally, once the particles reach the lysosomes they do not exit over at least a 24 hour time period, (Salvati et al., 2011) and this is likely also the case for the PNIPAM particles. In the case of nanoparticles with a high positive surface charge density, for example PAMAM dendrimers, excessive oxidative stress via the proton pump mechanism has been shown to result in endosomal or lysosomal rupture and release of the nanoparticles into the cytosol. However, such a mechanism is unlikely for these weakly anionic particles.

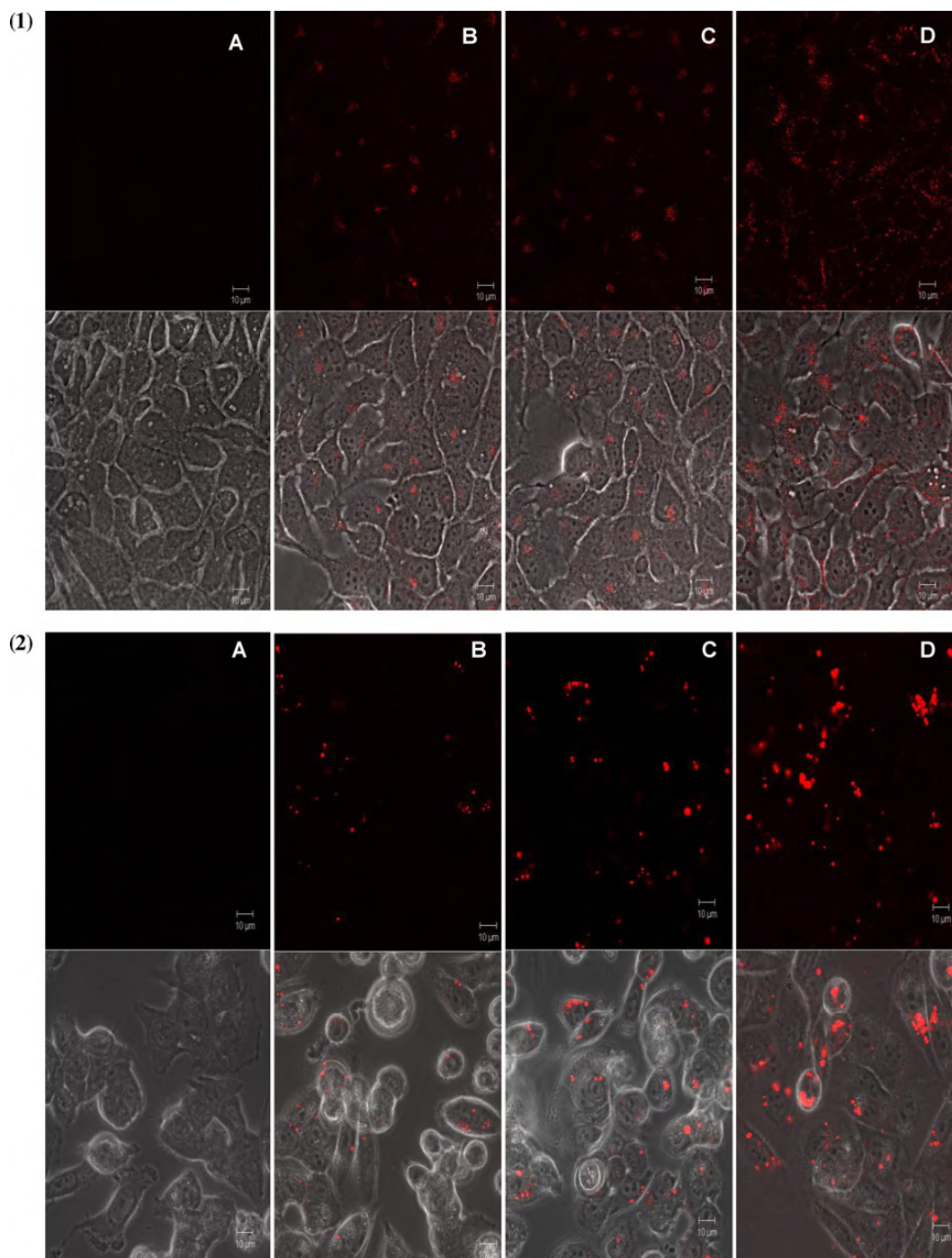


Figure 4.2. Confocal laser scanning micrograph (CLSM) of internalisation of fluorescent labelled PNIPAM nanoparticles in HaCaT and SW 480 cells after 24h of exposure (using a 63x oil immersion objective). Panel 1 represents the uptake study in the HaCaT cells and panel 2 represents the uptake study in SW 480 cells. In each figure Panel A represents the untreated control and Panels B, C and D, represent the nanoparticle exposure concentrations of 30, 50 and 100 mg/l respectively. Scale bar is 10 μ m.

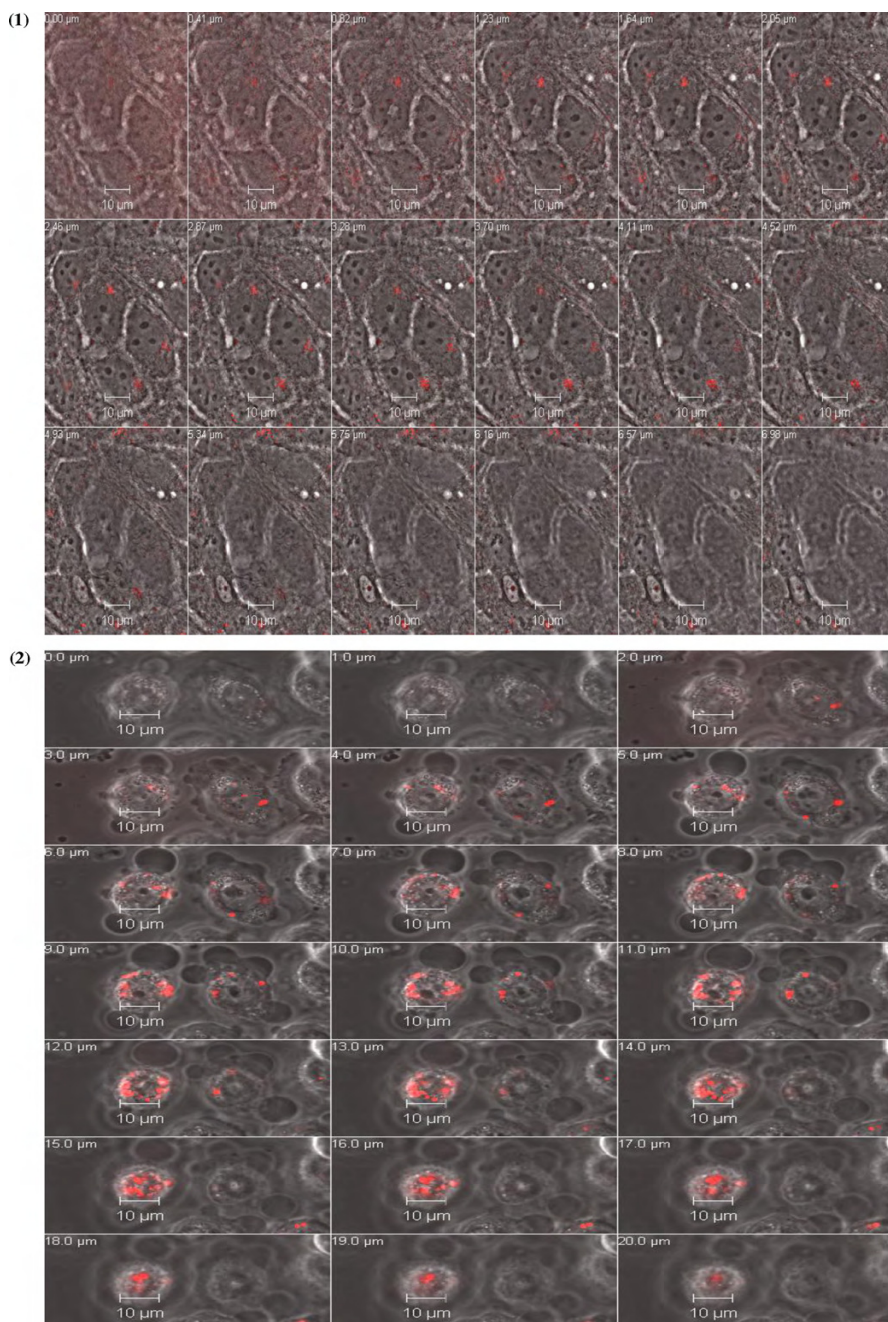


Figure 4.3. CLSM optical sections (z-sections) of the HaCaT and SW 480 cells showing the localisation of the nanoparticles at different sections (using a 63x oil immersion objective). Each optical section represents a particular plane of focus and nanoparticles have a different plane of focus indicating that they are internalised completely. Panel 1 represents the HaCaT cells (optical section thickness is 0.41 μm). Panel 2 represents the SW 480 cells (optical section thickness is 1.0 μm) with exposure concentration 50mg/l. Scale bar is 10μm.

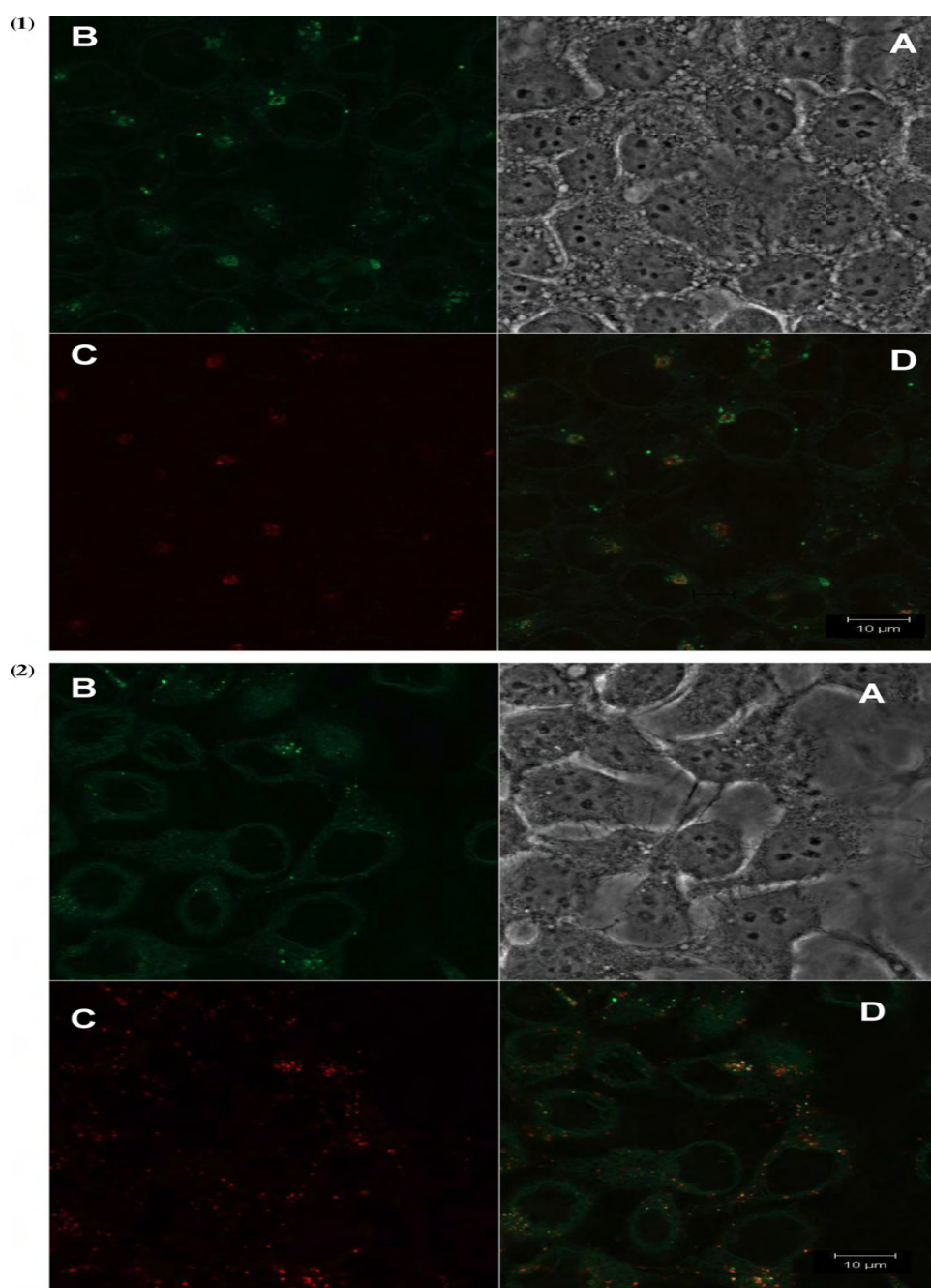


Figure 4.4. CLSM images of co-localisation of NIPAM nanoparticles with lysosomes, by co-staining the HaCaT cells with lysotracker green (using a 63x oil immersion objective). (1) and (2) are the 24 hour exposure to labelled PNIPAM nanoparticles at concentrations of 30 and 50 mg/l respectively. In each figure Panel A represents the brightfield image; Panel B shows the green fluorescence channel showing the localisation of the lysotracker dye and indicating the lysosomes; Panel C is the red fluorescence channel and shows the localisation of the PNIPAM nanoparticles; and Panel D is the overlay of Panels B and C (the green and red channels) and shows the co-localisation of the nanoparticles with the lysosomes. Scale bar is 10μm.

4.3.3 Cytotoxicity assessment of PNIPAM nanoparticles

The cytotoxicity of the unlabelled PNIPAM nanoparticles was studied in the HaCaT and SW480 cell lines. As administration routes of nanoparticle based drug delivery agents are likely to be transdermal or by ingestion, human dermal and gastrointestinal models were employed for this study. HaCaT is an immortalised non-cancerous human keratinocyte cells and SW 480 is a primary adenocarcinoma of human colon cells. These two cell lines are isolated from different organs of the human, and also have different morphology, metabolism and also antioxidant levels (Mukherjee et al., 2010). The assay was carried out by analysing the uptake of Alamar blue (AB), a water-soluble dye that has been previously used for quantifying *in vitro* viability of various cells (Fields and Lancaster, 1993; Ahmed et al., 1994). When added to cell cultures, the oxidized form of the AB enters the cytosol and is converted to the reduced form by mitochondrial enzyme activity, accepting electrons from NADPH, FADH, FMNH, and NADH as well as from the cytochromes. This redox reaction is accompanied by a shift in colour from indigo blue to fluorescent pink, which can be easily measured by colorimetric or fluorometric analysis (Al-Nasiry et al., 2007). The percentage of cell viability was determined by comparison with cells which were not exposed to nanoparticles i.e. the control group. The results are presented in figures 4.5 and 4.6 for HaCaT and SW 480 cell respectively. For the cytotoxicity assay, nanoparticles concentration from 25 to 1000 mg/l were tested in both cell lines at four different exposures times (24 h, 48 h, 72 h and 96 h). No significant cytotoxicity response has been observed in HaCaT and SW 480 cells (figure 4.5 and 4.6), even at the highest exposure doses and longest exposure times.

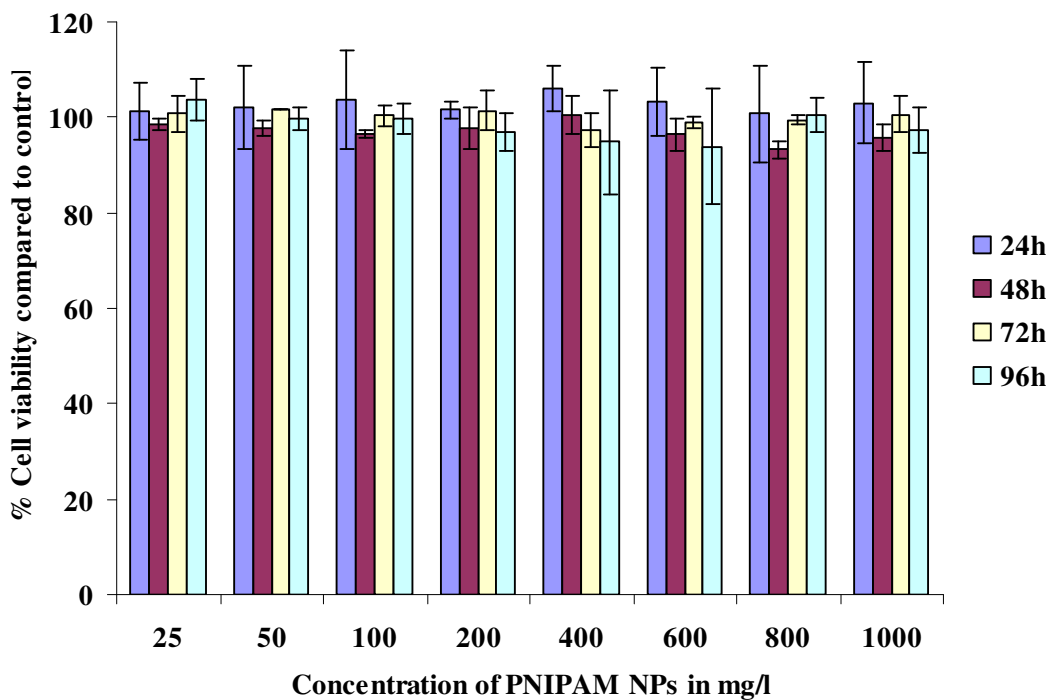


Figure 4.5. Cytotoxicological response of HaCaT cells after 24, 48, 72 and 96 h of exposure to increasing concentrations of PNIPAM nanoparticles.

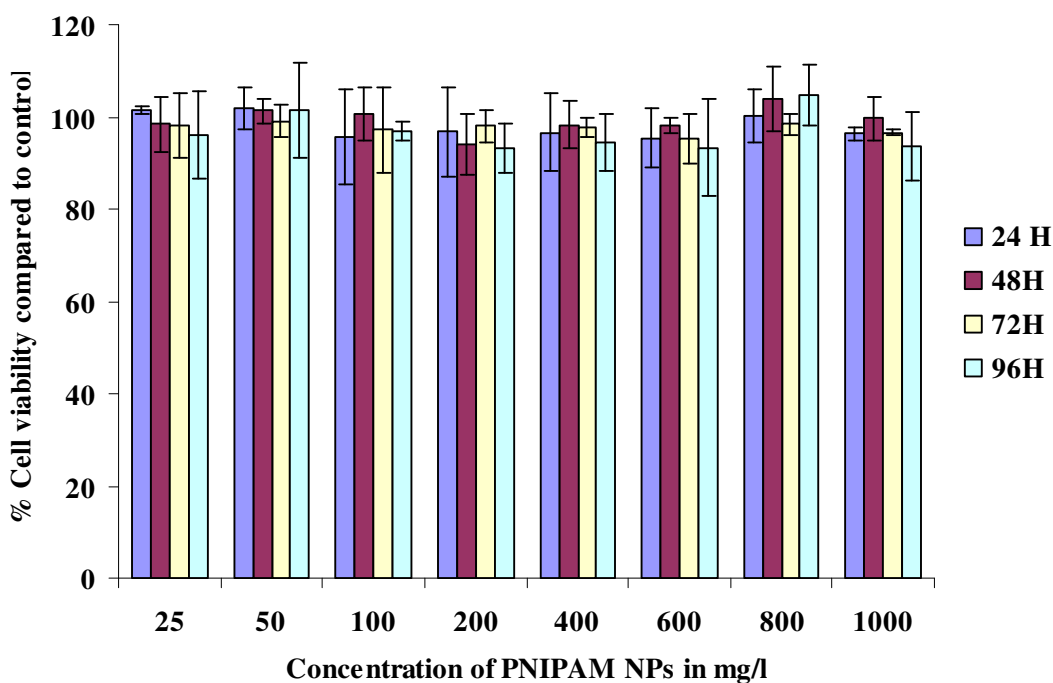
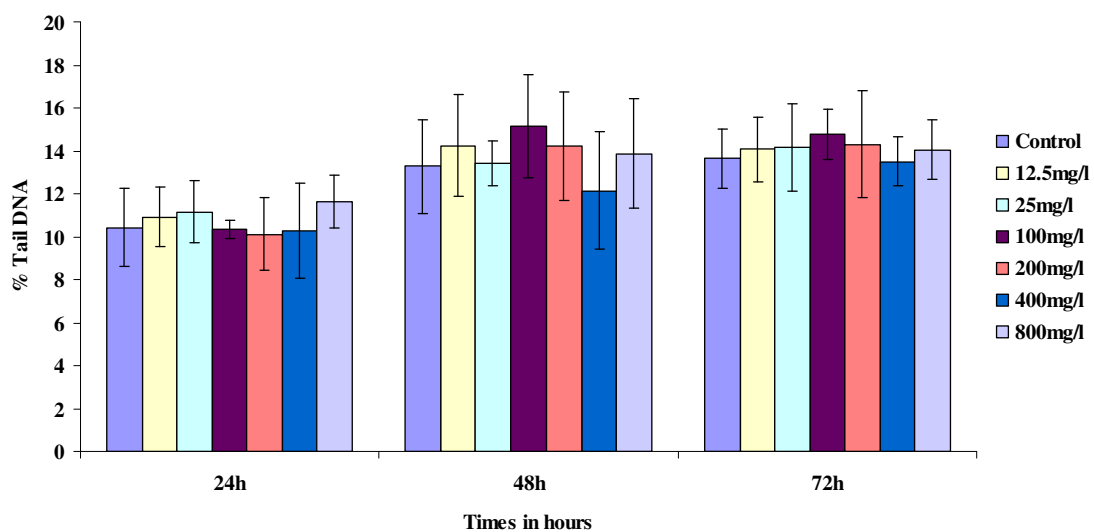


Figure 4.6. Cytotoxicological response of SW480 cells after 24, 48, 72 and 96 h of exposure to increasing concentrations of PNIPAM nanoparticles.

4.3.4 Genotoxicity assessment of PNIPAM nanoparticles

The genotoxicity of the PNIPAM nanoparticles in the concentration range from 12.5 $\mu\text{g/mL}$ to 800 $\mu\text{g/mL}$ was analysed in both HaCaT and SW480 cells for different concentrations and different exposure times. DNA damage was estimated by analyzing the OTM (Olive Tail Moment) and tail percentage DNA. At all concentrations and exposure times tested, no statistically significant DNA damage ($p \leq 0.5$) was observed as shown in Figures 4.7A and B; and 4. 8A and B for the case of HaCaT and SW480 cells respectively. Concentrations of PNIPAM nanoparticles in the range 12.5 to 800 mg/l were employed for the genotoxicity study for three different exposure times i.e 24 h, 48 h and 72 h. No significant DNA damage ($p \leq 0.5$) compared to the control group was observed even at the highest dose and longest exposure time in the case of both the cell lines (figure 4.7 and 4.8).

A.



B.

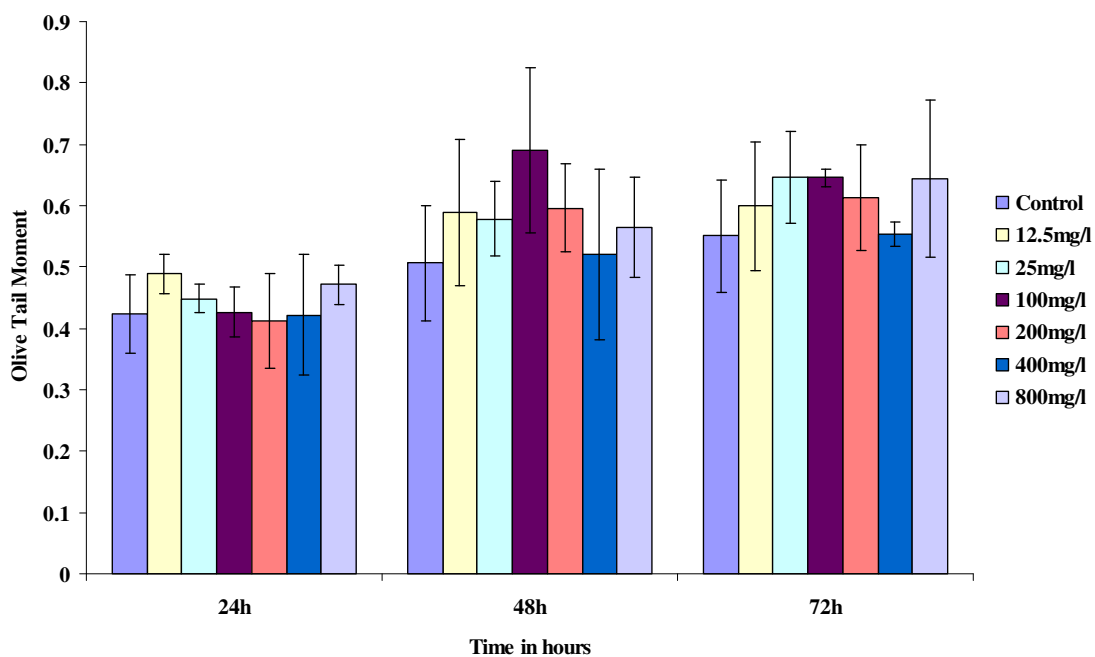
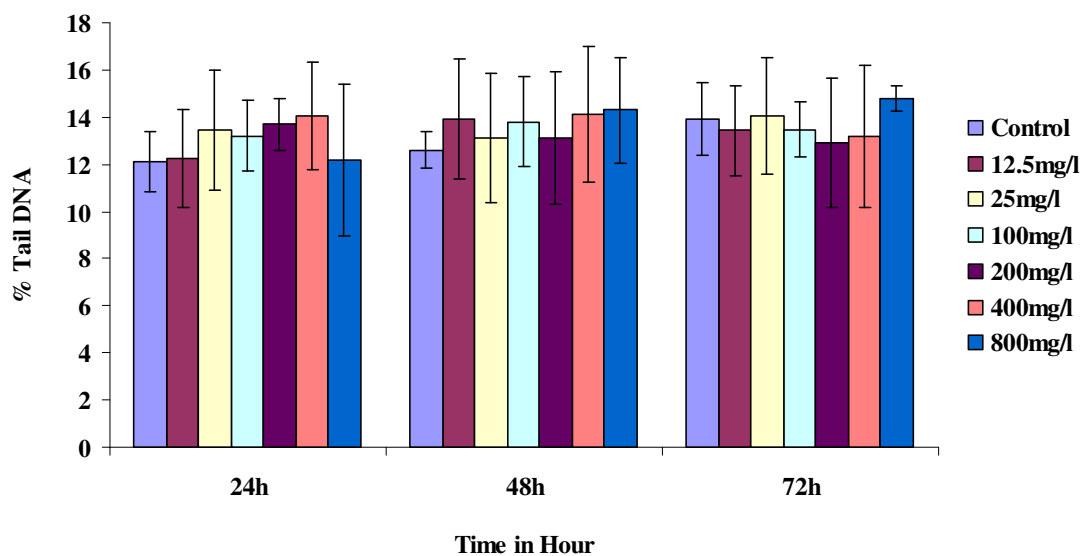


Figure 4. 7. Genotoxicity response of PNIPAM nanoparticles to HaCaT cells. Panel A represents the % tail DNA and Panel B represents the olive tail moment after exposure of the particles at three different time points. Data shown mean \pm SD (n=3).

A



B.

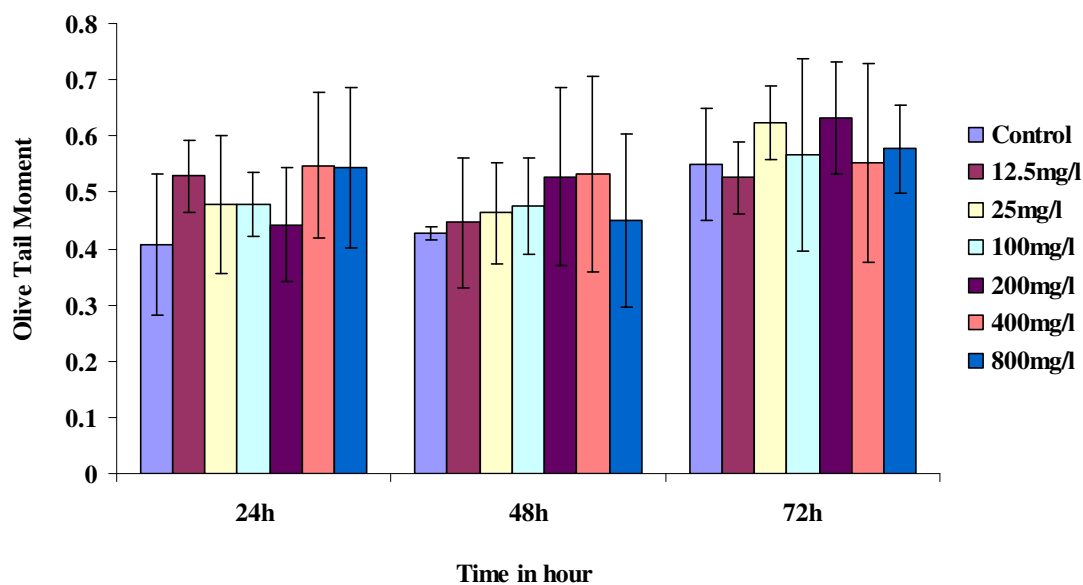


Figure 4.8. Genotoxicity response of PNIPAM nanoparticles to SW480 cells. Panel A represents the % tail DNA and Panel B represents the olive tail moment after exposure of the particles at three different time points. Data shown mean \pm SD (n=3).

4.4 Discussion

4.4.1 Characterisation of PNIPAM nanoparticles

Due to the thermoresponsive nature of the PNIPAM nanoparticles, the hydrodynamic diameter in the cell culture media was measured at increasing trend of temperature. This dramatic increase of particle size is characteristic of agglomeration (Naha et al., 2009b) and at the exposure temperature of 36°C - 38 °C, the particles in the supplemented media had sizes ~0.5- 1µm. Similar results were obtained using the fluorescently-labelled particles, where the presence of the covalently-linked rhodamine B did not affect the particle size, transition temperature or agglomeration behaviour significantly, confirming that labelled particles are representative of unlabelled ones, so that direct comparisons of their behaviour can be made. Thus, for the rhodamine-labelled NIPAM particles, the particle hydrodynamic diameter was confirmed by DLS as 76nm at 25°C with a polydispersity index (PDI) around 0.239.

An increasingly negative zeta potential value was observed when the nanoparticles were suspended in the protein supplemented cell culture media, although it must be noted that the values are always very low, which explains the agglomeration behaviour observed, as zeta potential values of at least ± 30 mV are considered necessary for charge stabilisation to be prominent. This increase may therefore be due to the interaction / adsorption of proteins on to the surface of the nanoparticles yielding a protein corona (Lynch et al., 2007). Such an increase in zeta potential towards negative values is attributable to shielding of the surface charge due to adsorption of and/or interaction with components of the medium by the nanoparticles, supporting the conclusions of the particle size measurements.

4.4.2 Intracellular uptake study

The results of the co-localisation study, in which lysosomes were co-stained using lysotracker green, provides evidence of PNIPAM nanoparticles localised in lysosomes (Figure 4.4). No evidence of localisation within the cell nuclei was observed. This is not unexpected, given the large size of the agglomerates in the cell culture medium. From the images of Figures 4.2 and 4.4, it appears that further particle agglomeration may be occurring intracellularly, or that particles are being accumulated into the lysosomes. Lysosomes have also been shown to be the final destination for polystyrene and silica nanoparticles following uptake by a range of cell types (Shapero et al., 2010). Additionally, once the particles reach the lysosomes they do not exit over at least a 24 hour time period, (Salvati et al., 2011) and this is likely also the case for the PNIPAM particles.

4.4.3 Cytotoxicity

Although the PNIPAM nanoparticles are clearly internalised in the mammalian cells and predominantly localised in the lysosomes, no statistically significant cytotoxicity was observed over a broad concentration range from 12.5 to 1000 $\mu\text{g/ml}$ in either cell line (Figure 4.5 and 4.6).

In the previous chapter (Chapter 3) which reported on the ecotoxicological analysis of PNIPAM nanoparticles, they were found to be similarly non-cytotoxic to fish cells, although a systematic increase in the ecotoxicity response was observed with increasing concentration of a more hydrophobic co-monomer, N-tert-butylacrylamide, BAM, in the NIPAM/BAM co-polymer nanoparticles (Naha et al., 2009b). Some nanomaterials such as single wall carbon nanotubes have been shown to produce toxic responses through medium depletion even without being internalised into the cells (Davoren et al.,

2007). More commonly, engineered nanoparticles of size ranges ≤ 100 nm such as titanium dioxide and silicon dioxide (crystalline), produce toxic effects by entering into cells causing stress, inflammation, genotoxicity and finally cell death (Nel et al., 2006; Donaldson et al., 2006; Oberdörster et al., 2005). In this study, however, although PNIPAM nanoparticles (~50 to 60 nm at 37 °C) are clearly internalised and localised specifically in lysosomes, no cytotoxicological response is observed for up to 96 hours of exposure. Similarly, Polylactic-co-glycolic acid (50:50) and Eudragit RS100 nanoparticles of size 200nm have recently been shown to elicit no cytotoxicological response in SW480 cells, although internalised, suggesting their potential as nano-carriers of drugs for delivery systems.

4.4.4 Genotoxicity

The Comet assay is widely accepted as a simple, sensitive, and rapid tool for assessing DNA damage in different test models and is extensively used for chemical testing (Dhawan et al., 2009). The assessment of nanoparticles for genotoxicity is required as although no cytotoxicological response is observed up to 1000 $\mu\text{g/ml}$, the absence of DNA damage is essential for biocompatibility. Although titanium dioxide nanoparticles show no cytotoxic response in V79 cells (Chinese hamster lung fibroblasts), significant genotoxicity has been observed. The micronucleus assay indicated both chromosome breakage as well as aneuploidy (Bhattacharya et al., 2008) and further indications of genotoxicity via induction of sister chromatid exchange and micronucleus formation in human white blood cells have been reported (Turkez et al., 2007). However, in the current study, no significant genotoxic response ($p \leq 0.05$) is observed, indicating excellent biocompatibility of PNIPAM particles with mammalian cells over 72 hours of exposure to concentrations up to 800 $\mu\text{g/ml}$ in an *in vitro* study. In a recent study of the genotoxicity of 34 nm amorphous silica nanoparticles, no genotoxic effects were

observed via the Comet assay at concentrations up to 400 $\mu\text{g}/\text{mL}$ (Barnes et al., 2008). The fact that the uptake and co-localisation studies suggested that the particles are localised in lysosomes and did not reach the nucleus would also suggest that DNA damage should be limited. However, direct contact between nanoparticles and DNA is not necessary in order to induce DNA damage, which can also result from inflammatory responses to nanoparticles, or oxidative stress (Singh et al., 2009). Amongst the polymeric nanoparticles used and proposed for various applications such as drug delivery etc., only a few have been analysed for genotoxicity (He et al., 2009). The chemical composition of nanomaterials has been shown to influence the mechanism of uptake, transport and toxic responses. For example the cationic $-\text{NH}_2$ surface coated PAMAM dendrimers have been shown to localise in mitochondria (Lee et al., 2009), eliciting a toxic response via production of reactive oxygen species, inflammation and apoptosis in mouse macrophage cells (Naha et al., 2010a). Neutral pegylated quantum dots have, however, been observed to be localised in lysosomes of HaCaT cells (Meade et al., 2009). The studies presented here indicate cellular uptake and localisation of PNIPAM particles in lysosomes. However, no adverse geno or cytotoxicological responses are observed up to the highest doses in either HaCaT or SW480 cell-lines, indicating excellent biocompatibility. It is of course noted that, although as synthesised and dispersed in MQ water the PNIPAM particles are of a size classified as nano, in the cell culture medium, agglomeration and interaction with the medium components results in an effective average size of the order 0.5-1 μm being presented to cells. Nevertheless, in terms of adverse toxicological effects, it can be stated that the as produced nanoparticles show negligible effects.

4.5 Conclusion

Fluorescently labelled PNIPAM particles are clearly seen to be internalised by HaCaT and SW480 cells after 24hrs, and are most likely localised in lysosomes, although some particles are observed in the cytoplasm not associated with the lysosomes.

Equivalent unlabelled PNIPAM nanoparticles are shown to elicit no significant cytotoxic response in HaCaT and SW480 cells, indicating that these particles are biocompatible in nature in an *in vitro* model. No significant difference in the cell viability upon exposure of either cell type to PNIPAM nanoparticles was found after 24, 48, 72 and 96h of exposure at concentrations ranging from 12.5 to 1000 mg/l. The biocompatibility of the unlabelled PNIPAM nanoparticles is further confirmed by the genotoxicity results, as there is no significant difference in the % tail DNA and OTM in either the HaCaT and SW480 cells upon exposure of the particles.

The observed interaction of the PNIPAM nanoparticles with the two different mammalian cell lines and the interpretation of the consequences of the particle fate and behaviour within the cells is an indication of the biocompatibility of these polymer particles in an *in vitro* model. Furthermore, from our previous study it has been observed that nanoparticulate PNIPAM has a negligible ecotoxicological response. However, although the *in vitro* study gives preliminary indications as to the biocompatibility or toxicity of a substance, such techniques are useful for preliminary screening only, and further *in vivo* studies are required, using animal models of increasing complexity (mice, rat, rabbit, monkey, and then human), to conclusively confirm biocompatibility.

References

- Ahmed, S. A., Gogal, R. M., and Walsh, J. E. 1994. A new rapid and simple non radioactive assay to monitor and determine the proliferation of lymphocyte: an alternative to [3H] thimidine incorporation assay *J. Immunol Method*, 170, 211-224.
- Al-Nasiry, S., Geusens, N., Hanssens, M., Luyte, C., and Pijnenborg, R. 2007. The use of alamar blue assay for quantitative analysis of viability, migration and invasion of choriocarcinoma cells *Human Production*, 22, 1304-1309.
- Barnes, C.A., Elsaesser, A., Arkusz, J., Smok, A., Palus, J., Lesniak, A., Salvati, A., Hanrahan, J.P., de Jong, W.H., Dziubałtowska, E., Stepnik, M., Rydzyński, K., McKerr, G., Lynch, I., Dawson, K.A., Howard, C.V. 2008. Reproducible Comet Assay of amorphous silica nanoparticles detects no genotoxicity. *Nano Letters*, 8, 3069-3074.
- Bhattacharya, K., Cramer, H., Albrecht, C., Schins, R., Rahman, Q., Zimmermann, U., Dopp E. 2008. Vanadium pentoxide-coated ultrafine titanium dioxide particles induce cellular damage and micronucleus formation in V79 cells. *J Toxicol Environ Health A*.71, 976-980.
- Blasi, P., S. Giovagnoli, A. Schoubben, M. Ricci, C. 2007. Solid lipid nanoparticles for targeted brain drug delivery. *Adv Drug Deliv Rev.* 59, 454-77.
- Cabaleiro-Lago, C., F. Quinlan-Pluck, I. Lynch, S. Lindman, A. M. Minogue, E. Thulin, D. M. Walsh, K. A. Dawson, and S. Linse. 2008. Inhibition of amyloid beta protein fibrillation by polymeric nanoparticles. *J Am Chem Soc.* 130, 15437-43.

- Cedervall, T., Lynch, I., Foy, M., Berggard, T., Donnelly, S. C., Cagney, G., Linse, S., and Dawson. K. A. 2007. Detailed identification of plasma proteins adsorbed on copolymer nanoparticles. *Angew Chem Int Ed Engl.* 46 , 5754-6.
- Contreras, J., Xie, J., Chen, Y. J, Pei, H., Zhang, G., Fraser, C. L., Hamm-Alvarez, S. F. 2010. Intracellular uptake and trafficking of difluoroboron dibenzoylmethane-poly lactide nanoparticles in HeLa cells. *ACS Nano.* 25, 2735-2747.
- Davoren, M., Herzog, E., Casey, A., Cottineau, B., Chambers, G., Byrne, H.J., Lyng, F.M. 2007. *In vitro* toxicity evaluation of single walled carbon nanotubes on human A549 lung cells. *Toxicol In Vitro,* 21, 438-48.
- Dhawan, A., Bajpayee, M., Parmar, D.2009. Comet assay: a reliable tool for the assessment of DNA damage in different models. *Cell Biol Toxicol.* 25, 5-32.
- Donaldson, K., Aitken, R., Tran, L., Stone, V., Duffin, R., Forrest, G., and Alexander. A. 2006. Carbon nanotubes: a review of their properties in relation to pulmonary toxicology and workplace safety. *Toxicol Sci.* 92, 5-22.
- Fields R D and Lancaster M V. 1993. Dual-attribute continuous monitoring of cell proliferation / cytotoxicity *Am. Biotechnol Lab.* 11, 48-50.
- He, L., Yang, L., Zhang, Z. R., Gong, V., Deng, L., Gu, Z., Sun. X. 2009. *In vitro* evaluation of the genotoxicity of a family of novel MeO-PEG-poly(D,L-lactic-co-glycolic acid)-PEG-OMe triblock copolymer and PLGA nanoparticles. *Nanotechnology* 20, 455102.
- Hsiue, G. H., Chang, R. W., Wang, C. H ., Lee. S. H. 2003. Development of in situ thermosensitive drug vehicles for glaucoma therapy. *Biomaterials,* 24 , 2423-30.
- Hsiue, G. H., Hsu, S. H., Yang, C. C., Lee, S. H., Yang. I. K. 2002. Preparation of controlled release ophthalmic drops, for glaucoma therapy using thermosensitive poly-N-isopropylacrylamide. *Biomaterials* 23, 457-62.

- Ito, F., Fujimori, H., Honnami, H., Kawakami, H., Kanamura, K., Makino, K. 2008. Effect of polyethylene glycol on preparation of rifampicin-loaded PLGA microspheres with membrane emulsification technique. *Colloids Surf B Biointerfaces* 66, 65-70.
- Kavanagh, C. A., Gorelova, T. A., Selezneva, I.I, Rochev, Y. A., Dawson, K. A. Gallagher, W. M., Gorelov, A. V., Keenan. A. K. 2005. Poly(N-isopropylacrylamide) copolymer films as vehicles for the sustained delivery of proteins to vascular endothelial cells. *J Biomed Mater Res A* 72, 25-35.
- Lee, J.H., Cha, K.E., Kim, M.S., Hong, H.W., Chung, D.J., Ryu, G., Myung, H. 2009. Nanosized polyamidoamine (PAMAM) dendrimer-induced apoptosis mediated by mitochondrial dysfunction. *Toxicol Lett.* 190 , 202–207.
- Lin, C. C., and Metters. A. T. 2006. Hydrogels in controlled release formulations: network design and mathematical modeling. *Adv Drug Deliv Rev* 58, 1379-408.
- Lynch, I., Cedervall, T., Lundqvist, M., Cabaleiro-Lago, C., Linse, S., Dawson, K. A. 2007. The nanoparticle–protein complex as a biological entity; a complex fluids and surface science challenge for the 21st century. *Advances in Colloid and Interface Science*, 134-135, 167–174.
- Meade, A.D., Clarke, C., Bonnier, F., Poon, K., Garcia, A., Knief, P., Ostrowska, K., Salford, L., Nawaz, H., Lyng, F.M., Byrne, H.J., 2009. Functional and Pathological Analysis of Biological Systems using Vibrational Spectroscopy with Chemometric and Heuristic Approaches. *First Workshop on Hyperspectral Image and Signal Processing: Evolution in Remote Sensing*, Pages: 111-114 (2009)

- Meng, H., Chen, Z., Xing, G., Yuan, H., Chen, V., Zhao, F., Zhang, C., Zhao, Y. 2007. Ultrahigh reactivity provokes nanotoxicity: explanation of oral toxicity of nano-copper particles. *Toxicol Lett.* 175, 102-10.
- Naha, P. C., Kanchan, V., Manna, P. K., and Panda, A. K. 2008. Improved bioavailability of orally delivered insulin using Eudragit-L30D coated PLGA microparticles. *J Microencapsul.* 25, 248-56.
- Naha, P. C., Kanchan, V., and A. K. Panda. 2009a. Evaluation of parenteral depot insulin formulation using PLGA and PLA microparticles. *J Biomater Appl.* 24, 309-25.
- Naha, P. C., Casey, A., Tenuta, T., Lynch, I., Dawson, K. A., Byrne, H. J., Davoren, M. 2009b. Preparation, Characterization of *NIPAM* and *NIPAM/BAM* Copolymer Nanoparticles and their Acute Toxicity Testing using an Aquatic test battery. *Aquat. Toxicol.* 92, 146-154.
- Naha, P.C., Davoren M., Lyng F.M., Byrne, H.J. 2010a. Oxidative stress induced inflammatory response and cytotoxicity of PAMAM dendrimers in J774A.1 cells. *Toxicology and Applied Pharmacology* (Accepted/ doi: 10.1016/j.taap.2010.04.014).
- Nel, A., Xia, T., Madler, L., Li, N. 2006. Toxic potential of materials at the nanolevel. *Science* 311, 622-7.
- Nel, A.E., Mädler, L., Velegol, D., Xia, T., Hoek, E.M.V., Somasundaran, P., Klaessig, F., Castranova V., and Thompson, M. 2009. Understanding biophisicochemical interactions at the nano–bio interface. *Nature materials*, 8, 543-557.

- Neun, B. W, Stern, S. T. 2011. Monitoring lysosomal activity in nanoparticle-treated cells. *Methods Mol. Biol.* 697, 207-212.
- Oberdorster, G., Oberdorster, E., Oberdorster. J. 2005. Nanotoxicology: an emerging discipline evolving from studies of ultrafine particles. *Environ Health Perspect* 113, 823-39.
- Papageorgiou, I., Brown, C., Schins, R., Singh, S., Newson, R., Davis, S., Fisher, J., Ingham, E., Case. C. P. 2007. The effect of nano- and micron-sized particles of cobalt-chromium alloy on human fibroblasts *in vitro*. *Biomaterials* 28, 2946-58.
- Peppas, N. A., Bures, P., Leobandung, W., Ichikawa. H., 2000. Hydrogels in pharmaceutical formulations. *Eur J Pharm Biopharm* 50, 27-46.
- Poland, C. A., Duffin, R., Kinloch, I., Maynard, A., Wallace, W.A., Seaton, A., Stone, V., Brown, S., Macnee, W., Donaldson. K. 2008. Carbon nanotubes introduced into the abdominal cavity of mice show asbestos-like pathogenicity in a pilot study. *Nat Nanotechnol* 3, 423-8.
- Shapero, K., Fenaroli, F., Lynch, I., Cottell, D.C., Salvati, A., Dawson. K.A., 2010. Time and space resolved uptake study of silica nanoparticles by human cells. *Molecular biosystem*, DOI: 10.1039/c0mb00109k.
- Salvati, A., Santos, T., Varela, J., Åberg, C., Pinto, P., Lynch, I., Dawson, K.A. 2011. Experimental and theoretical approach to comparative nanoparticle and small molecule intracellular import, trafficking, and export. *Nanomedicine* (In press),
- Shi, H., He, X., Yuan, Y., Wang, K., Liu, D. 2010. Nanoparticle-based biocompatible and long-life marker for lysosome labeling and tracking. *Anal Chem.*82, 2213-2220.

- Silva, C. M., Ribeiro, A. J., Ferreira, D., Veiga, F. 2006. Insulin encapsulation in reinforced alginate microspheres prepared by internal gelation. *Eur J Pharm Sci* 29, 148-59.
- Singh, N., Manshian, B., Jenkins, G. J., Griffiths, S. M., Williams, P.M., Maffeis, T. G., Wright, C. J., Doak, S. H. 2009. NanoGenotoxicology: the DNA damaging potential of engineered nanomaterials. *Biomaterials*, 30, 3891-914.
- Singh, S., Shi, T., Duffin, R., Albrecht, C., van Berlo, D., Hohr, D., Fubini, B., Martra, G., Fenoglio, I., Borm, P. J., Schins, R. P. 2007. Endocytosis, oxidative stress and IL-8 expression in human lung epithelial cells upon treatment with fine and ultrafine TiO₂: role of the specific surface area and of surface methylation of the particles. *Toxicol Appl Pharmacol* 222, 141-51.
- Turkez, H., Geyikoglu, F. 2007. An *in vitro* blood culture for evaluating the genotoxicity of titanium dioxide: the responses of antioxidant enzymes. *Toxicol Ind Health*. 23, 19-23.
- Xu, F. J., Kang, E. T., Neoh, K. G. 2006. pH- and temperature-responsive hydrogels from crosslinked triblock copolymers prepared via consecutive atom transfer radical polymerizations. *Biomaterials*, 27, 2787-97.
- Xu, F. J., Zhong, S. P., Yung, L. Y., Kang, E. T., Neoh, K. G. 2004. Surface-active and stimuli-responsive polymer--Si(100) hybrids from surface-initiated atom transfer radical polymerization for control of cell adhesion. *Biomacromolecules* 5, 2392-403.
- Zhang, X. Z., Jo Lewis, P., Chu, C. C. 2005. Fabrication and characterization of a smart drug delivery system: microsphere in hydrogel. *Biomaterials* 26, 3299-309.

Zhang, J., Misra, R.D.K. 2007. Magnetic drug-targeting carrier encapsulated with thermosensitive smart polymer: Core-shell nanoparticle carrier and drug release response. *Acta Biomaterialia* 3, 838–850

Chapter 5

Ecotoxicology of PAMAM dendrimers (G4, G5 and G6)

Adapted from “An Ecotoxicological Study of *Poly (amidoamine)* Dendrimers – Towards Quantitative Structure Activity Relationships”. *Environmental science and Technology*, 2009, 43, 6864-6869.

Authors: Pratap C. Naha, Maria Davoren, Alan Casey, Hugh J. Byrne

5.1 Introduction

Dendritic polymer nanostructures are highly branched radial polymers that have specific and systematically variable size, shape and chemical structure (Boas and Heegaard, 2004). Polyamidoamine (PAMAM) dendrimers contain a 2-carbon ethylenediamine core and primary amino groups on the surface (<http://www.dendritech.com/pamam.html>). The potential applications of the PAMAM dendrimers are described in introduction chapter-1. There have also been recent reports on the ecotoxicological evaluation of various metal based nanomaterials (Lovern et al., 2007; Heinlaan et al., 2008; Gagné et al., 2008; Mortimer et al., 2008; Navarro et al., 2008; Franklin et al., 2007; Mueller and Nowack, 2008). A recent study has explored the toxicity of PAMAM dendrimers G 3.5 and G 4 in a zebra fish embryo model (Heiden et al., 2007). However, the field of eco-(nano) toxicology is still relatively new and there is a dearth of quantitative structure activity relationships established for nanomaterials. Our previous study of N-isopropylacrylamide/N-tert-butylacrylamide copolymer nanoparticles demonstrated a clear relationship between the toxicity observed in a range of test models and the physico-chemical properties of the nanoparticles (Chapter 3; Naha et al., 2009).

To date there have been no reports on the environmental impacts of PAMAM dendrimers. The range of potential applications may result in their unintentional release into the environment, however, so that an assessment of their potential environmental impact is imperative. The structurally well defined and variable macromolecules can also provide a further basis upon which to establish structure activity relationships governing ecotoxicological responses which may serve to develop a fundamental understanding of their interactions and as guidelines for the future prediction of responses.

The aim of the present investigation was the characterization and ecotoxicological evaluation of three commercially available PAMAM dendrimers (G4, G5 and G6). Successive generations increase in diameter and therefore effective surface area, while the surface chemistry is unchanged, thus enabling an assessment of the influence of particle size alone on the toxic response. Acute ecotoxicological effects of G4, G5 and G6 were evaluated using a battery of bioassays representing different trophic levels. The tests employed included a bacterial model, two crustaceans and *in vitro* tests employing two different fish cell lines to represent vertebrate models, in accordance with the EU policy of Reduction, Replacement and Refinement (RRR), (Directive 86/609/EEC) on the protection of animals used for experimental and scientific purposes. Indeed, previous studies have demonstrated that fish cell lines are versatile tools in ecotoxicology and found that *in vitro* cytotoxicity is positively correlated with acute toxicity *in vivo* (Fent, 2001). The particle size and zeta potential combined with pH were monitored in the range of test media. UV/visible spectroscopic analysis of these particles in two different cell culture media was performed to investigate any potential changes to the effective medium composition which could contribute to an indirect or secondary toxicity (Casey et al., 2008).

5.2 Experimental methods

The experimental methods are described in chapter 2. Particle size measurement and zeta potential are described in chapter 2, section 2.2.1.1 and 2.2.1.2. Interactions of PAMAM dendrimers with cell culture media were carried out by spectroscopic study and the methodology is described in section 2.2.1.3. All the ecotoxicity protocols and cytotoxicity assays are described in section 2.2.2 and 2.2.2.6 of chapter 2.

5.3 Results

5.3.1 Characterisation of particles

5.3.1.1 Particle size

The average hydrodynamic diameter of G4, G5 and G6 as measured in the different test media are shown in Table 5.1. The values compare well to those quoted by the manufacturers (G4- 4.5 nm, G5- 5.4 nm and G6-6.7 nm) and no significant agglomeration of the particles is indicated (<http://www.dendritech.com/pamam.html>). In the case of the particle sizes observed in the cell culture media, the comparatively high values may indicate an interaction with components of the media yielding a “protein corona” as has been observed with other nanoparticles (Lynch et al., 2007).

Table 5.1. Hydrodynamic diameter of PAMAM dendrimers in different test media (measured at 20 °C). Data show the mean \pm SD, (n=3).

Different Media	Test	PAMAM G4 Size in nm (Diameter)	PAMAM G5 Size in nm (Diameter)	PAMAM G6 Size in nm (Diameter)
Microtox (MD)	Diluent	4.0 \pm 0.1	5.5 \pm 0.2	7.6 \pm 0.15
Daphnia (DM)	Media	4.1 \pm 0.05	5.4 \pm 0.15	5.7 \pm 0.10
Thamnocephalus Media (TM)		4.0 \pm 0.15	5.6 \pm 0.11	6.6 \pm 0.15
PLHC-1 Media		6.6 \pm 0.23	6.6 \pm 0.26	11.5 \pm 0.26
RTG-2 Media		6.6 \pm 0.23	10.2 \pm 0.23	13.6 \pm 0.23

5.3.1.2 Zeta potential

The zeta potential of each the dendrimer was measured in each of test media employed and these values are shown graphically in Figure 5.1. Each of the particles tested gave a positive zeta potential in all the media (with the exception of the cell culture media) as a result of the positively charged NH_2 surface groups. It is noted, however, that the magnitude of the zeta potential does not change monotonically with generation number, except in MQ. The G4 dendrimer is minimally perturbed compared to the value in MQ in all media, again with the exception of the PLHC-1 and RTG-2 media. The PLHC-1 and RTG-2 media differ from the DMEM medium in that they contain additional FCS. It is suggested therefore that the additional protein adsorbs onto the surface of the particles masking the intrinsic surface charge. In DM, TM and MD, the zeta potentials of G5 and G6 are considerably perturbed suggesting a significant interaction with the medium.

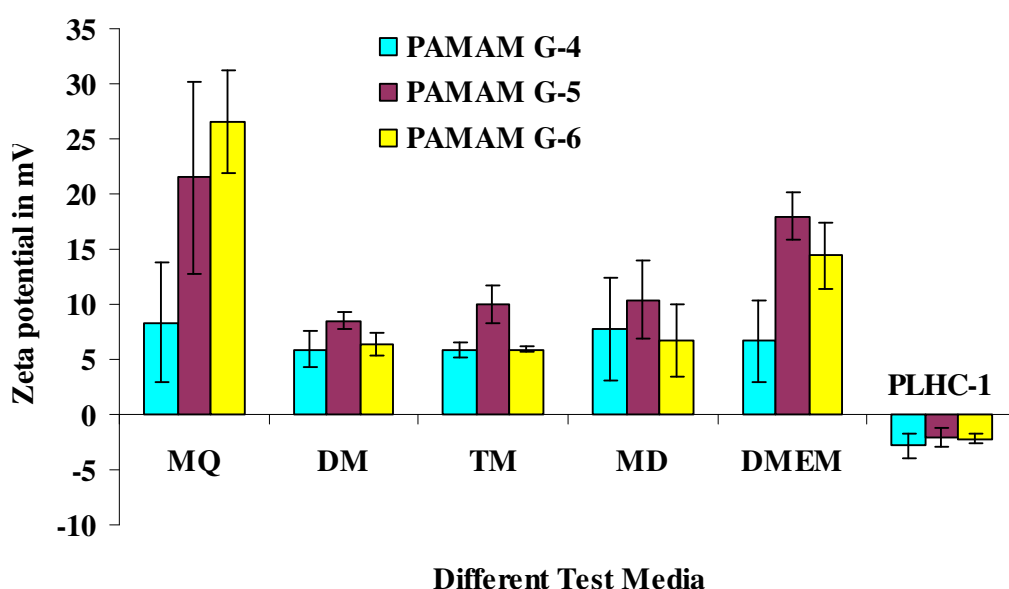


Figure 5.1. Zeta potential of PAMAM dendrimer in different test media. Data presented as mean \pm SD (n=6).

5.3.1.3 Spectroscopic analysis

Both the particle size and zeta potential measurements point towards an interaction of the dendrimers with the cell culture medium. Such interactions have previously been observed for single walled carbon nanotubes (Casey et al., 2008) and were characterized using UV/visible absorption spectroscopy (Casey et al., 2007).

The UV-Visible absorption spectrum of the DMEM medium shows characteristic peaks at ~270, ~360, ~410 and ~560 nm (Figure 5.2 A). The feature at ~360 nm can be attributed to riboflavin (Posadaz et al., 2000; Zirak et al., 2005), a vitamin present in the medium, whereas the feature at ~560 nm can be assigned to the phenol red indicator within the medium. At ~270 nm, there are contributions from the range of amino acids and other molecular components contained within the medium. Upon addition of FCS, in PLHC-1 and RTG-2, a further feature at ~ 410 nm evolves and the feature at ~ 270 nm increases significantly. Most notably, upon addition of the FCS to the DMEM medium, there is a visible colour change manifest spectroscopically as a significant and progressive decrease of the characteristic absorption feature of the phenol red pH indicator at ~560 nm indicating that the additional proteins affect a change in the pH of the medium.

Upon addition of the dendrimers to the cell culture media, a visible colour change was also observed. Figure 5.2C, shows the absorption spectra of the 5% FCS supplemented DMEM medium, PLHC-1, with and without the dendrimer particles added. The phenol red absorption at ~560 nm is seen to increase, the change increasing according to the sequence G6~G5<G4. This is essentially a reversal of the changes observed in the pure medium DMEM upon addition of the 5% FCS. Also notable in Figure 5.2 are the changes to the spectral feature at ~410nm, associated with the FCS. There is a progressive reduction of the absorbance from that observed in the pure medium in the

sequence G6~G5>G4. The same behaviour and indeed trend is observable in the RTG-2 10% serum supplemented cell culture medium. (Figure 5.2B).

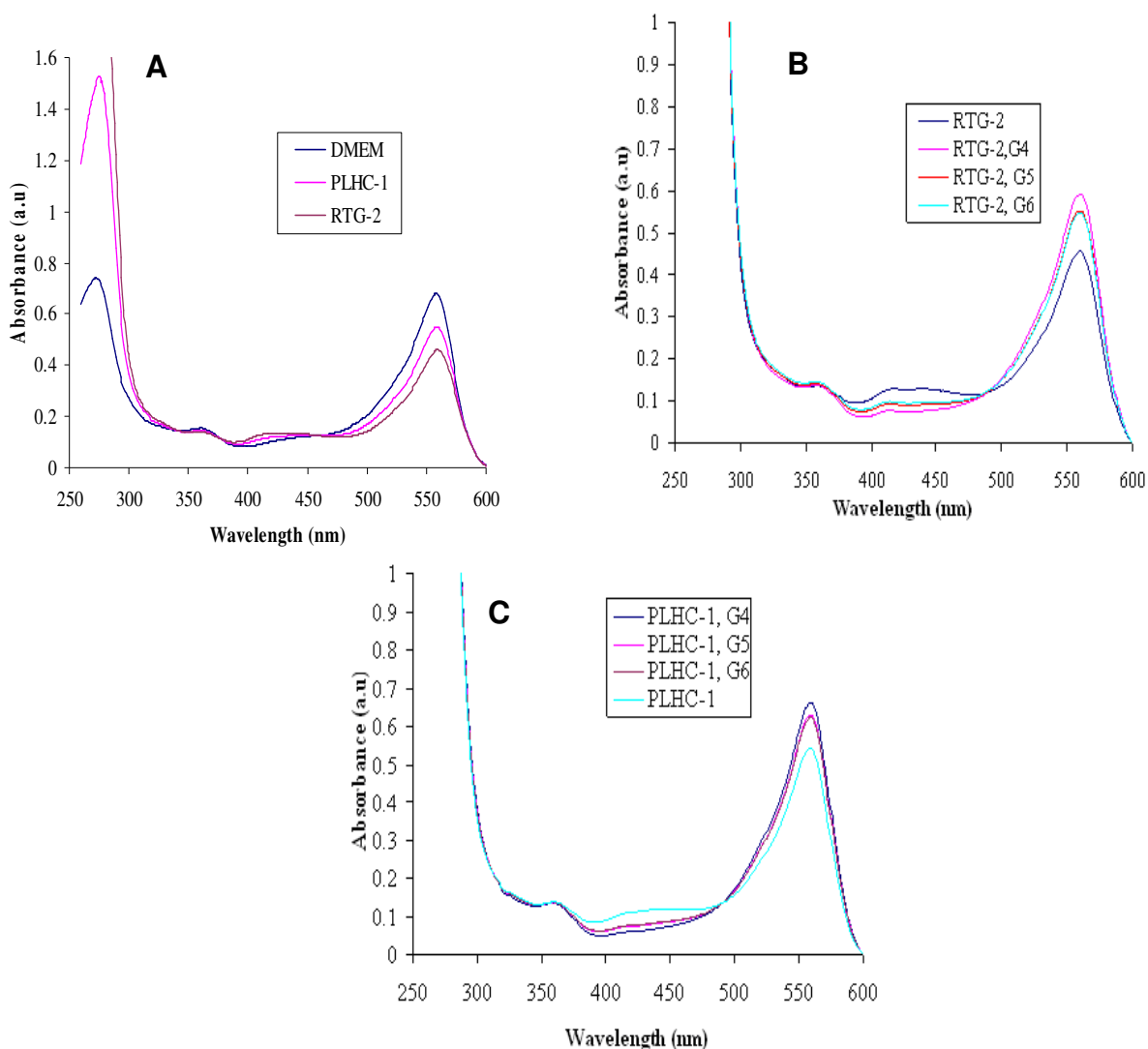


Figure 5.2. Medium interaction study of PAMAM (G4, G5 and G6) dendrimers in PLHC-1 media by UV-Visible absorption spectroscopy. Figure A represents UV-Visible absorption spectra of DMEM F-12 HAM, PLHC-1 and RTG-2 media; Figure B represents UV-Visible absorption spectra of RTG-2 media with PAMAM (G4, G5 and G6) dendrimers; Figure C represents UV-Visible absorption spectra of PLHC-1 media with PAMAM (G4, G5 and G6) dendrimers.

The observed spectroscopic changes can be associated with changes in the pH of the medium. Upon addition of FCS to DMEM, the pH is reduced from 7.9 to 7.6 (5%) and

7.4 (10%). Upon addition of the dendrimer nanoparticles to the media, the pH was seen to recover significantly, most notably for G4.

The reduction of the absorbance feature associated with the FCS and the concurrent reversal of the pH changes caused by the addition of the FCS to the pure medium points towards an interaction of the particles with the FCS by adsorption. This changes the contribution of the serum to the pH and the effective composition of the medium.

Comparatively high values of the particle sizes observed in the cell culture media may indicate an interaction with components of the media yielding a “protein corona” as has been observed with other nanoparticles (Lynch et al., 2007). The values of the zeta potential of the dendrimers in the cell culture media are negative which suggests that the additional protein adsorbs onto the surface of the particles. In addition, the changes to the spectral feature at ~410nm, associated with the FCS, also indicate an interaction of the nanoparticles with the protein. There is a progressive reduction of the absorbance from that observed in the pure medium in the sequence G6~G5>G4. The same behavior and indeed trend is observable in the RTG-2 10 % serum supplemented cell culture medium. (Figure 5.2B and C). Notably, however, no changes to the absorption features at ~ 360 nm are discernible, indicating that the medium interaction is primarily with the FCS.

5.3.2 Ecotoxicity

Testing of the reference chemicals, phenol and potassium dichromate, was carried out in tandem with the nanoparticles to ensure the validity of each test method. Endpoints of all reference toxicity tests were within those stipulated in each respective standard guideline or reported in other previous studies (Chapter 2. section 2.2.2). Consistent results were achieved for each test control in accordance with the criteria for validity of each test guideline.

For all assays, 0-5% (mostly less than 5%) death was observed in the control (untreated) group. According to data of the range finding study, concentration ranges of different particles were chosen to achieve 10-90% effect. As the trend of toxicity in PAMAM dendrimers is $G6 > G5 > G4$, different concentration ranges were identified by the respective range finding tests for successive generations.

According to the range finding study, concentration ranges of different particles were chosen to achieve 10-90% effect. As the trend of toxicity in PAMAM dendrimers is $G6 > G5 > G4$, different concentrations were identified by the respective range finding tests for successive generations.

5.3.2.1 Ecotoxicity tests with PAMAM Dendrimer G4, G5 and G6

The results of the ecotoxicity assessment of PAMAM dendrimers G4, G5 and G6 from different test systems are presented in Tables 5.2, 5.3 and 5.4 respectively. Dose dependent response of PAMAM dendrimers is presented in figures 5.3 and 5.4 for the *T. platyurus* and *D. magna* assays. The cytotoxic effects of G4, G5 and G6 in the PLHC-1 and RTG-2 cell lines are presented in Figures 5.5 and 5.6 respectively.

The concentrations of PAMAM dendrimers determined by the range finding study for the toxicity study of *T. platyurus* were 1-7 μM , 0.05-6 μM and 0.05-4 μM of G4, G5 and G6 respectively. A significant difference of mortality as compared to the control group and also a significant dose dependent response (figure 5.3) was observed ($p \leq 0.05$). In the case of *D. magna*, concentration employed were 0.25-3.0 μM , 0.1-1.5 μM and 0.05-0.75 μM for G4, G5 and G6 respectively. A significant immobilisation of *D. magna* as compared to control group, as well as a significant dose dependent response (figure 5.4) was observed ($p \leq 0.05$). The cytotoxicity effect of PAMAM dendrimers to the fish cells is presented in figure 5.5 and 5.6 for PLHC-1 and RTG-2 cell- lines respectively. Here also a significant cytotoxicity response was observed as compared to

control group ($p \leq 0.05$). Overall, a significant generation dependent ecotoxicity response was observed with PAMAM dendrimers and the trend of toxicity is $G6 > G5 > G4$ ($p \leq 0.05$) for the range of test models employed, except the case of *V. Fischeri*. *D. magna* is found to be most sensitive test model and RTG-2 cells the least, according to the calculated EC_{50}/LC_{50} value (Table 5.2-5.4) for the case of G4, G5 and G6 PAMAM dendrimers. The LOEC and NOEC of all the PAMAM dendrimers for the entire range of test models employed here is described in table 5.2-5.4.

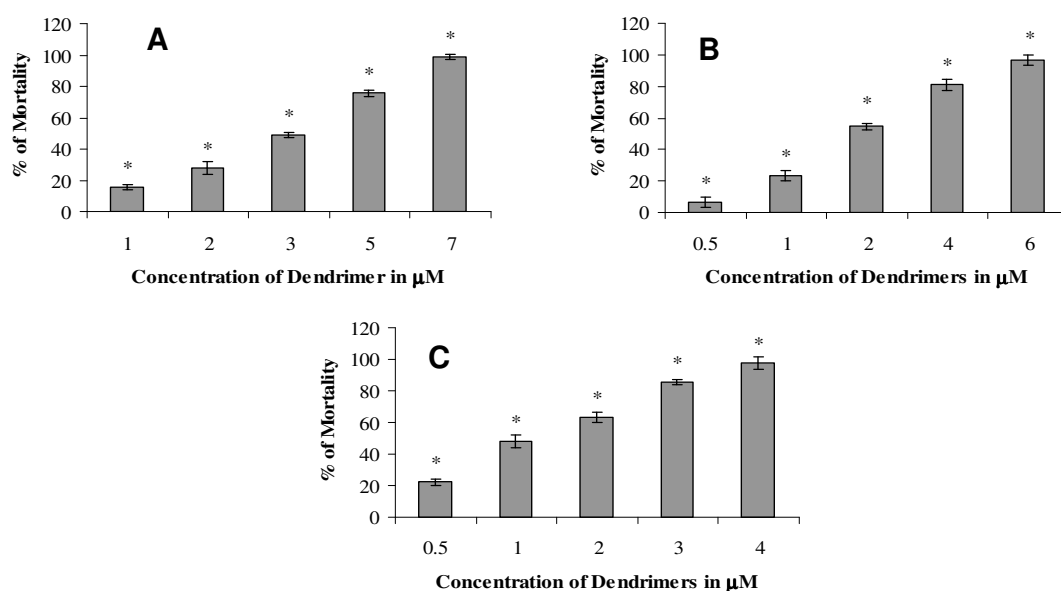


Figure 5.3. Dose dependent response of PAMAM dendrimers in *T. platyurus* , Figures A, B and C represents results for the PAMAM dendrimers G4, G5 and G6 respectively.

* Denotes significant difference of mortality as compared to control group ($p \leq 0.05$).

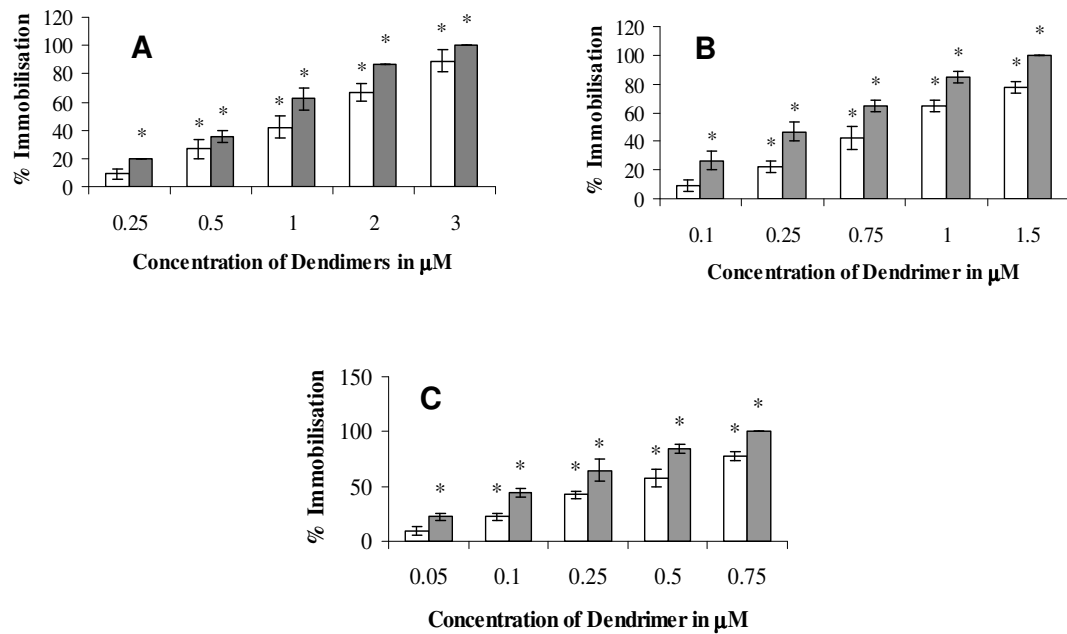


Figure 5.4. Dose dependent response of PAMAM dendrimers in *D.magna* , Figures A, B and C represents results for the PAMAM dendrimers G4, G5 and G6 respectively. (□) 24 hour and (■) 48 hours exposure time. * Denotes significant difference of immobilisation as compared to control group ($p \leq 0.05$).

Table 5.2. Ecotoxicity of PAMAM dendrimer G4.

Test Model	End Point and Concentration Range tested (μM)	EC₅₀/LC₅₀ (μM)	NOEC (μM)	LOEC (μM)
<i>V. fischeri</i>	5 min inhibition (0.195 – 50)	16.30	3.1	6.25
<i>V. fischeri</i>	15 min inhibition (0.195 – 50)	6.17	1.5	3.1
<i>V. fischeri</i>	30 min inhibition (0.195 – 50)	3.11	0.195	0.39
<i>D. magna</i>	24 h immobilisation (0.25 – 3)	1.13	0.25	0.5
<i>D. magna</i>	48 h immobilisation (0.25 – 3)	0.68	< 0.25	0.25
<i>T. platyurus</i>	24 h lethality (1 – 7)	2.90	< 1	1
PLHC-1	96 h Cytotoxicity (0.176 – 13)	2.08	0.176	0.352
RTG-2	96 h Cytotoxicity (1- 80)	12.93	< 1	1

Table 5.3. Ecotoxicity of PAMAM dendrimer G5.

Test Model	End Point and Concentration Range tested (μM)	EC₅₀/LC₅₀ (μM)	NOEC (μM)	LOEC (μM)
<i>V. fischeri</i>	5 min inhibition (0.097 – 25)	15.18	0.195	0.39
<i>V. fischeri</i>	15 min inhibition (0.097 – 25)	5.08	0.195	0.39
<i>V. fischeri</i>	30 min inhibition (0.097 – 25)	2.3	0.097	0.195
<i>D. magna</i>	24 h immobilisation (0.1 – 1.5)	0.72	0.1	0.25
<i>D. magna</i>	48 h immobilisation (0.1 – 1.5)	0.27	< 0.1	0.1
<i>T. platyurus</i>	24 h lethality (0.05 – 6)	1.81	< 1	1
PLHC-1	96 h Cytotoxicity (0.062 – 5)	0.56	0.125	0.25
RTG-2	96 h Cytotoxicity (0.625 – 50)	6.07	< 0.625	0.625

Table 5.4. Ecotoxicity of PAMAM dendrimer G6.

Test Model	End Point and Concentration Range tested (μM)	EC₅₀/LC₅₀ (μM)	NOEC (μM)	LOEC (μM)
<i>V. fischeri</i>	5 min inhibition (0.048 – 12.5)	4.80	0.195	0.39
<i>V. fischeri</i>	15 min inhibition (0.048 – 12.5)	1.64	0.195	0.39
<i>V. fischeri</i>	30 min inhibition (0.048 – 12.5)	0.83	0.195	0.39
<i>D. magna</i>	24 h immobilisation (0.05 – 0.75)	0.32	0.05	0.1
<i>D. magna</i>	48 h immobilisation (0.05 – 0.75)	0.13	< 0.05	0.05
<i>T. platyurus</i>	24 h lethality (0.5 – 4)	1.11	< 1	1
PLHC-1	96 h Cytotoxicity (0.037 – 3)	0.21	0.037	0.075
RTG-2	96 h Cytotoxicity (0.031 – 25)	2.51	< 0.31	0.31

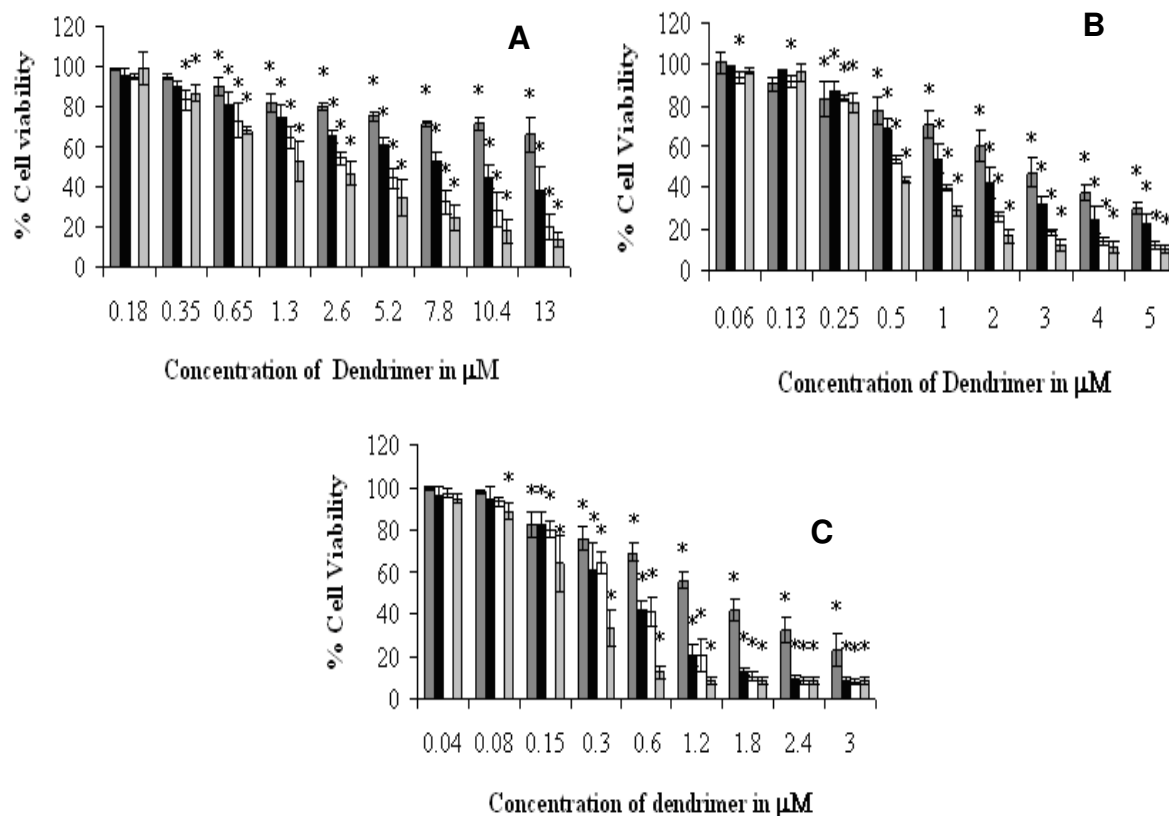


Figure 5.5 Cytotoxicity of PAMAM dendrimer in PLHC-1 cells as quantified using the AB Assay. A, B and C represent G4, G5 and G6 respectively. Data presented as mean \pm SD (N=3). * Denotes significant difference from control ($p \leq 0.05$). 24 h (■); 48 h (■); 72 h (□) and (96 h (□)).

The results of the ecotoxicological assessment of the three generations of PAMAM dendrimer nanoparticles are summarised in Table 5.2 to 5.4. Although the different models cannot be quantitatively compared, and we acknowledge that generally fish cell lines are at least an order of magnitude less sensitive than the whole organism (Davoren and Fogarty 2006), the figure illustrates the differing sensitivities of the models, and most significantly the consistent systematic structural dependence of the response. In the case of the *Vibrio fischeri* test model, the toxicity of each dendrimer was found to increase linearly with increasing exposure time.

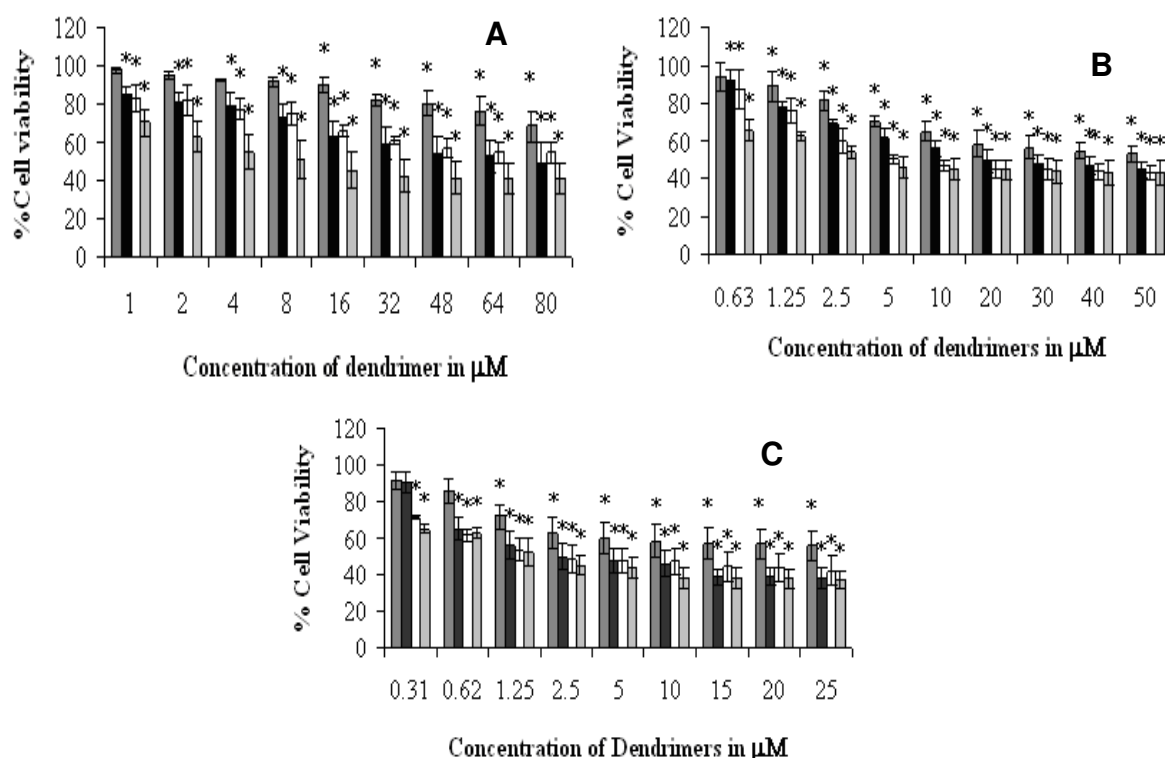


Figure 5.6. Cytotoxicity of PAMAM dendrimer in RTG-2 cells as quantified using the AB Assay. A, B and C represent G4, G5 and G6 respectively. Data presented as mean \pm SD (N=3). * Denotes significant difference from control ($p \leq 0.05$). 24 h (■); 48 h (■); 72 h (□) and (96 h (□)).

5.4 Discussion

The most sensitive test endpoint for each of the dendrimers was the 48 h immobilisation assay with the *Daphnia magna*. For each of the dendrimer nanoparticles, the RTG-2 cells were found to be the least sensitive model. The PLHC-1 cells were found to be an order of magnitude more sensitive than the RTG-2 cells. The higher susceptibility observed in PLHC-1 cells may be explained by the difference in the origin of each cell line, the different growth temperatures (Teneva et al., 2003 and 2005), higher in PLHC-1 than in RTG-2 cells; different species of fish (Kotak et al., 1996). A similar behavior of greater sensitivity of the PLHC-1 model compared to RTG-2 cells has been observed

on exposure to Microcystins (Pichardo et al., 2005; Caminada et al., 2006). Microcystins (MCs) represent a group of more than 80 cyclic heptapeptides, which mediate cytotoxicity via specific protein phosphatase (PP) inhibition. Because of the structure and size of MCs, active uptake into cells occurs via organic anion-transporting polypeptides (OATP/Oatp), as confirmed for liver-specific human *OATP1B1* and *OATP1B3*, mouse *Oatp1b2* (*mOatp1b2*), skate *Oatp1d1*, and the more widely distributed *OATP1A2* expressed at the blood–brain barrier. These are tissue specific and cell type specific expression of OATP/Oatp transporters and specific transport of MC congeners. (Feurstein et al., 2010).

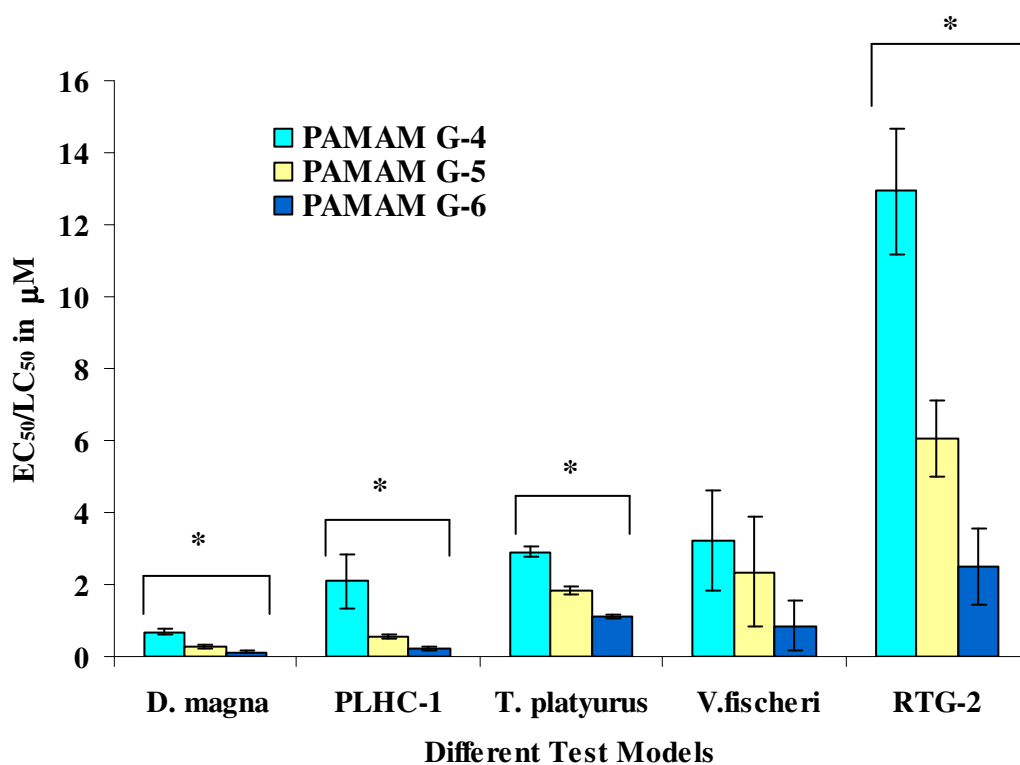


Figure 5.7. Toxicity profile of PAMAM dendrimers based on EC_{50}/LC_{50} values in different test models. Data presented as mean \pm SD ($n=3$). * Denotes significant difference of EC_{50}/LC_{50} responses between G4, G5 and G6 ($p \leq 0.05$).

The toxicity of the PAMAM dendrimer series was found to increase as a function of increasing generation and this effect was observed with all the test models ($p \leq 0.05$) except *Vibrio fischeri*. The trend of toxicity of the PAMAM dendrimers according to the calculated EC_{50}/LC_{50} value are *D.magna* > PLHC-1 > *T.platyurus* > *V. fischeri* > RTG-2. This relationship with increasing generation is shown graphically in Figure 5.7. *D.magna* is the most sensitive test model where as RTG-2 cells are the least test model for the case of G4, G5 and G6 PAMAM dendrimers. The systematic trend observed must be relatable therefore to the systematically varied physico-chemical properties of the dendrimer series, pointing towards structure activity relationships governing the toxic response. The recorded EC_{50} is seen to be approximately linear dependent on the measured surface area, as calculated from the measured particle size as shown in Figure 5.8. Such a dependence of toxic and inflammatory response on surface area of different nanoparticles has previously been reported (Brown et al., 2001; Sayes et al., 2007; Stoeger et al., 2009).

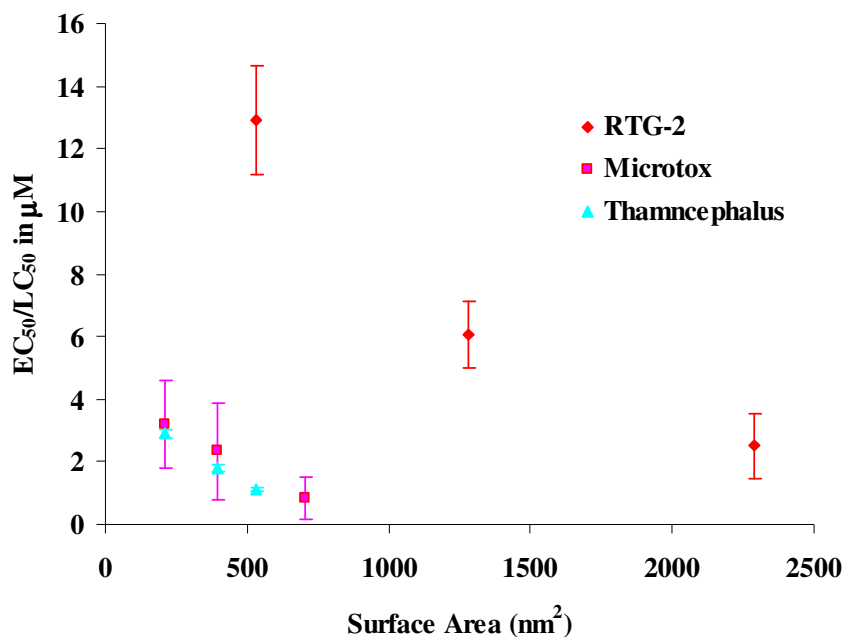


Figure 5.8. Correlation between measured surface areas of PAMAM dendrimers with EC_{50}/LC_{50} in different test models

In the neutral environment of MQ, the measured zeta potentials show a clear correlation with dendrimer generation due to the increased number of the cationic hydrophilic amino groups (G4:64, G5:128, G6: 256). As shown in Figure 5.1, the zeta potential for G4 is minimally altered in all other media, but those of G5 and G6 are significantly altered, such that in DM, TM, MD and DMEM, G5 consistently exhibits the highest zeta potential value. This behaviour can be better understood by considering the change in the zeta potential rather than the observed value, which monotonically increases with generation number in each of the media.

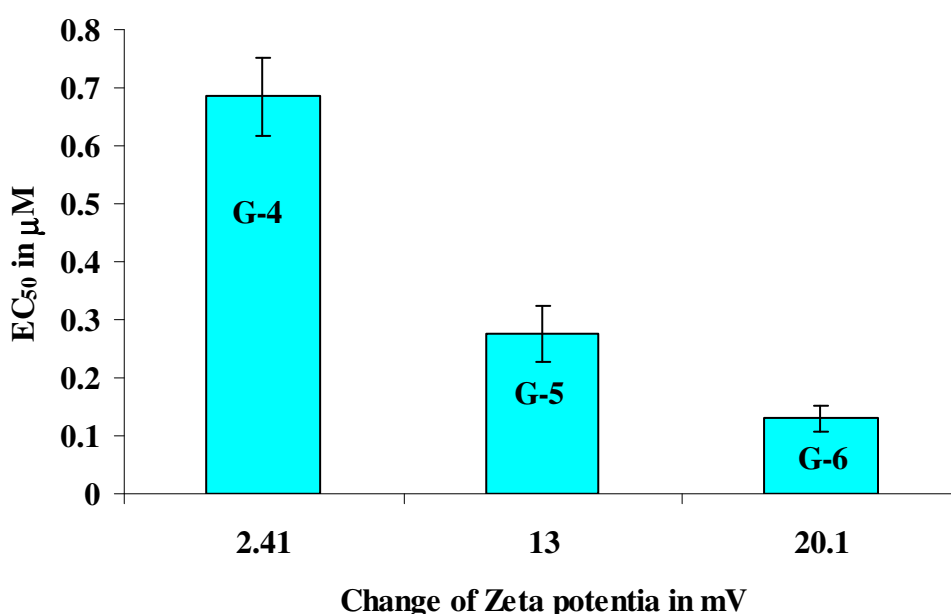


Figure 5.9. Correlation between change of zeta potential and EC₅₀ of PAMAM dendrimer (G4, G5 and G6) in immobilisation of *Daphnia magna*.

Spectroscopic investigation revealed that the spectroscopic changes were largely associated with an interaction of the dendrimer nanoparticles with the FCS. The interaction results in a concomitant change in the pH of the medium and of the zeta potential. Again, no direct correlation between the change in zeta potential and the

change in pH was observed. Notably, the trend of the degree of interaction of G4>G5~G6 does not correlate with the observed trends in the toxic response of G4<G5<G6, indicating that changes to the effective medium concentration due to adsorption of the protein are not the dominant factor governing the toxic response, and that a direct response to the interaction of the cells with the protein covered particles is most likely (Lynch et al., 2007). As for the bacterial and crustacean models, however, there is a correlation between the observed change in the zeta potential and the toxic response potentially pointing towards an indirect toxic mechanism.

The PAMAM dendrimers tested in this study were found to be more toxic, according to the differences of the EC₅₀s to the same test models compared to the PNIPAM and NIPAM/BAM copolymer nanoparticles previously tested (Naha et al., 2009). From the previous study it was demonstrated that the most sensitive model for PNIPAM and NIPAM/BAM 85:15 nanoparticles is *Daphnia magna* (EC₅₀ 413.6 and 449.6 mg l⁻¹ respectively). For NIPAM/BAM 65:35 and NIPAM/BAM 50:50 the most sensitive model was found to be *Vibrio fischeri* (EC₅₀ 40 and 25 mg l⁻¹ respectively). For the PAMAM dendrimers tested in this study the *Daphnia magna* was the most sensitive model, EC₅₀ 0.68 μM (~ 9.6 mg l⁻¹), 0.27 μM (~ 7.7 mg l⁻¹) and 0.13 μM (~ 7.4 mg l⁻¹) respectively.

For the PAMAM dendrimer series, the surface chemistry is the same for each generation, but in successive generations there is a systematic increase in molecular weight, number of surface amino groups and particle size. The toxicity also linearly increased with the increase in generation of PAMAM dendrimer (G6 > G5 > G4) with all the test models which point towards physico-chemical properties as well as structure activity relationship.

5.5 Conclusion

In summary, polyamidoamine (PAMAM) dendrimers show a significant eco and cytotoxicological response at concentrations ranges from 0.13 μM to 16.30 μM . For all generations of PAMAM dendrimer tested the *Daphnia magna* was demonstrated to be the most sensitive test model with the RTG-2 cell line being the least sensitive. The toxicological response was seen to correlate well with the generation of PAMAM dendrimers and therefore with the particle surface area. The surface chemistry is unaltered in successive generations, and thus a clear and direct relationship between the physical parameter and the toxic response is inferred. The physico-chemical characteristics, most notably the zeta potential of the particles, were seen to change dependant on the dispersion medium, however, and the correlation of the toxic response to these changes may point towards an interaction with the medium resulting in a change in effective composition as an underlying source of the toxic response. Successive generations present a larger surface area for interaction with the media, and thus a larger toxic response. Such an indirect effect cannot be considered as the sole origin; however, as is seen by comparison of the PAMAM dendrimers with the NIPAM/BAM copolymer nanoparticles and mechanisms of internalisation resulting in a direct toxic response should be investigated for all models.

While this study has established the initial ecotoxicity of these PAMAM (G4, G5 and G6) dendrimers, consideration should now be directed towards understanding the mechanisms behind the observed toxicity for these dendrimers, as presented in the next chapter.

References

- Boas, U., Heegaard, P. M. H. 2004. Dendrimers in drug research. *Chem. Soc. Rev.* 33, 43-63.
- Boaru, D. A., Dragos, N., Schirmer, K. 2006. Microcystin-LR induced cellular effects in mammalian and fish primary hepatocyte cultures and cell lines: a comparative study. *Toxicology*, 218, 134–148.
- Brown, D. M., Wilson, M. R., MacNee, W., Stone, V., Donaldson, K. 2001. Size-Dependent Proinflammatory Effects of Ultrafine Polystyrene Particles: A Role for Surface Area and Oxidative Stress in the Enhanced Activity of Ultrafines. *Toxicology and Applied Pharmacology*, 175, 191–199.
- Caminada, D., Escher, C., Fent, K. 2006. Cytotoxicity of pharmaceuticals found in aquatic systems: Comparison of PLHC-1 and RTG-2 fish cell lines. *Aquat. Toxicol.* 79, 114-123.
- Casey, A., Herzog, E., Lyng, F. M., Byrne, H. J., Chambers, G., Davoren, M. 2008. Single walled carbon nanotubes induce indirect cytotoxicity by medium depletion in A549 lung cells. *Toxicol. Lett.* 179, 78-84.
- Casey, A., Davoren, M., Herzog, E., Lyng, F. M., Byrne, H. J., Chambers, G. 2007. Probing the interaction of single walled carbon nanotubes within cell culture medium as a precursor to toxicity testing. *Carbon*, 45, 34–40.
- Chandrasekhar, D., Sistla, R., Ahmad, F. J., Khar, R. K., Diwan, P. V. 2007. The development of folate-PAMAM dendrimer conjugates for targeted delivery of anti-arthritic drugs and their pharmacokinetics and biodistribution in arthritic rats. *Biomaterial*, 28, 504-512.
- Colvin, V. L. 2003. The potential environmental impact of engineered nanomaterials. *Nat. Biotechnol.* 21, 1166–70.

- Davoren, M., Fogarty, A.M. 2006. *In vitro* cytotoxicity assessment of the biocidal agents sodium o-phenylphenol, sodium o-benzyl-p-chlorophenol, and sodium p-tertiary amylphenol using established fish cell lines. *Toxicol. In Vitro*, 7, 1190-1201.
- Duncan, R., Izzo, L. 2005. Dendrimer biocompatibility and toxicity. *Adv. Drug Deliv. Rev.* 57, 2215-2237.
- Emanuele, A. D., Attwood, D. 2005. Dendrimer-drug interactions. *Adv. Drug Deliv. Rev.* 57, 2147-2162.
- Franklin, N. M., Rogers, N. J., Apte, S. C., Batley, G. E., Gadd, G. E., Casey, P.S. 2007. Comparative Toxicity of Nanoparticulate ZnO, Bulk ZnO, and ZnCl₂ to a Freshwater Microalga (*Pseudokirchneriella subcapitata*): The Importance of Particle Solubility. *Environ. Sci. Technol.* 41, 8484–8490.
- Fent, K. 2001. Fish cell lines are versatile tools in ecotoxicology: assessment of cytotoxicity, cytochrome P4501A induced potential and estrogenic activity of chemicals and environmental samples. *Toxicology in vitro*, 15, 477-488.
- Feurstein, D., Kleinteich, J., Heussner, A.H., Stemmer, K., Dietrich, D.R. 2010. Investigation of microcystin congener-dependent uptake into primary murine neurons. *Environmental Health and Perspective*, 118, 370-375.
- Foley, S., Crowley, C., Smaih, M., Bonfils, C., Erlanger, B., Seta, P., Larroque, C. 2002. Cellular localisation of a water-soluble fullerene derivative. *Biochem. Biophys. Res. Commun.* 294, 116–119.
- Gagné, F., Auclair, J., Turcotte, P., Fournier, M., Gagnon, C., Sauve, S., Blaise, C. 2008. Ecotoxicity of CdTe quantum dots to fresh water mussels: Impacts on immune system, oxidative stress and genotoxicity. *Aquat. Toxicol.* 86, 333-340.

- Heiden, T. C., Dengler, E., Kao, W. J., Heideman, W., Peterson, R. E. 2007. Developmental toxicity of low generation PAMAM dendrimers in zebrafish. *Toxicol Appl Pharmacol.* 225, 70-79.
- Heinlaan, M., Ivask, A., Blinova, I., Dubourguier, H. C., Kahru, A. 2008. Toxicity of nanosized and bulk ZnO, CuO and TiO₂ to bacteria *Vibrio fischeri* and crustaceans *Daphnia magna* and *Thamnocephalus platyurus*. *Chemosphere*, 71, 1308-1316.
- Hong, S. P., Bielinska, A. U., Mecke, A., Keszler, B., Beals, J. L., Shi, X. Y., Balogh, L., Orr, B. G., Baker, J. R., Holl, M. M. B. 2004. Interaction of poly(amidoamine) dendrimers with supported lipid bilayers and cells: hole formation and the relation to transport. *Bioconjugate Chem.* 15, 774-782.
- <http://www.dendritech.com/pamam.html>.
- Kotak, B. J., Semalulu, S., Friyzt, D. L., Prepas, E. E., Hrudehy, S. E., Coppock, R.W. 1996. Hepatic and renal pathology of intraperitoneally administered microcystin-LR in rainbow trout (*Oncorhynchus mykiss*). *Toxicol*, 34, 517-525.
- Labieniec, M., Gabryelak, T. 2008. Preliminary biological evaluation of poly(amidoamine) (PAMAM) dendrimer G3.5 on selected parameters of rat liver mitochondria. *Mitochondrion*, 8, 305-312
- Leroueil, P. R., Berry, S. A., Duthie, K., Han, G., Rotello, V. M., McNerny, D. Q., Baker, J. R., Orr, B. G., Holl, M. M. B. 2008. Wide varieties of cationic nanoparticles induce defects in supported lipid bilayers. *Nano Letters*. 8, 420-424.
- Leroueil, P. R., Hong, S. Y., Mecke, A., Baker, J. R., Orr, B. G., Holl, M. M. B. 2007. Nanoparticle interaction with biological membranes: Does nanotechnology present a janus face? *Acc. Chem. Res.* 40, 335-342.

- Lovern, S. B., Strickler J. R., Klaper, R. 2007. Behavioural and physiological changes in *Daphnia magna* when exposed to nanoparticle suspensions (titanium dioxide, nano-C60, and C60HxC70Hx). *Environ. Sci. Technol.* 41, 4465-7.
- Lynch, I., Cedervall, T., Lundqvist, M., Cabaleiro-Lago, C., Linse, S., Dawson, K. A. 2007. The nanoparticle–protein complex as a biological entity; a complex fluids and surface science challenge for the 21st century. *Advances in Colloid and Interface Science*, 134-135, 167–174.
- Malik, N., Wiwattanapatapee, R., Klopsch, R., Lorenz, K., Frey, H., Weener, J. W., Meijer, E. W., Paulus, W., Duncan, R. 2000. Dendrimers: relationship between structure and biocompatibility *in vitro*, and preliminary studies in the biodistribution of 125I-labelled polyamidoamine dendrimers *in vivo*. *Journal of Controlled Release*. 65, 133-148.
- Mortimer, M., Kasemets, K., Heinlaan, M., Kurvet, I., Kahru, A. 2008. High throughput kinetic *Vibrio fischeri* bioluminescence inhibition assay for study of toxic effects of nanoparticles. *Toxicol. In Vitro*, 22, 1412-1417.
- Mueller, N. C., Nowack, B. 2008. Exposure Modelling of Engineered Nanoparticles in the Environment. *Environ. Sci. Technol.* 42, 4447–4453.
- Naha, P. C., Casey, A., Tenuta, T., Lynch, I., Dawson, K. A., Byrne, H. J., Davoren, M. 2009. Preparation, Characterization of NIPAM and NIPAM/BAM Copolymer Nanoparticles and their Acute Toxicity Testing using an Aquatic test battery. *Aquat. Toxicol.* 92, 146-154.
- Navarro, E., Piccapietra, F., Wagner, B., Marconi, F., Kaegi, R., Odzak, N., Sigg, L., Behra, R. 2008. Toxicity of Silver Nanoparticles to *Chlamydomonas reinhardtii*. *Environ. Sci. Technol.* 42, 8959–8964.

- Perinotto, A. C., Caseli, L., Hayasaka, C. O., Riul, A., Oliveira, O. N., Zucolotto, V. 2008. Dendrimer-assisted immobilization of alcohol dehydrogenase in nanostructured films for biosensing: Ethanol detection using electrical capacitance measurements, *Thin Solid Films*, 516, 9002–9005.
- Pichardo, S., Jos, A., Zurita, J. L., Salguero, M., Camean, A. M., Repetto, G. 2005. The use of the fish cell lines RTG-2 and PLHC-1 to compare the toxic effects produced by microcystins LR and RR. *Toxicol. In vitro*, 19, 865–873.
- Posadaz, A., Sanchez, E., Gutierrez, M.I., Calderon, M., Bertolotti, S., Biasutti, M.A., Garcia, N.A. 2000. Riboflavin and rose Bengal sensitised photo-oxidation of sulfathiazole and succinylsulfathiazole kinetic study and microbiological implications. *Dyes and Pigments*, 45, 219–228.
- Roberts, J. C., Bhalgat, M. K., Zera, R. T. 1996. Preliminary biological evaluation of polyamidoamine (PAMAM) Starburst™ dendrimers. *J. Biomed. Material Research*, 30, 53-65.
- Sayes, C. M., Reed, K. L., Warheit, D. B. 2007. Assessing Toxicity of Fine and Nanoparticles: Comparing *In vitro* Measurements to *In vivo* Pulmonary Toxicity Profiles. *Toxicological Sciences*, 97, 163–180.
- Shieh, M. J., Peng, C. L., Lou, P. J., Chiu, C. H., Tsai, T. Y., Hsu, C. Y., Yeh, C. Y., Lai, P. S. 2008. Non-toxic phototriggered gene transfection by PAMAM-porphyrin conjugates. *J. Control. Rel.* 129, 200-206.
- Stoeger, T., Takenaka, S., Frankenberger, B., Ritter, B., Karg, E., Maier, K., Schulz, H., Schmid O. 2009. Deducing *in vivo* Toxicity of Combustion-Derived Nanoparticles from a Cell-Free Oxidative Potency Assay and Metabolic Activation of Organic Compounds. *Environmental Health Perspectives*, 117, 54-60.

- Svenson, S., Tomalia, D. A. 2005. Dendrimers in biomedical applications – reflections on the field. *Adv. Drug Deliv. Rev.* 57, 2106-2129
- Teneva, I., Asparuhova, D., Dzhambazov, B., Mladenov, R., Schirmer, K. 2003. The freshwater cyanobacterium *Lyngbya aerugineo-coerulea* produces compounds toxic to mice and to mammalian and fish cells. *Environmental Toxicology*, 18, 9–20.
- Teneva, I., Dzhambazov, B., Koleva, L., Mladenov, R., Schirmer, K. 2005. Toxic potential of five freshwater *Phormidium* species (Cyanoprokaryota). *Toxicon*, 45, 711–725.
- Venuganti, V. V. K., Perumal, O. P. 2008. Effect of Poly(amidoamine) (PAMAM) dendrimer on skin permeation of 5-fluorouracil. *Int. J. Pharm.* 361, 230-238.
- Vergun, O., Reynolds, I. J. 2005. Distinct characteristics of Ca²⁺ induced depolarization of isolated brain and liver mitochondria. *Biochim. Biophys. Acta.* 1709, 127–137.
- Xu, Y. H., Zhao, D.Y. 2005. Removal of copper from contaminated soil by use of poly(amidoamine) dendrimers. *Environ. Sci. Technol.* 39, 2369-2375.
- Xu, Y. H., Zhao, D. Y. 2006. Removal of lead from contaminated soils using poly(amidoamine) dendrimers. *Ind. Eng. Chem. Res.* 45, 1758-1765.
- Zirak, P., Penzkofer, A., Schiereis, T., Hegemann, P., Jung, A., Schlichting, I. 2005. Absorption and fluorescence spectroscopic characterisation of BLUF domain of AppA from *Rhodobacter sphaeroides*. *Chemical Physics*, 315, 142–154.

Chapter 6

Genotoxicity and apoptosis of PLHC-1 Cells upon exposure to PAMAM dendrimers

Adapted from Reactive oxygen species induced genotoxicity and apoptosis of PLHC-1 cells upon exposure of PAMAM dendrimers. (Manuscript in preparation)

6.1 Introduction

Eco (nano) toxicology is a relatively new area of research and, notably, in comparison to human nanotoxicology, there is a dearth of quantitative structure activity relationships established for nanomaterials. The study of N-isopropylacrylamide/N-tert-butylacrylamide copolymer nanoparticles demonstrated a clear relationship between the observed toxicity in a range of fresh water test models, representing different trophic levels, and the physico-chemical properties of the nanoparticles (Chapter 3, Naha et al., 2009). Similarly clear structural dependences of the responses of all trophic levels have been observed with nano-sized PAMAM dendrimers in the same range of fresh water ecological organisms and fish cells (Chapter 5, Naha et al., 2009). There have been other recent reports on the ecotoxicological evaluation of various metal-based nanomaterials (Lovern et al., 2007; Heinlaan et al., 2008; Gaghe et al., 2008; Mortimer et al., 2008; Navarro et al., 2008; Franklin et al., 2007; Mueller and Nowack, 2008). However, the majority of studies to date have been phenomenological and in the main have not explored the mechanisms of interaction.

These systematically varied molecular nanostructures also present a route towards an understanding of the dependence of the interactions with biosystems on the physico-chemical properties of nanomaterials. As well as their potential importance in nanomedical applications, the structurally well-defined and variable macromolecules can also provide a further basis upon which to establish structure activity relationships governing eco-toxicological responses which may serve to develop a fundamental understanding of their interactions as described in chapter 5.

Oxidative stress has been established as one of the key factors determining the toxicity of several nanomaterials (Nel et al., 2006; Lanone et al., 2006; Donaldson et al., 2006; Obedoster et al., 2005). Free radical formation causes damage to biological components

through oxidation of lipids, proteins and DNA damage and finally leads to apoptotic cell death. Oxidative stress may have a role in the induction of inflammation through up regulation of redox sensitive transcription factors, NF- κ B and activator protein-1 (AP-1), and kinases involved in inflammation (Lanone et al., 2006; Rahman, 2000; Rahman et al., 2005; Park and Park 2009). However, there is a range of reactive oxygen species which can be generated, dependent upon the chemical nature of the toxicant. Also different species of ROS lead to different intracellular responses. For example, the hydroxyl radical can lead to adduct formation in the base pairs of DNA such as 8-OHdG (8-hydroxy2'-deoxyguanosine) production, which mediates the pathophysiology of a wide variety of diseases including cancer, atherosclerosis, neurodegenerative disorders and the aging process (Halliwell and Gutteridge, 1999). Because of its importance, the potential of nanoparticles to elicit such a response should be investigated.

The ecotoxicological assessment of PAMAM dendrimers was previously conducted in a multitrophic battery of bioassays representing different trophic levels (Chapter 5). Within the battery, the PLHC-1 fish cell line, derived from a hepatocellular carcinoma in an adult female topminnow (*Poeciliopsis lucida*), was seen to be the second most sensitive bioassay and a clear and systematic dependence of the toxic response on the dendrimer generation was observed. In this chapter, the mechanism of the toxicity pathway of PAMAM dendrimers is explored in the PLHC-1 fish cell line. Analysis of the generation of reactive oxygen species, DNA damage and apoptosis was performed to understand the cell death process. The PLHC-1 cell line represents vertebrate models, in accordance with the EU policy of Reduction, Replacement and Refinement (RRR), (Directive 86/609/EEC on the protection of animals used for experimental and scientific purposes).

6.2 Experimental methods

All the experimental methods employed are described in chapter 2. The protocols for intracellular reactive oxygen species (ROS) detection and quantification in PLHC-1 cells is described in section 2.2.2.9. The genotoxic response of PLHC-1 cells exposed to PAMAM dendrimers was detected by the alkaline comet assay described in section 2.2.2.12. The procedure for DNA extraction after exposure to PAMAM dendrimers is outlined in section 2.2.2.11.1. The 8-OHdG assay was carried out by ELISA as described in section 2.2.2.11.2 and the apoptosis assay is described in section 2.2.2.13 of chapter 2.

6.3 Results

6.3.1 Particle characterization and Cytotoxicity

Particle characterisation (particle size, zeta potential, spectroscopic studies) and the cytotoxicity data were provided in chapter 5. Due to the observed relatively higher sensitivity of the PLHC-1 cells, the mechanistic pathways are explored in PLHC-1 cells.

6.3.2 Intracellular reactive oxygen species (ROS)

Quantitative measurement of the intracellular ROS generation in PLHC-1 cells was performed at different time points (1h, 2h, 4h, 6h and 12h) and with different exposure concentrations of each dendrimer (G4, G5 and G6). For all generations, the exposure time points and the concentration of PAMAM dendrimer (0.15 μM to 6 μM) used were the same, in order to correlate intracellular ROS production by the three generations of PAMAM dendrimers and also to enable comparison with the cytotoxic and genotoxic responses, as well as apoptosis and cell death. Intracellular ROS generation in PLHC-1 cells upon the exposure to PAMAM dendrimers was visualised using confocal

fluorescence microscopy, as shown in figure 6.1, for the case of 2 h exposure of each dendrimer at a concentration of 2 μM (G4, G5 and G6) and 400 μM for H_2O_2 . The confocal images were taken using a 63x oil immersion objective lens. It should be noted that the regions of white coloration are present in the control samples and therefore are not due to nanoparticles, but may be due to the reflection of the white light. The concentration dependent increase in ROS production for the five different time points for the three dendrimer generations was monitored using the fluorescence plate reader and the results are shown in figure 6.2. Intracellular ROS production was found to be dendrimer generation and time dependent (Figure 6.3). A significant generation dependent ROS production $\text{G6} > \text{G5} > \text{G4}$ was observed at 1, 2, and 12 h exposure time period ($p \leq 0.05$) as illustrated in figure 6.3.

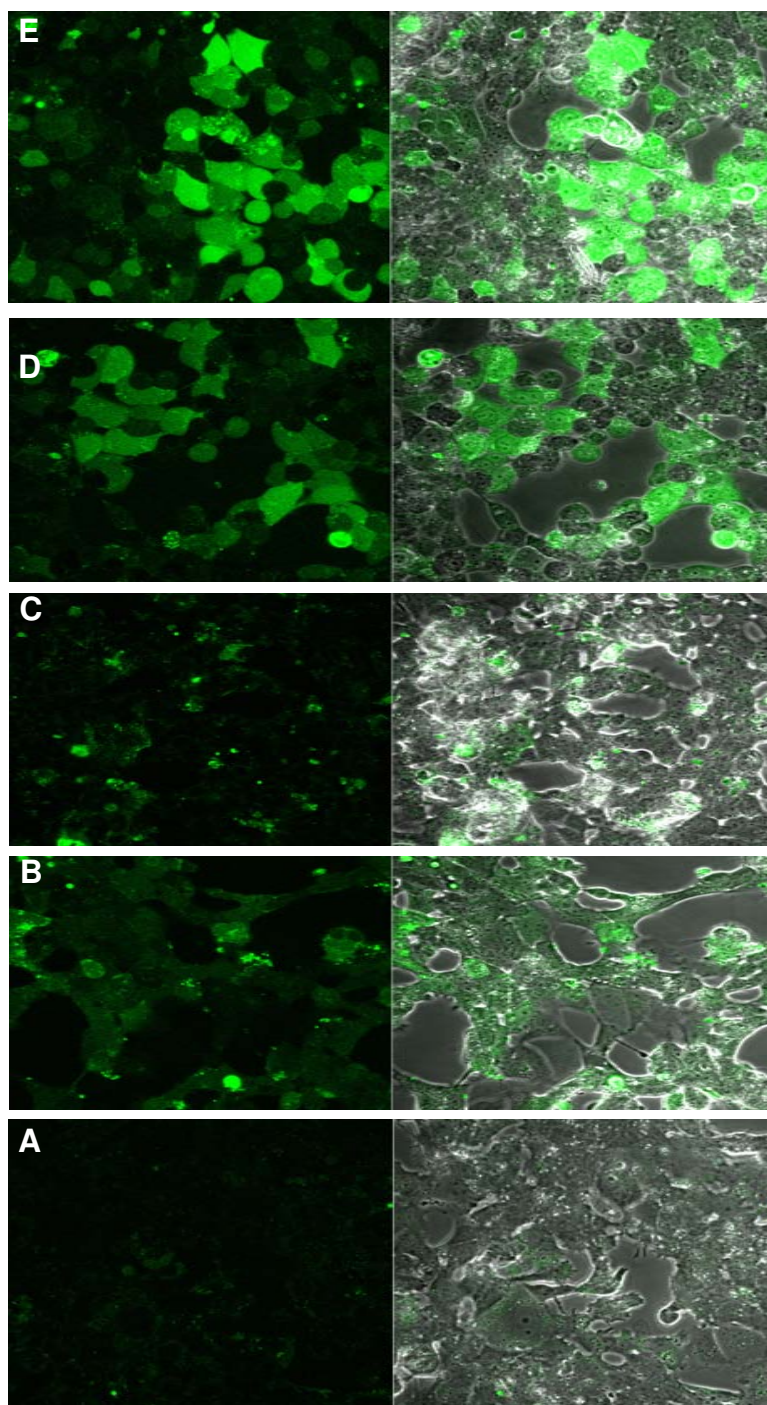


Figure 6.1 Confocal laser scanning micrograph (CLSM) of PLHC-1 cells showing intracellular ROS production upon exposure of PAMAM dendrimers to the PLHC-1 cells at 2 h exposure time period. Figure A, B, C, D and E represent the Negative control, H₂O₂, PAMAM G4, G5 and G6 respectively at 2 μM concentration for the case of PAMAM and 400 μM H₂O₂. Magnification is at 63x.

Figure 6.4A describes the relationship between the intracellular ROS production and the primary surface amino group of the PAMAM dendrimer for a fixed concentration of 0.6 μM at 2 h exposure time period. Similar to the case of the cytotoxic response, the

generation dependent ROS levels appear to be correlated with increasing generation, following the trend of G6 > G5 > G4 as shown in figure 6.3. This trend mirrors that of the cytotoxic response (Figure 5.7, chapter 5).

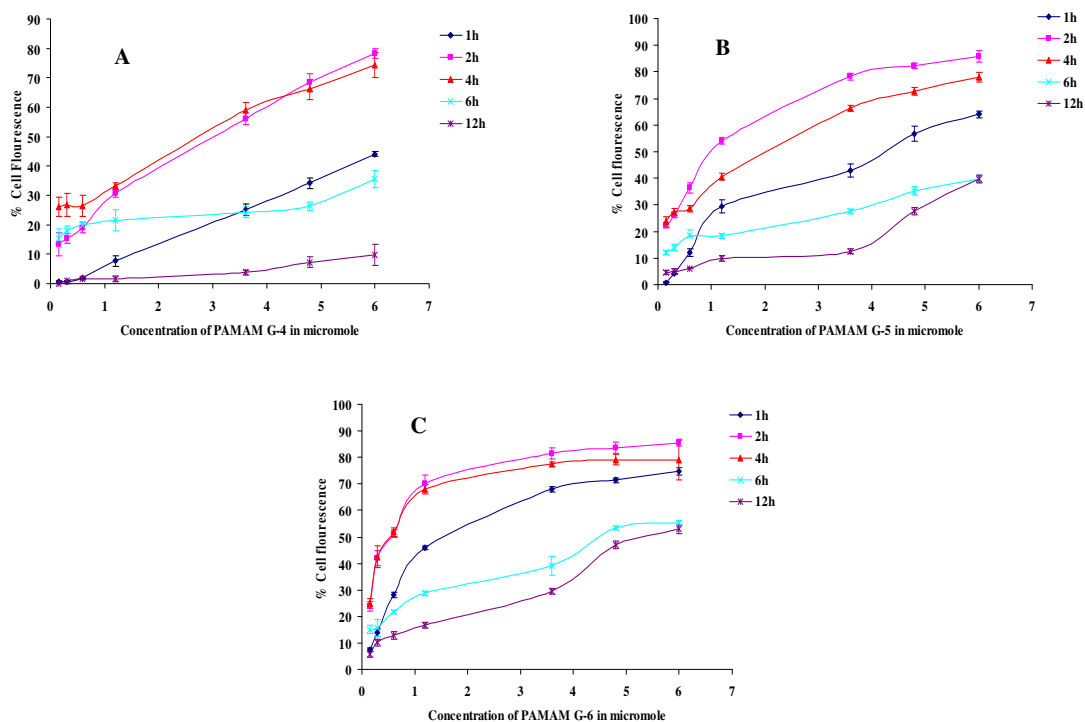


Figure 6.2. Concentration and time dependent intracellular ROS generation, upon the exposure of PAMAM dendrimers (A) G4 (B) G5 and (C) G6. The data are presented as mean \pm SD (n=3). % of cell fluorescence (% cell fluorescence as compared to control).

The intracellular ROS production in PLHC-1 cells is systematically dependent on generation and concentration of PAMAM dendrimers. At the lower concentrations, exposure results in a monotonic increase in the intracellular ROS production at all time points. At higher concentrations, a saturation of ROS production was observed (figure 6.2). As a function of time, for all generations and concentrations, the ROS levels are seen to increase initially, reach a maximum before decaying to control levels (figure 6.3). For all PAMAM generations (G4, G5 and G6) the maximum level of ROS

production is approximately 90% and this maximum level is reached after ~2h for G5 and G6, while for the case of G4, the maximum level is reached at ~ 4h. The generation of ROS is counteracted by the natural intracellular antioxidants which act to minimize the oxidative stress (Sies, 1993). In general, the time evolution of the ROS is not very well understood, but similar behaviour has been observed in other studies (Mukherjee et al.,2010)

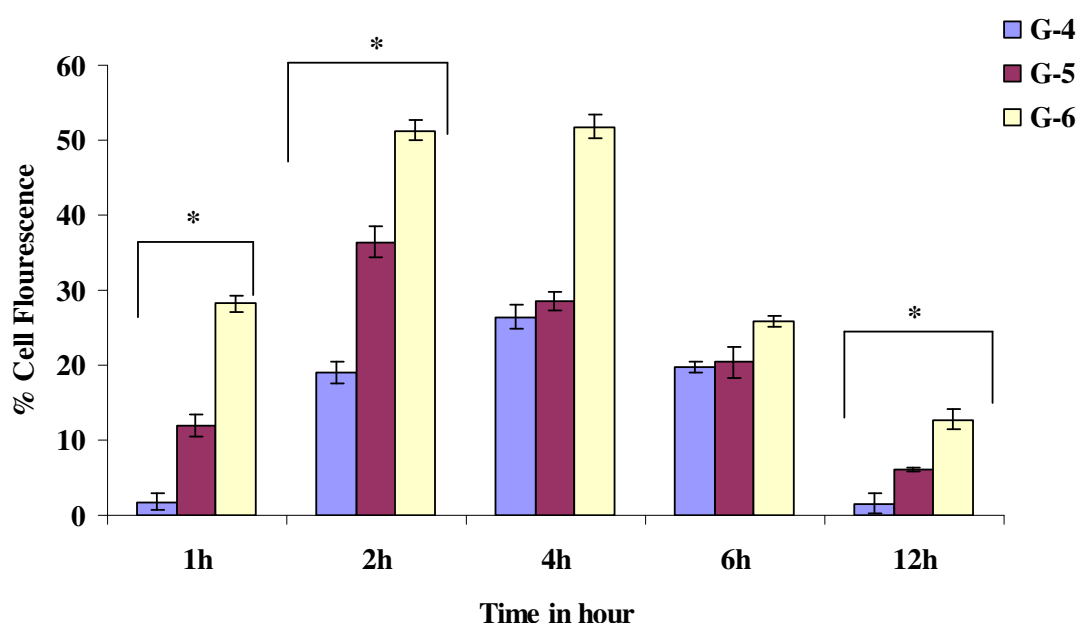
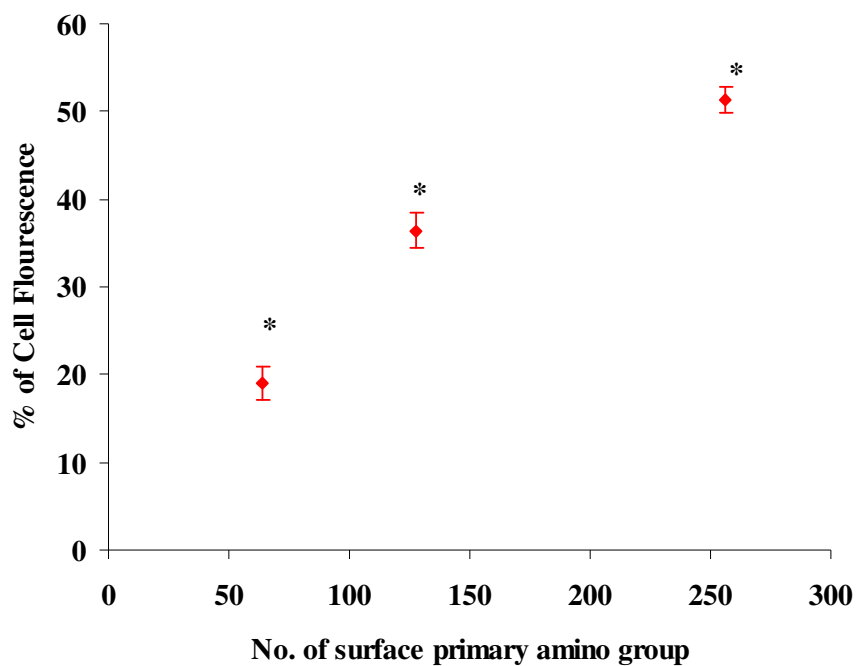


Figure 6.3. Plot showing the generation dependent intracellular ROS production at a concentration of $0.6\mu\text{M}$. *Denotes significant difference of ROS production between G4, G5 and G6 in all the exposure time period 1, 2, and 12 h ($p \leq 0.05$).

Notably, however, when the concentration is expressed in terms of effective number of amino groups (molar dose \times number of amino groups per dendrimer), the ROS generation curves for a fixed time point overlap almost exactly, as shown in Figure 6.4(B).

A



B

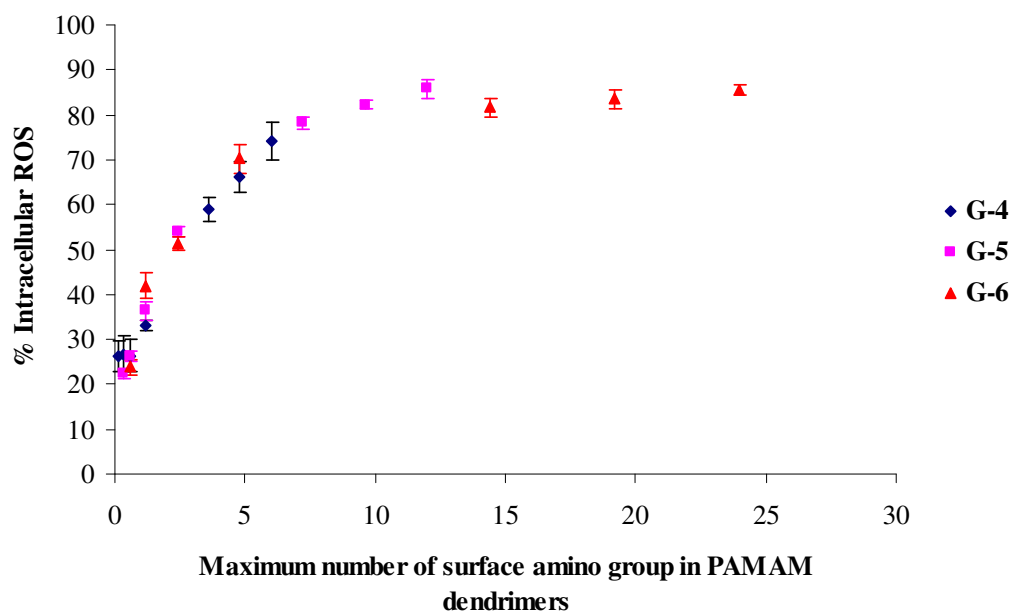


Figure 6.4. (A) Plot showing the relationship between the intracellular ROS production and the number of surface primary amino group of the PAMAM dendrimers at 2 hour exposure time period of $0.6\mu\text{M}$ concentration. *Denotes significant difference of ROS production with increases in the surface primary amino groups ($p \leq 0.05$); (B)

relationship between maximum surface amino group and the intracellular ROS production in PLHC-1 cells.

6.3.3 Genotoxicity response of PAMAM dendrimers

The genotoxicity of the PAMAM dendrimers was evaluated in PLHC-1 cells at a concentration range from 0.125 μM to 1 μM for the cases of G4, G5 and G6, for different exposure times (6h, 12h and 24h). For all dendrimer generations, the concentration range is one of approximately linear increase in levels of ROS (figure 6.2). DNA damage was estimated by analyzing the tail percentage DNA in the Comet assay. Representative micrographs of observed comets are shown in figure 6.5, after 24 hour exposure to PAMAM dendrimers at a concentration of 0.5 μM . A dose dependent genotoxicity response was observed in all three generations of PAMAM dendrimers in PLHC-1 cells (Figure 6.6). Significant genotoxicity response was observed in PLHC-1 cells as compared to control group ($p \leq 0.05$) after exposure of PAMAM dendrimers. Also a generation dependent level of DNA damage was observed with the PAMAM dendrimers (Figure 6.7). Significant generation dependent ($p \leq 0.05$) genotoxicity response was observed at 24 hour exposure time period. However, after 6 and 12 h exposure, a significant difference of genotoxicity response between G4, G6, and between G5, G6 ($p \leq 0.05$) is observed at a concentration of 0.5 μM (Figure 6.7).

The toxic responses of all organisms studied are well correlated with the physico-chemical characteristic of the PAMAM dendrimers (Chapter 5, Naha et al., 2009), and here the same is observed for the generation of intracellular ROS and the genotoxic response in PLHC-1 cells, indicating that the paradigm of oxidative stress as the source of the toxic mechanism of nanoparticles, outlined by Nel et al., 2006, is applicable for PAMAM dendrimers. Notably, both the oxidative stress and the genotoxic response are

correlated with the number of surface amino groups per dendrimer as shown in shown in figure 6.4A and 6.8.

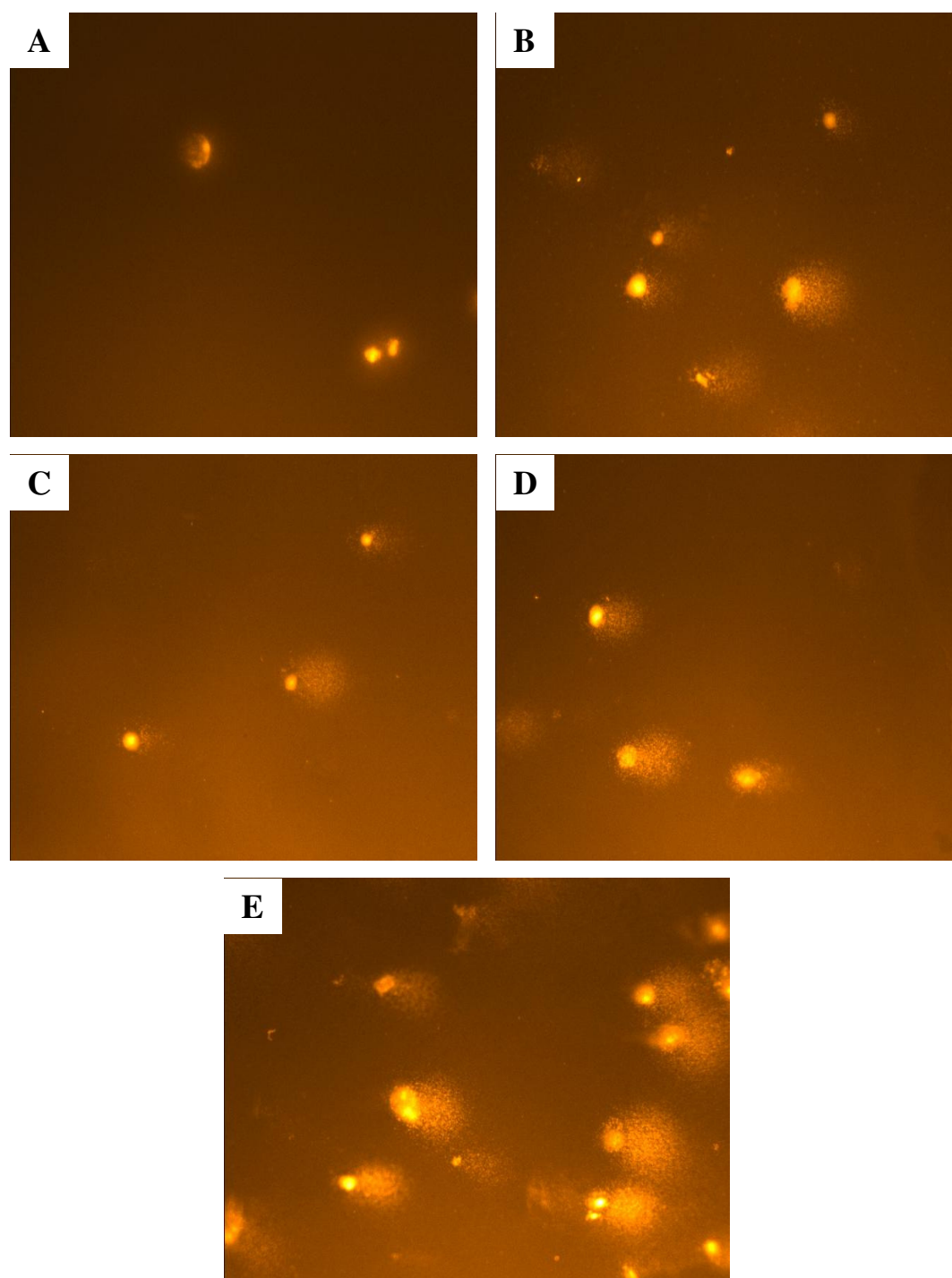


Figure 6.5. Representative micrographs showing comets of PLHC-1 cells after 24 hour exposure of PAMAM dendrimers. Panel A represents control, Panel B, Represents ENU (Ethyl nitrosourea), Panels C, D and E represent G4, G5 and G6 respectively.

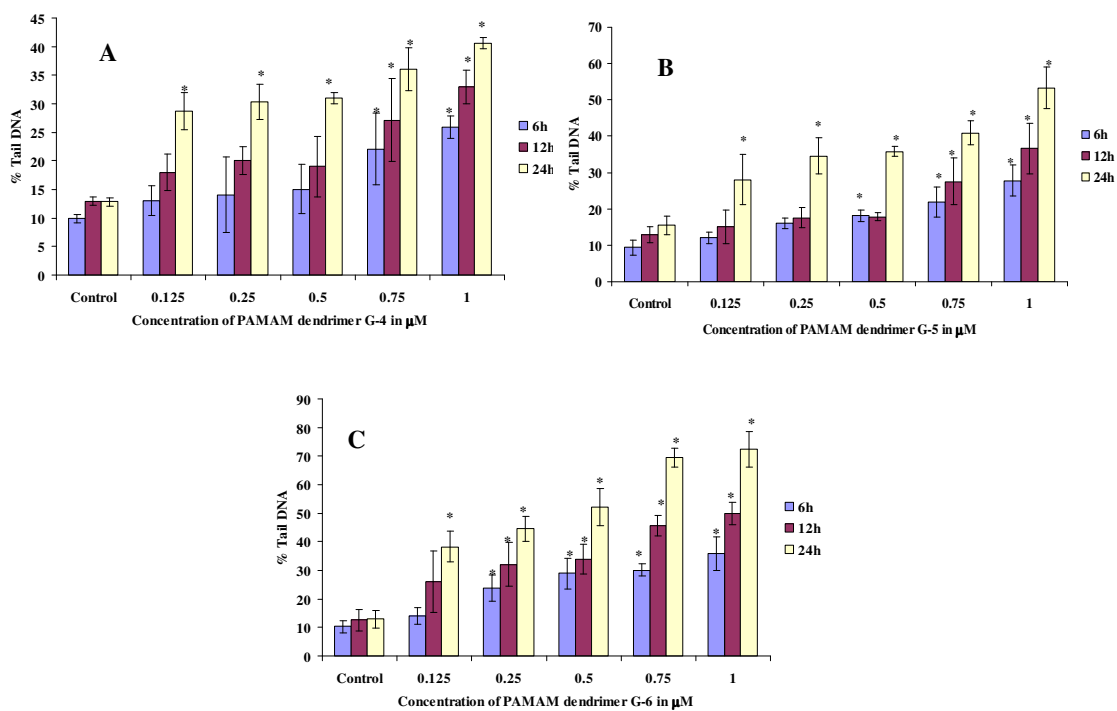


Figure 6.6. Genotoxicity response of PAMAM dendrimers at 6h, 12h and 24h exposure, Panels A, B and C represent PAMAM G4, G5 and G6 respectively. *Denotes significant difference genotoxicity response as compared to control group ($p \leq 0.05$).

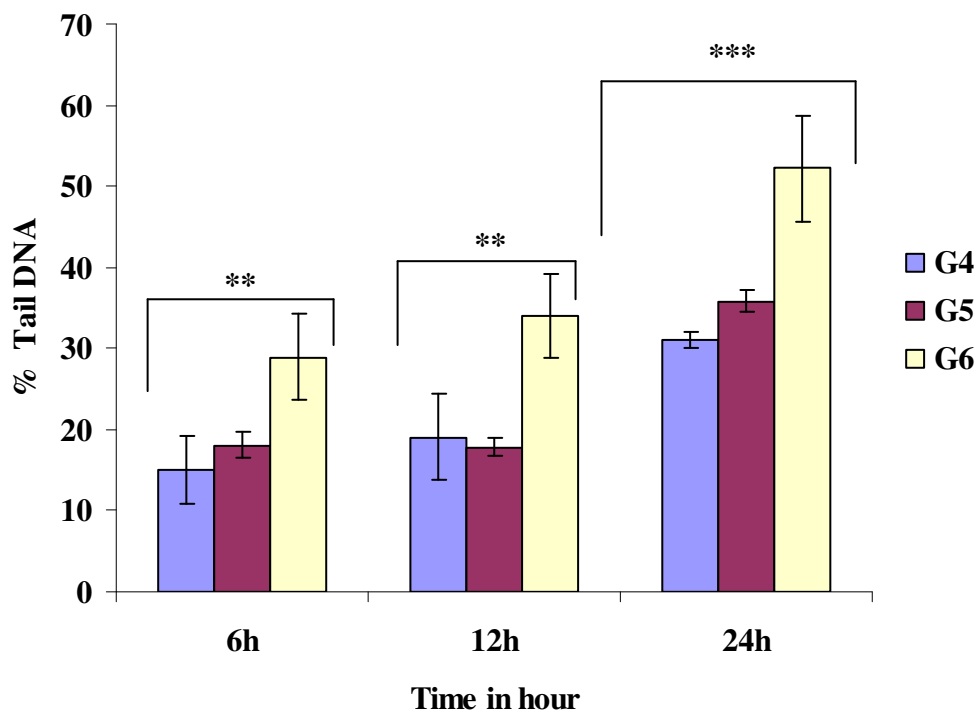


Figure 6.7. Generation dependent genotoxicity response of PAMAM dendrimers at 6h, 12h and 24h exposure at 0.5 μ M concentration. ***Denotes significant difference of genotoxicity response between G4, G5 and G6 ($p \leq 0.05$). **Denotes significant difference genotoxicity response between G4, G6, and between G5, G6 ($p \leq 0.05$).

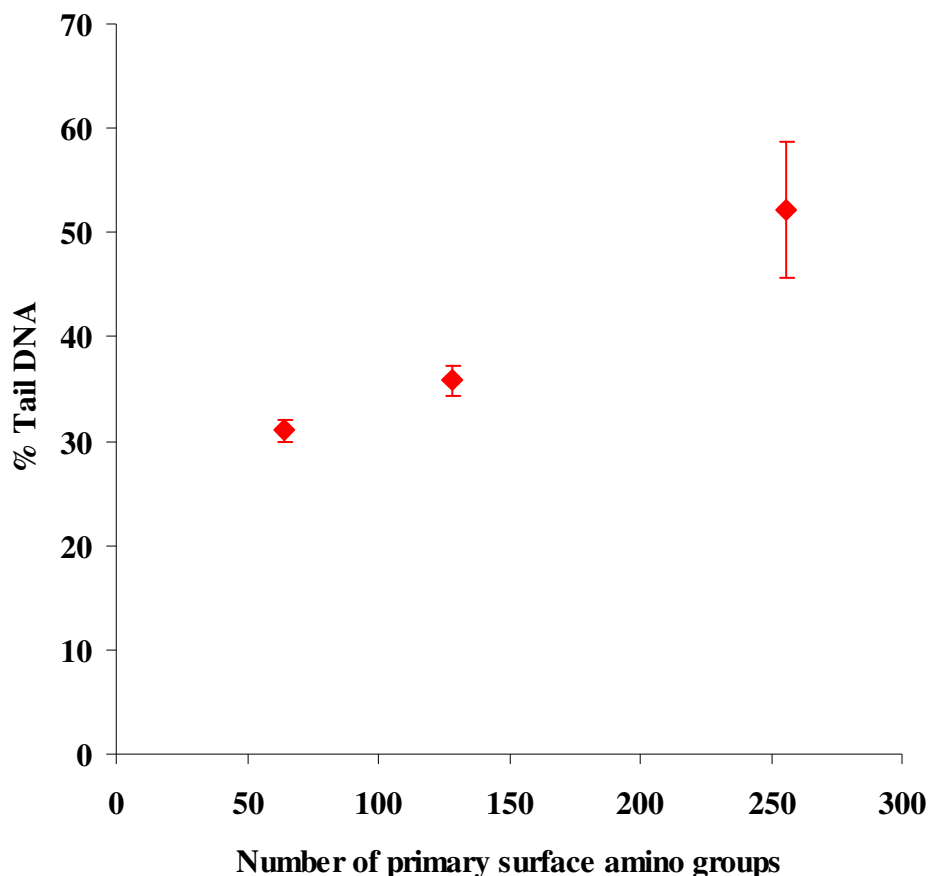


Figure 6.8. Relationship between the % Tail DNA and number of primary surface amino groups of the PAMAM dendrimers (Data shown 24 h exposure at 0.5 μ M concentration. Data showed mean \pm SD).

6.3.4 8-OHdG assay

Oxidative damage to DNA in cells by ROS is a well reported process (Zhang et al., 2009). The level of 8-OHdG (8-hydroxy-2'-deoxyguanosine) production was measured by a competitive *in vitro* enzyme-linked immunosorbant assay for quantitative measurement of the oxidative DNA adduct 8-hydroxy-2'-deoxyguanosine. The levels of 8-OHdG production in the PLHC-1 cells to the PAMAM dendrimers are presented in Table 6.1. As the genotoxicity and intracellular ROS study was investigated in the PLHC-1 cells and at 0.5 μ M significant genotoxicity and intracellular ROS response

was observed, this cell line and the same concentration was used for the detection of 8-OHdG formation. The exposure concentration is 0.5 μM of G4, G5 and G6, each at 6h, 12h and 24h time periods. Notably there is no significant difference between the control group and the PAMAM exposure group. However, there is a significant difference in the level of 8-OHdG production upon exposure to the positive control, H_2O_2 (Shown in table 6.1). Increased levels of 8-OHdG production upon the exposure to PAMAM dendrimers were not detectable over the entire exposure time period. Although a significant degree of DNA damage has been observed as compared to the control group ($p \leq 0.05$) at lower concentrations of 0.125 μM , 0.25 μM and 0.5 μM after 24h exposure (figure 6.6) , no 8-OHdG formation was observed at a concentration of 0.5 μM at the same time of exposure. The results suggests that 8-OHdG is not produced upon the exposure of PAMAM dendrimers in PLHC-1 cells, which is a positive outcome given the potential pathophysiological importance, although significant genotoxic response has been observed at the same concentration (0.5 μM) in PLHC-1 cells.

Table 6.1. Levels of 8-OHdG formation in the PLHC-1 cells to PAMAM dendrimers exposure.

	6h 8-OHdG level in ng/ml	12h 8-OHdG level in ng/ml	24h 8-OHdG level in ng/ml
Control	< 0.125	< 0.125	< 0.125
H_2O_2	0.573 ± 0.29	2.895 ± 0.32	15.704 ± 0.275
G4	< 0.125	< 0.125	<0.125
G5	<0.125	< 0.125	< 0.125
G6	< 0.125	<0.125	<0.125

6.3.5 Apoptosis Assay

The apoptosis study performed with PLHC-1 cells exposed to PAMAM G4, G5 and G6 dendrimers suggests that, with increasing concentration, the percentage of healthy cells

decreases, whereas the early apoptotic, late apoptotic and dead cell populations increase, as shown in Tables 6.2, 6.3 and 6.4 for 6h, 12h and 24h exposure respectively. After 6 hour exposure, a significant early apoptotic cell population was observed as compared to control groups. A significant difference ($p < 0.05$) of early apoptotic cell population at exposure concentrations of 0.6 and 1.2 μM in the case of G6 and 2 μM in the case of G5 as compared to control has been observed. However, a significant ($p < 0.05$) late apoptotic cell population was observed at all the exposure concentrations except 0.65 μM of G4 after 6h exposure (Table 6.2). After 12 hour exposure of PAMAM dendrimers, significant ($p < 0.05$) early and late apoptotic cell populations were observed in PLHC-1 cells except at 0.65 μM concentration of G4, as compared to control (Table 6.3). However, after 24 hour exposure, all the exposure concentrations of PAMAM dendrimer (G4, G5 and G6) employed show significant ($p < 0.05$) early and late apoptotic cell populations, as compared with the control group (Table 6.4). No significant difference between response to the G4, G5 and G6 PAMAM dendrimers was observed at 6 and 12 h (figure 6.9 A and B), although a significant difference ($p < 0.05$) in early and late apoptotic cell populations was observed between G4 and G6 at 24 hour exposure (figure 6.9 C). Furthermore, a significant difference ($p < 0.05$) is observed between the late apoptotic cell population after 24 hour exposure to G5 and G6 dendrimers (figure 6.9 C).

Table 6.2. Percentage of cell populations in different stages of apoptosis of the PLHC-1 cells to PAMAM dendrimers at 6h exposure time period. Data provided here is the mean \pm SD, (N=3).

Different Events	Negative Control	Camptothecin	PAMAM G4 (μ M)			PAMAM G5 (μ M)			PAMAM G6 (μ M)		
			0.65	2.6	5.2	0.25	1	2	0.15	0.6	1.2
% Healthy	92 \pm 5	73 \pm 6	85 \pm 5	81 \pm 5	77 \pm 6	82 \pm 6	79 \pm 6	73 \pm 5	75 \pm 5	67 \pm 5	65 \pm 5
% Early Apoptotic	1.3 \pm 0.3	7.6 \pm 2.1	3.3 \pm 0.3	4.2 \pm 2.8	7.0 \pm 1.2	3.5 \pm 1.7	4.1 \pm 1.9	8.1 \pm 2.1	5.3 \pm 2.4	8.1 \pm 2.5	9.1 \pm 3.1
% Late Apoptotic	0.1 \pm .02	6.5 \pm 2.1	4 \pm 1.8	6.4 \pm 1.4	7.2 \pm 2.3	4.7 \pm 1.7	6.9 \pm .7	8.4 \pm 0.9	6.2 \pm 0.8	7.6 \pm 1	10.1 \pm 1.4
% Dead cells	6.2 \pm 0.9	12. \pm 1.4	7.6 \pm 1.7	8.14 \pm .5	9 \pm 0.7	9.6 \pm 0.8	9.8 \pm 1.2	11. \pm 1.4	13.6 \pm 1.3	17 \pm 1.9	16 \pm 2

Table 6.3. Percentage of cell populations in different stages of apoptosis of the PLHC-1 cells to PAMAM dendrimers at 12h exposure time period. Data provided here is the mean \pm SD, (N=3).

Different Events	Negative Control	Camptothecin	PAMAM G4 (μ M)			PAMAM G5 (μ M)			PAMAM G6 (μ M)		
			0.65	2.6	5.2	0.25	1	2	0.15	0.6	1.2
% Healthy	91.5 \pm 5	52.5 \pm 4.6	81.7 \pm 5	76 \pm 5.8	71.7 \pm 4.2	66.3 \pm 5.9	59.5 \pm 5.1	55.9 \pm 5.7	69.5 \pm 6.2	62.1 \pm 5.9	54.4 \pm 4.2
% Early Apoptotic	1.2 \pm 0.2	17.2 \pm 2.3	6 \pm 3.2	8.2 \pm 2.1	9.1 \pm 2.2	9.9 \pm 1.5	11.7 \pm 1.8	13 \pm 1.1	7.9 \pm 1.4	10.9 \pm 2.5	12.9 \pm 2.1
% Late Apoptotic	0.2 \pm 0.3	16.9 \pm 1.1	7.1 \pm 1.3	9.5 \pm 1.2	10 \pm 2.9	11.8 \pm 2.7	13.9 \pm 1.7	13.8 \pm 1.9	9.8 \pm 0.9	10.6 \pm 1.2	14.5 \pm 2.4
% Dead cells	7.2 \pm 2.9	13.3 \pm 0.9	5 \pm 0.5	6.2 \pm 1.2	9.1 \pm 1.7	11.7 \pm 1.5	14.8 \pm 1.3	17.1 \pm 2.5	12.7 \pm 1.4	16 \pm 1.9	18 \pm 2.1

Table 6.3. Percentage of cell populations in different stages of apoptosis of the PLHC-1 cells to PAMAM dendrimers at 24h exposure time period. Data provided here is the mean \pm SD, (N=3).

Different Events	Negative Control	Camptothecin	PAMAM G4 (μ M)			PAMAM G5 (μ M)			PAMAM G6 (μ M)		
			0.65	2.6	5.2	0.25	1	2	0.15	0.6	1.2
% Healthy	88.4 \pm 5.4	34.5 \pm 5.8	61.7 \pm 4.7	55 \pm 4.3	52 \pm 5.2	56.3 \pm 5.5	51.5 \pm 4.1	47.9 \pm 5.7	39.7 \pm 5.6	32.3 \pm 4.2	27.5 \pm 5.4
% Early Apoptotic	2.1 \pm 0.2	13.4 \pm 1.1	10.9 \pm 2.1	13 \pm 1.8	12.8 \pm 3.2	10.5 \pm 1.6	12.7 \pm 1.7	15.8 \pm 2.3	17.6 \pm 1.4	19.9 \pm 1.5	19.2 \pm 1.9
% Late Apoptotic	3.4 \pm 1.3	17.9 \pm 2.5	12.2 \pm 1.5	15.5 \pm 1.2	15.7 \pm 2.4	15 \pm 1.9	14.9 \pm 1.6	14.9 \pm 1.1	19.9 \pm 0.9	20.8 \pm 1.1	21.9 \pm 1.4
% Dead cells	6 \pm 0.9	33.9 \pm 1.4	15.1 \pm 1.7	16.2 \pm 0.5	19.3 \pm 0.7	18 \pm 0.87	20.8 \pm 1.2	21.2 \pm 1.5	22.7 \pm 3.3	26.9 \pm 3.8	31.8 \pm 4.1

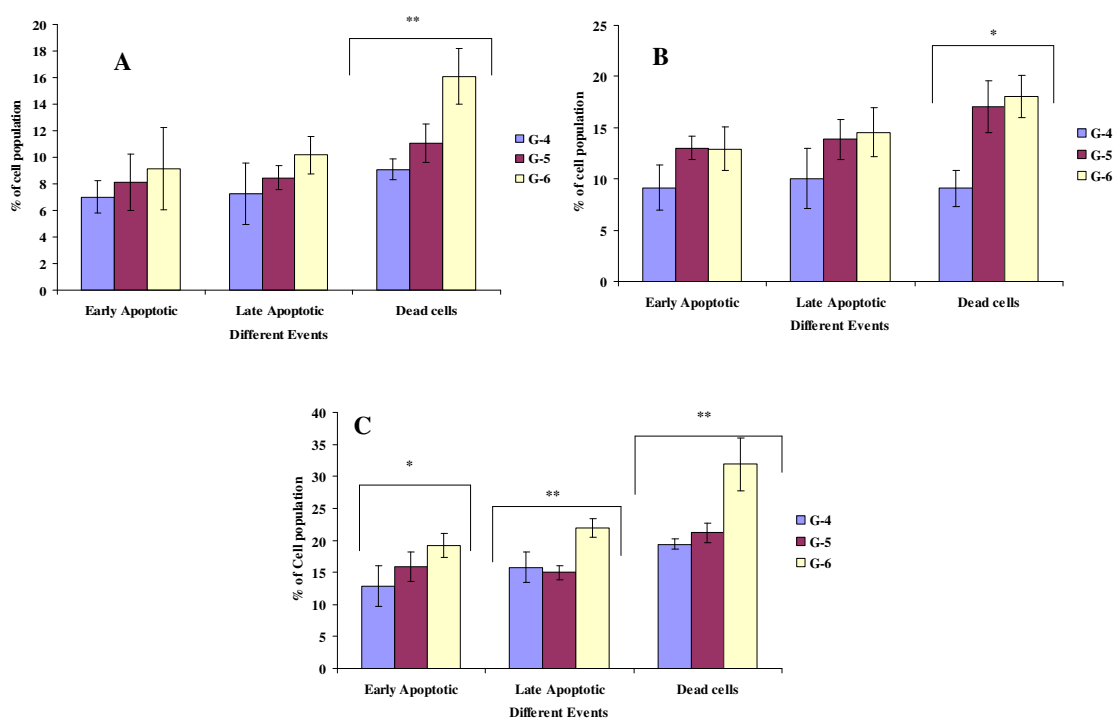


Figure 6.9. Generation dependent apoptosis of the PLHC-1 cells to PAMAM dendrimers and the exposure concentration is 5.2, 2 and 1.2 μM for G4, G5 and G6 respectively. Figure A, B and C represent 6 h, 12h and 24h exposure respectively. ** Denotes the significant difference ($p \leq 0.05$) between G4, G6 and between G5 G6; * denotes the significant difference between G4 and G6 ($p \leq 0.05$).

6.4 Discussion

In the case of the PAMAM dendrimer series, the surface chemistry is the same for each generation, but in successive generations there is a systematic increase in molecular weight, particle size and number of surface amino groups per particle. The toxicity also linearly increases with the increase in generation of PAMAM dendrimer ($G6 > G5 >$

G4) with all the species examined (Chapter 5), which points towards the importance of the physico-chemical properties as well as underlying structure activity relationships.

The generation of intracellular ROS by PAMAM dendrimers is clearly one of the most relevant toxic pathways and a clear generation dependence of increased intracellular ROS production is shown in figure 6.3. The sequence of increased ROS generation is $G6 > G5 > G4$. This response is also well related with the number of surface primary amino groups of the PAMAM dendrimers, as shown in figure 6.4A. This indicates that the cationic surface amino groups play a direct role in the production of ROS. Increased intracellular ROS generation suggests that the PAMAM dendrimers can lead to disruption of the mitochondrial electron transduction chain which leads to additional O_2^- production and perturbs the mitochondrial permeability transition pore, which leads to release of pro-apoptotic factors and programmed cell death (Oberdörster et al., 2005). Intracellular ROS production can lead to inflammation, as demonstrated for a number of different nanoparticles (Li et al., 2008; Stone et al., 2007; Lubos et al., 2008; Driscoll, 2000).

The genotoxicity assay was performed by the Comet assay, which is widely accepted as a simple, sensitive, and rapid tool for assessing DNA damage in different test models and is extensively used for chemical testing (Dhawan et al., 2009). A significant ($p < 0.05$) genotoxic response is observed with PAMAM dendrimers as compared to control in PLHC-1 cells. The response is systematic and clearly dependent on the generation of the PAMAM dendrimers only at 24h exposure (Figure 6.7). Similar generation dependent responses have been observed with the production of reactive oxygen species and cytotoxicity. The percentage of DNA damage is clearly dependent upon the number of surface primary amino groups (as shown in Figure 6.8). Generation dependent of intracellular ROS production, cytotoxicity and genotoxicity was observed with

PAMAM dendrimers in PLHC-1 cells. As the PAMAM generation increases, there is an increase in the number of surface amino groups (64, 128 and 256 amino groups for G4, G5 and G6 respectively) which makes the particle more cationic. As a result, the observed ROS, DNA damage and cytotoxicity may be considered to be primarily due to the surface amino group. Cationic PAMAM dendrimers have been shown to localise in mitochondria (Lee et al., 2009), eliciting a toxic response via production of reactive oxygen species and inflammation in mouse macrophage cells (Naha et al., 2010), as described in the following chapter.

Apoptosis is a programmed cell death mechanism in multicellular organisms (Kerr et al., 1972). It involves a series of biochemical events leading to changes in characteristic cell morphology, including blebbing, changes to the cell membrane, such as loss of membrane asymmetry and attachment, cell shrinkage, nuclear fragmentation, chromatin condensation, and chromosomal DNA fragmentation, and finally cell death (Kerr et al., 1972). Oxidative stress, reported to lead to alteration of mitochondrial function and decreased cell viability was observed, and therefore a further check was carried out to determine whether PAMAM dendrimers caused apoptosis. Apoptosis was detected in cells treated with dendrimers (Table 6.2 to 6.4), as measured by FACS (Fluorescence associated cell sorter) analysis using Yo-Pro[®] and propidium iodide. It has been reported that a strong interaction between cationic dendrimers and lipid bilayers results in enhanced pore formation (Lee and Larson, 2009). In fact, cationic linear polymers in contact with only a single bilayer do not perforate membranes, whereas the relatively rigid dendrimers penetrate the bilayer, since they can achieve a similar degree of contact between charged groups by interacting with both layers (Lee and Larson, 2009). Thus, perforation by a dendrimer itself could be one of the mechanisms responsible for mitochondrial damage. It has been reported that G5 PAMAM dendrimers induce

expression of caspases 3, 9, and Bax proteins and decreased Bcl-2 expression which is an indication of apoptosis (Lee et al., 2009). The results presented here agree with the published literature. However after 24 hour exposure, all the exposure concentration of PAMAM dendrimer (G4, G5 and G6) employed shows significant ($p < 0.05$) early and late apoptotic cell populations as compared with control group (Table 6.4). It has been observed that no significant difference of early and late apoptotic cell populations between the G4, G5 and G6 PAMAM dendrimers at 6 and 12 h (figure 6.9 A and B), however a significant difference ($p < 0.05$). However, there was a significant difference of early and late apoptotic cell population was observed between G4 and G6 at 24 hour exposure time period (figure 6.9 C).

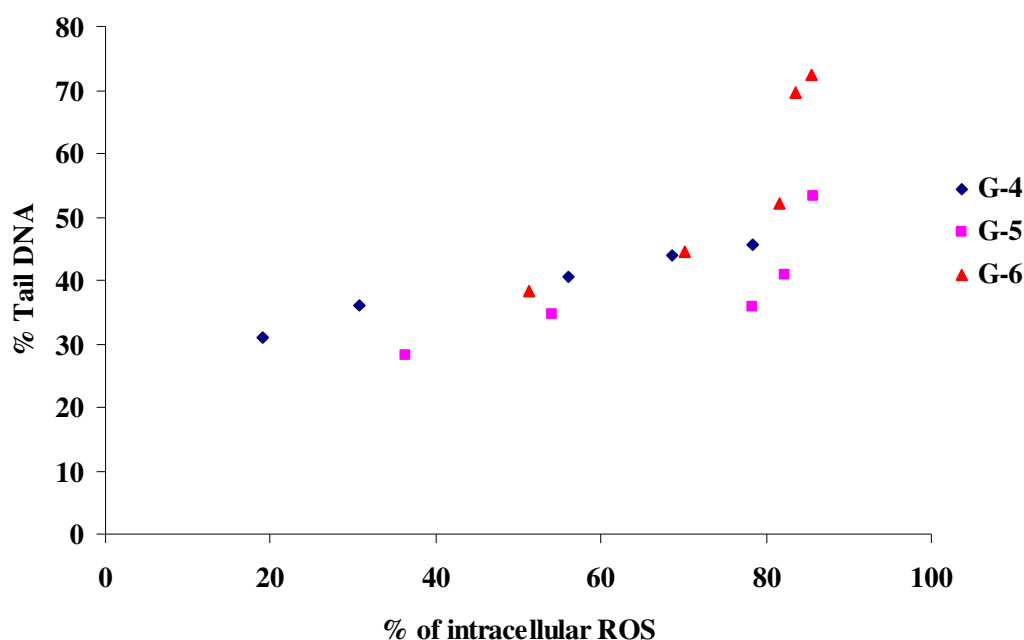


Figure 6.10. Relation between maximum DNA damage and maximum intracellular ROS production upon the exposure of PAMAM dendrimers G4, G5 and G6. (DNA damage 24h and ROS 2h Data).

Notably, an approximately linear dependence of intracellular ROS and genotoxicity response is observed, as presented in figure 6.10. However, there is saturation of intracellular ROS production at the higher concentrations of PAMAM dendrimers employed in the study. In the apoptosis assay, the percentage of dead cells increases with the increase in concentration of PAMAM dendrimers. At the higher concentration exposures employed here, the percentages of healthy cells and apoptotic cells are lower than the lower concentration exposure. The higher concentration exposure employed in the study induced cell death might be due to necrosis. At the same time, there is a saturation of intracellular ROS production at the higher concentration exposure (Figure 6.10). Saturation of intracellular ROS production and cell death at higher concentration exposure are well correlated and this may be an indication of necrotic cell death at the higher dose of PAMAM dendrimer exposure in PLHC-1 cells.

6.5 Conclusion

PAMAM dendrimers show a significant cytotoxic response in PLHC-1 cells. The generation dependence ($G6 > G5 > G4$) of the production of increased intracellular ROS, DNA damage and cytotoxicity indicates the direct effects of the positively charged surface amino groups. The toxicity starts with production of reactive oxygen species, which induces DNA damage, apoptosis and finally cell death upon the exposure of PAMAM dendrimers in PLHC-1 cells. As the generation increases, there is increase of surface primary amino group, molecular weight as well as the diameter of the PAMAM dendrimer. Toxic response in terms of generation of ROS, genotoxicity and cell death is systematically correlated with the generation of PAMAM dendrimer ($G6 > G5 > G4$). Structure activity relationship of PAMAM dendrimer points towards mechanistic approaches of cell death.

References

- Chandrasekhar, D., Sistla, R., Ahmad, F. J., Khar, R. K., Diwan, P. V. 2007. The development of folate-PAMAM dendrimer conjugates for targeted delivery of anti-arthritic drugs and their pharmacokinetics and biodistribution in arthritic rats. *Biomaterial*, 28, 504-512.
- Dhawan, A., Bajpayee, M., Parmar, D. 2009. Comet assay: a reliable tool for the assessment of DNA damage in different models. *Cell Biol Toxicol*. 25, 5-32.
- Donaldson, K., Aitken, R., Tran, L., Stone, V., Duffin, R., Forrest, G., Alexaner, A. 2006. Carbon nanotubes: a review of their properties in relation to pulmonary toxicology and work place safety. *Toxicol. Sci*. 92, 5-22.
- Donaldson, K., Tran, L., Jimenez, L.A., Duffin, R., Newby, D.E., Mills, N., MacNee, W., Stone, V. 2005. Combustion-derived nanoparticles: a review of their toxicology following inhalation exposure. *Part Fibre Toxicol*. 2, 10.
- Driscoll K.E. 2000. TNF- α and MIP-2: role in particle induced inflammation and regulation by oxidative stress. *Toxicol Lett*. 112-113, 177-184.
- Franklin, N. M., Rogers, N. J., Apte, S. C., Batley, G. E., Gadd, G. E., Casey, P.S. 2007. Comparative Toxicity of Nanoparticulate ZnO, Bulk ZnO, and ZnCl₂ to a Freshwater Microalga (*Pseudokirchneriella subcapitata*): The Importance of Particle Solubility. *Environ. Sci. Technol*. 41, 8484–8490.
- Gagné, F., Auclair, J., Turcotte, P., Fournier, M., Gagnon, C., Sauve, S., Blaise, C. 2008. Ecotoxicity of CdTe quantum dots to fresh water mussels: Impacts on immune system, oxidative stress and genotoxicity. *Aquat. Toxicol*. 86, 333-340.
- Heinlaan, M., Ivask, A., Blinova, I., Dubourguier, H. C., Kahru, A. 2008. Toxicity of nanosized and bulk ZnO, CuO and TiO₂ to bacteria *Vibrio fischeri* and crustaceans *Daphnia magna* and *Thamnocephalus platyurus*. *Chemosphere*, 71, 1308-1316.

<http://probes.invitrogen.com/media/pis/mp13243>

- Kerr, J.F., Wyllie, A.H., Currie, A.R. 1972. Apoptosis: a basic biological phenomenon with wide-ranging implications in tissue kinetics. *Br. J. Cancer* 26, 239–257.
- Lanone, S., Boczkowski, J. 2006. Biomedical Applications and Potential Health Risks of Nanomaterials: Molecular Mechanisms. *Curr Mol Med.* 6, 651-63.
- Lee, H., Larson, R.G., 2009. Multiscale modeling of dendrimers and their interactions with bilayers and polyelectrolytes. *Molecules* 19, 423–438.
- Lee, J.H., Cha, K.E., Kim, M.S., Hong, H.W., Chung, D.J., Ryu, G., Myung, H. 2009. Nanosized polyamidoamine (PAMAM) dendrimer-induced apoptosis mediated by mitochondrial dysfunction. *Toxicol Lett.* 190, 202–207.
- Li, N., Xia, T., Nel, A.E. 2008. The role of oxidative stress in ambient particulate Matter-induced lung diseases and its implications in the toxicity of engineered nanoparticles. *Free Radical Biol. Med.* 44, 1689–1699.
- Lovern, S. B., Strickler J. R., Klaper, R. 2007. Behavioural and physiological changes in *Daphnia magna* when exposed to nanoparticle suspensions (titanium dioxide, nano-C60, and C60HxC70Hx). *Environ. Sci. Technol.* 41, 4465-7.
- Lynch, I., Cedervall, T., Lundqvist, M., Cabaleiro-Lago, C., Linse, S., Dawson, K. A. 2007. The nanoparticle–protein complex as a biological entity; a complex fluids and surface science challenge for the 21st century. *Advances in Colloid and Interface Science*, 134-135, 167–174.
- Lubos, E., Handy, D.E., Loscalzo, J. 2008. Role of oxidative stress and nitric oxide in atherothrombosis. *Front. Biosci.* 13, 5323–5344.
- Mortimer, M., Kasemets, K., Heinlaan, M., Kurvet, I., Kahru, A. 2008. High throughput kinetic *Vibrio fischeri* bioluminescence inhibition assay for study of toxic effects of nanoparticles. *Toxicol. In Vitro*, 22, 1412-1417.

- Mukherjee, S.P., Lyng, F.M., Garcia, A., Davoren, M., Byrne, H.J. 2010. Mechanistic studies of *in vitro* cytotoxicity of poly (amidoamine) dendrimers in mammalian cells. *Toxicol Appl Pharmacol.* 248, 259-68.
- Mueller, N. C., Nowack, B. 2008. Exposure Modelling of Engineered Nanoparticles in the Environment. *Environ. Sci. Technol.* 42, 4447–4453.
- Navarro, E., Piccapietra, F., Wagner, B., Marconi, F., Kaegi, R., Odzak, N., Sigg, L., Behra, R. 2008. Toxicity of Silver Nanoparticles to *Chlamydomonas reinhardtii*. *Environ. Sci. Technol.* 42, 8959–8964.
- Nel, A., Xia, T., Madler, L., Ning, L. 2006. Toxic potential of materials at nanolevel. *Science* 311, 622-627.
- Obedoster, G., Obedoster, E., Obedoster, A. 2005. Nanotoxicology: an emerging discipline evolving from studies of ultrafine particles. *Environ. Health Perspect.* 113, 823-839.
- Shieh, M. J., Peng, C. L., Lou, P. J., Chiu, C. H., Tsai, T. Y., Hsu, C. Y., Yeh, C. Y., Lai, P. S. 2008. Non-toxic phototriggered gene transfection by PAMAM-porphyrin conjugates. *J. Control. Rel.* 129, 200-206.
- Sies H.1993. Strategies of antioxidant defense. *Eur J Biochem.* 215, 213-219.
- Zhang, R., Kang, K.A., Piao, M.J., Maeng, Y.H., Lee, K.H., Chang, W.Y., You, H.J., Kim, J.S., Kang, S.S., Hyun, J.W. 2009. Cellular protection of morin against the oxidative stress induced by hydrogen peroxide, *Chem. Biol. Interact.* 177, 21–27.

Chapter 7

Immunotoxicity of PAMAM dendrimers (G4, G5 and G6)

Adapted from “Reactive Oxygen Species (ROS) induced cytokine production and cytotoxicity of PAMAM dendrimers in J774A.1 cells”. *Toxicology and applied Pharmacology*, 2010, 246, 91-99.

Authors: Pratap C. Naha, Maria Davoren, Fiona M. Lyng and Hugh J. Byrne

7.1 Introduction

The interaction of PAMAM dendrimers with PLHC-1 cells, representative of fresh water vertebrate species was described in chapter 6. In this chapter, the immunotoxicity of the PAMAM dendrimers is explored. Macrophages were chosen as the target cells for the *in vitro* model, as macrophages are one of the professional antigen presenting cells (APC). J774A.1 cells, derived from the blood of the female BALB/c mouse. Although both PLHC-1 and J774A.1 cells are considered to represent vertebrate species, they are derived from different species and thus have different metabolic activity. The application of nanomaterials as intravenous drug delivery platforms may depend on avoiding rapid elimination from systemic circulation by cells of the immune system. When nanoparticles enter into the bloodstream, they immediately encounter a complex environment of plasma proteins and immune cells. The interaction of nanoparticles with immune cells may occur both in the blood stream via monocytes, platelets, leukocytes, and dendritic cells (DC) and in tissues by resident phagocytes, e.g., Kupffer cells in liver, DC in lymph nodes, macrophages and B cells in the spleen (Dobrovolskaia et al., 2008). As PAMAM dendrimers are potentially proposed for vaccine and intracellular gene delivery applications, and macrophages are the main target cells to produce or improve the immunogenicity of the different antigens, this study explores the interaction with and toxicity to macrophages cells of PAMAM (G4, G5 and G6) dendrimers. ROS and subsequent cytokine production are monitored as indicators of oxidative stress and inflammatory response.

In addition to a study of the PAMAM dendrimer materials in their own right, the systematically varied molecular nanostructures potentially provides a route towards an understanding of the dependence of the interactions on the physico-chemical properties of nanomaterials. In a recent study, the toxicity of PAMAM dendrimers in mammalian

cells has been demonstrated to be generation dependent (Mukherjee et al., 2009), potentially laying the foundation for structure-activity relationships underlining the mechanistic responses. Conjugation of poly (ethylene glycol) (PEG) to the surface of PAMAM dendrimers has been observed to improve their biocompatibility, reducing the cytotoxic response (Wang et al., 2009). The objective of the present work is an *in vitro* assessment of the immunotoxicological response of three generations of the cationic PAMAM dendrimers (G4, G4 and G6) in mouse macrophage cells (J774A1). The systematically varied structure and size allows an evaluation of the dependence of the response on the physico-chemical properties. The PAMAM dendrimers were characterized in terms of particle size and zeta potential in cell culture media with and without protein (FBS). In accordance with the EU policy of Reduction, Replacement and Refinement (RRR) an *in vitro* rather than animal model is employed to assess the cytotoxic response and underlying mechanisms of these materials. (Directive 86/609/EEC on the protection of animals used for experimental and scientific purposes). Cytotoxicological effects of PAMAM dendrimers were evaluated using the Alamar blue and MTT [(3-(4, 5-Dimethylthiazol-2-yl)-2, 5- diphenyltetrazolium bromide, a tetrazole)] assays. Intracellular reactive oxygen species (ROS) were measured following exposure of the macrophages to PAMAM dendrimers for time periods of 1h, 2h, 4h and 6h. The visualisation of ROS production by the cells was performed by confocal laser scanning microscopy. The secretion of the cytokines and chemokines, Macrophage Inflammatory Protein-2 (MIP-2), Tumour Necrosis Factor - α (TNF- α) and Interleukin - 6 (IL-6), following exposure of the macrophage cells to PAMAM dendrimers was measured quantitatively by enzyme linked immunosorbant assay (ELISA).

7.2 Experimental methods

All the relevant experimental methods are described in chapter 2. Particle size and zeta potential measurement are described in chapter 2, sections 2.2.1.1 and 2.2.1.2. Intracellular reactive oxygen species (ROS) detection in J774A.1 cells is described in section 2.2.2.9; Cytokine expression upon the exposure of PAMAM dendrimers in J774A.1 cells was detected by ELISA as described in section 2.2.2.10. The cytotoxicity assays employed are described in section 2.2.2.6 of chapter 2.

7.3 Results

7.3.1 Characterisation of PAMAM dendrimers

The PAMAM dendrimers (G4, G5 and G6) were characterised in terms of particle size, and zeta potential. As described in chapter 5, the hydrodynamic diameter correlated well with that quoted by the manufactures (Naha et al., 2009). In the J774A.1 cell culture media, the hydrodynamic diameter of G4, G5 and G6 was $6.2 \text{ nm} \pm 0.3 \text{ nm}$; $7.5 \text{ nm} \pm 0.3 \text{ nm}$ and $10.3 \text{ nm} \pm 0.4 \text{ nm}$ respectively. The slight increase in size in cell culture media may be due to interaction with proteins or other components of the cell culture media producing a ‘protein corona’ as has been observed with other nanoparticles (Lynch et al., 2007).

Table 7.1. Zeta potential of PAMAM dendrimers in different media

Different media	PAMAM G4 in mV	PAMAM G5 in mV	PAMAM G6 in mV
Milli-Q water	8.3 ± 5.5	21.5 ± 8.7	26.5 ± 4.7
DMEM	6.7 ± 3.7	18.0 ± 2.1	14.4 ± 3.0
5 % J774A.1 Cell culture media	-2.9 ± 1.1	-3.1 ± 0.9	-3.9 ± 0.4

In Milli Q water and DMEM cell culture medium, the zeta potential of the PAMAM dendrimers was observed to be positive, due to the cationic surface amino groups. However, the surface charge was observed to be negative in the J774A1 cell culture medium containing 5% FBS due to the interaction of proteins with the surface amino groups, as described previously (Chapter 4, Naha et al., 2009). The zeta potential of G4, G5 and G6 was found to be -2.9 ± 1.1 ; -3.1 ± 0.9 ; and -3.9 ± 0.4 mV respectively (Table 7.1). This is a clear indication of the interaction of the protein with the PAMAM dendrimers as shown previously (Naha et al., 2009).

7.3.2 Cytotoxicity assay

The cytotoxicity of PAMAM dendrimers was determined using two different assays for an exposure time of 24h and the results are shown in Figure 7.1, with the EC_{50} values shown in Table 7.2. The toxic response observed in both assays is well matched and there is no significant difference between the calculated EC_{50} from both the assays in J774A1 cells.

Table 7.2. EC₅₀ data of PAMAM dendrimers G4, G5 and G6 for the Alamar blue (AB) and MTT assays for 24 hour exposure in J774A.1 cells.

PAMAM Dendrimer	EC ₅₀ of AB assay in (μM)	EC ₅₀ of MTT assay in (μM)
G4	1.6 ± (0.3)	1.4 ± (0.3)
G5	0.5 ± (0.2)	0.5 ± (0.2)
G6	0.3 ± (0.1)	0.2 ± (0.1)

A time and generation dependent toxic response was furthermore observed as shown in Figure 7.2a. Maximum cell death occurs at 72 h exposure for all three generations of PAMAM dendrimers. The trend of toxic response was G6 > G5 > G4, as observed previously for aquatic species and fish cell lines (Chapter 5, Naha et al., 2009) as well as mammalian cell lines (Mukherjee et al., 2009). Notably, the toxic response in terms of inverse EC₅₀ (Ragnvaldsson et al., 2007) shows a monotonic increase with increasing number of surface primary amino groups present in the PAMAM dendrimers which is shown in Figure 7.2.b for the case of 24 h exposure, demonstrating a clear structure-activity relationship. In order to further explore the mechanisms of cell death, the induced oxidative stress and inflammatory response were explored.

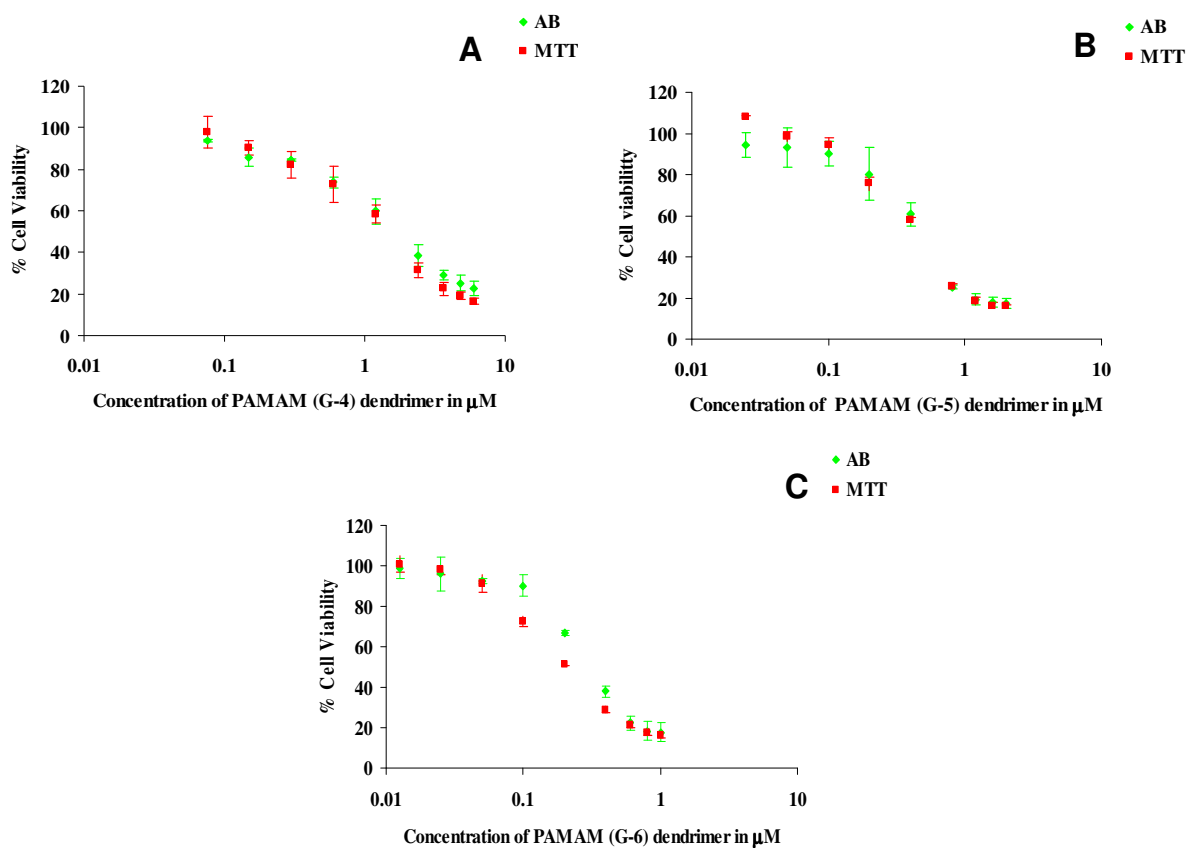


Figure 7.1. Comparison of cytotoxicity assays AB and MTT of (A) G4, (B) G5 and (C) G6 PAMAM dendrimers in J774A.1 cells after 24h exposure. The data shown mean \pm SD (n=3).

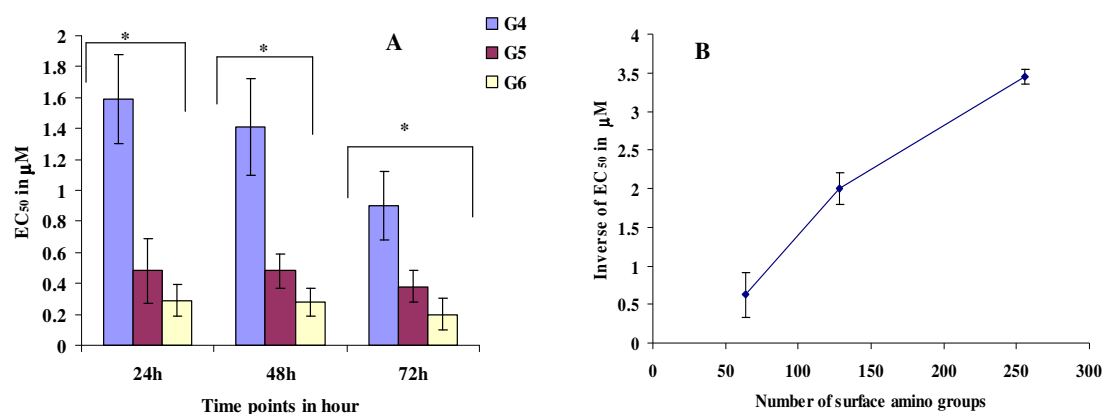


Figure 7.2. (A) Time and generation dependence of toxic response of PAMAM dendrimers (G4, G5, G6); *Denotes significant difference of EC₅₀ between G4, G5 and G6 in all the exposure time period 24, 48 and 72 h ($p \leq 0.05$). (B) Plot showing relationship between number of surface amino groups and the toxic response of PAMAM dendrimers at 24h exposure (AB assay). All the data are expressed in mean \pm SD (n=3).

7.3.3 Intracellular Reactive oxygen species (ROS)

The intracellular ROS study was performed at different time points (1, 2, 4 and 6h) and with different exposure concentrations of each dendrimer (G4, G5 and G6). For all generations, the exposure time points and the concentration of PAMAM dendrimer (0.031 μ M to 3 μ M) used were the same, in order to correlate the increased ROS production by the three generations of PAMAM dendrimers and also to enable comparison with the cytotoxic and inflammatory response. Intracellular ROS production in the macrophage cells upon exposure to PAMAM dendrimers was easily visualised using confocal fluorescence microscopy, as shown in figure 7.3 for the case of 2 h exposure of each dendrimer at a concentration of 1 μ M. The fluorescence was quantified using a plate reader, which provides an average of the statistically variable

response of individual cells (Elbekai and El-Kadi, 2005). This *in situ* method was favoured over flow cytometry as J7741.A cells are strongly adherent and do not detach easily from the flask after trypsinisation. The concentration dependent increase in ROS production for four different time points for the three dendrimer generations was monitored and the results are shown in Figure 7.4. Increased ROS production was found to be dendrimer generation and time dependent (Figure 7.5A). In a previous study of poly (propyleneimine) dendrimers (PPI), a similar generation dependent intracellular ROS production and reduction of mitochondrial membrane potential was observed in macrophages (Kuo et al., 2007). The generation dependence follows the trend of G6 > G5 > G4, as was seen for the cytotoxic response. Similar to the case of the cytotoxic response, the generation dependent ROS levels appear to be correlated with the increase in number of surface primary amino groups with increasing generation, as shown in figure 7.5B for the case of 1 h exposure.

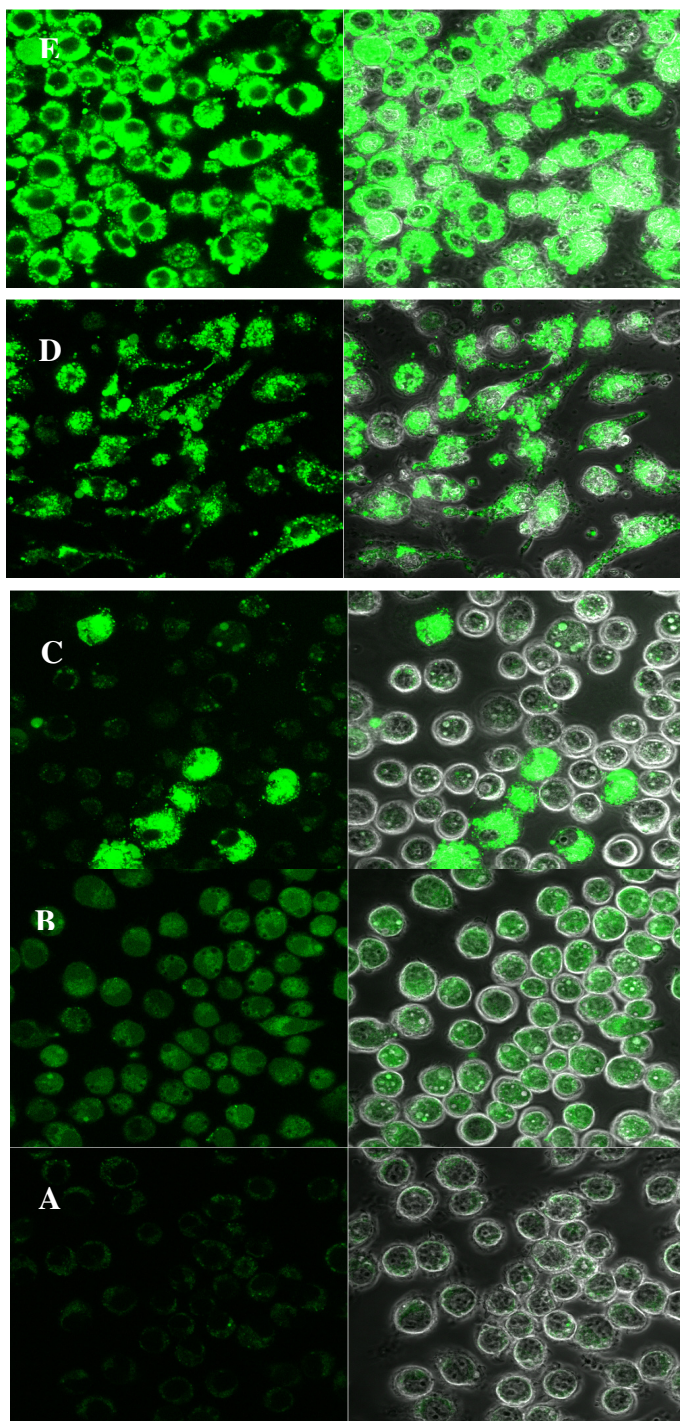


Figure 7.3. Confocal fluorescence and phase contrast micrographs of intracellular ROS generation following exposure to (A) negative control, (B) positive control (H_2O_2), (C) PAMAM G4, (D) PAMAM G5 and (E) PAMAM G6. The data are shown after 2h exposure of PAMAM dendrimers. Magnification is 63 x.

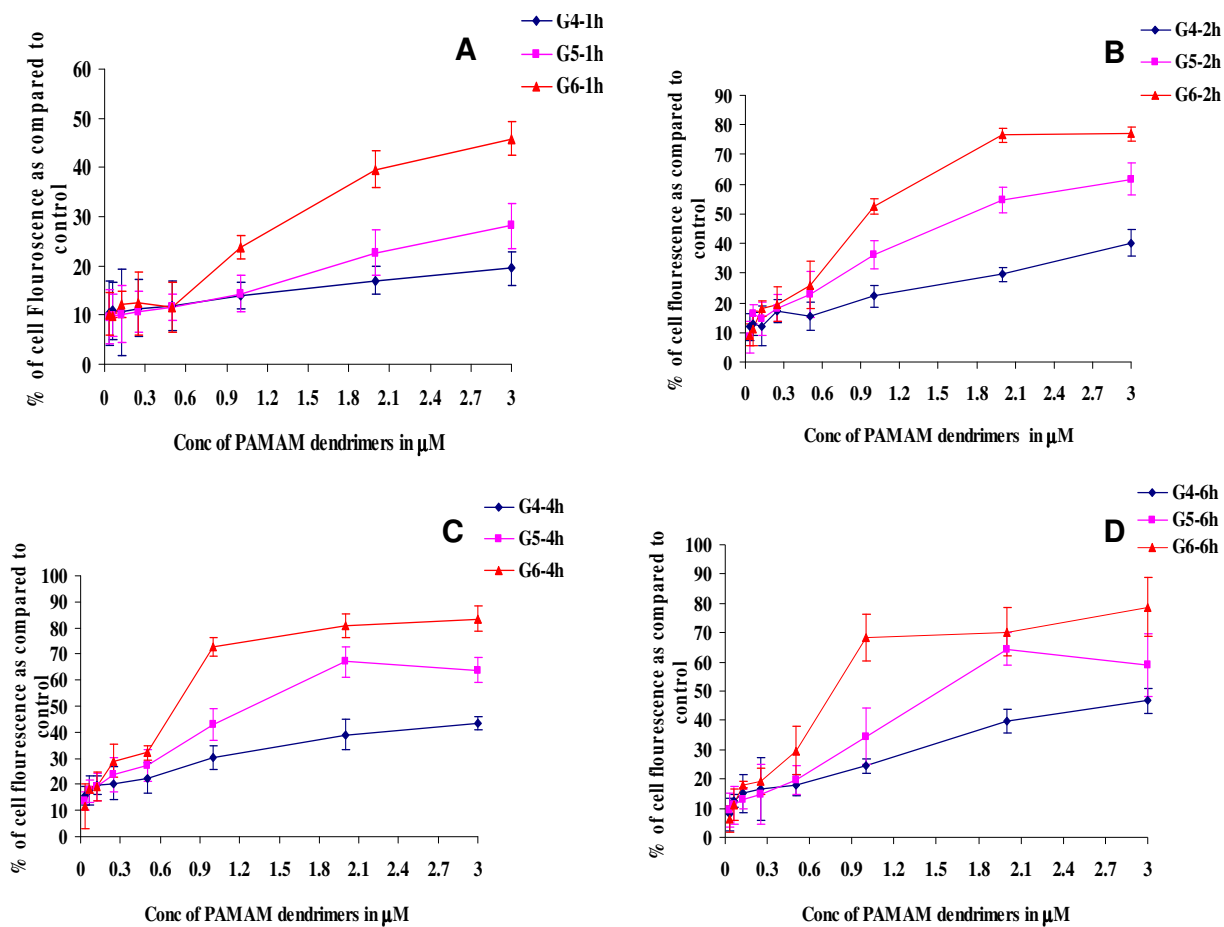


Figure 7.4. Concentration and time dependent intracellular ROS generation by G4, G5 and G6 at (A) 1, (B) 2, (C) 4 and (D) 6 h exposure time points. The data are presented as mean \pm SD (n=3).

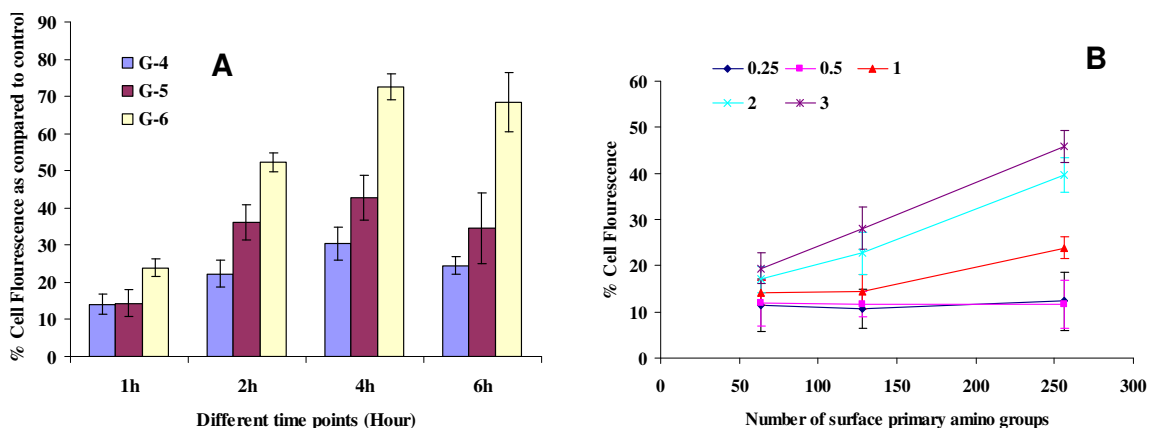


Figure 7.5. (A) generation dependent intracellular reactive oxygen species (ROS) production following exposure to PAMAM dendrimers (G4, G5 and G6) in J774A.1 cells at an exposure concentration of $1\mu\text{M}$. The data are presented in mean \pm SD ($n=3$), (B) correlation between the production of intracellular ROS and number of surface primary amino groups.

As was observed for the PHLC-1 fish cell line, when the molar concentration is expressed in terms of the total number of surface amino groups, (Figure 7.6) the % of ROS generation as a result of exposure of J774A.1 to each of the PAMAM dendrimers shows approximately the same response, indicating the cationic surface amino groups are the source of the ROS production.

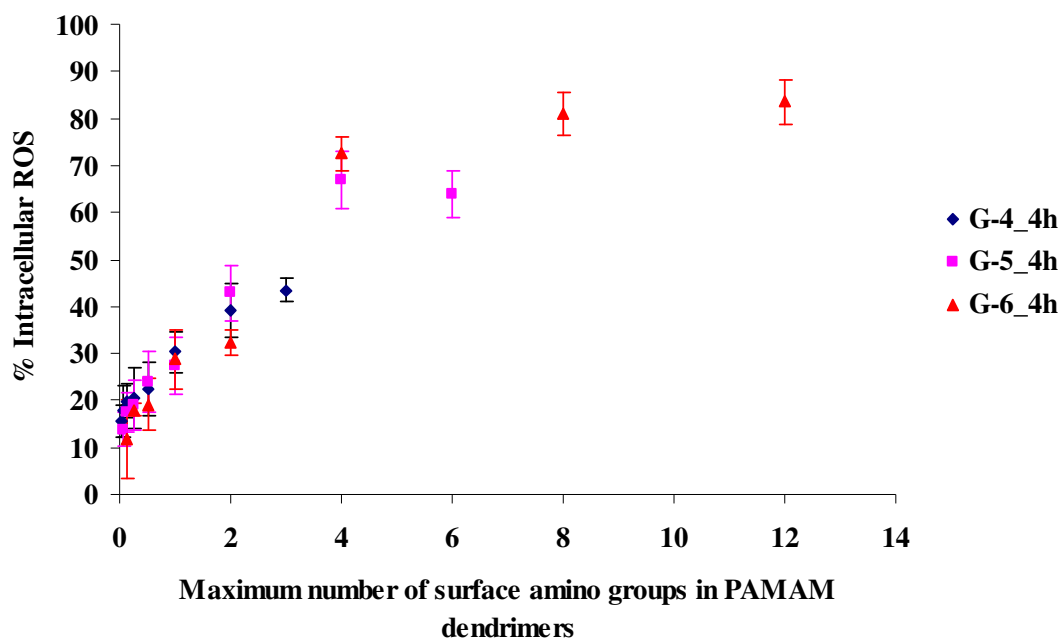


Figure 7.6 Correlation between maximum ROS production and the maximum number of surface primary amino groups of PAMAM dendrimers at 4 hour exposure.

7.3.4 Cytokines production

7.3.4.1 Macrophage inflammatory protein-2 (MIP-2)

The level of macrophage inflammatory protein-2 (MIP-2) secretion by the J774A.1 cells following exposure to PAMAM dendrimers was analysed from the cell culture supernatant after exposure to 5 different concentrations of each dendrimer and also at 5 different exposure time periods (6, 12, 24, 48 and 72h). MIP-2 levels at different exposure time periods were calculated from the standard curve of the MIP-2 standards (ranging from 10 to 800 pg/ml).

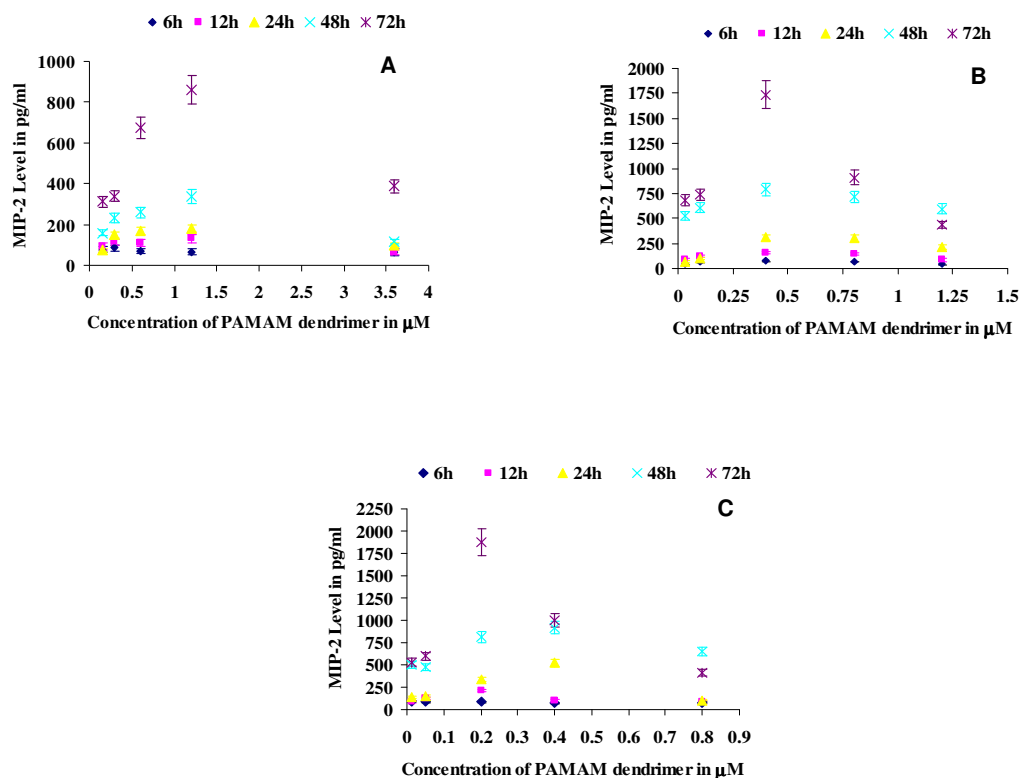


Figure 7.7. The level of MIP-2 secreted after exposure of J774A.1 cells to (A) G4, (B) G5 and (C) G6 PAMAM dendrimers for 6h, 12h, 24h, 48h and 72h. These data are presented in mean \pm SD (n=3).

The secretion of MIP-2 was found to be time, PAMAM generation and concentration dependent, as shown in Figures 7.7 and 7.10. Maximum levels of MIP-2 were generated at all the time points at concentrations of G4 (1.2 μM); G5 (0.4 μM) and G6 (0.2 μM) and the secretion of MIP-2 protein from the macrophage cell was found to be generation dependent, G6 producing the highest level and G4 the lowest, (G6 > G5 > G4) which is well correlated with the cytotoxic response and the ROS generation. Although a linear dependence is not obvious, the MIP-2 protein secretion levels increase monotonically

with the number of surface primary amino groups of the PAMAM dendrimers, as shown in Figure 7.11 A.

7.3.4.2 Interleukin-6 (IL-6)

After different exposure time periods (6, 12, 24, and 48 h) of PAMAM dendrimers, the levels of IL-6 were calculated from the standard curve (standards ranging from 10 to 800 pg/ml). In the case of G4 (0.6 μM); G5 (0.4 μM) and G6 (0.2 μM), the maximum levels of IL-6 were observed after 24 h exposure. A time, concentration and generation dependent IL-6 secretion from the macrophage cells was observed upon the exposure to PAMAM dendrimers as shown in Figure 7.8 and 7.10. PAMAM dendrimer G6 producing the highest levels and G4 the lowest ($G6 > G5 > G4$) which is well correlated with the cytotoxic response. Again the level of IL-6 secretion by the J774A.1 cells increases monotonically with the surface area of each dendrimer generation, as shown in Figure 7.11 B.

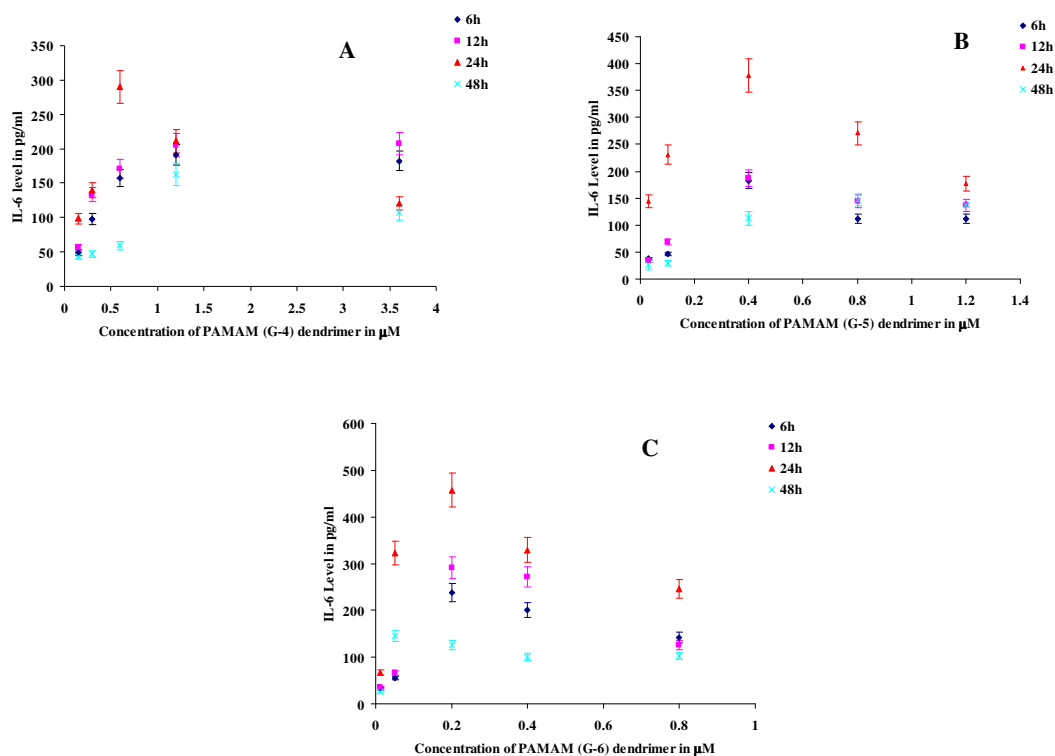


Figure 7.8. Secretion of IL-6 following exposure to (A) G4, (B) G5 and (C) G6 in J774A.1 cells at 6, 12, 24 and 48 h time points. The data are presented as mean \pm SD (n=3).

7.3.4.3 Tumour necrosis factor- α (TNF- α)

The TNF- α levels at different exposure times (6, 12, 24, and 48 h) were calculated from the standard curve of TNF- α standards (ranging from 10 to 800 pg/ml). Maximum levels of TNF- α were generated at concentrations of G4 (1.2 μ M); G5 (0.8 μ M) and G6 (0.2 μ M) after 24h exposure. A time, concentration and generation dependent TNF- α secretion from the macrophage cells was observed upon the exposure to PAMAM dendrimers as shown in Figure 7.9 and 7.10. PAMAM dendrimer G6 producing the highest levels and G4 the lowest, (G6 > G5 > G4) which is well correlated with the cytotoxic response. Again the levels of TNF- α secretion by the J774A.1 cells increase

monotonically with the number of surface primary amino group of the PAMAM dendrimer, shown in Figure 7.11 C.

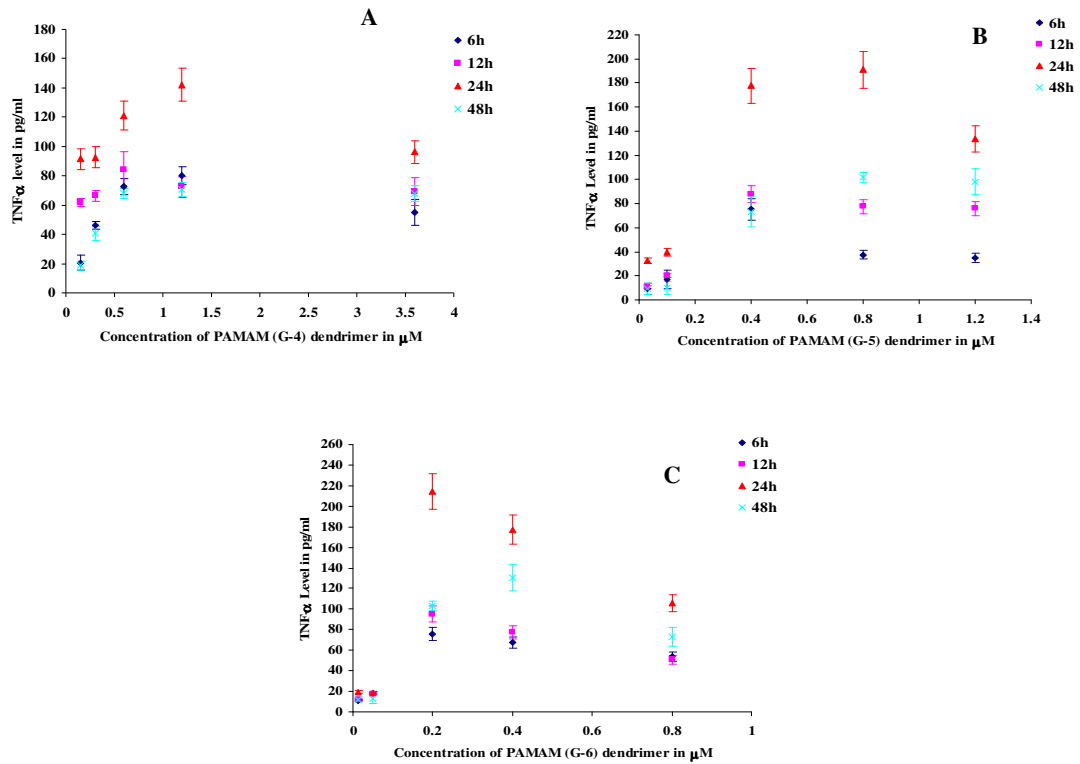


Figure 7.9. Secretion of TNF- α upon the exposure to (A) G4, (B) G5 and (C) G6 in J774A.1 cells at 6, 12, 24 and 48 h time points. The data are presented as mean \pm SD (n=3).

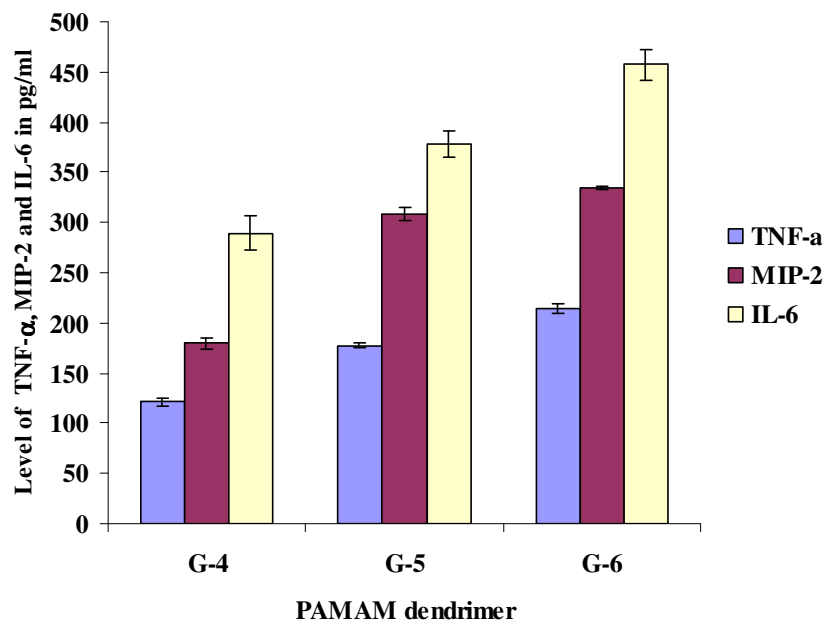


Figure 7.10. Generation dependent MIP-2, IL-6 and TNF- α secretion after 24h exposure of PAMAM dendrimers (G4, G5 and G6) in J774A.1 cells. The data are shown as mean \pm SD (n=3).

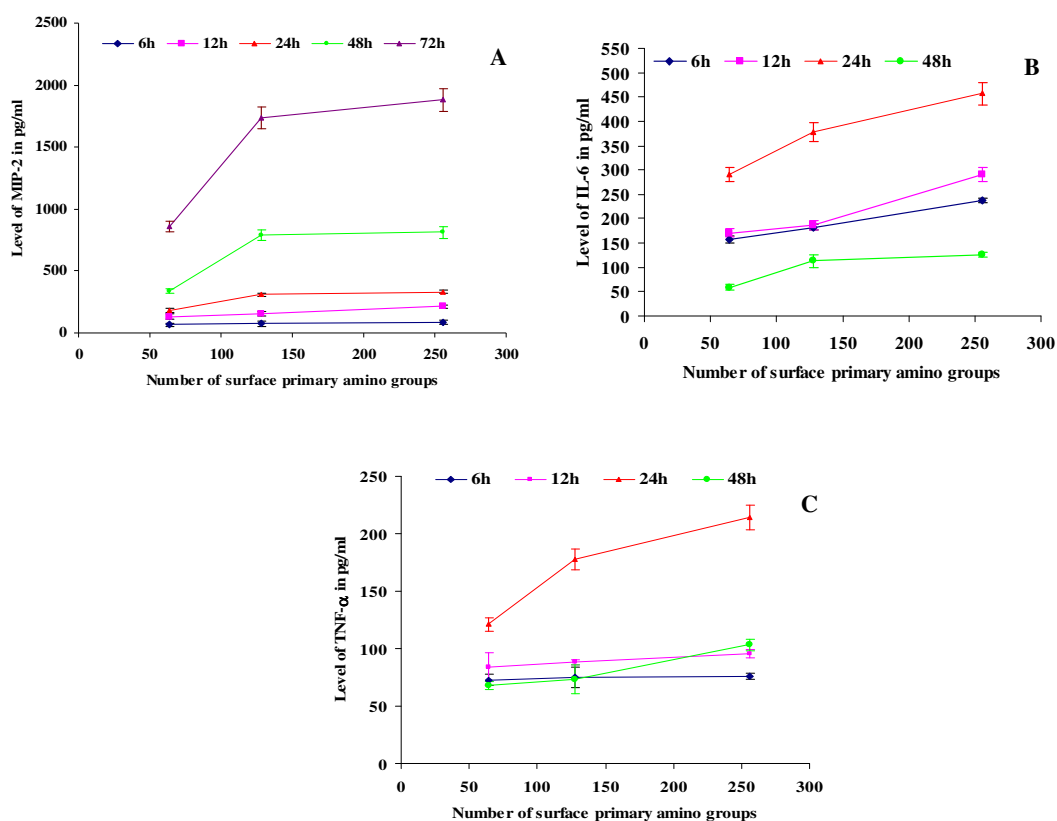


Figure 7.11. Correlation between inflammatory mediator (A) MIP-2, (B) IL-6 and (C) TNF- α response and the surface area of PAMAM dendrimers (G4, G5 and G6). All the data are presented in mean \pm SD (n=3).

7.4 Discussion

The cytotoxic response of J774A.1 cells to the PAMAM dendrimers, with varying numbers of $-\text{NH}_2$ surface group (G4, G5 and G6), was evaluated using the Alamar blue (AB) and MTT assays. The EC_{50} was calculated and no significant difference was observed between the assays after 24 h exposure (Figure 7.1). Alamar blue is a water-soluble dye and the oxidized form enters the cytosol and is converted to the reduced form by mitochondrial enzyme activity by accepting electrons from NADPH, FADH, FMNH, NADH as well as from the cytochromes (Al-Nasiry et al., 2007). Mitochondrial

activity was determined by the MTT assay. MTT is reduced to the purple formazan in the mitochondria of living cells. This reduction takes place only when mitochondrial reductase enzymes are active, and therefore conversion can be directly related to the number of viable (living) cells. MTT is completely reduced by mitochondrial enzyme. The close agreement of the EC_{50} as determined by the two assays is an indication of significant mitochondrial injury as origin of the cytotoxic response.

The toxic response was seen to increase with dendrimer generation and therefore size. A similar generation dependent toxicological response was previously seen with fish cells (Naha et al., 2009) and also mammalian cells lines (Mukherjee et al., 2009). A toxic response which increases with nanoparticle diameter would appear to go against the commonly accepted trends of increased toxicity with decreased nanoparticle size, but can be understood in terms of the linear correlation with the number of surface amino groups of PAMAM dendrimer as shown in Figure 7.2 B.

The surface primary amino groups render the dendrimers cationic and as the generation of PAMAM dendrimer increases, there is a linear increase in the number of surface amino groups (Dendritech, Inc. <http://www.dendritech.com/pamam.html>). The observed generation dependence suggests that the toxic response has origin in the actions of the surface charge (Figure 7.2B).

Cationic nanoparticles, like amino-terminated PAMAM dendrimers enter into an endosomal compartment and escape from the lysosomes by inhibiting the lysosomal proton pump (Nel et al., 2009) and become localized in the mitochondria (Lee et al., 2009) producing reactive oxygen species and inducing cell death (Mukherjee et al., 2010). But in case of PNIPAM, the particles remain in the lysosomes for 24 hours.

In this study, intracellular ROS generation by PAMAM dendrimers is clearly one of the toxic pathways and a clear generation dependence of intracellular increased ROS production is shown in Figure 7.5A. The sequence of increased ROS generation is G6 > G5 > G4. This response is also well correlated with the number of surface primary amino group of PAMAM dendrimers, as shown in Figure 7.5B. This indicates that the cationic surface amino groups play a direct role in the production of ROS. Generation dependent intracellular ROS, cytotoxicity and also cytokines production has been observed with the PAMAM dendrimers in J774A.1 cells. As the PAMAM generation increases, there is an increase in the number of surface amino groups (64, 128 and 256 amino groups for G4, G5 and G6 respectively) which makes the particle more cationic. The toxicity of the PAMAM dendrimers has also been reported to decrease upon modification of the number of functional groups (Khandare et al., 2010). In a recent study, it has been proposed that amino-terminated PAMAM dendrimers enter into an endosomal compartment whereupon the unsaturated amino groups are capable of sequestering protons that are supplied by the v-ATPase. They thus inhibit the lysosomal proton pump mechanism, leading to rupture and deposition of the particles and the lysosomal content in the cytoplasm and ultimately cell death (Nel et al., 2009).

Increased intracellular ROS generation suggests that the PAMAM dendrimers can lead to disruption of the mitochondrial electron transduction chain which may lead to additional O_2^- production, which has been observed with carbon based nanoparticles (Donaldson et al., 2005) and perturbs the mitochondrial permeability transition pore, which leads to release of pro-apoptotic factors and programmed cell death (Oberdörster et al., 2005).

Intracellular ROS production can lead to inflammation, as demonstrated for a number of different nanoparticles (Li et al., 2008; Stone et al., 2007; Lubos et al., 2008; Driscoll,

2000). Oxidative stress activates the MAPK signalling pathway, inducing transcription factors such as NF κ B and AP-1, and these transcription factors induce mRNA expression of pro-inflammatory mediators and finally cause inflammation (Park and Park 2009). Macrophage inflammatory protein-2 (MIP-2) plays a major role in mediating the neutrophilic inflammatory response to nanoparticles (Driscoll et al., 1995). It is a potent neutrophil chemoattractant and epithelial cell mitogen and is involved in acute pulmonary inflammation and mediates tissue damage (Walley et al., 1997; Chung et al., 2003). It is induced by LPS (Lipopolysaccharide), oxidative stress in a wide range of cells including alveolar macrophages, mast cells, peritoneal macrophages, epithelial cells and fibroblasts (Monteiller et al., 2007).

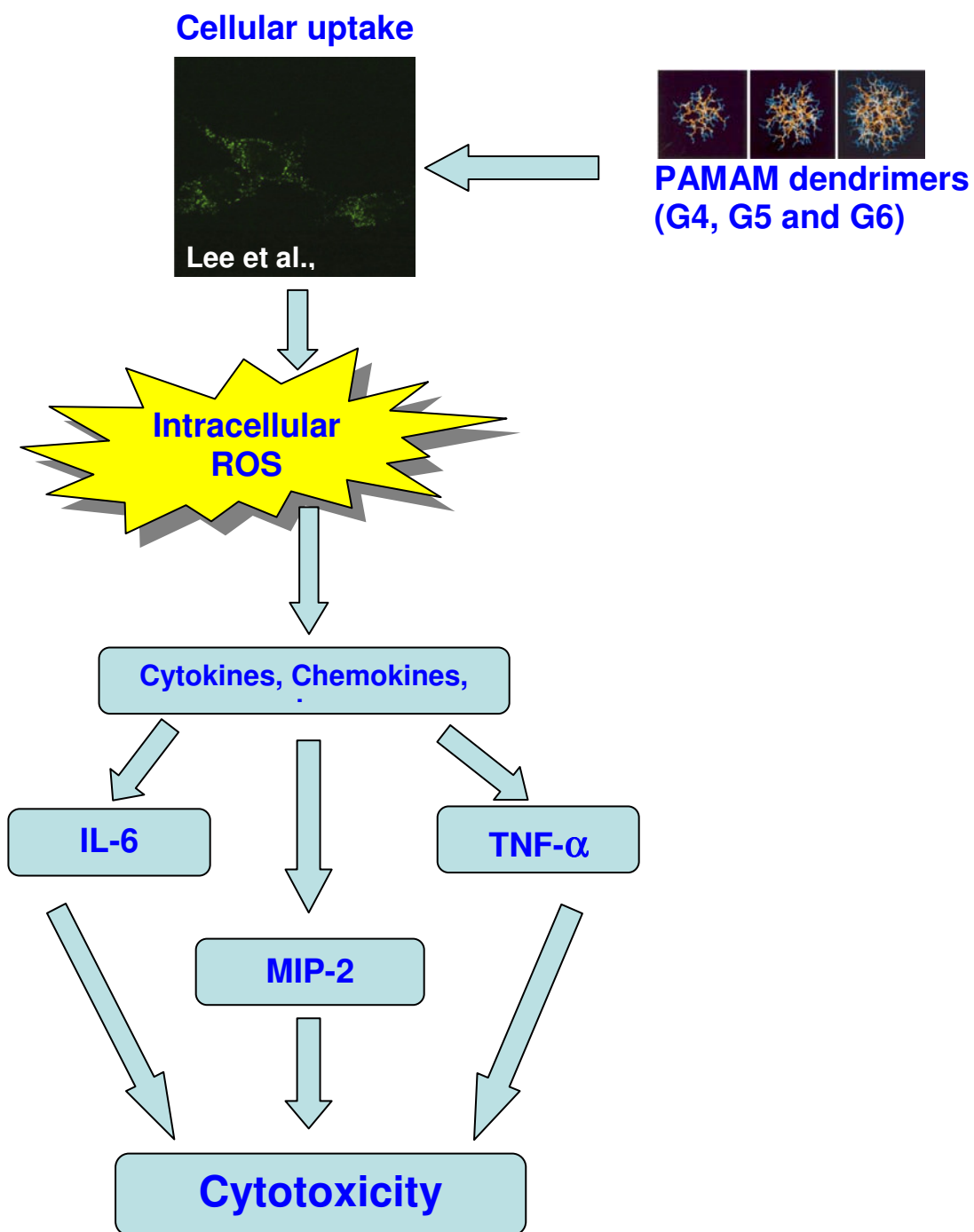


Figure 7.12. Schematic of the systematic sequence of events in J774A.1 cells following exposure to PAMAM dendrimers.

Inflammatory response induced by nanoparticles is thus a further toxic mechanism (Monteiller et al., 2007), and in this work the inflammatory mediators (MIP-2, TNF- α and IL-6) induced by PAMAM dendrimers are highlighted. The level of secretion of all three inflammatory mediators, MIP-2, TNF- α and IL-6 following exposure of macrophage cells to PAMAM dendrimers is dependent on the concentration, time of exposure and the generation of PAMAM dendrimers, as well as the cytotoxic response. A generation dependent cytokine production was found in all cases and the trend was G6 > G5 > G4. Thus the ROS production, inflammatory response and cytotoxicity all show similar trends in terms of dendrimer structure. The pathway of the toxic response induced by PAMAM dendrimers may therefore be one of localisation in the mitochondria (Lee et al., 2009) which could be leading to disruption of the mitochondrial electron transduction chain, and additional O₂⁻ production resulting in oxidative stress (Figure 7.3 and Figure 7.4). The systematic mechanistic pathways of cell death due to PAMAM dendrimers is presented in Figure 7.12, and the sequence of responses as a function of time is shown in Figure 7.13. Within the resolution of the measurements performed, the timing sequence is identical for all three dendrimer generations. In figure 7.13, the systematic sequence of events as function of time is presented. Initially, maximum levels of ROS are produced after 4 h, and this is followed by a maximum level of IL-6 and TNF- α expressed at 24 h and the maximum level of MIP-2 and cytotoxicity observed at 72 h after the exposure of PAMAM dendrimers to J774A.1 cells. This indicates that the intracellular ROS production is one of the key origins of toxic response of PAMAM dendrimers in J774A.1 cells.

Although the toxic responses can be well correlated with the dendrimer generation structures, it should be noted that the particle size was seen to increase in the cell culture medium and furthermore that the zeta potential of the PAMAM dendrimers changed

polarity from positive to negative. These observations point towards the interaction of proteins and/or other molecular components of the medium with the particle surface. In our previous study, we have seen spectroscopically the interaction of FBS with the PAMAM dendrimers (Naha et al., 2009), as has been documented for other nanoparticles, leading to the formation of a protein corona (Lynch et al., 2007).

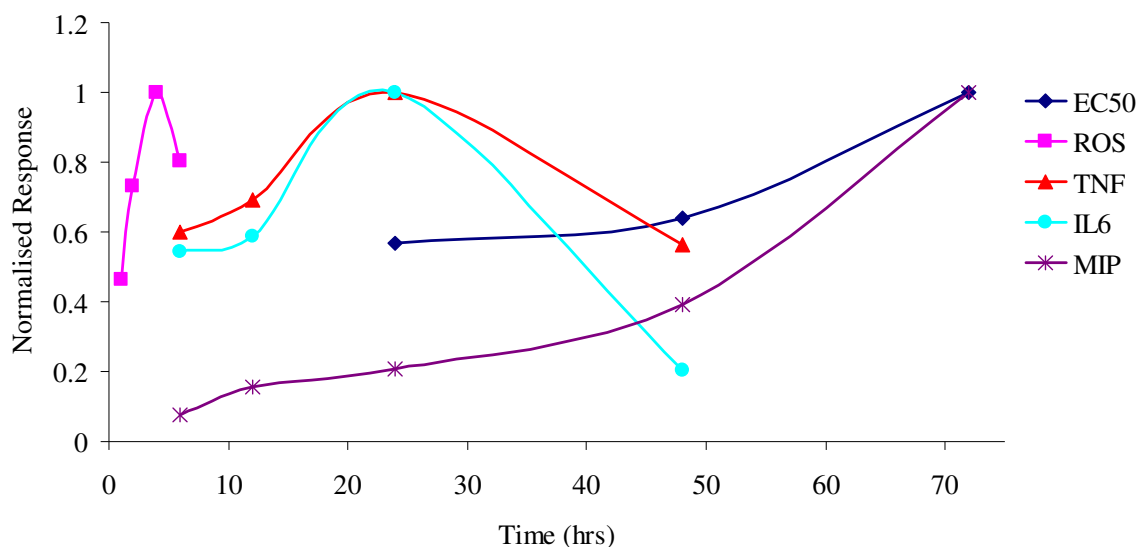


Figure 7.13. Graphical representation of the of different responses as a function of time upon the exposure of PAMAM dendrimers (for the case of G4) in J774A.1 cells.

In the case of carbon nanotubes, such interactions have been shown to result in medium depletion and a secondary or indirect toxicity (Casey et al., 2008) even though the carbon nanotubes are not seen to be taken up by the cells (Davoren et al., 2007). From this point of view it is important to understand whether toxic responses originate from the interaction of particles external or internal to the cells.

Significant ROS generation has also been seen from carbon nanotubes external to the cells (Herzog et al., 2009). Thus it is conceivable that the ROS, cytokines production, cytotoxicity cascade could be initiated from external stress (Herzog et al., 2009). However, a recent study has clearly demonstrated the internalisation of PAMAM

dendrimers and their localisation in the mitochondria (Lee et al., 2009). Thus, although there may be external stress leading to some degree of indirect toxic response, it is proposed that the principal response is a direct result of internalisation of the nanomaterials.

7.5 Conclusions

PAMAM dendrimers show a significant cytotoxic response in mouse macrophage cells (J774A.1) *in vitro* at a concentration of 0.013 to 6 μM . The generation dependence ($G6 > G5 > G4$) of the production of increased intracellular ROS, inflammatory mediators and the cytotoxicity indicates the direct effects of the positively charged surface amino groups. The mechanism of the toxic response is proposed to be one of localisation of the cationic particles in the mitochondria, leading to significant increase in ROS generation, induction of cytokines production and ultimately cell death. The generation dependent intracellular ROS levels, cytokines production and cytotoxicity of PAMAM dendrimers point towards the basis of structure activity relationships.

Reference

- Al-Nasiry, S., Geusens, N., Hanssens, M., Luyte, C., and Pijnenborg R. 2007. The use of Alamar Blue assay for quantitative analysis of viability, migration and invasion of choriocarcinoma cells. *Human Production* 22, 1304-1309.
- Batista, M.L Jr., Santos, R.V., Cunha, L.M., Mattos, K., Oliveira, E.M., Seelaender, M.C., Costa Rosa, L.F. 2006. Changes in the pro-inflammatory cytokine production and peritoneal macrophage function in rats with chronic heart failure. *Cytokine*, 34, 284-290.
- Casey, A., Herzog, E., Lyng, F. M., Byrne, H. J., Chambers, G., Davoren, M. 2008. Single walled carbon nanotubes induce indirect cytotoxicity by medium depletion in A549 lung cells. *Toxico Lett.* 179, 78–84.
- Cheng, Y., Xu, Z., Ma, M., Xu, T. 2008. Dendrimers as drug carrier: applications in different routes of drug administration. *J. Pharm. Sci.* 97, 123-143.
- Chung, Y-J., Yang, G H., Islam, Z., Pestka J. J. 2003. Up-regulation of macrophage inflammatory protein-2 and complement 3A receptor by the trichothecenes deoxynivalenol and satratoxin G. *Toxicology* 186, 51-65.
- Davoren, M., Herzog, E., Casey, A., Cottineau, B., Chambers, G., Byrne, H.J., Lyng, F.M. 2007. *In vitro* toxicity evaluation of single walled carbon nanotubes on human A549 lung cells. *Toxicol In Vitro*, 21,438-48.
- Dendritech, Inc. <http://www.dendritech.com/pamam.html>. accessed on 16th June 2009.
- De Jong W.H. NanoImpactNet workshop on Protocols for assessment of biological hazards of engineered nanoparticles, Lausanne, March 2009.

- Dobrovolskaia, M.A., Aggarwal, P., Hall, J.B., McNeil, S.E. 2008. Preclinical study to understand nanoparticle interaction with the immune system and its potential effects on nanoparticle biodistribution. *Mol. Pharm.* 5, 487-495.
- Donaldson, K., Tran, L., Jimenez, L.A., Duffin, R., Newby, D.E., Mills, N., MacNee, W., Stone, V. 2005. Combustion-derived nanoparticles: a review of their toxicology following inhalation exposure. *Part Fibre Toxicol.* 2, 10.
- Donaldson, K., Aitken, R., Tran, L., Stone, V., Duffin, R., Forrest, G., Alexander, A. 2006. Carbon nanotubes: a review of their properties in relation to pulmonary toxicology and work place safety. *Toxicol. Sci.* 92, 5-22.
- Driscoll K.E. 2000. TNF- α and MIP-2: role in particle induced inflammation and regulation by oxidative stress. *Toxicol Lett.* 112-113, 177-184.
- Driscoll, K.E., Hassenbein, D.G., Howard, B.W., Isfort, R.J., Cody, D., Tindal, M.H., Carter, J.M. 1995. Cloning, expression, and functional characterization of rat macrophage inflammatory protein 2: a neutrophil chemoattractant and epithelial cell mitogen. *J. Leuk. Biol.* 58, 359–364.
- Duncan, R., Izzo, L. 2005. Dendrimer biocompatibility and toxicity. *Adv. Drug Delivery Rev.* 57, 2215–2237
- Emanuele, A. D., Attwood, D. 2005. Dendrimer-drug interactions. *Adv. Drug Delivery Rev.* 57, 2147–2162.
- Elbekai, R.H and El-Kadi, A.O.S., 2005. The role of oxidative stress in the modulation of aryl hydrocarbon receptor-regulated genes by As³⁺, Cd²⁺, and Cr⁶⁺. *Free Radical Biol. Med.* 39, 1499–1511.
- Gillies, E.R., Frechet, J.M.J. 2005. Dendrimers and dendritic polymers in drug delivery. *Drug Discovery Today* 10, 35-43.

- Herzog, E., Byrne, H.J., Casey, A., Davoren, M., Lenz, A-G., Maier, K.L., Duschl, A., Oostingh, G.J. 2009. SWCNT suppress inflammatory mediator responses in human lung epithelium *in vitro*. *Toxicology and Applied Pharmacology* 234, 378-390.
- <http://probes.invitrogen.com/media/pis/g002.pdf>, accessed on 16th June 2009.
- Huang, R.Q., Qu, Y.H., Ke, W.L., Zhu, J.H., Pei, Y.Y., Jiang, C. 2007. Efficient gene delivery targeted to brain using a transferrin conjugated polyethylene glycol modified polyamidoamine dendrimer. *FASEB J.* 21, 1117-1125.
- Hulikova, K., Benson, V., Svoboda, J., Sima, P., Fiserova, A. 2009. N-Acetyl-D-glucosamine-coated polyamidoamine dendrimer modulates antibody formation via natural killer cell activation. *International Immunopharmacology* 9, 792–799.
- Kang, H., De-Long, R., Fisher, M.H., Juliano, R.L. 2005. Tat-conjugated PAMAM Dendrimers as delivery agents for antisense and siRNA oligonucleotides. *Pharmaceutical research*, 22, 2099-2106.
- Khandare, J., Mohr, A., Calderón, M., Welker, P., Licha, K., Haag, R. 2010. Structure-biocompatibility relationship of dendritic polyglycerol derivatives. *Biomaterial*, 31, 4268-4277.
- Kuo, J.H., Jan, M.S., Lin, Y.L. 2007. Interactions between U-937 human macrophages and poly(propyleneimine) dendrimers. *J. Control Release.* 120, 51-9.
- Kukowska-Latallo, J.F., Candido, K.A., Cao, Z., Nigavekar, S.S., Majoros, I.J., Thomas, T.P., Balogh, L.P., Khan, M.K., Baker, J.R. 2005. Nanoparticle targeting of anticancer drug improves therapeutic response in animal model of human epithelial cancer. *Cancer Res.* 65, 5317-24.
- Lanone, S., Boczkowski, J. 2006. Biomedical Applications and Potential Health Risks of Nanomaterials: Molecular Mechanisms. *Curr Mol Med.* 6, 651-63.

- Lee, C.C., MacKay, J.A., Frechet, J.M.J., Szoka, F.C. 2005. Designing dendrimers for biological applications. *Nat Biotechnol.* 23, 1517–1526.
- Lee, J.H., Cha, K.E., Kim, M.S., Hong, H.W., Chung, D.J., Ryu, G., Myung, H. 2009. Nanosized polyamidoamine (PAMAM) dendrimer-induced apoptosis mediated by mitochondrial dysfunction. *Toxicol Lett.* 190, 202–207.
- Li, N., Sioutas, C., Cho, A., Schmitz, D., Misra, C., Sempf, J., Wang, M, Oberley, T., Froines, J., Nel, A. 2003. Ultrafine particulate pollutants induce oxidative stress and mitochondrial damage. *Environ Health Perspect.* 111, 455-60.
- Li, N., Xia, T., Nel, A.E. 2008. The role of oxidative stress in ambient particulate Matter-induced lung diseases and its implications in the toxicity of engineered nanoparticles. *Free Radical Biol. Med.* 44, 1689–1699.
- Lubos, E., Handy, D.E., Loscalzo, J. 2008. Role of oxidative stress and nitric oxide in atherothrombosis. *Front. Biosci.* 13, 5323–5344.
- Lynch, I., Cedervall, T., Lundqvist, M., Cabaleiro-Lago, C., Linse, S., Dawson, K. 2007. A. The nanoparticle-protein complex as a biological entity; A complex fluids and surface science challenge for the 21st century. *Adv. Colloid Interface Sci.* 13, 4–135.
- Maeda, H., Matsumura, Y. 1986. A new concept on macromolecular therapeutics in cancer chemotherapy: mechanism of tumouritropic accumulation of proteins and the antitumour agents SMANCS. *Cancer Res.* 46, 6387-6392.
- Monteiller, C., Tran, L., MacNee, W., Faux, S., Jones, A., Miller, B., Donaldson, K. 2007. The proinflammatory effect of low toxicity low solubility particles, nanoparticles and fine particles on epithelial cell *in vitro*: the role of surface area. *Occup. Environ. Med.* 64, 609-615.

- Mukherjee, S.P., Davoren, M., Byrne, H.J. 2010. *In vitro* mammalian cytotoxicological study of PAMAM dendrimers - Towards quantitative structure activity relationships Toxicol. In Vitro, 24, 169-77.
- Mukherjee, S.P., Lyng, F.M., Garcia, A., Davoren, M., Byrne, H.J. 2010. Mechanistic studies of *in vitro* cytotoxicity of poly (amidoamine) dendrimers in mammalian cells. Toxicol Appl Pharmacol. 248, 259-68.
- Naha, P.C., Davoren, M., Casey, A., Byrne, H.J. 2009. An ecotoxicological study of poly(amidoamine dendrimers-towards quantitative structure activity relationship. Environ. Sci. Technol. 43, 6864-6869.
- Nel, A., Xia, T., Madler, L., Ning, L. 2006. Toxic potential of materials at nanolevel. Science 311, 622-627.
- Nel, A.E., Mädler, L., Velegol, D., Xia, T., Hoek, E.M.V., Somasundaran, P., Klaessig, F., Castranova V., and Thompson, M. 2009. Understanding biophysicochemical interactions at the nano–bio interface. Nature materials, 8, 543-557.
- Obedoster, G., Obedoster, E., Obedoster. A. 2005. Nanotoxicology: an emerging discipline evolving from studies of ultrafine particles. Environ. Health Perspect. 113, 823-839.
- Organisation for Economic Co-operation and Development, 2001, Guideline (423) for Testing of Chemicals: Acute Oral Toxicity – Acute Toxic Class Method (<http://www.oecd.org/dataoecd/17/50/1948370.pdf>, accessed on 16th March 2010)
- Osuchowski, M.F., Siddiqui, J., Copeland, S., Remick D.G. 2005. Sequential ELISA to profile multiple cytokines from small volumes. Journal of Immunological Methods, 302, 172–181

- Osuchowski, M.F., Welch, K., Siddiqui, J., Remick, D.G. 2006. Circulating Cytokine/Inhibitor Profiles Reshape the Understanding of the SIRS/CARS Continuum in Sepsis and Predict Mortality. *Journal of Immunology*, 177, 1967-74.
- Park, E.J., Park, K. 2009. Oxidative stress and pro-inflammatory response induced by silica nanoparticles *in vitro* and *in vivo*. *Toxicology Letters* 184, 18-25.
- Ragnvaldsson, D., Berglind, R., Tysklind, M., and Leffler, P. 2007. Environmental Hazard Screening of a Metal-polluted Site Using Pressurized Liquid Extraction and Two *In vitro* Bioassays. *A Journal of the Human Environment* 36,494-501.
- Rahman, I. 2000. Regulation of nuclear factor- κ B, activator protein-1, and glutathione levels by tumor necrosis factor- α and dexamethasone in alveolar epithelial cells, *Biochem. Pharmacol.* 60, 1041–1049.
- Rajananthanan, P., Attard, G. S., Sheikh, N. A., Morrow, W. J. 1999. Evaluation of novel aggregate structures as adjuvants: composition, toxicity studies and humoral responses. *Vaccine* 17, 715–730.
- Sheng, K. C., Kalkanidis, M., Pouniotis, D.S., Esparon, S., Tang, C.K., Apostolopoulos, V., Geoffrey, A., Pietersz, G.A. 2008. Delivery of antigen using a novel mannosylated dendrimer potentiates immunogenicity *in vitro* and *in vivo* *Eur. J. Immunol.* 38, 424–436.
- Stone, V., Johnston, H., Clift, M.J. 2007. Air pollution, ultrafine and nanoparticles toxicology: cellular and molecular interactions. *IEEE Trans. Nanobiosci.* 6, 331–340.
- Svenson, S., Tomalia, D. A. 2005. Dendrimers in biomedical applications-reflections on the field. *Adv. Drug Delivery Rev.* 57, 2106–2129.
- Venuganti, V. V. K., Perumal, O. P. 2008. Effect of Poly(amidoamine) (PAMAM) dendrimer on skin permeation of 5-fluorouracil. *Int. J. Pharm.* 361, 230–238.

- Walley, K.R., Lukacs, N.W., Standiford, T.J., Strieter, R.M., Kunkel, S.L. 1997. Elevated levels of macrophage inflammatory protein 2 in severe murine peritonitis increase neutrophil recruitment and mortality. *Infect. Immun.* 65, 3847-3851.
- Wang, W., Xiong, W., Wan, J., Sun, X., Xu, H., Yang, X. 2009. The decrease of PAMAM dendrimer-induced cytotoxicity by PEGylation via attenuation of oxidative stress. *Nanotechnology*, 11;20(10):105103.
- Xia, T., Kovichich, M., Liong M., Zink J.I., Nel, A. E. 2008. Cationic Polystyrene Nanosphere Toxicity Depends on Cell-Specific Endocytic and Mitochondrial Injury Pathways. *ACS Nano*, 2, 85-96.
- Xia, T., Kovichich, M., Brant, J., Hotze, M., Sempf, J., Oberley, T., Sioutas, C., Yeh, J. I., Wiesner, M. R., Nel, A. E. 2006. Comparison of the Abilities of Ambient and Manufactured Nanoparticles to Induce Cellular Toxicity According to an Oxidative Stress Paradigm. *Nano Lett.* 6, 1794–1807.
- Yoo, H., Juliano, R.L. 2000. Enhanced delivery of antisense oligonucleotides with fluorophore-conjugated PAMAM dendrimers. *Nucleic acid Research.* 28, 4225-4231.

Chapter 8

Conclusion

Polymeric nanoparticles have been investigated for a wide range of potential applications, especially in the biomedical field, in terms of drug, gene, and vaccine delivery vectors as well as for MRI contrast agents for diagnosis. Given the potential widespread use of both the series of polymeric nanomaterials (PAMAM dendrimers, PNIPAM and NIPAM/BAM copolymer nanoparticles), there is an urgent need for information regarding the human health and environmental implications of exposure to these polymeric nanomaterials. In terms of human exposure, considerable attention has been devoted of late to the potential effects of exposure to nanomaterials. However, the field of eco-(nano) toxicology is still relatively new and there is a dearth of quantitative structure activity relationships established for nanomaterials. Thus, this study has utilised both human and aquatic models.

In the case of polymeric nanoparticles, the structurally well defined and variable macromolecules can also provide a further basis upon which to establish structure activity relationships governing eco and mammalian-toxicological responses which may serve to develop a fundamental understanding of their interactions and as guidelines for the future prediction of responses. In the case of PNIPAM and NIPAM/BAM nanoparticles, a systematically varied surface morphology is achieved as the ratio of BAM increases, the amount of N-H groups exposed at the surface decreases, and the amount of $-C-(CH_3)_3$ groups increases, reducing the hydrophilicity of the resulting copolymer. The systematically varied molecular PAMAM dendrimer nanostructures potentially provide a route towards an understanding of the dependence of the interactions on the physico-chemical properties of nanomaterials. Both the polymer particles were selected to understand the correlation between physico-chemical properties and toxicological impact of these nanomaterials to the human health as well as to the environment. As such, independent of their potential applications, the particle

series have been chosen as potential models for positive controls for nanoparticle toxicity.

PNIPAM and NIPAM/BAM are well known thermoresponsive polymers which can be used to generate well defined nanoparticles. However, no eco or mammalian toxicity data of PNIPAM and NIPAM/BAM co-polymer nanoparticles was available prior to this study. The most sensitive ecotoxicological assay for PNIPAM and NIPAM/BAM 85:15 nanoparticles was the immobilisation of *Daphnia magna* (48 hour EC₅₀) and for NIPAM/BAM 65:35 and NIPAM/BAM 50:50 nanoparticles was the Microtox[®] assay (*Vibrio fischeri*, 5 minutes EC₅₀). The least sensitive bioassay was *Pseudokirchneriella subcapitata* (72 h EC₅₀) for the four nanomaterials tested. An important conclusion from the study therefore is that the sensitivity of each assay is dependent on the physico-chemical characteristics of the particle, emphasising the importance of a multi-trophic approach. This is possibly indicative of different mechanisms of uptake and/or toxic response for particles of differing physico-chemical properties, but further studies would be required to qualify the observations. As the ratio of BAM increases in the copolymer nanoparticles the toxic response increased in all the test species, despite the fact that the particles with the highest ratio of BAM were highly agglomerated. The toxicity trend for different nanoparticles was PNIPAM < NIPAM/BAM 85:15 < NIPAM/BAM 65:35 < NIPAM/BAM 50:50, which suggests that there is a significant effect due to particle hydrophobicity and the surface free energy (Lynch et al., 2005). This is confirmed by the correlation of the toxic response with the observed zeta potential of the particles in the medium. The correlation of the toxic response in *Daphnia magna* with the reduction in zeta potential points towards a contribution of secondary effects due to modification of the medium. No dependence of the toxic response on the particle size (hydrodynamic diameter, measured in DLS) was observed

however. Nevertheless the study gives a clear dependence of the toxic response on the particle composition pointing towards structure-activity relationships.

Mammalian toxicological evaluation of PNIPAM nanoparticles indicated no significant cytotoxic response in HaCaT and SW480 cells, which seems that particles could be biocompatible, but the result presented here is the only obtained from the *in vitro* assay, further studies are required, like *in vivo* study in rat or rabbit model to confirm this. No significant difference in the cell viability upon exposure of either cell type to PNIPAM nanoparticles was found after 24h, 48h, 72h and 96h of exposure at concentrations ranging from 12.5 to 1000 mg/l. The biocompatibility of the PNIPAM nanoparticles is further confirmed by the genotoxicity results, as there is no significant difference in the % tail DNA and olive tail moment (OTM) in either the HaCaT and SW480 cells upon exposure of the particles. Fluorescently labelled PNIPAM particles are clearly seen to be internalised by HaCaT and SW480 cells after 24hrs, and there are some evidence that the particles are localised in lysosomes and also some particles are in cytoplasm not associated with the lysosomes.

The observed interaction of the PNIPAM nanoparticles with the two different mammalian cell lines and the interpretation of the consequences of the particle fate and behaviour within the cells is an indication of the biocompatibility of these polymer particles. In addition to this, as it was observed that PNIPAM nanoparticles do not elicit an ecotoxicological response in range of test model employed. The data presented here would suggest that these particles have significant potential as drug delivery agents in the form of hydrogels or as scaffolds in the field of tissue engineering.

However the ecotoxicological study of Polyamidoamine (PAMAM) dendrimers demonstrated significant eco and cytotoxicological responses at concentration ranges

from 0.13 μM to 16.30 μM . For all generations of PAMAM dendrimer tested, the *Daphnia magna* was shown to be the most sensitive test model, the RTG-2 cell line being the least sensitive. The ecotoxicological response was seen to correlate well with the generation of PAMAM dendrimers and therefore with the particle surface area. The surface chemistry is unaltered in successive generations, and thus a clear and direct relationship between the physical parameter and the toxic response is inferred. The physico-chemical characteristics, most notably the zeta potential of the particles, were seen to change dependant on the dispersion medium, however, and the correlation of the toxic response to these changes may point towards an interaction with the medium resulting in a change in effective composition as an underlying source of the toxic response. Successive generations present a larger number of surface amino groups for interaction with the media, and thus a larger toxic response. Such an indirect effect can not be considered as the sole origin; however, as is seen by comparison of the PAMAM dendrimers with the NIPAM/BAM copolymer nanoparticles and mechanisms of internalisation resulting in a direct toxic response should be investigated for all models. A significant genotoxicity and apoptosis response in PLHC-1 cells was observed upon the exposure to PAMAM dendrimers. The generation dependence ($G6 > G5 > G4$) of the production of increased intracellular ROS, DNA damage, apoptosis and the cytotoxicity in the PLHC-1 cells, indicates the direct effects of the positively charged surface amino groups.

The immunotoxicity of PAMAM dendrimers was investigated in mouse macrophage cells (J774A.1) *in vitro* at a concentration of 0.013 to 6 μM . Generation dependent immunotoxicological response of PAMAM dendrimer was observed in J774A.1 cells. The generation dependence ($G6 > G5 > G4$) of the production of increased intracellular ROS, inflammatory mediators and the cytotoxicity. The mechanism of the toxic

response is proposed to be one of localisation of the cationic particles in the mitochondria, leading to significant increase in ROS generation, induction of cytokines production, DNA damage, apoptosis and ultimately cell death.

The ecotoxicological study of the NIPAM/BAM series of nanoparticles shows significant toxic effects at higher concentration. As the ratio of BAM increases in the nanomaterial composite there is a systematic increase of toxic response. However, in case of PNIPAM nanoparticles, no toxicological response was observed with mammalian cells even at higher doses.

PAMAM dendrimers show significant toxic responses at the concentration employed in the studies, both fresh water ecological organisms and mammalian cells. Clear structure property relationships are indicated for the toxic responses in both cases. An evolving paradigm of toxic responses to nanomaterials begins with the generation of intracellular ROS, followed by lysosomal and/or mitochondrial damage, which leads to DNA damage, mutation, apoptosis and finally cell death (Nel et al., 2009, Xia et al., 2006 and 2008). PAMAM dendrimer induced cell death has been demonstrated to follow this mechanistic pathway.

In general, polymeric nanomaterials, having systematic structural variations in molecular weight, surface chemistry and size, represent ideal model systems to explore structure property relationships governing toxicological response. In addition, PAMAM dendrimers hold potential as gene transfecting agents due to the positive charge on the surface and are also employed as vaccine delivering agents. Understanding their mode of interaction and cellular transport can lead to improved guidelines for the design of drug delivery systems.

Ultimately, the development of quantitative structure activity relationships governing the interaction of nanoparticles with cellular systems is desirable. This study has

indicated that systematic variation of physic-chemical properties may be the foundation of such relationships.

References

- Lynch, I., Blute, I.A., Zhmud, B., MacArtain, P., Tosetto, M., Allen, L.T., Byrne, H.J., Farrell, G.F., Keenan, A.K., Gallagher, W.M., Dawson, K.A. 2005. Correlation of the Adhesive Properties of Cells to *N*-Isopropylacrylamide/*N*-*tert*-Butylacrylamide Copolymer Surfaces with Changes in Surface Structure Using Contact Angle Measurements, Molecular Simulations, and Raman Spectroscopy. *Chem. Mater.* 17, 3889 - 3898.
- Nel, A.E., Mädler, L., Velegol, D., Xia, T., Hoek, E.M.V., Somasundaran, P., Klaessig, F., Castranova V., and Thompson, M. 2009. Understanding biophysicochemical interactions at the nano–bio interface. *Nature materials*, 8, 543-557.
- Xia, T., Kovoichich, M., Liong, M., Mädler, L., Gilbert, B., Shi, H., Yeh, J.I., Zink, J.I., Nel A.E. 2008. Comparison of the mechanism of toxicity of zinc oxide and cerium oxide nanoparticles based on dissolution and oxidative stress properties. *Am. Chem. Soc. Nano.* 2, 2121–2134.
- Xia, T., Kovoichich, M, Brant J., Hotze, M., Sempf, J., Oberley, T., Sioutas, C., Yeh, J. I., Wiesner, M. R., Nel, A.E. 2006. Comparison of the abilities of ambient and manufactured nanoparticles to induce cellular toxicity according to an oxidative stress paradigm. *Nano Letter.* 6, 1794–1807.

Appendices

Appendix I: Supporting Information

1.1 PNIPAM and NIPAM/BAM co-polymer nanoparticles

Poly *N*-isopropylacrylamide (PNIPAM) and *N*-isopropylacrylamide-co-*N*-*tert*-butylacrylamide (NIPAM/BAM) copolymer particles with systematically varied ratios of the respective monomers (85:15, 65:35, and 50:50 NIPAM/BAM) were made available by University College Dublin through the “Integrated NanoScience Platform for Ireland” collaborative programme (www.inspirenano.com). They were synthesised by free radical polymerisation (Cedervall, et al., 2007). In brief, the synthetic procedure, as supplied by UCD, was as follows: 2.8g monomers (in the appropriate ratios by weight), and 0.28g crosslinker (N,N-methylenebisacrylamide) were dissolved in 190 ml MilliQ water (MQ) with 0.8 g Sodium Dodecyl Sulphate (SDS) and the solution was degassed by bubbling with nitrogen gas for 30 minutes. Polymerisation was induced by adding 0.095g ammonium persulfate initiator in 10 ml MQ water and heating at 70°C for 4 hours. Particles were extensively dialysed with MQ water for several weeks, the water being changed daily, until no traces of monomers, crosslinker, initiator or SDS could be detected by proton NMR (spectra acquired in D₂O using a 500 MHz Varian Inova spectrometer). Particles were freeze-dried and stored in the fridge until used. Due to the inverse solubility of PNIPAM and NIPAM/BAM particles, solutions for exposure studies were prepared by dispersing the particles on ice to ensure good solubility of the particles (i.e. to ensure that the solutions are below the lower critical solution temperature of the particles and thus that polymer-water contacts are more favourable than polymer-polymer contacts which would result in uptake of water and swelling of the particles), before gradually warming them to the test conditions. Fluorescently tagged NIPAM nanoparticles with nominally 500 fluorescent labels per particle were also synthesized within the “Integrated NanoScience Platform for Ireland”

collaborative programme (www.inspirenano.com). In brief, the synthetic procedure, as supplied by UCD, was as follows. 0.1 g of SDS was mixed with 0.0044 g of methacryloxyethyl thiocarbamoyl Rhodamine B in 10 ml of MQ water and the mixture was sonicated using a Covaris S2 system at a frequency of 450 kHz for 500 seconds until most of the dye was visibly dissolved. The solution was transferred into a falcon tube adding an additional 10 ml MQ water together with the rest the SDS (0.3 g) and was then sonicated using an ultrasonic bath (Branson 1510) at a frequency of 42 kHz for 5 hours continuously until the dye was completely dissolved in the SDS. The monomers (1.4 g of NIPAM, 0.14 g of cross linker) were added to this solution with 75 ml of MQ water, stirred for 30 minutes under nitrogen flow to remove dissolved O₂, heated at 70°C and then the synthesis was performed by adding a degassed solution composed of 0.0475 g of initiator diluted in 5 ml of MQ water. The reaction was carried out for 12 hours at 70°C and under nitrogen flow. The labelled particles were dialysed against ethanol for 6 days and then extensively dialysed in ultrapure water, freeze dried and stored at 4°C. Any unreacted dye was removed by extensive dialysis to ensure that the fluorescence detected during internalisation studies was truly representative of nanoparticles. (Personal communication, Iseult Lynch).

1.2 Transmission electron microscopy (TEM) study

In the case of PNIPAM particles, particle size was also determined by Electron Microscopy. Samples were prepared by negative-contrast staining as described previously (Gorelov et al 1997). Briefly, stock solutions of tungstophosphoric acid (TPA, 200 mg / ml) (Fluka) and labelled NIPAM nanoparticles (5mg / ml) were prepared in water, and were left in a drying cabinet for about 2 hours at 55°C. The mixing of the final solution and the sample preparation was performed in the drying cabinet at a constant temperature of 55 °C. The final solution contained 20 mg / ml of

TPA and 4.5 mg /ml of NIPAM nanoparticles, and was left in the drying cabinet for about 15 minutes together with the TEM grids. A drop of this final solution was placed on the grid and immediately soaked with filter paper in order to leave on the grid a thin film of nanoparticles, in this way minimising the nanoparticle agglomeration during the drop drying time. Samples were investigated in a TECNAI G² 12 TWIN TEM using an acceleration voltage of 120 kV and objective aperture of 20 µm. Digital images were recorded with a MegaView III (SIS) camera.

Appendix II: Publications

- **Pratap C. Naha**, V. Kanchan, P.K. Manna, Amulya K. Panda. 2008. Improved bioavailability of orally delivered insulin using Eudragit L 30D coated PLGA microparticle. **Journal of Microencapsulation**, 25, 248-256.
- **Pratap C. Naha**, V. Kanchan and Amulya K. Panda. Evaluation of parenteral depot insulin formulation using PLGA and PLA microparticles. **Journal of Biomaterial Applications**, 2009. 24 (4):309-25.
- **Pratap C. Naha**, Alan Casey, Tiziana Tenuta, Iseult Lynch, Kenneth A. Dawson, Hugh J. Byrne, Maria Davoren. Preparation and characterisation of *NIPAM* and *NIPAM/BAM* co-polymer nanoparticles and their acute toxicity testing using an aquatic test battery. **Aquatic Toxicology**, 2009. 92, 146-154.
- **Pratap C. Naha**, Maria Davoren, Alan Casey and Hugh J. Byrne. An Ecotoxicological study of Poly (amidoamine) Dendrimers-Towards Quantitative Structure Activity Relationship. **Environmental Science and Technology**, 2009. 43(17):6864-6869.
- **Pratap C. Naha**, Maria Davoren, Fiona M. Lyng and Hugh J. Byrne. Oxidative stress induced inflammatory response and cytotoxicity of PAMAM dendrimers in J774A.1 cells. (2010). **Toxicology and Applied Pharmacology**, 246 (1-2), 91-99.
- **Pratap C. Naha**, Kunal Bhattacharya, Tiziana Tenuta, Kenneth A. Dawson, Iseult Lynch, Amaya Gracia, Fiona M. Lyng , Hugh J. Byrne. Intracellular localisation, Geno- and Cytotoxic response of Poly *N*-isopropylacrylamide (PNIPAM) nanoparticles to human keratinocyte (HaCaT) and colon cells (SW 480). **Toxicology Letters**. (2010), 198, 134-143.
- **Pratap C. Naha**, S. Madhusudan, P. K Manna, Hugh J. Byrne and Amulya K. Panda. Role of polymeric excipients on controlled release profile of Glipizide from PLGA and Eudragit RS 100 Nanoparticles. (December, 2010), **Biomedical materials**. (Submitted).
- Kunal Bhattacharya, **Pratap C. Naha**, Andrew Kellet, Fiona Lyng, Izabela Neydenova, Svetlana Mintova, Hugh J Byrne. Biocompatibility of silica based Zeolite-MFI nanoparticles in human lung cells. (2011). (In Preparation).

- **Pratap C. Naha** and Hugh J. Byrne. Oxidative stress induced DNA damage and apoptosis by PAMAM dendrimers in PLHC-1 cells. (2011), (In preparation).

Appendix III: Presentations

- **Pratap C. Naha**, Maria Davoren, Iseult Lynch, Kenneth Dawson, Hugh J. Byrne. Preparation, characterisation and ecotoxicological evaluation of P(NIPAM) and NIPAM:BAM co-polymer nanoparticles. **NanoimpactNet Conference**, 25th March, 2009. **Lausanne, Switzerland**. (Oral Presentation)
- **Pratap C. Naha** and Hugh J. Byrne. Ecotoxicological Assessment of Polymeric Nanoparticles of Technological Relevance. 6th May 2009, **NanoBio INSPIRE meeting, Tyndal Institute, Cork, Ireland**. (Oral Presentation)
- **Pratap C. Naha**, Hugh J. Byrne, Iseult Lynch, Kenneth A. Dawson, Maria Davoren. Physico-Chemical Properties And Structure Activity Relationship Are Key Factors For Ecotoxicity Of Polymeric Nanoparticles. 1st June 2009, 19th Annual Meeting **SETAC Europe. Goteborg, Sweden**. (Poster presentation).
- **Pratap C. Naha**, Maria Davoren, Tiziana Tenuta, Iseult Lynch, Kenneth Dawson, Hugh J. Byrne. Structurally Dependent Ecotoxicity of Polymeric Nanoparticles. 15th & 16th October 2009. **INSPIRE NanoBio conference, Dublin, Ireland**. (Poster presentation).
- **Pratap C. Naha**, Maria Davoren, Fiona M. Lyng and Hugh J. Byrne. Oxidative stress induced inflammatory response and cytotoxicity of PAMAM dendrimers in J774A.1 cells. 2nd - 4th June 2010. **3rd International Conference on Nanotoxicology, Edinburgh Napier University, Edinburgh UK**. (Poster presentation).
- **Pratap C. Naha**; Tiziana Tenuta; Kenneth A. Dawson; Iseult Lynch; Fiona M. Lyng; Hugh J. Byrne. Interaction of Poly *N*-isopropylacrylamide (PNIPAM) nanoparticles with human keratinocyte (HaCaT) and colon cells (SW 480). 20-21st October 2010, **INSPIRE NanoBio conference, Dublin, Ireland**. (Poster presentation).
- **Pratap C. Naha**, Maria Davoren and Hugh J. Byrne. Interaction of nanosized Poly (amido) amine dendrimers with fresh water ecological organisms and fish cells. 15th -19th May 2011., 21st Annual Meeting **SETAC Europe. Milan, Italy**. (Oral presentation).
-

Appendix IVI: Conference and Workshop Attendance

1. 2nd International Conference on Nanotoxicology September, 2008, Zurich, Switzerland.
2. NanoImpactnet workshop, June 2008, UCD, Dublin, Ireland.
3. 1ST NanoImpactnet Conference March 2009, Lusanne, Switzerland.
4. 19th SETAC Annual meeting June 2009, Goteborg, Sweden.
5. 1st International NanoBio Conference, October 2009, Dublin, Ireland
6. 3rd International Conference on Nanotoxicology 2nd - 4th June 2010. 3rd International Conference on Nanotoxicology, Edinburgh Napier University, Edinburgh UK.
7. NanoImpactnet workshop, 6-9 September 2010, Hazard Assessment of Nanomaterials.UCD, Dublin, Ireland.
8. BioNano Conference, 20-21st October 2010. UCD, Dublin, Ireland.
9. VIth Annual meeting of Irish cytometry society. November 17th and 18th 2010, Dublin, Ireland.
10. 21st SETAC Annual meeting May 2011, Milan, Italy

Curriculum Vitae



Pratap C. Naha
 Radiation and Environmental Science Centre (RESC)
 FOCAS Research Institute.
 Dublin Institute of Technology
 Kevin Street, Dublin-8,
 Ireland
 E Mail : pratap.naha@dit.ie
 pratapnaha@gmail.com
 nahapc@yahoo.com
 Phone : +353 1 402 7956 (Office)
 +353 879421303 (Mobile)



Educational Qualification

2008/05 – 03/2011 : Ph.D
 Dublin Institute of Technology
 Supervisor: Prof. Hugh J. Byrne
 2006/07 – 2008/04: Project assistance
 National Institute of Immunology
 Supervisor: Dr. Amulya K. Panda
 2004 – 2006:
 Master in Pharmacy (M. Pharm; Pharmacology)
 Dept. of Pharmacy; Annamalai University;
 First Division with GPA 8.58.
 2000-2004:
 Bachelor in Pharmacy (B.Pharm.)
 Institute of Pharmacy and Technology,
 Biju Pattnaik University of Technology, (BPUT)
 First Division (77% marks).

Research Experience

05/2008 – 03/2011: (Focas Research Institute, DIT, Dublin, Ireland)

- *Eco and In vitro mammalian toxicological assessment of Polymeric nanomaterials.*

07/2006 – 04/2008: (National Institute of Immunology; New Delhi, India)

- *Scale up and evaluation of biodegradable polymer particle formulations for single dose vaccine.*
- *Improved immunogenicity of enterovirus antigen by use of microparticle carrier: a proof of principle study for development of multi-variant enterovirus vaccine.*

2004–2006: (Dept. of Pharmacy, Annamalai University and National Institute of Immunology)

- *Development and Characterization of Novel Polymeric Microspheres for sustained oral and intramuscular delivery of Insulin.*

Scientific Skills

During Ph.D

- Characterization of nanoparticles in terms of hydrodynamic diameter, zeta potential, and the BET surface area measurement.
- Cell culture like HaCaT, SW480, J774A.1, PLHC-1 and RTG-2 cells.
- Cytotoxic Assays like, MTT, Alamar blue, Neutral red, Clonogenic assay.
- Interaction of nanomaterials with dye and cell culture medium study was performed with UV/Visible spectroscopy and fluorometric technique.
- Uptake and co-localisation study of nanoparticles within the cells by Confocal Laser Scanning Microscope (CLSM) and live cell observer.
- Mechanistic pathway of nanoparticles induced toxicity was studied in terms of Reactive Oxygen Species (ROS) generation, Mitochondrial membrane potential (MMP), DNA damage (by Alkaline Comet assay), Oxidative DNA damage, like formation of DNA adduct (8-OHdG), inflammatory response (IL-6, IL-8, TNF- α , and MIP-2, by ELISA), and Apoptosis assay (by Flowcytometer).

- Toxicological screening procedure of PAMAM dendrimers (G4, G5 and G6) and PNIPAM/BAM series of nanoparticles in both mammalian cells and fresh water organisms, representing different trophic level for the Ecotoxicological evaluation.
- Ecotoxicity assessment of PAMAM dendrimers (G4, G5 and G6) and PNIPAM/BAM series of nanoparticles using a battery of bioassays like Microtox assay, Algal growth inhibition assay, Immobilisation of *Daphnia magna*, *Thamnocephalus* assay, chronic toxicity assay with *Daphnia magna* (Reproductive toxicity) and the cytotoxicity assessment in two fish cell line (PLHC-1 and RTG-2) to represent a secondary consumer in fresh water ecosystem.

During Project Assistant at National Institute of Immunology, India.

- Techniques related to development of novel drug delivery systems e.g. liposome's, microspheres, nanoparticles, SLN (solid-lipid nanoparticles) and Dendrimers. Spray-drying technique for production of polymeric nano and microparticles and development of delivery system for poorly soluble drugs and proteins.
- Improvement of immunogenicity (of viral proteins like Rota virus and Enterovirus; Tetanus Toxoid; DPT; HB_sAg) by polymeric microparticles.
- *In vivo* study (Rat and Mice model) for the immunological response of the antigen entrapped polymeric microparticles; especially for the evaluation of humoral and T- cell response. And also for the memory response against the antigen (TT, DPT) entrapped polymeric microparticles (PLA and PLGA).
- *In vivo* anti-diabetic evaluation of insulin loaded Eudragit coated PLGA microparticles in rat model (Both oral and parenteral route).

- Isolation and high throughput protein purification techniques (Human growth hormone, SOD etc).
- Techniques like ELISA, RIA, ELISPOT, Flow Cytometry, Western Blot, SDS-PAGE and chromatographic techniques (like FPLC, Ion exchange, Size exclusion) for protein purification.

Publications

- **Pratap C. Naha**, V. Kanchan, P.K. Manna, Amulya K. Panda. 2008. Improved bioavailability of orally delivered insulin using Eudragit L 30D coated PLGA microparticle. **Journal of Microencapsulation**, 25, 248-256.
- **Pratap C. Naha**, V. Kanchan and Amulya K. Panda. Evaluation of parenteral depot insulin formulation using PLGA and PLA microparticles. **Journal of Biomaterial Applications**, 2009. 24 (4):309-25.
- **Pratap C. Naha**, Alan Casey, Tiziana Tenuta, Iseult Lynch, Kenneth A. Dawson, Hugh J. Byrne, Maria Davoren. Preparation and characterisation of *NIPAM* and *NIPAM/BAM* co-polymer nanoparticles and their acute toxicity testing using an aquatic test battery. (2009), **Aquatic Toxicology**, 92, 146-154.
- **Pratap C. Naha**, Maria Davoren, Alan Casey and Hugh J. Byrne. An Ecotoxicological study of Poly (amidoamine) Dendrimers-Towards Quantitative Structure Activity Relationship. (2009). **Environmental Science and Technology**, 43(17):6864-6869.
- **Pratap C. Naha**, Maria Davoren, Fiona M. Lyng and Hugh J. Byrne. Oxidative stress induced inflammatory response and cytotoxicity of PAMAM dendrimers in J774A.1 cells. (2010). **Toxicology and Applied Pharmacology**. 246 (1-2), 91-99.

- **Pratap C. Naha**, Kunal Bhattacharya, Tiziana Tenuta, Kenneth A. Dawson, Iseult Lynch, Amaya Gracia, Fiona M. Lyng , Hugh J. Byrne. Intracellular localisation, Geno- and Cytotoxic response of Poly *N*-isopropylacrylamide (PNIPAM) nanoparticles to human keratinocyte (HaCaT) and colon cells (SW 480). (2010) **Toxicology Letters**, 198, 134-143.
- **Pratap C. Naha**, S. Madhusudan, P. K Manna, Hugh J. Byrne and Amulya K. Panda. Role of polymeric excipients on controlled release profile of Glipizide from PLGA and Eudragit RS 100 Nanoparticles. **Biomedical Materials**, (Submitted, December 2010).
- Kunal Bhattacharya, **Pratap C. Naha**, Andrew Kellet, Fiona Lyng, Izabela Neydenova, Svetlana Mintova, Hugh J Byrne. Biocompatibility of silica based Zeolite-MFI nanoparticles in human lung cells. (2011). (In Preparation).
- **Pratap C. Naha** and Hugh J. Byrne. Oxidative stress induced DNA damage and apoptosis by PAMAM dendrimers in PLHC-1 cells. (In preparation).

Conference Presentations

- **Pratap C. Naha**, Maria Davoren, Iseult Lynch, Kenneth Dawson, Hugh J. Byrne. Preparation, characterisation and ecotoxicological evaluation of P(NIPAM) and NIPAM:BAM co-polymer nanoparticles. NanoimpactNet Conference, 25th March, 2009. Lausanne, Switzerland. (Oral Presentation)
- **Pratap C. Naha** and Hugh J. Byrne. Ecotoxicological Assessment of Polymeric Nanoparticles of Technological Relevance. 6th May 2009, NanoBio INSPIRE meeting, Tyndal Institute, Cork, Ireland. (Oral Presentation)

- Pratap C. Naha, Hugh J. Byrne, Iseult Lynch, Kenneth A. Dawson, Maria Davoren. Physico-Chemical Properties And Structure Activity Relationship Are Key Factors For Ecotoxicity Of Polymeric Nanoparticles. 1st June 2009, 19th Annual Meeting SETAC Europe. Goteborg, Sweden. (Poster presentation).
- Pratap C. Naha, Maria Davoren, Tiziana Tenuta, Iseult Lynch, Kenneth Dawson, Hugh J. Byrne. Structurally Dependent Ecotoxicity of Polymeric Nanoparticles. 15th & 16th October 2009. INSPIRE NanoBio conference, Dublin, Ireland. (Poster presentation).
- Pratap C. Naha, Maria Davoren, Fiona M. Lyng, Hugh J. Byrne. Oxidative stress induced inflammatory response and cytotoxicity of PAMAM dendrimers in J774A.1 Cells. 2nd -4th June 2010, 3rd International Nanotoxicology conference. Edinburgh, UK. (Poster presentation).

Reference

Prof. Hugh J. Byrne
Director, FOCAS Research Institute,
Dublin Institute of Technology (DIT).
Kevin Street, Dublin-8.
Ireland.
E mail: hugh.byrne@dit.ie
Phone : +353 1 4027900
Fax : +353 1 402 7901

I, hereby assure that the statements mentioned in this CV are true in the best of my knowledge.

Dublin, Ireland.

Pratap C. Naha